Functionalised 1,3-dithiole derivatives exhibiting intramolecular donor-acceptor properties

Andrew Green

Functionalised 1,3-Dithiole Derivatives Exhibiting Intramolecular Donor-Acceptor Properties

Andrew Green B.Sc. (Hons.)
St. Aidans College

Department of Chemistry
University of Durham

A thesis submitted for the degree of Doctor of Philosophy at the University of Durham.

July 1997

Declaration

The work described in this thesis was carried out by the author, unless otherwise acknowledged, in the Department of Chemistry, University of Durham between October 1993 and September 1996. It has not been submitted previously for a degree at this or any other University.

Statement of Copyright

Abstract

Functionalised 1,3-Dithiole Derivatives Possessing Intramolecular Donor-Acceptor Properties

by

Andrew Green B.Sc.(Hons.)

A thesis submitted for the degree of Doctor of Philosophy at the University of Durham

July 1997

A variety of functionalised 1,3-dithiole derived donor-π-acceptor systems linked by an alkenic bridge have been synthesised, the acceptor units being dicyanomethylene and cyanoimine. They exhibit intramolecular electron transfer from the electron donor moiety to the electron acceptor moiety. The presence of electron donating substituents on the 1,3-dithiole ring increases the degree of overall charge transfer; this process has been studied by UV-VIS spectroscopy and X-ray crystallography. The latter technique indicates a significant amount of intramolecular electron transfer in the ground state.

A selection of functionalised donor-π-acceptor systems linked by an anthracene spacer unit have been prepared which possess greater donor-π-acceptor characteristics; however, the degree of electron transfer measured by X-ray crystallography of one derivative appears to be less.

The 1,3-diselenole donor unit has also been utilised as an electron donor unit in donor-π-acceptor systems however, for all derivatives the diselenole unit is inferior to the 1,3-dithiole unit.

The linking of a 1,3-dithiole donor unit to two acceptor units produces charge transfer bands that are red shifted compared to the parent donor-π-acceptor systems. Exchange of one acceptor unit for a donor unit leads to a similar red shift.

Solution electrochemical studies, non-linear optical properties, ultra-fast spectroscopy and solvatochromic analysis have been performed on a range of systems.

Acknowledgements

I would like to express my heartfelt thanks to the people without whose help and friendship I would have found the last three years incredibly difficult.

Firstly, I would like to thank my supervisor Prof. Martin Bryce for his constant encouragement and help during the past three years.

Thanks also to my industrial supervisor Dr Paul Wight for his encouragement in the early days.

To Prof. Carlos Seoane and Nazario Martín for hosting my visit to Madrid and Louis Sanchez for helping me around an unfamiliar lab.

Special thanks to the people who have shared their extensive experience with me during my time in Durham, especially to:-

Dr. Adrian Moore for his constant help with practical problems, for performing preliminary experiments to the work discussed in chapter 2 and for being around to go for a beer when things got too much.

Dr. Antony Chesney for his help with preliminary experiments for chapter 5 and for correcting my English.

I couldn't finish this section without thanking Dr. Mark Blower who taught me a great deal about practical chemistry in the early days. Thanks to you all.

Thanks to the past and present members of the Bryce group; working with you all has been a pleasure (in no particular order) Mike, Graham, Alex, Jules, Reinhold, Shimon, Pilar, Derek and Brian.

In the small amount of time that I wasn't performing chemistry thanks to the friends that have helped cheer me up when thing got me down; Graham (again), Tracy, Suzanne, Lisa, Rocky (The skiing crew, long may it continue), Alton and Dianne (don't forget how you both met!!). Ade, Colin, Adam, Shimon, and Chez (the Drobbers five aside team) Sherrie, Lisa, Lynne, Rachel, Karen, Adrian, Burnadet, Steve, Sarah, Ian and anyone else that I may have forgotten you're all very special to me.

Thanks to the technical staff in the department for providing Mass spectra, CHN analysis and NMR Spectra, especially Mrs. Julia Say for variable temperature NMR spectra, Dr. Andrei Batsanov and Prof. Judith Howard for the X-ray crystal structures within this thesis, Dr. Igor Lednev, Dr. John Moore and Prof. Ron Hester (University of York) for performing the ultra-fast spectroscopic studies, Dr. M. Hucknell (Zeneca Specialties) for performing the statistical calculations for chapter 3 and Dr. I. Ledoux (French Telecom, Paris) for the NLO data.

Thanks to the EPSRC for their financial support and Zeneca (Specialties) for providing a CASE award.

Finally, to my family for all their help and support during my student years.

Contents

Chapter 1

Introduction

1.1 Intermolecular Charge Transfer Complexes of the TTF-TCNQ Genre

The possibility that organic materials could exhibit electrical conductivity was first suggested in the early 20th century.[1,2] However, the majority of organic compounds are insulators with a room temperature conductivity ($\sigma_{RT}<10^{-10}$ S cm^{-1}). The mixing of an electron donor (D) with an electron acceptor (A) can form complexes (D^+A^-) and much higher conductivity values ($\sigma_{RT}=1\text{-}10^{-2}$ S cm^{-1}) may be found in these charge transfer complexes. The first reported example of an organic conducting material ($\sigma_{RT}=1$ S cm^{-1}) was an unstable perylene bromine salt.[3] The first major breakthrough in the synthesis of highly conducting charge transfer complexes followed the synthesis of the strong electron acceptor tetracyano-*p*-quinodimethane (TCNQ) **1**.[4] A wide variety of complexes of TCNQ were formed which exhibited semiconducting behaviour ($\sigma_{RT}=10^{-6}\text{-}10^{-4}$ S cm^{-1}). The first true organic metal was not reported until 1973:[5] a charge transfer complex of tetrathiafulvalene (TTF) **2** and TCNQ **1** [$TTF^{+\cdot}TCNQ^{-\cdot}$] which exhibit a room temperature conductivity of 500 S cm^{-1} with conductivity increasing with decreasing temperature down to 54K. Below this temperature the material behaves as an insulator due to Peierls distortion (a lattice distortion inherent to low dimensional chain materials).[6,7]

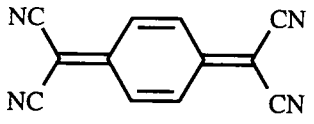

1

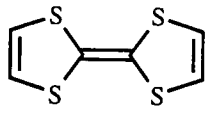

2

1.1.2 TTF-TCNQ

In 1970 Wudl established that TTF **2** is a powerful electron donor.[8] The solution electrochemistry of **2** exhibits two reversible one-electron oxidation waves at 0.34V and 0.71V respectively (*vs.* Ag/AgCl). The second oxidation occurs at relatively high potential due to the formation of a dication state in which both charges are in close proximity leading to coulombic repulsive forces (fig.1.1).

In 1972 it was discovered that the chloride salt of TTF was conducting[9] ($\sigma_{RT}=0.2$ S cm^{-1}) and in the following year TTF-TCNQ was reported. The crystal structure of TTF-TCNQ[10] (fig.1.2) consists of TTF radical cations and TCNQ radical anions aligned in interlocking segregated stacks.

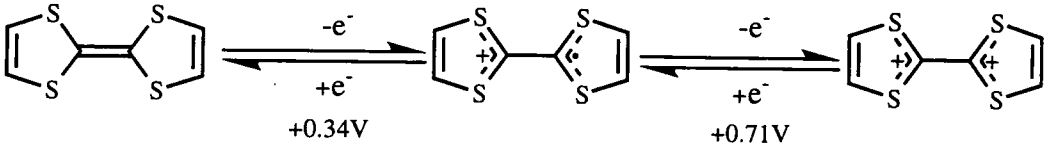

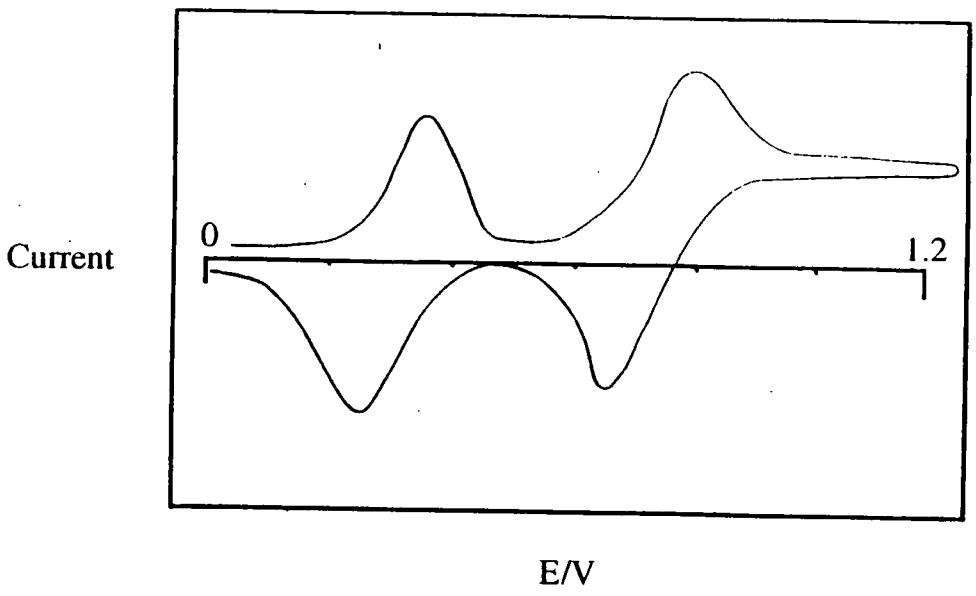

Fig.1.1 Cyclic Voltammogram of TTF. Pt working and counter electrodes, Ag/AgCl reference electrode

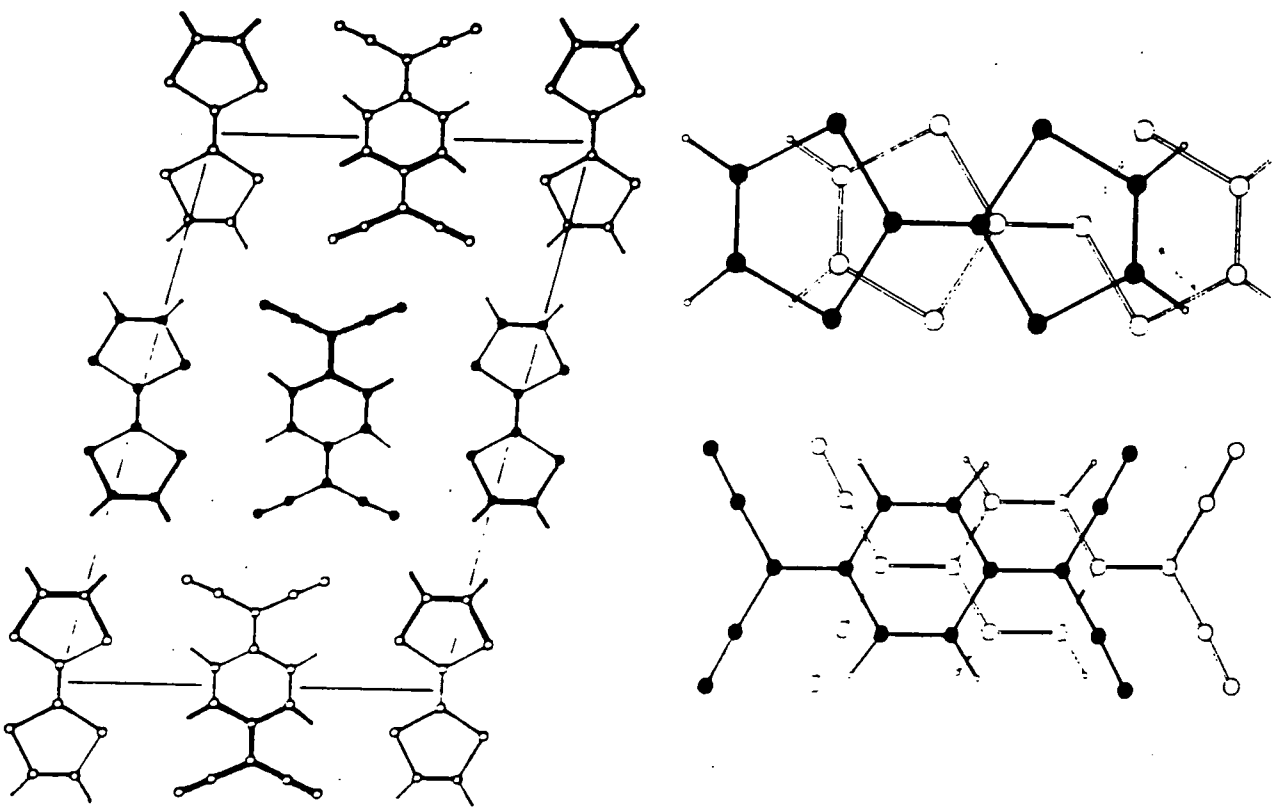

Fig.1.2 X-Ray Structure of TTF:TCNQ

Infra-red spectroscopy indicated that charge transfer is incomplete with only 0.59 electrons being transferred from the donor to the acceptor.[11] This leads to a structure with partially filled orbitals which give rise to the metallic conductivity within both stacks due to the long range delocalisation of unpaired electrons. The conductivity in TTF-TCNQ is highly anisotropic, and is primarily along the stacking axis. This complex is, therefore, known as a one-dimensional organic conductor.

1.1.3 Modifications to the TTF Unit

Modification of the core TTF unit is usually concerned with interchanging the sulfur atoms for more polarisable Se and Te atoms. To this end tetraselenafulvalene (TSF) **3**[12] and tetratellurafulvalene (TTeF) **4**[13] were synthesised. In both cases the charge transfer complexes formed with TCNQ exhibited higher conductivity than TTF-TCNQ (700-800 S cm^{-1} for TSF-TCNQ; 2200 S cm^{-1} for TTeF-TCNQ) which was attributed to increased intra- and inter-stack interactions due to the more diffuse nature of the Se and Te atomic orbitals.

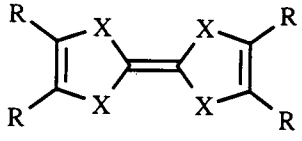

2 X=S R=H
3 X=Se R=H
4 X=Te R=H
5 X=S R=Me
6 X=Se R=Me

Extending the σ–bond framework by the addition of the electron releasing methyl groups provided tetramethyl-TTF (TMTTF) **5**[14] and tetramethyl-TSF (TMTSF) **6**.[15] The corresponding tellurium derivative has, to date, not been reported. A great deal of work has been performed on TMTSF **6** as it was the first donor to form salts which exhibited organic superconductivity.

1.1.3.1 TMTSF the First Organic Superconductor

Bechgaard *et al*[16] formed the first series of salts of TMTSF **6** with monovalent counterions: $(TMTSF)_2X$ ($X=PF_6^-$, AsF_6^-, TaF_6^-, NbF_6^-, SbF_6^-, ClO_4^-). The ClO_4^- salt was the first such salt to exhibit ambient pressure superconductivity with T_c=1.4K.

The X-ray structure of $(TMTSF)_2BrO_4^-$ salt can be seen in fig.1.3. As with TTF-TCNQ the donor unit is essentially planar and stacked in a ring-over-bond fashion with the anion occupying channels between the donors. There is considerable interstack interactions between the donor units due to selenium--selenium contacts which leads to a two dimensional complex in which the expected Peierls distortion, which occurs in TTF-TCNQ, was suppressed leading to a superconducting material.

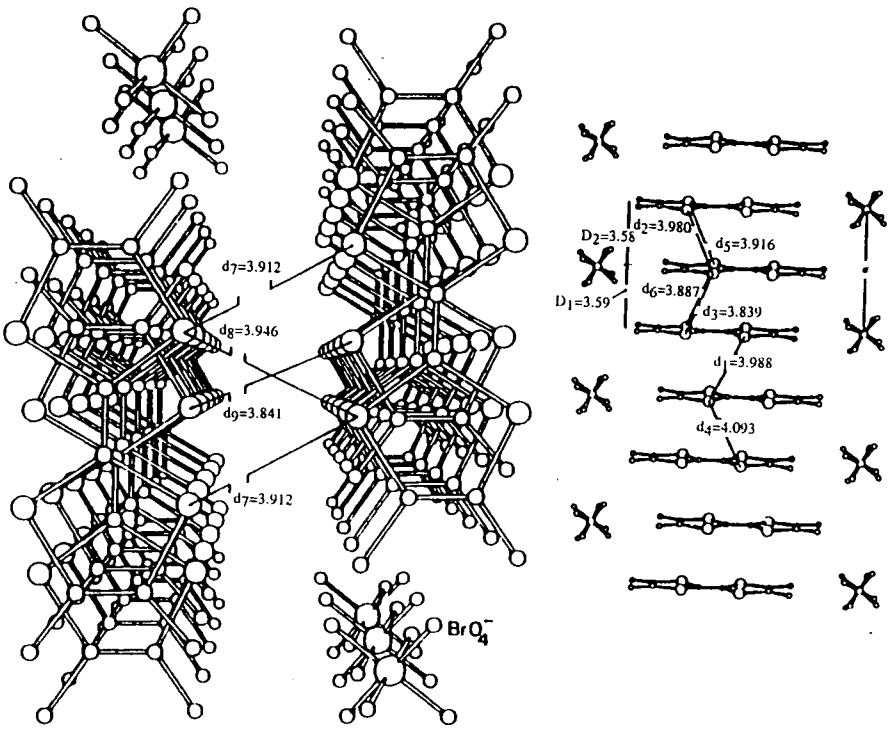

Fig 1.3 X-Ray Structure of $(TMTSF)_2BrO_4^-$

1.1.3.2 Increasing the Dimensionality of TTF Salts

The dimensionality of TTF can be improved by interconverting the core TTF sulfur atoms for selenium or tellurium (Section 1.1.3) or by the incorporation of more chalcogen atoms into the donor structure. In order to achieve this, bis(ethylenedithio)-TTF (BEDT-TTF or ET) **7** was synthesised.[17] It was also found that linear, inorganic, symmetrical, monovalent anions (I_3^-, IBr_2^-, AuI_2^-) afforded ambient pressure superconducting salts of ET. Currently, at least 40 superconducting salts of ET have been synthesised, with the three highest temperature superconductors of this class being salts of ET (T_c=10.4-12.8K).

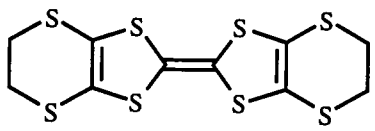

7

A noticable feature of these salts is the formation of kappa phase structures (orthogonal dimers of ET) rather than simple stacks: this leads to the formation of three-dimensional S--S interactions (fig.1.4)

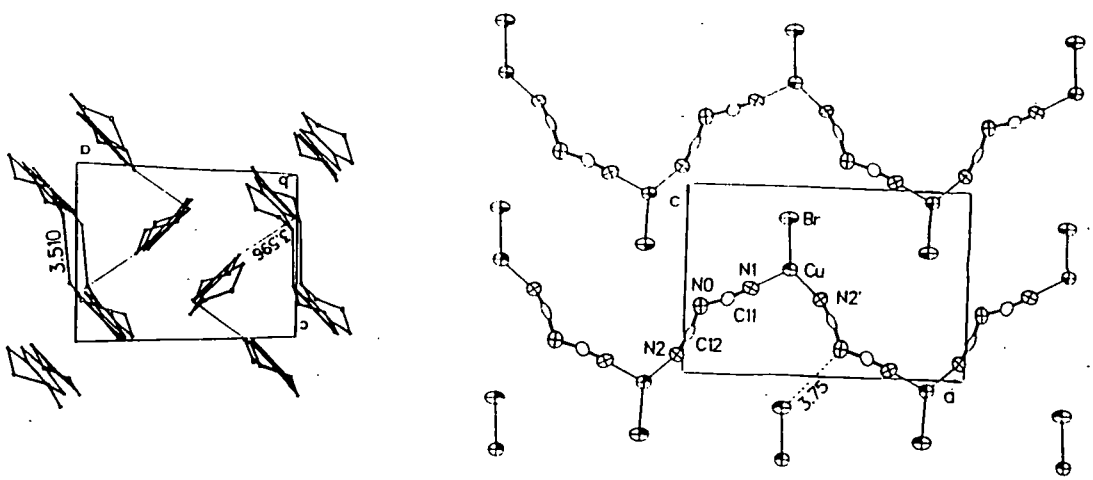

Fig.1.4 X-Ray Crystal Structure of κ-$(ET)_2Cu[N(CN)_2]Br$

1.1.4 The Addition of a Spacer Group Between 1,3-Dithiole Units

The inclusion of a conjugated spacer between the two 1,3-dithiole units in TTF **2** was expected to alleviate coulombic repulsion in oxidised states. In 1982 Yoshida *et al* prepared compounds **8**[18] and **9**[19]. The increased stability of the radical cation and dication, relative to TTF **2** was demonstrated in the CV data for these compounds which are shown in Table 1.1.

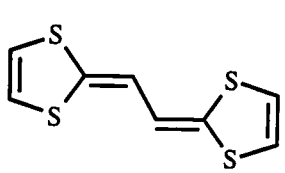

8

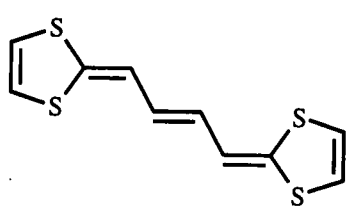

9

Compound	E_1/V	E_2/V	E_2-E_1/V
2	0.34 (1)	0.71 (1)	0.37
8	0.20 (1)	0.36 (1)	0.16
9	0.22 (2)	-	-
10	0.34 (2)	-	-

Table 1.2 CV Data for TTF 2 and Compounds 8-10 (Values in Parenthesis Indicate Number of Electrons Involved)

On passing from TTF to compound **8**, which contains one further π-bond spacer unit between the dithiole rings, both the first and second oxidation potentials were lowered. Indeed, for compound **9**, a single, two-electron oxidation wave was observed which indicates that the coulombic repulsion between the two 1,3-dithiolium cations was eradicated, with both dithioles acting as separate redox entities. Similarly, in compound **10**,[20] which possesses an anthracene spacer unit, the dication state is stabilised and a single two-electron oxidation was observed at 0.34V.

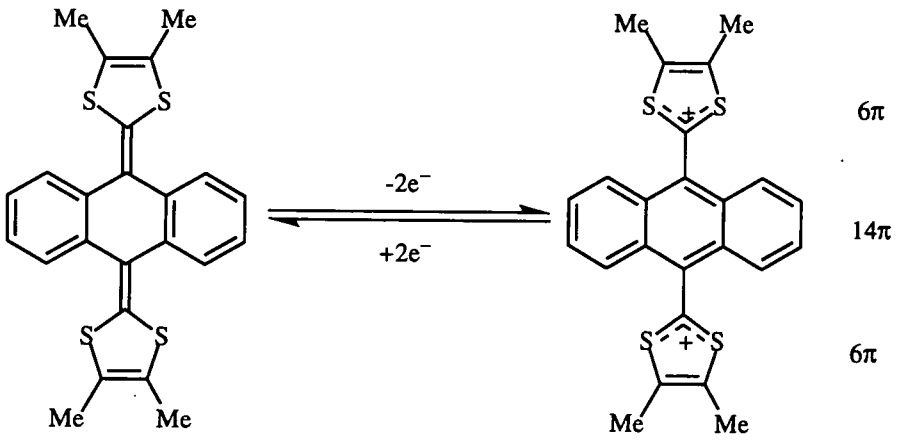

10 **10^{2+}**

In the neutral state molecule **10** is non-planar adopting a butterfly conformation (fig. 1.5a) which is attributed to disfavourable S-H peri interactions between the dithiole sulfurs and the anthracene unit. The 1:4 TCNQ salt, however, adopts a markedly different structure[21] to that of the neutral donor (fig. 1.5b). In the dication state the dithiole units of compound **10** are almost orthogonal to the now planar anthracene unit. Furthermore, both the 1,3-dithiolium cations and the anthracene spacer units are now aromatic (possessing 6 and 14π electrons, respectively) which further stabilises the dication state. This TCNQ salt was conducting and exhibited semi-metallic behaviour with σ_{RT}=60 S cm^{-1}, this value remaining constant down to 60K. The

structural aspects of **10** and 10^{2+} are relevant to new donor-anthracene-acceptor systems discussed in chapter 3.

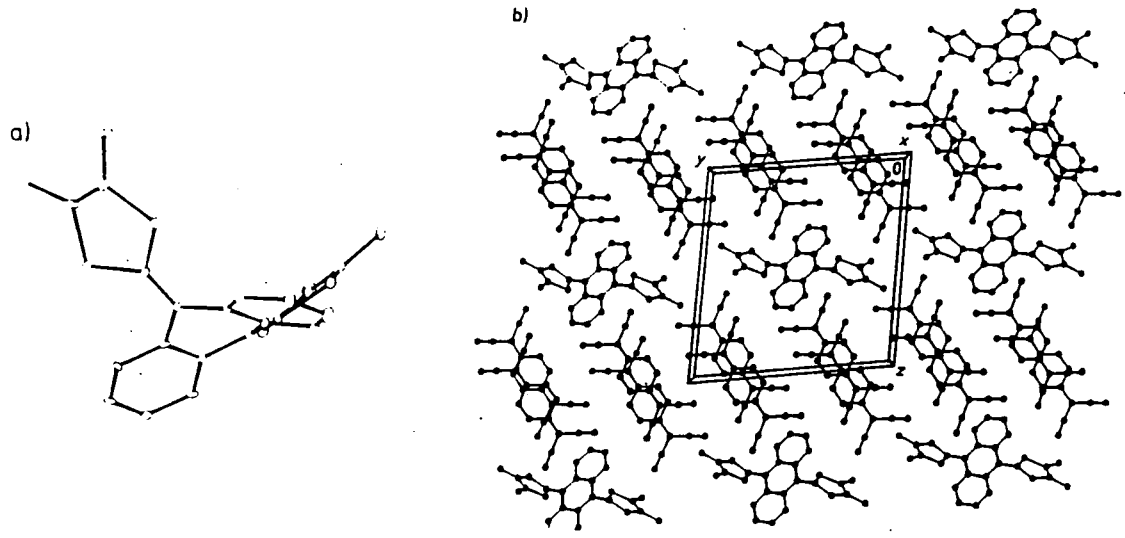

Fig.1.5 X-Ray Crystal Structure of a) The Neutral Donor 10 and b) the 1:4 TCNQ Salt $10^{2+}(TCNQ_4)^{2-}$

1.1.5 Modification of TCNQ

In contrast to the huge developments that have occurred within TTF chemistry, the modification of the TCNQ unit has received far less attention.

1.1.5.1 *N,N,'*-Dicyanoquinonediimine Acceptor Systems

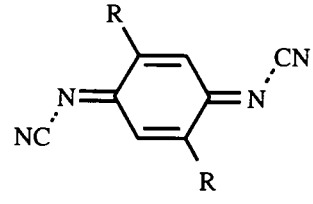

11 R=H
12 R=Me

In 1984 Hünig *et al* synthesised the new electron acceptor *N,N'*-dicyanoquinonediimine (DCNQI) **11** in which the sterically bulky dicyanomethylene groups of TCNQ were replaced by the less sterically demanding cyanoimine groups.[22] The charge transfer complex of **11** with TTF[23] exhibited a room temperature conductivity of 10 S cm^{-1} which, although lower than TTF-TCNQ the charge transfer

salts of **11** retained planarity which is an important prerequisite for organic conductivity.

The most important materials developed thus far from DCNQI are the radical anion salts of 2,5-disubstituted derivatives **12** of the general structure $[R_1, R_2\text{-DCNQI}]_2M$ (M= Li, Na, K, NH_4, Tl, Cu and Ag).[24] These materials possess high one-dimensional conductivity σ_{RT} = *ca.* 100-1000 S cm^{-1} with the exception of the copper salt which exhibits three-dimensional metallic behaviour. The conductivity was attributed to the packing of this material in the crystal lattice (fig.1.6). The copper ions are arranged like a string of pearls along the c-axis with the DCNQI units linked to the copper atoms in a nearly tetrahedral geometry which allows electrons to be transported along the c axis *via* the stacks of acceptors. The copper atoms which are too far apart to interact with each other can transfer electrons between stacks thereby assisting the metallic conductivity.

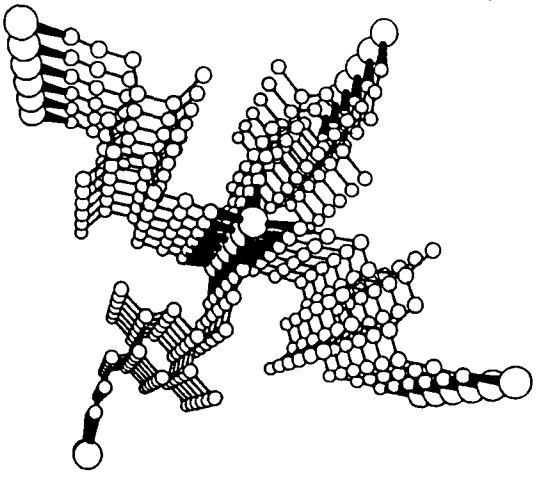

Fig.1.6 X-Ray Crystal Structure of $(Me_2DCNQI)_2Cu$

1.1.5.2 Donor-Acceptor Systems Based Upon Modified TCNQ

The admixture of an electron donor (D) and electron acceptor (A) often results in charge transfer complexes with uncontrollable stoichiometries. Becker *et al* [25] proposed that the linking of the donor to the acceptor by a sigma bond could induce regular stacking patterns in both the donor and the acceptor whilst attaining a known donor:acceptor ratio. The linking of two donor units to an acceptor *via* a flexible sigma link could induce the donors and acceptors to stack in a controllable way (fig.1.7) which is required to facilitate the formation of conducting complexes.

Fig.1.7 Proposed Aggregation of D-A-D Molecules

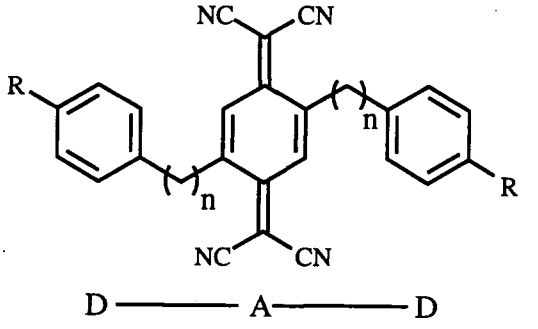

13 R=H n=1
14 R=H n=3

In 1988, 2,5-dibenzyl-7,7,8,8-tetracyano-*p*-quinodimethane (DBTCNQ) **13** was synthesised as a prototypical donor-σ-acceptor-σ-donor system.[26] However, the linking of the weakly donating phenyl group to the TCNQ acceptor unit *via* a sigma bond lead to no observable inter- or intra-molecular electron transfer in the UV-VIS spectra. A variety of electron releasing groups R was appended to the donor unit but again no charge transfer was observed which was mainly attributed to the stacking motif observed. The donor fragments were twisted almost perpendicularly to the acceptor preventing any regular stacking of the donor units (fig.1.8) due to steric interactions between the central TCNQ acceptor unit and the phenyl donor fragments. There are, however, isolated triplets of donor-acceptor-donor units formed by two different phenyl groups and a central TCNQ unit, and an infinite stack of acceptor units was observed within the isolated triplets of D-σ-A-σ-D units. The only previous examples of stacked TCNQ units was in charge transfer complexes in which the TCNQ unit was partially ionic (Section 1.1.2).

In an extension to this work, Martín *et al* recently presented similar systems with even longer sigma frameworks between the donor and the acceptor components[27] in an attempt to negate possible steric interactions with the central TCNQ unit. Compound **14** was synthesised containing a 3 carbon chain spacer between the donor and the acceptor; however, these systems exhibited a similar structural motif in the solid state with no observable acceptor interactions or electron transfer.

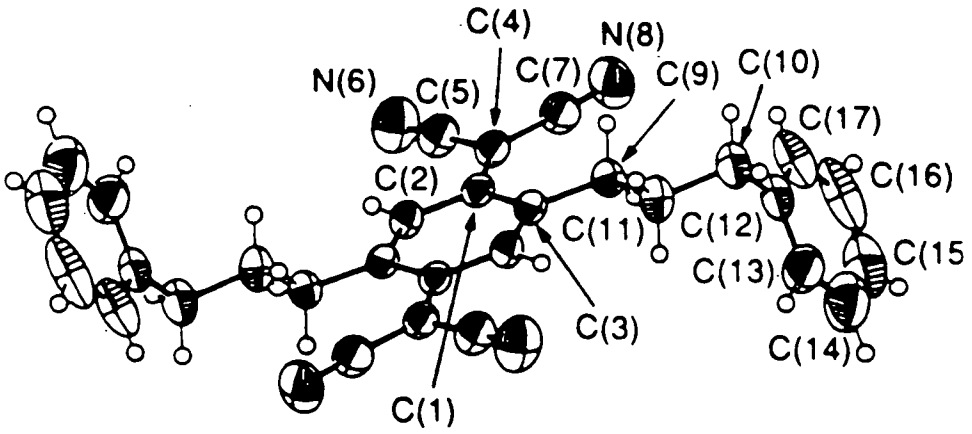

Fig.1.8 X-Ray Structure of Compound 14

To prevent the donor attaining an orthogonal alignment to the acceptor, compound **15** was proposed in which the donor fragment was tethered at two positions locking the molecule into a rigid conformation. However, in the attempted synthesis of **15** from **16** by Hanack *et al*,[28] the fully aromatised acceptor unit tetracyanopentacenequinodimethane (TCPQ) **17** was the only isolated product (Scheme 1.1).

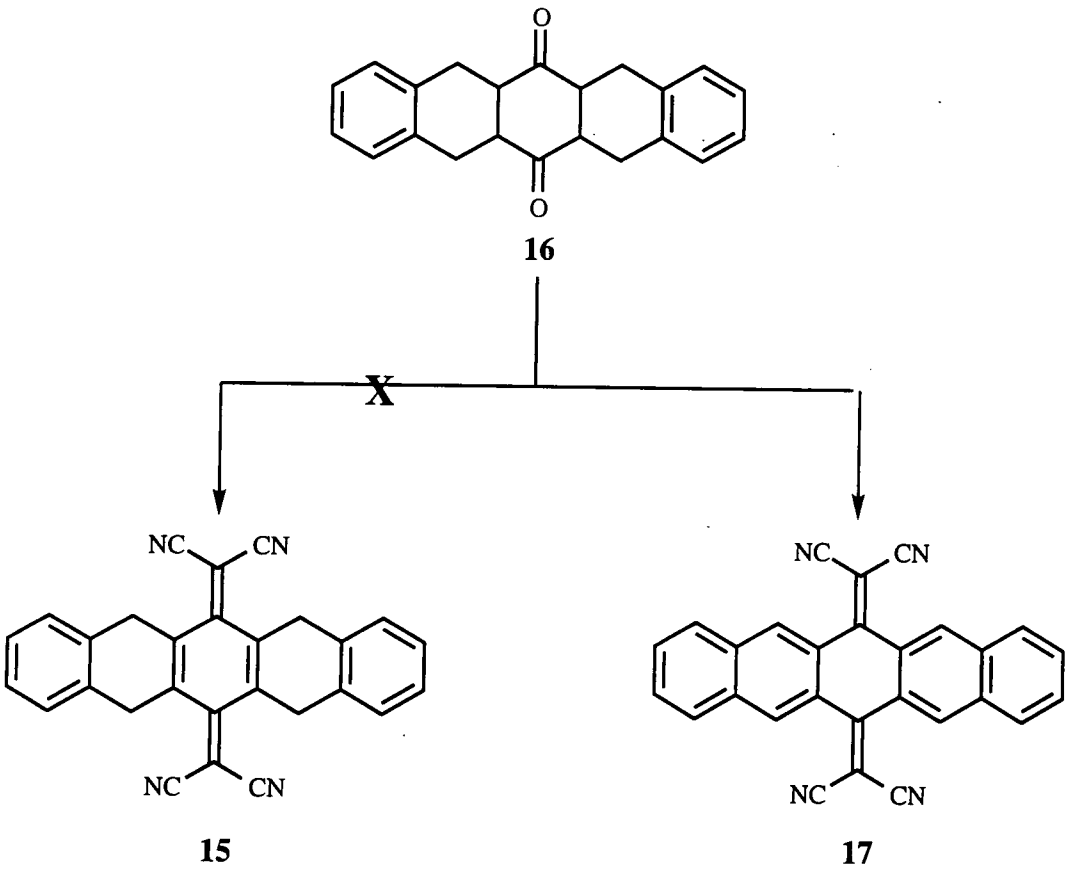

Scheme 1.1 Attempted Synthesis of Compound 15

As a refinement, heteroatom bridged system **18** was synthesised in which no aromatisation of the TCNQ units was anticipated. In compounds **18a,b**[29] intramolecular charge transfer was detected by the presence of a low energy absorption band in the UV-VIS spectra. This band was, predictably, shifted to even lower energy (bathochromically) when the aromatic donor was functionalised with electron donating methyl groups (Table 1.2). The nature of the charge transfer was attributed to the heterocyclic donor fragment within the sigma framework, with the weakly donating phenyl group having a nominal effect on the position of the charge transfer bands observed. This was surpported by data for compound **19** in which the dithiin unit was replaced by an oxathiin fragment. The improved p-π electron donation of the oxygen atom within the latter ring leads to bathochromically shifted charge transfer bands compared to compound **18**. Thus the nature of electron transfer was probably due to resonance structures **18'** and **19'** (Scheme 1.2) which was only slightly effected by functionalising the phenyl group with electron releasing methyl substituents.

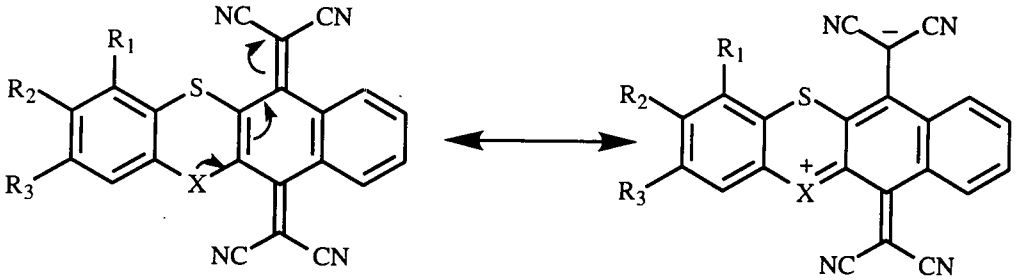

18 X=S
19 X=O

18' X=S
19' X=O

Scheme 1.2

Compound	X	R_1	R_2	R_3	λ_{max}/nm
18a	S	H	H	H	515
18b	S	H	Me	H	538
19a	O	H	H	H	594
19b	O	H	Me	H	606
19c	O	H	H	Me	603
19d	O	Me	H	Me	621

Table 1.2

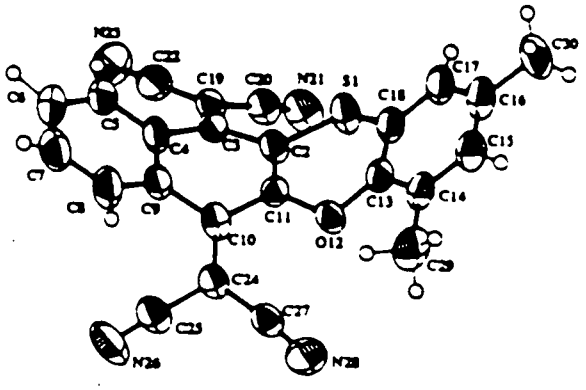

Fig.1.9 X-Ray Crystal Structure of 19 Demonstrating the Buckled Structure

The orthogonality inherent in compounds **13-14** was not observed for compound **19**, although its structure is still far from planar with the TCNQ unit and the oxathiine ring adopting a boat conformation (fig.1.9). The dicyanomethylene units were again buckled out of plane due to steric interactions, adopting a similar conformation to analogous acceptor systems[30] in which interaction between the dicyanomethylene group and the aromatic protons predominate.

1.1.5.3 Molecular Rectifiers Based on TTF and TCNQ

The linking of a more powerful electron donor to an electron acceptor *via* a sigma bond could lead to a material that has the potential to act as a molecular rectifier by allowing unidirectional electron flow, similar to a diode. Compound **20** was proposed by Aviram and Ratner as a model material which could perform such a task.[31]

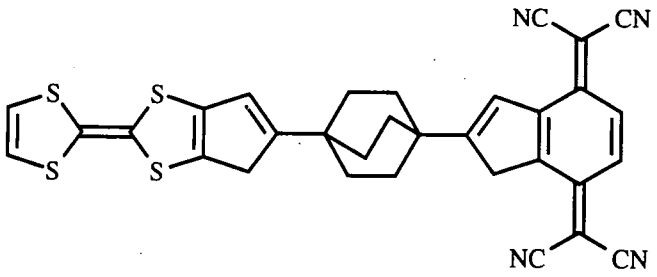

20

In order for D-σ-A systems to act as a molecular rectifier electrons from the cathode must transfer to the acceptor, forming the relatively stable A^-; subsequent electron flow to the donor through the sigma bridge and thence to the anode would complete the circuit with current flowing in this direction (fig.1.10) forming stable entities (*i.e.* D^+A^-). However, if the current was reversed the opposite scenario should not be possible (forming the unstable D^-A^+).

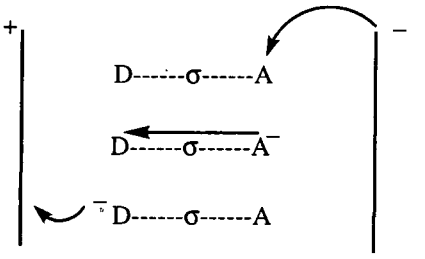

Fig 1.10 Theory of Molecular Rectification

Compound **20** has, to date, not been reported but analogous systems have recently been synthesised in which TTF is linked to TCNQ *via* ester **21-22** and carbamate **23** linkages as the sigma component in the original design.[32,33]

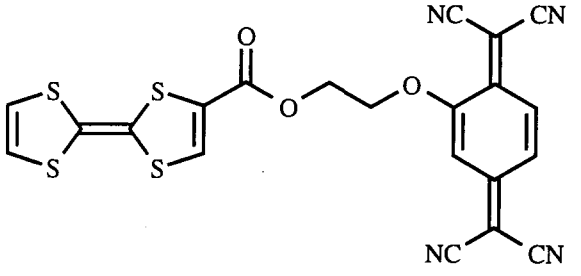

21

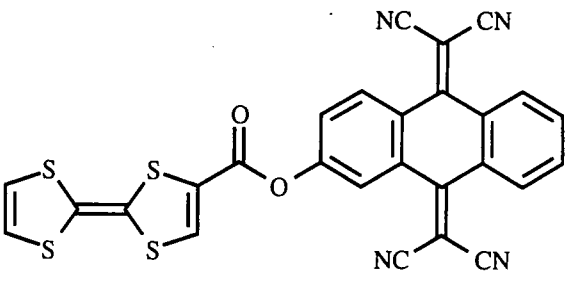

22

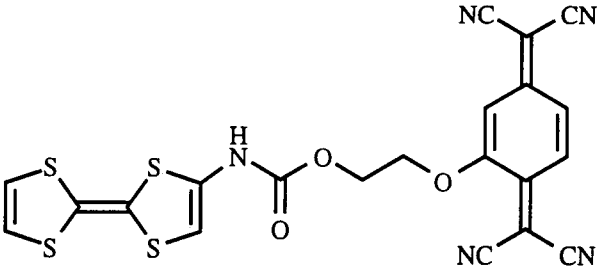

23

Noteworthy amongst the results obtained thus far is that compound **21**[34] (a black solid formed from TTF acid chloride and TCNQ alcohol) exhibits a nitrile stretching frequency in the IR spectrum at 2180 cm^{-1} (TCNQ-OH ν_{CN}=2210 cm^{-1}). Such nitrile shifts have been associated with the formation of the TCNQ radical anion.[35]

These preliminary results indicate that the synthesis of the target compound **20** could be an exciting breakthrough within the field of molecular rectification. Only one example of molecular rectification has been reported, which consists of an electron donating unit conjugatively linked to a modified TCNQ acceptor unit **24**.[36] This molecule, when aligned as a metal / organic multilayer / metal structure exhibits rectifier-like forward bias current dependency, which was attributed to the formation of zwitterionic intermediate **24'** (Scheme 1.3).[37]

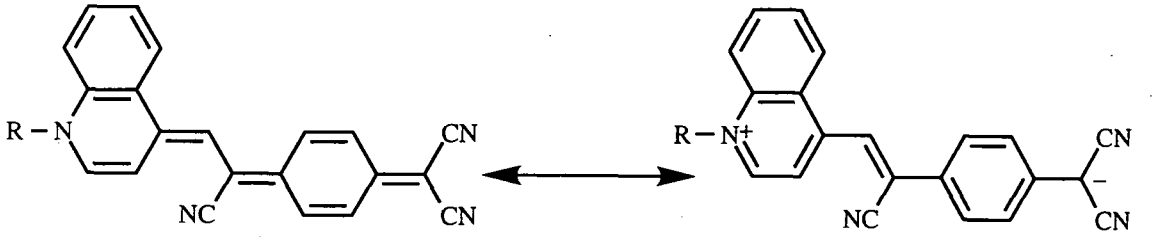

24 R=$C_{16}H_{33}$ **24'** R=$C_{16}H_{33}$

Scheme 1.3 The Zwitterionic state of compound 24

Systems such as **18-19** and **24** can also be considered as materials which exhibit intramolecular electron transfer from the donor to the acceptor which is manifested as a low energy absorption band in their UV-VIS spectra.

1.2 Intramolecular Donor-Acceptor Systems

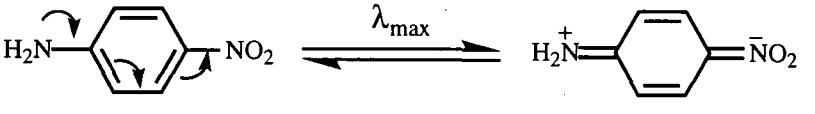

25a **25a'**

Scheme 1.4 Intramolecular Charge Transfer in *Para*-nitro aniline

The linking of an electron donor to an electron acceptor *via* a conjugated link leads to a system with the general formula D-π-A which is classically exemplified by the

model system *para*-nitroaniline **25a** which exhibits an absorption at λ_{max} or λ_{CT} =378 nm in the UV-VIS spectra. This is attributed to electron delocalisation with a contribution from the quinoidal zwitterionic structure **25a'** (Scheme 1.4).

The wavelength of this charge transfer band can be tuned by judicious choice of donor, acceptor and conjugated spacer units (Table 1.3). From these data the donor strength is seen to increase in the order:

$$Me<OMe<NH_2<N(Me)_2$$

Similarly, for a given donor unit, the nitro group is superior to the cyano group as an acceptor, as in all cases the charge transfer band for the nitro derivative was red-shifted compared to the cyano analogues (Table 1.3).

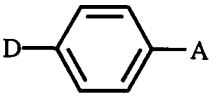

λ_{max}/nm

	Donor (D)			
Acceptor (A)	Me	OMe	NH_2	$N(Me)_2$
CN	232	247	269	297
NO_2	280	314	378	418

Table 1.3 λ_{max} Values for Donor-π-Acceptor Systems

1.2.1 Donor-π-Acceptor Systems as Materials for Non-linear Optics (NLO)

The presence of a donor and an acceptor in conjugation is also the major constituent of materials which produce large second order non-linear optical responses.

1.2.1.1 Theory of Non-linear Optics

Non-linear optics is primarily concerned with the interaction of electromagnetic fields with various media to produce new fields altered in phase, amplitude or frequency. The media through which this non-linear effect is observed may be an inorganic or organic material. The polarisation (P) induced in a molecule by an applied electric field (E) can be expressed by equation (**1**).

$$P=\alpha E+ \beta E^2 + \gamma E^3 + ... \quad (1)$$

If we assume, for simplicity, that the polarisation term is a scalar quantity, then the first coefficient of the electric field α was attributed to simple linear polarisation which is responsible for the refractive index of the material. Polarisation may be induced in a suitable material by interaction with an electric field, and in a non-linear medium this induced polarisation is itself non-linear. This is illustrated in fig.1.11 in which the first non-linear term β has the effect of doubling the frequency (or halving the wavelength) of the incident wave.

A medium exhibiting a non-linear response should be able to achieve asymmetric charge distribution and thus be polarised. It is, therefore, intuitive that donor-π-acceptor systems are ideal candidates for non-linear optical materials. This frequency doubling effect is called second harmonic generation (as the second harmonic of the frequency is generated) and the coefficient β (the molecular hyperpolarisability) dictates the efficiency of a medium to effect this phenomenon.

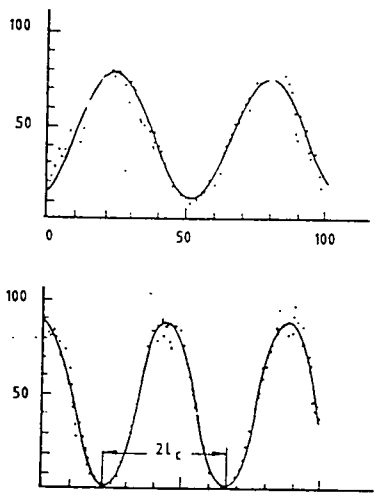

Fig.1.11 Non-linear Response to an Applied Field

1.2.1.2 Molecular Hyperpolarisability

Molecules which contain delocalised π electrons exhibit large values of β which are largest for materials which exhibit low energy charge transfer bands. If we, therefore consider the three isomers of nitroaniline **25a-c** there will be CT bands observed for the *ortho* and *para* isomers due to conjugation between the donor and the acceptor, but none will be observed for the *meta* isomer.

The contribution to β for these materials can be separated into two parts for isomeric nitroanilines (**2**).[38,39]

$$\beta=\beta_{add}+\beta_{CT} \qquad (2)$$

In which β_{add} is the vector sum of the values for the monosubstituted species and β_{CT} is the quantum mechanical calculated contribution to the overall value of β. It is evident from table 1.4 that the values for β_{CT} are responsible for the increase in the overall value of β for species in which charge transfer is possible. The values of β, β_{add} and β_{CT} for a variety of nitroanilines and the parent compounds are summarised in Table 1.4.

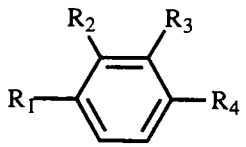

25a $R_1=NH_2$ $R_2=H$ $R_3=H$ $R_4=NO_2$
25b $R_1=H$ $R_2=NH_2$ $R_3=NO_2$ $R_4=H$
25c $R_1=NH_2$ $R_2=H$ $R_3=NO_2$ $R_4=H$

Compound	$\beta_{exp}/10^{-30}$esu	β_{add} (esu)	β_{CT} (esu)
25a	34.5	3.4	19.6
25b	10.2	1.7	10.9
25c	6.0	3.3	4.0
Nitrobenzene	2.2	-	-
Aniline	1.1	-	-

Table 1.4 Variation of β For a Variety of Nitroanilines

Some of the earliest measurements of β for simple functionalised aromatic systems with delocalised π electrons were performed on compounds such as **25a-c** by Levine [40] and Oudar.[41] This work, which can be considered to be in parallel with the experimental measurement of the values of λ_{max}, which leads to a quantitative model of the effect that differing donor groups have on the value of β. This is exemplified in Table 1.5, which if allied with the data in Table 1.3 indicates that an increased value of λ_{max} corresponds to a larger value of β.

λ_{max}/nm [$\beta/10^{-30}$esu]

Donor (D)				
Acceptor (A)	Me	OMe	NH_2	$N(Me)_2$
CN	232 [2.92]	274 [4.83]	269 [13.34]	297 [14.24]
NO_2	280 [9.12]	314 [17.35]	378 [47.67]	418 [52.75]

Table 1.5 Comparison of λ_{max} and β values

Systems which exhibit intramolecular electron transfer are of interest not only in tuning the position of the charge transfer bands, but also in the context of their second order hyperpolarisability value β. The following sections will be concerned with progress within these two fields, with the aim of modulating both the value of λ_{max} and β.

1.2.1.3 Variation of the Conjugated Spacer Group Between The Donor and The Acceptor Units

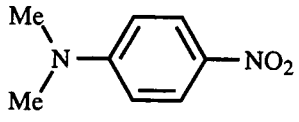

25a

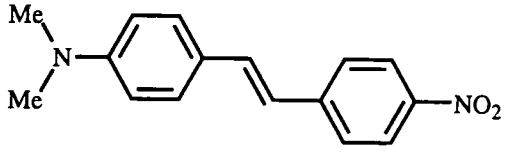

26

Compound	μ/D^a	$\beta/10^{-30}esu^b$	$\mu\beta/10^{-48}$esu
25a	7.53	52.75	392
26	-	-	580

[a] $1D=10^{-18}$ esu

[b] Measured at 1907 nm

Table 1.6 UV-VIS and NLO Data for Compounds 25a and 26

The effect of the length of the conjugated spacer between donor (dialkylamino) and acceptor (nitro) units has been extensively studied by Oudar:[41] increasing the conjugated length from that of *para*-nitroaniline **25a** to the corresponding stilbene

derivative **26** considerably increases the value of μβ (the product of the dipole moment μ and β) (Table 1.6).

It has been demonstrated that there is a quadratic dependence of β with increasing chain length within these systems.[42] Similarly, the nature of the spacer unit also has a marked effect on both the position of the charge transfer band and the overall values of β.

1.2.1.3.1 Aromatic *vs.* Aliphatic Spacer Groups

The effect that an aromatic or aliphatic spacer group has on charge transfer properties is exemplified for compounds **26** and **27**. The former is linked to the nitro acceptor by 5π bonds compared to the latter which is linked by only 4π bonds: the value of β for **27**, however, is 50% greater than for **26**. This is attributed to the destabilising effect of the aromatic spacer unit upon charge transfer, in which the spacer unit becomes quinoidal losing aromatic stabilisation energy.

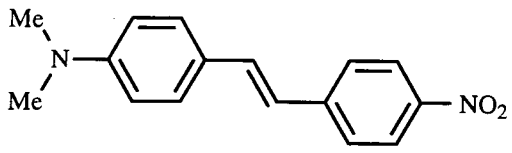

26

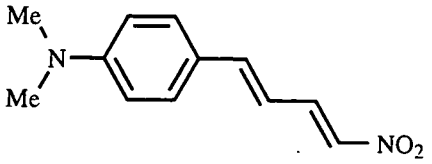

27

In order to limit this destabilising effect, Jen *et al* replaced the benzene spacer units by thiophene, which having a lower delocalisation energy than benzene, lead to an increase in the values of both λ_{max} and μβ.[43] Thus, commencing with stilbene derivative **28** replacement of one of the benzene rings with thiophene (compound **29**) leads to an increase in both λ_{max} and μβ. Incorporating a second thiophene unit (compound **30**) produced a further increase, with the value of μβ double that for compound **28** as can be observed in Table 1.7.

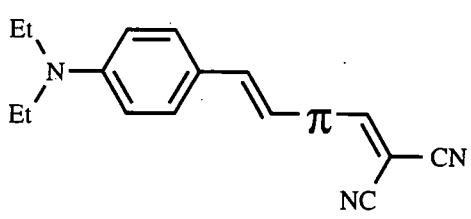

28 π=benzene
29 π=thiophene

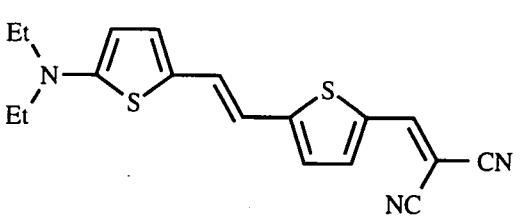

30

Compound	λ_{max}/nm[a]	$\mu\beta/10^{-48}$esu[b]
28	468	1100
29	513	1300
30	584	2600

[a] all spectra measured in dioxane solution

[b] measured at 1907 nm

Table 1.7 UV-VIS and NLO Data for Compounds 28-30

In conclusion, increasing the length of the conjugated spacer between the donor and the acceptor produces materials which exhibit increased bathochromic shifts in the position of the charge transfer bands. The use of an alkenic spacer produces improved results over aromatic spacer units due to the loss of aromaticity which occurs in the latter upon charge transfer. This destabilising effect may be limited by employing thienyl spacer units. There is, however, a point at which the values of λ_{max} and β no longer increase as the conjugated spacer unit becomes larger, beyond this point (termed the "saturation" point) the position of the charge transfer absorption is shifted hypsochromically (to high energy).[44]

1.2.2 Variation of The Acceptor Unit

The majority of the work discussed thus far has dealt with simple aromatic acceptor units substituted with nitro and cyano groups. The most important criterion for a good electron acceptor unit is the ability to accommodate and stabilise a negative charge. If the nitro acceptor was exchanged for one which was better able to delocalise the negative charge then the values of both λ_{max} and β should increase.

Ullman *et al* discovered that the methyl sulfonyl group was a promising electron acceptor unit,[45] and a variety of donor-π-acceptor systems were synthesised containing the dialkylamino donor linked to this new acceptor *via* alkenic and azo spacer units; the values of λ_{max} for the different spacer units are summarised in Table 1.8.

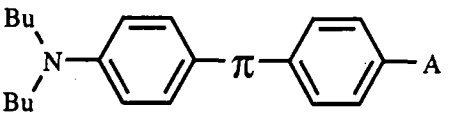

A	π	λ_{max}/nm[a]	$\varepsilon/10^4 M^{-1}cm^{-1}$
NO_2	N=N	500	4.37
NO_2	CH=CH	453	2.91
$MeSO_2$	N=N	464	4.08
$MeSO_2$	CH=CH	390	2.33

[a] All spectra recorded in dichloromethane solution

Table 1.8 UV-VIS Data for Compound 31

From this work it is noteworthy that not only is the methyl sulfonyl group a poorer acceptor than the corresponding nitro group, but the use of an azo derived spacer lead to bathochromically shifted charge transfer bands compared to the simple alkenic spacer. The values of β were similarly reduced compared to the nitro acceptor units. This blue shift is encouraging as frequency doubling often produces light within the visible region (from an infra red-laser) and, thus, it is important that the NLO material is transparent within this spectral range. The wavelength at which absorption due to charge transfer is complete is also important and is known as the cut off point, designated λ_{cutoff}. This leads to a trade off between increasing the extent of charge transfer to increase the values of β, whilst attempting to produce materials which do not interfere with the frequency doubling process by self absorption.

Ogura and co-workers introduced the sulfonyl-vinyl acceptor group with the intention of producing materials with low values of λ_{cutoff} whilst still maintaining NLO activity.[46] In this work the little used methoxy-furanyl and thienyl units were utilised due to their weaker donor abilities, compared to the dimethyl-amino group, producing a variety of donor-π-acceptor systems of the general structures **32** and **33** (Table 1.9).

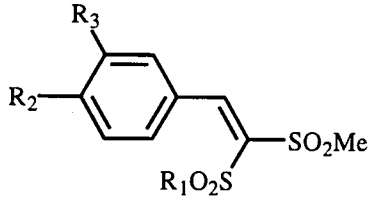

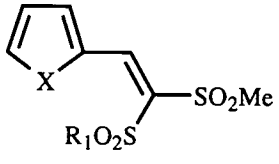

32a R_1=Me R_2=H R_3=H
32b R_1=*p*-Tol R_2=OMe R_3=H
32c R_1=*p*-Tol R_2=OMe R_3=OMe
32d R_1=Me R_2=OMe R_3=H

33a R_1=*p*-Tol X=O
33b R_1=Me X=O
33c R_1=*p*-Tol X=S
33d R_1=Me X=S

Compound	λ_{max}/nm[a]	λ_{cutoff}/nm	$\beta/10^{-30}$esu[b]
32a	282	322	4.7
32b	330	-	8.3
32c	352	-	10.6
32d	325	377	6.4
33a	329	388	5.2
33b	322	380	5.1
33c	333	-	4.5
33d	327	338	4.0

[a] All spectra measured in ethanol solution

[b] Measured at 1064 nm

Table 1.9 UV-VIS and NLO Data for Compounds 32 and 33

As expected, the methoxy substituents **32b-d** led to increased value of β compared to the unsubstituted systems **32a**. The charge transfer bands were all at relatively high energy, indicating that the conjugated linking of a weak donor unit to the sulfonyl vinyl group leads to poor intramolecular donor-π-acceptor characteristics with moderate values of β.

1.2.2.1 Materials Which Exhibit Low Values of λ_{max}

An interesting method for modulating the values of λ_{max} was recently reported by Grahn *et al.*[47] They set out to provide materials with relatively large non-linear optical responses without linking the donor to the acceptor *via* a conjugated pathway thereby producing materials with low values of λ_{max}. The linking of a donor and an acceptor to the 1,8-positions of naphthalene provides a cross conjugated system (Scheme 1.5) where the donor and the acceptor cannot interact intramolecularly but interact in an intermolecular fashion in a manner similar to TTF-TCNQ (Section 1.1). The donor (D) and the acceptor (A) were systematically modified producing values of β greater than for *p*-nitroaniline **25a** whilst considerably lowering the values of both λ_{max} and λ_{cutoff}. Some comparative examples, containing the relatively weakly donating methoxy substituent, are collected in Table 1.10 along with similar data for *para*-nitroaniline **25a**.

Some interaction between the donor and acceptor units in compounds **33a,b** was indicated by a significant high field shift in the ^1H NMR spectra of the donor and acceptor regions which was attributed to electronic interactions. Similarly the X-ray structure of compound **34** shows that both the phenyl rings are substantially twisted, leading to a face-to-face orientation (fig.1.12).

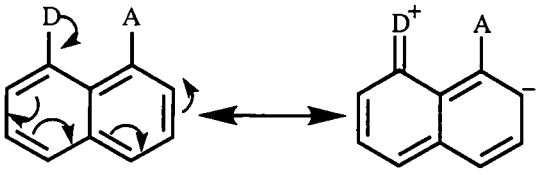

33a D=OMe A=CF_3
33b D=OMe A=CN
34 D=OMe A=NO_2

Scheme 1.5 The Linking of a Donor to an Acceptor via a Non-conjugated Pathway

Compound	A	D	λ_{max}/nm[a]	λ_{cutoff}/nm	$\beta/10^{-30}$esu[b]
33a	CF_3	OMe	320	360	35
33b	CN	OMe	298	375	26
34	NO_2	OMe	308	428	32
25a	-	-	350	428	17

[a] All measurements performed in chloroform solution

[b] measured at 1064 nm

Table 1.10 UV-VIS and NLO Data for Compounds 25a, 33-34

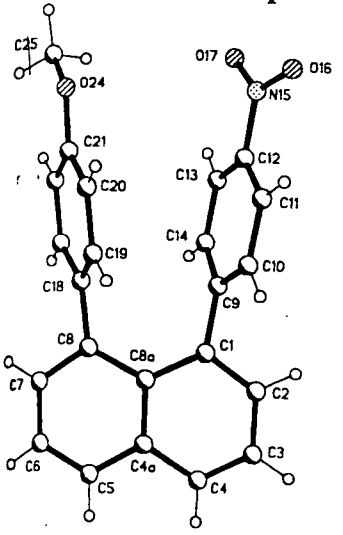

Fig 1.12 X-Ray Crystal Structure of Compound 34

The use of the more elaborate rhodanine acceptor unit to confer large values of both λ_{max} and β was first realised by Ikeda who studied the NLO response of rhodanine-methine derivative **36**.[48] Later studies by Rao *et al* elegantly demonstrated that the rhodanine unit was an excellent electron acceptor, as exemplified by the λ_{max} and $\mu\beta$ values for compounds **35-37** (Table 1.11) with data for compound **25a** added for comparison.[49]

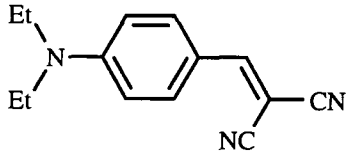

35

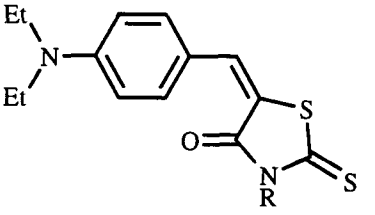

36 R=H
37 R=Et

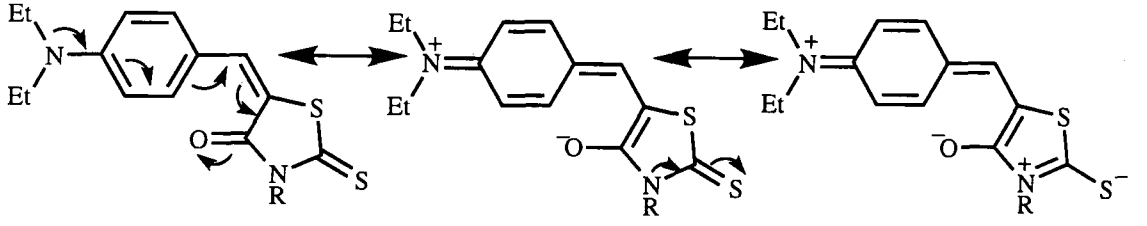

Scheme 1.6 Modes of Charge Transfer in Rhodanine Derived Donor-π-Acceptor Systems

Compound	λ_{max}/nm[a]	$\mu\beta/10^{-48}$esu[b]
25a	370	110
35	419	300
36	452	300
37	465	420

[a] all spectra measured in dioxane solution
[b] measured at 1907 nm

Table 1.11

Compounds **35-37** differ only in the nature of the electron acceptor; however, the position of the charge transfer band and the values of $\mu\beta$ were significantly enhanced for the rhodanine derivatives. The attachment of electron releasing substituents to the heterocyclic nitrogen atom had a positive effect on the values of $\mu\beta$ which may be

attributed to the partial gain in aromaticity due to electron transfer from the heterocyclic nitrogen to the thione (Scheme 1.6).

1.2.3 Cyanovinyl Acceptor Units

In 1987 Katz *et al* utilised the dicyanomethylene and tricyanomethylene units as electron acceptors linked to the dimethylamino donor unit producing compounds **38** and **39**.[50] Both materials exhibited an increase in the value of β over the parent compound **25a** (Table 1.12).

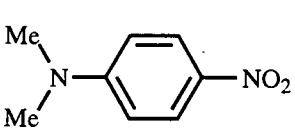

25a

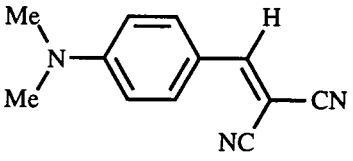

38

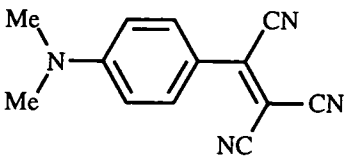

39

Compound	$\beta_0/10^{-30}$esu[a]	$\mu\beta_0/10^{-48}$esu
25a	12	85.2
38	16	139.3
39	26	283.4

[a] measured at 1300 nm

Table 1.12

This increase in the value of β_0 was attributed to the stabilising effects that the two nitrile units exert on the adjacent anion, with the tricyanovinyl group acting as a stronger acceptor. This was elegantly demonstrated by a plot of the Hammet parameter for the three acceptor groups, which exhibited excellent correlation compared to the observed value of β (fig 1.13).

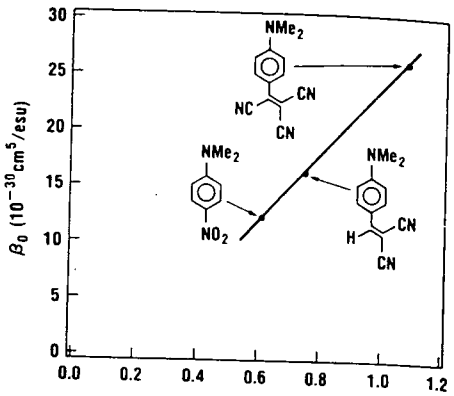

Fig.1.13 Plot of β_0 *vs.* σ_r^- for compounds 25 and 38-39

During the course of this work Katz also pioneered the use of the 1,3-dithiole-2-ylidene donor unit. The remainder of this chapter will be devoted to the use of the 1,3-dithiole donor fragment as a π electron donor.

1.3 The Use of the 1,3-dithiole-2-ylidene Unit as a π Electron Donor

The exchange of the dimethylamino donor unit in compounds **25a** and **39** for a 1,3-dithiole group yielded **40** and **41** which exhibited markedly increased values of $\mu\beta_0$ (Table 1.13).[50] This increase was far greater than would be expected if considering the simple Hammet coefficients and was attributed to an excited state property.

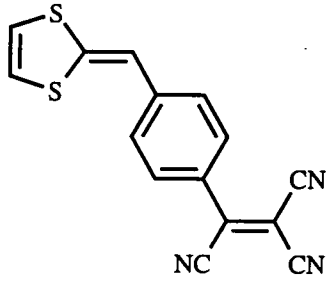

40

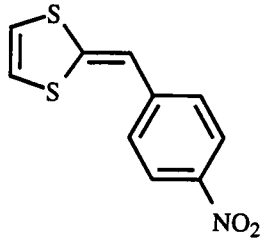

41

Compound	$\beta/10^{-30}$esu[a]	$\mu\beta/10^{-48}$esu	$\mu\beta_0/10^{-48}$esu
25a	21	149.1	85.2
39	78	850	283.4
40	-	1200	-
41	52	358	172.5

[a] measured at 1300 nm

Table 1.13 The Effect of The Donor on NLO Properties

The cation located on the dithiole in compound **40'** leads to an aromatic dithiolium cation which could stabilise the zwitterionic species leading to increased values of β and hence increased values of λ_{max} (Scheme 1.7).

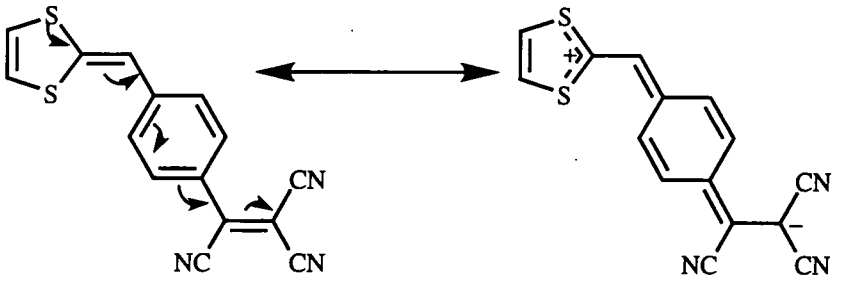

40 40'

Scheme 1.7 The Formation of an Aromatic Dithiolium Cation upon Intramolecular Charge Transfer

The earliest reports of a dithiole derived donor-π-acceptor system was by Gompper and Kutter[51] and Mayer and Gebhardt[52] in the mid 1960's in which they, independently, linked the 1,3-dithiole donor unit *via* a single π bond to the powerful dicyanomethylene acceptor unit yielding compound **42**. Unfortunately, neither paper reported the UV-VIS spectra of this compound.

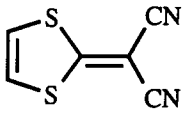

42

1.3.1 The Ketene Dithioacetal as a π-Electron Donor

In order to gain further insight into the stabilising effects of the 1,3-dithiole donor units Rao investigated the ketene dithioacetal unit which contains a similar donor motif to the 1,3-dithiole.[53] A variety of donor-π-acceptor systems **43-44** containing both donor units were synthesised: their λ_{max}, $\mu\beta$ and $\mu\beta_0$ values are summarised in Table 1.14.

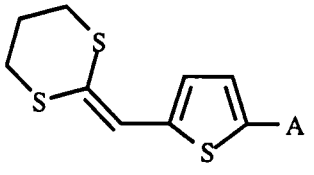

43a A=NO_2
43b A=$C(CN)C(CN)_2$

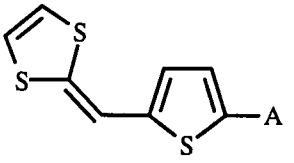

44a A=NO_2
44b A=$C(CN)C(CN)_2$

Compound	λ_{max}/nm[a]	$\mu\beta/10^{-48}$esu[b]	$\mu\beta_0/10^{-48}$esu[b]
43a	493	350	292
43b	438	200	150
44a	625	1600	815
44b	558	940	565

[a] All spectra measured in dioxane solution

[b] Measured at 1907 nm

Table 1.14 UV-VIS and NLO Data for Compounds 43-44

It is noticeable from Table 1.14 that the 1,3-dithiole derivatives possess increased values of both λ_{max} and $\mu\beta_0$. This may be attributed to the fact that the 1,3-dithiole unit attains aromaticity upon charge transfer (Scheme 1.8) whereas the ketene dithioacetal unit does not.

1.3.2 1,3-Dithiole Derived Donor-π-Acceptor Systems from TTF

An interesting dithiole derived donor-π-acceptor system has recently been synthesised by Hopf *et al* during attempts to form an intermolecular charge transfer complex of cyano(ethynyl)-ethane **45** with TTF **2**.[54] Instead of isolating a charge transfer complex compound **46** was formed *via* a 2+2 π cycloaddition reaction (Scheme 1.9).

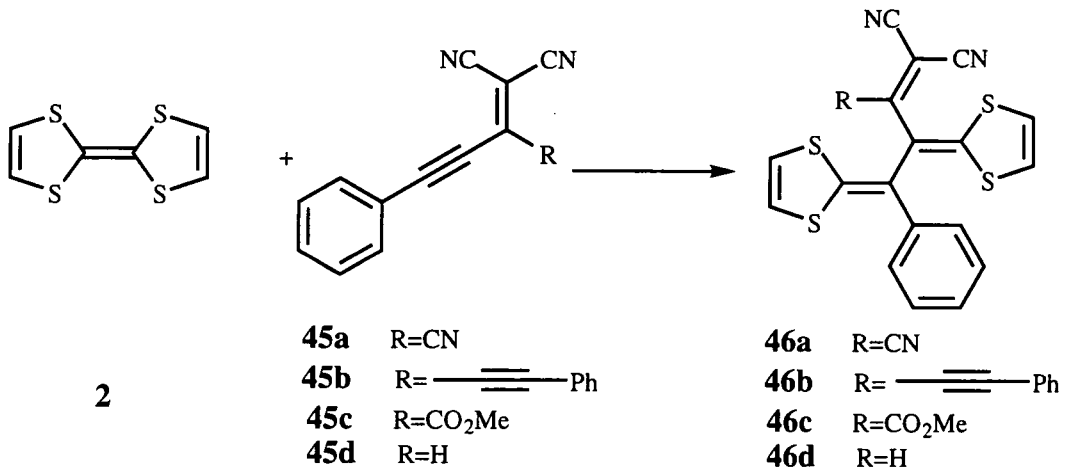

2

45a R=CN
45b R= —≡— Ph
45c R=CO_2Me
45d R=H

46a R=CN
46b R= —≡— Ph
46c R=CO_2Me
46d R=H

Scheme 1.9 Synthesis of Compounds 46a-d

In the crystal structure of compound **46a** the tricyanovinyl acceptor group and one of the 1,3-dithiole units were coplanar. This coplanarity between donor and acceptor led to an intramolecular charge transfer absorption at λ_{max}= 511 nm.

We noted that at the outset of the present work the use of the 1,3-dithiole group as a π electron donor did not address the possibility of utilising functionalised dithiole derivatives to modify or enhance the donor abilities.

1.3.3 Benzodithiole Derived Donor-π-Acceptor Systems

Lehn *et al* were the first to study functionalised 1,3-dithioles donor units in a systematic manner. In this seminal work they utilised the benzodithiole donor unit to synthesise a wide variety of donor-π-acceptor systems in which the acceptor and the conjugated spacer unit were systematically modified.[55] The benzodithiole Wittig **47** and Wittig-Horner reagents **48** were condensed with several dialdehydes to yield **49a**-**52a**. The terminal aldehyde was then converted into the dicyanomethylene **b**, pyridine **c**, *N*-methylpyridinium **d**, *p*-cyanophenyl **e**, and *p*-nitrophenyl **f** derivatives (Scheme 1.10).

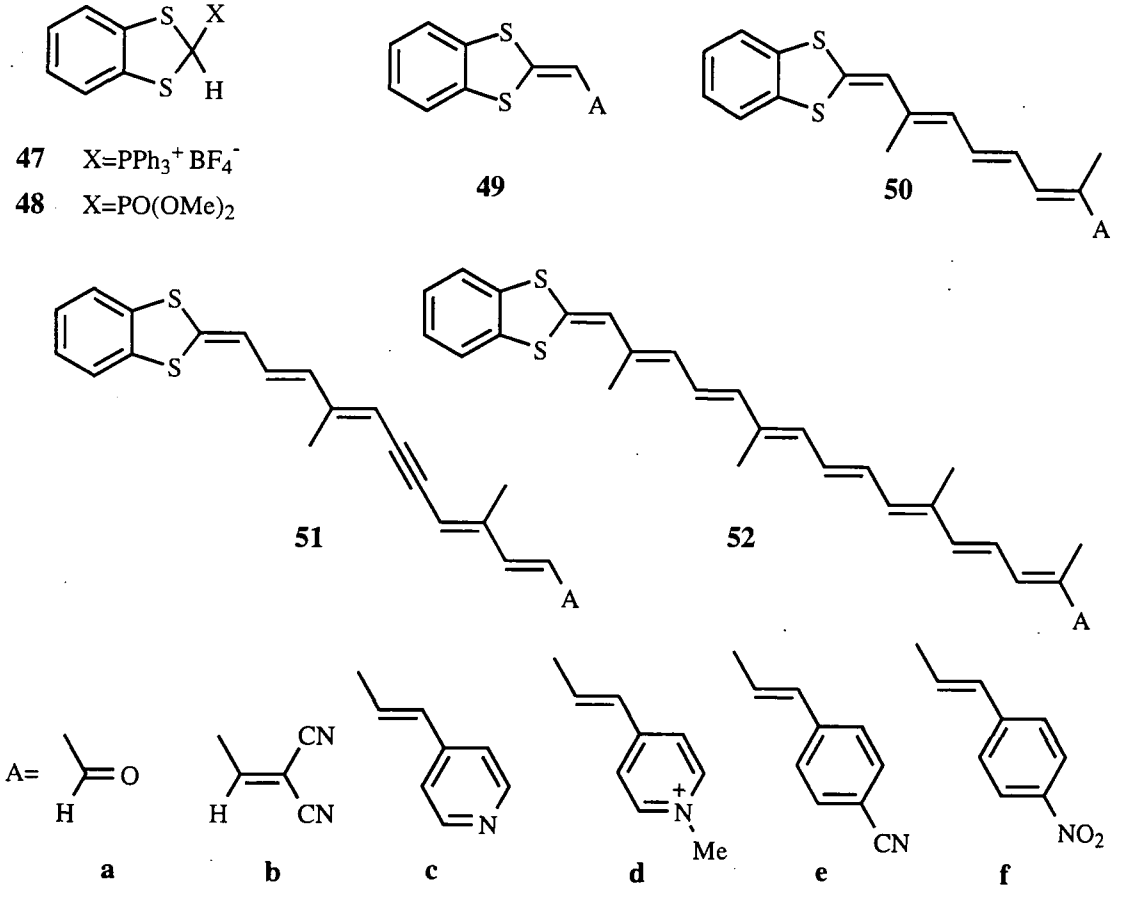

Scheme 1.10 1,3-Dithiole Donor-Acceptor Systems

Compounds **49-52** exhibited broad and intense absorption bands within the visible region of the UV-VIS spectra (Table 1.15) which was attributed to internal charge transfer from the donor to the acceptor. As the length of the alkenic spacer was increased the charge transfer band was shifted to lower energy. The replacement of one double bond for a triple bond produced a hypsochromic shift in the charge transfer band which was attributed to a disruption in the electronic motion due to the presence of the sp hybridised carbons. The position of the charge transfer band depended on the polarity of the solvent (solvatochromism) which is often indicative of NLO activity.

This work also indicated the relative strength of the acceptor units employed. It is evident from Table 1.15 that the acceptor strength varies from aldehyde (weakest) to methylpyridinium (strongest) *via* the *para*-cyano, *para*-nitro, pyridine and dicyanomethylene acceptors, respectively. The large value of λ_{max} for the methylpyridinium acceptor may be attributed not only to its obvious acceptor ability, but also to the fact that the UV-VIS spectra was performed in DMSO solution which is a highly polar solvent causing an increased red shift due to solvatochromism. Allied to the presence of this charge transfer band, compounds **49-52** were also highly NLO active. These materials were used as a basis for an in-depth study of the nature of the donor, conjugated spacer and acceptor unit upon the values of λ_{max} and β.[56]

	λ_{max}/nm[a]			
	49	**50**	**51**	**52**
a	372	456	466	500
b	446	562	540	588
c	394	457	452	505
d[b]	476	534	493	540
e	410	465	457	-
f	452	488	467	-

[a] in chloroform solution

[b] in DMSO solution

Table 1.15 UV-VIS Data for Compounds 49-52

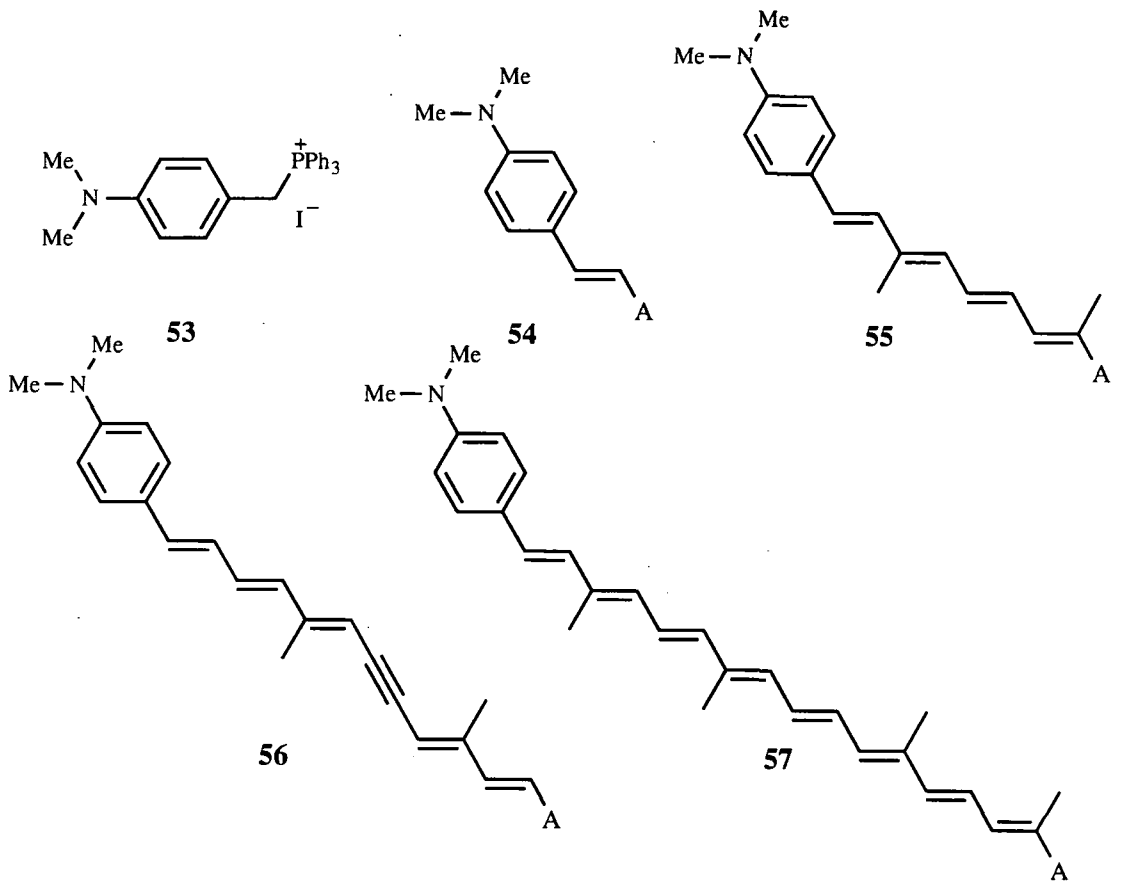

Scheme 1.11 Dimethylamino Donor-Acceptor Systems

Exchanging the 1,3-dithiole unit for *N,N*-dimethylaniline, using Wittig reagent **53** lead to analogous materials **54-57** (Scheme 1.11). A comparison of their UV-VIS spectra and $\mu\beta_0$ values are collected in Table 1.16.

Compound	λ_{max}[a]/nm	$\mu\beta/10^{-48}$esu[b]	$\mu\beta_0/10^{-48}$esu[b]
54a	384	320	200
55a	450	2000	1000
56a	461	4200	2000
57a	498	8900	3400
49a	372	30	20
50a	456	1200	570
51a	466	2200	1000
52a	500	7250	2800

[a] All spectra recorded in chloroform solution

[b] Determined at 1340 nm

Table 1.16 UV-VIS and NLO Data for Compounds 49-52 and 54-57

For these series of molecules it is evident that the dimethylamino derived donor-π-acceptor systems exhibit lower values of λ_{max} whilst similarly producing larger values of $\mu\beta_0$. The increase in the values of $\mu\beta_0$ with increasing conjugated length has previously been shown to exhibit a quadratic dependence on conjugated length. Within these series, a plot of log $\mu\beta_0$ and λ_{max} *vs.* the length of the conjugated spacer exhibited a dependence on $\mu\beta_0$ for compounds **49-52** proportional to $n^{2.4}$ whereas for compounds **54-57** the dependence was quadratic as expected, with no indication of saturation with increasing values of n. The values of λ_{max} show a marked tendency to level off with increasing values of n, leading to a saturation point being achieved. It is, therefore, evident that for this series of molecules the dimethylamino unit is superior as a donor to the benzodithiole donor in both values of both $\mu\beta_0$ and λ_{max}; however, this discrepancy appears to decrease as the conjugated length increases.

1.3.3 Benzodithiole Donor-π-Acceptor Systems as Molecular Devices

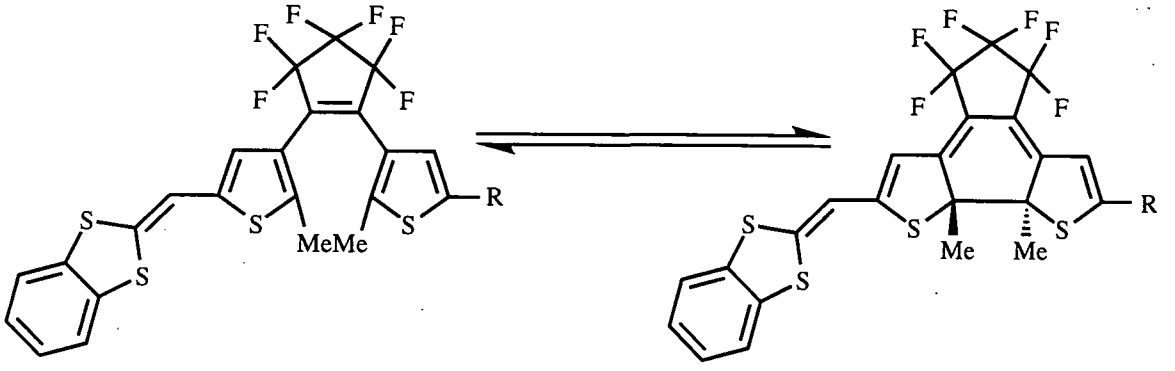

58 R=CHO
59 R=CHC(CN)$_2$

58' R=CHO
59' R=CHC(CN)$_2$

Scheme 1.12 Photocyclisation of 58 and 59 into 58' and 59'

The benzodithiole donor unit has been utilised as part of photochemically switchable materials **58** and **59**. When irradiated with UV light at 365 nm a marked colour change was observed along with a concomitant change in the ^{1}H NMR and UV-VIS spectra.[57]

The colour change was attributed to photocyclisation to **58'** and **59'** (Scheme 1.12) in which the benzodithiole donor is now linked to the acceptor by a conjugated pathway producing a charge transfer band within the visible region. This cyclisation was conveniently monitored by a marked up-field shift in the ^{1}H NMR spectrum for the thiophene proton and a smaller downfield shift for the thiophene methyl group. The extent of cyclisation was generally >98% after irradiation for 15 min.

Compound	λ_{max}/nm[a]	$\Delta\lambda_{max}$	$\mu\beta/10^{-48}$esu[b]
58	350	362	260
58'	713	-	1100
59	350	352	-
59'	702	-	-

[a] All spectra recorded in C_6D_6

[b] Measured at 1064 nm

Table 1.17 UV-VIS and NLO Data For Compounds 58-59

Cyclisation resulted in a bathochromic shift in the values of λ_{max} into the red or even near infra red regions which is indicated in Table 1.17. The fact that the conversion from open to closed state is so high allows an efficient "on/off" type switching function to be observed. More importantly, the closed isomer may be reconverted in 100% yield into the open isomer by irradiating at 600 nm.

The closed isomer predictably exhibited both solvatochromism and increased values of $\mu\beta$ compared to the open isomer for which conjugation between the donor and the acceptor is prohibited.

Chapter 2

1,3-Dithiole Derived Donor-π-Acceptor Systems

2.1 1,3-Dithiole Derived Donor-π-Acceptor Systems

Prior to the outset of this work the use of the 1,3-dithiole-2-ylidene donor fragment within the context of donor-π-acceptor systems has received only sporadic attention. This was surprising as the 1,3-dithiole heterocycle has a major advantage as a π-electron donor over simple aromatic donor units in that upon electron transfer from the donor to the acceptor the dithiolium cation attains 6π aromaticity which should stabilise the zwitterionic state, **50b'**. In contrast, the simple functionalised aromatic donor **38** units loses aromaticity in structure **38'** which is correspondingly destabilising (Scheme 2.1).

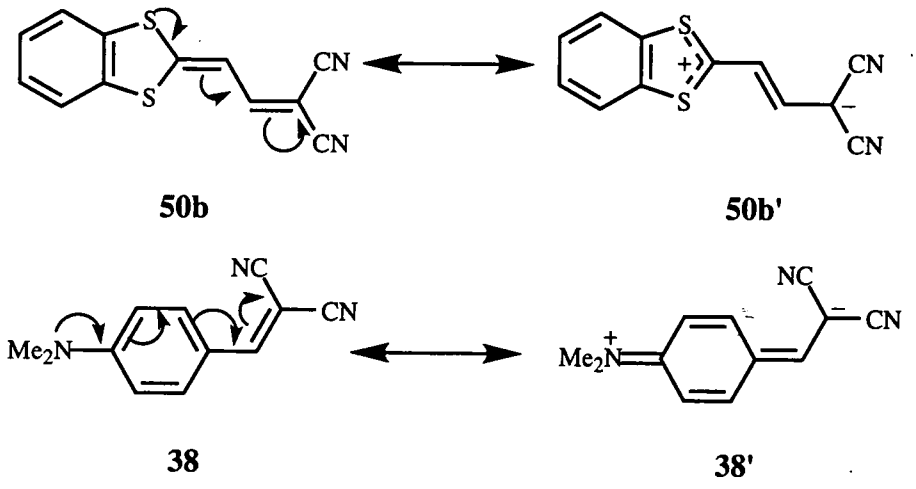

50b **50b'**

38 **38'**

Scheme 2.1 The Neutral and Zwitterionic States in Donor-π-Acceptor Systems

With the exception of the work performed by Lehn *et al*[55] (Section 1.3.3.1) no donor-π-acceptor systems utilising a functionalised dithiole unit were known. The effect of functionalising the periphery of a 1,3-dithiole should provide insights into the nature of intramolecular electron delocalisation within these systems. With this in mind, this chapter will briefly review the synthetic pathways to functionalised 1,3-dithiole derivatives and their subsequent incorporation into donor-π-acceptor systems.

2.2 Functionalised 1,3-Dithiole Donor Units

In our preliminary studies the functionality on the 1,3-dithiole was chosen to provide derivatives covering a range of donor properties: *viz.* 4,5-dimethyl (strongly electron donating), 4,5-dimethylthio (donating due to conjugation of the lone pair of electrons on the sulfurs) and 4,5-dicarbomethoxy (electron withdrawing).

2.2.1 Dithiole Donor Synthesis

2.2.2 Synthesis of 4,5-Dimethyl-1,3-dithiole-2-thione 65

The electron donating dimethyl dithioles were synthesised *via* modification of a literature procedure (Scheme 2.2).[58] To a solution of piperidine **60** was added sodium hydroxide followed by carbon disulfide which afforded piperidinodithiocarbamate **61** as a white precipitate to which was added 3-chloro-2-butanone **62** to afford **63**. This was subsequently cyclised to the iminium salt **64** by addition of concentrated sulfuric acid followed by hexafluorophosphoric acid. **64** was subsequently converted into thione **65** by treatment with sodium hydrosulfide in acetic acid.

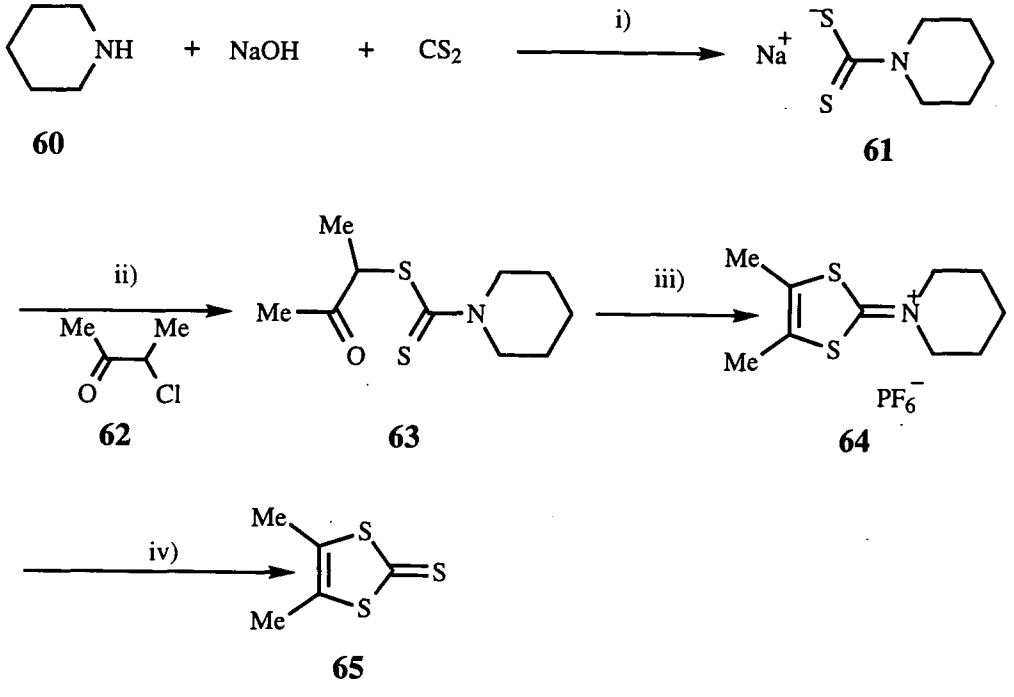

Scheme 2.2 Synthesis of 65 Reagents i) EtOH, 20°C, ii) EtOH, 20°C, iii) c.H_2SO_4, HPF_6 iv) NaSH, Acetic acid

2.2.3 Synthesis of 4,5-Dimethylthio-1,3-dithiole-2-thione 69

Methylthio substituted 1,3-dithiole-2-thione derivatives may be prepared from "zincate" salt **66** which was prepared *via* the chemical reduction of carbon disulfide in the presence of sodium.[59] The mechanism of this reaction has been the focus of much debate since it was first reported in 1927 by Fetkenhauer.[60] The major product, trapped by the addition of chloromethane, was initially assigned as dimethyl tetrathioxalate **67**, which is analogous to the chemical reduction of carbon dioxide to

oxalic acid **68** performed by Kolbe in 1868[61] (Scheme 2.3). It was not until 1974 that Wawzonek correctly identified the product as 4,5-dimethylthio-1,3-dithiole -2-thione **69** (Scheme 2.4).

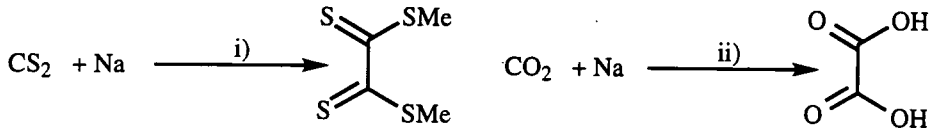

67 **68**

Scheme 2.3 Synthesis of 67 and 68 Reagents i) DMF, 0°C, MeCl, ii) DMF, 0°C, H^+

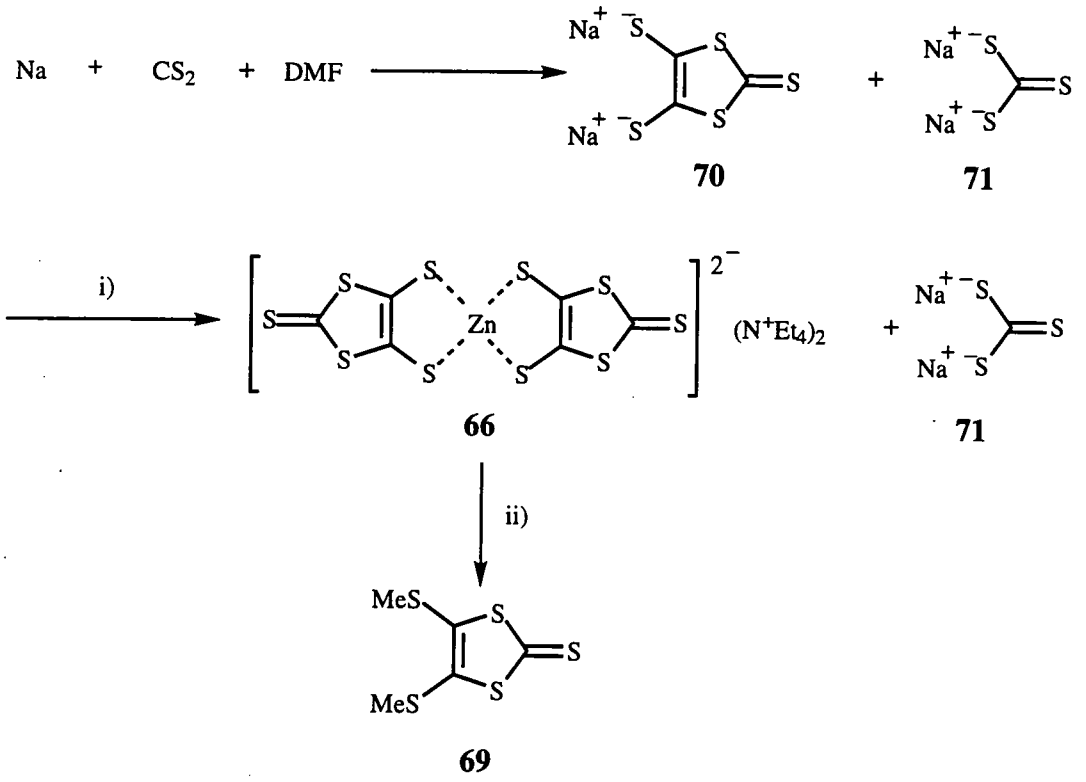

70 **71** **66** **71** **69**

Scheme 2.4 The Synthesis of 'Zincate' Salt 66 and 69 Reagents i) $ZnCl_2$, Et_4NBr, ii) MeI, Acetone

This reaction produces equimolar amounts of the desired 4,5-dithiolato-1,3-dithiole-2-thione **70** and 1,3-dithiolato-2-thione **71** which may be separated by the addition of zinc chloride which selectively forms an adduct with the former product isolated as the tetraethylammonium salt **66** (Scheme 2.4).

Alkylated species of **66** may be prepared by treatment with a variety of electrophiles.[62] Thus, the reaction with methyl iodide in acetone leads to the formation of 4,5-dimethylthio-1,3-dithiole-2-thione **69**[63] (Scheme 2.4).

2.2.4 Synthesis of 4,5-Dicarbomethoxy-1,3-dithiole-2-thione 74

This may be prepared in a one-step 3+2 cycloaddition reaction between ethylene trithiocarbonate **72** and dimethylacetylenedicarboxylate (DMAD) **73** in toluene to yield **74** (Scheme 2.5).

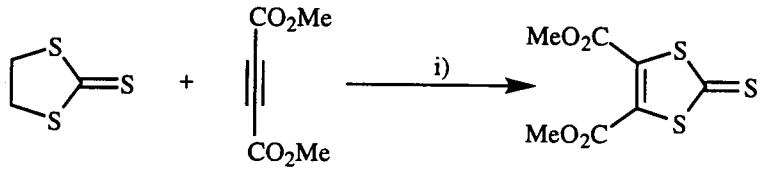

72 **73** **74**

Scheme 2.5 The Synthesis of Compound 74 Reagents i) Toluene, reflux

2.3 Synthesis of Dithiole Donor-Acceptor Systems.

During the initial work by Gompper *et al*[51] (Section 1.3) the simplest dithiole donor-π-acceptor system **42** was synthesised by the addition of malononitrile to methylthiolium iodide salt **76** (Scheme 2.6). We chose to adopt this synthetic route using functionalised dithiole units to investigate the effect that functionalisation of the 1,3-dithiole has on the nature of intramolecular charge transfer properties.

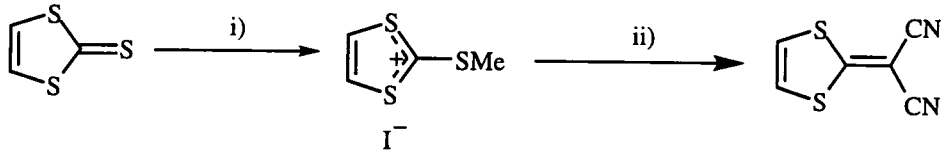

75 **76** **42**

Scheme 2.6 Gompper's Synthesis of Dithiole Derived Donor-π-Acceptor Systems Reagents i) MeI, ii) $CH_2(CN)_2$, pyridine, Et_3N

2.3.1 Synthesis of Methylated Salts of 77a,b,c

Thiones **65**, **69** and **74** were methylated using methyltrifluoromethyl sulfonate in dichloromethane to yield salts **77a-c** in excellent yields following the addition of diethyl ether (Scheme 2.7).

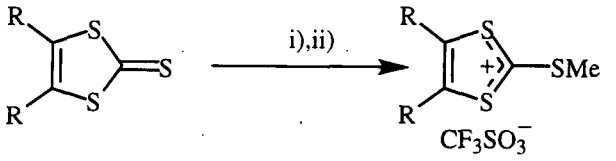

65 R=Me
69 R=SMe
74 R=CO_2Me

77a R=Me
77b R=SMe
77c R=CO_2Me

Scheme 2.7 Synthesis of Salts 77a-c Reagents i) $MeSO_3CF_3$, DCM, 20°C, ii) Et_2O

2.3.2 Synthesis of Dithiole Derived Donor-π-Acceptor Systems

Salts **77a,c** were transformed into their corresponding dicyanomethylene derivatives **78a,c** in good yields by treatment with malononitrile and pyridine in propan-2-ol and isolated as tan crystals (Scheme 2.8). The reaction of the 2,4,5-trimethylthio-1,3-dithiolium trifluoromethyl sulfonate **77b** under the same experimental conditions did not produce the expected product **78b**. However, performing this reaction in THF solution afforded **78b** in good yield as a pale yellow solid.

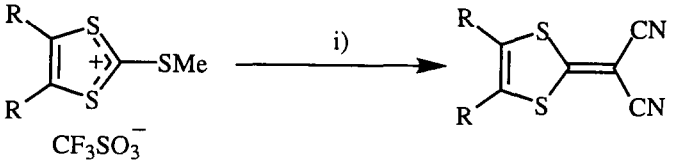

77a R=Me
77b R=SMe
77c R=CO_2Me

78a R=Me
78b R=SMe
78c R=CO_2Me

Scheme 2.8 The Synthesis of Functionalised Dithiole Donor-π-Acceptor Systems Reagents R=Me, CO_2Me i) $CH_2(CN)_2$, pyridine, propan-2-ol; R=SMe i) $CH_2(CN)_2$, pyridine, THF

2.3.3 UV-VIS Spectra of Compounds 78a-c

The solution UV-VIS spectra of these donor-π-acceptor systems notably exhibited a broad low energy absorption band (fig.2.1) of which the values of λ_{max} and the corresponding extinction coefficient (ε) are collected in Table 2.1. This low energy absorption has previously been attributed to intramolecular electron transfer from donor (dithiole) to acceptor (dicyanomethylene) for similar species producing zwitterionic species **78a'-c'** in solution (Scheme 2.9).[55]

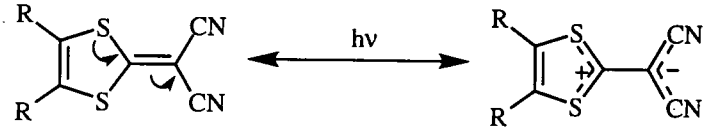

78a-c **78a'-c'**

Scheme 2.9 Zwitterionic States of Compounds 78a-c

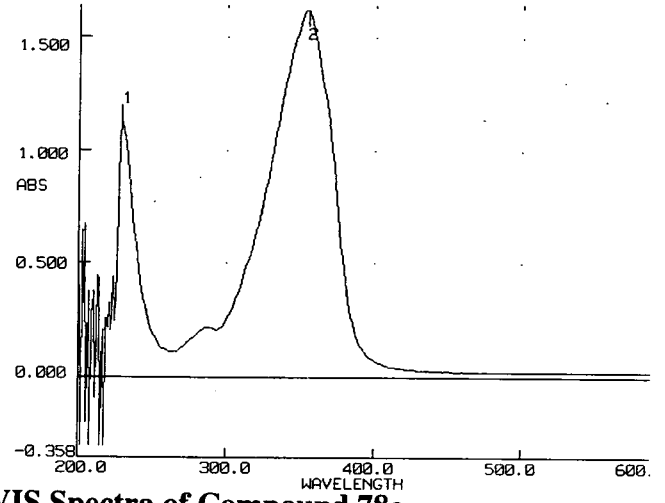

Fig.2.1 UV-VIS Spectra of Compound 78c

Compound	λ_{max}/nm	$\varepsilon/10^4 M^{-1}cm^{-1}$
78a	387	4.8
78b	364	1.3
78c	354	2.3

Table 2.1 λ_{max} Values for Compounds 78a-c

The presence of this intramolecular electron transfer band was highly encouraging as it is in agreement with the results obtained by Lehn *et al* employing shorter spacer units.[55] The presence of the electron donating methyl groups in derivative **78a** shifts

the position of this band to low energy by 33 nm, compared to the electron withdrawing ester groups. The methylthio functionalised system appears to be acting as relatively poor donor units compared to the dimethyl derivative. It was expected that the electron donation of the pπ electrons on sulfur would impart an electron donating effect onto the system. It appears, however, that in this system the methylthio group acts as a relatively poor electron donor. This may be attributed to the ability of sulfur to act as both a pπ donor and a dπ acceptor with the dπ acceptor contribution apparently predominating. It is therefore, evident that the functionality on the 1,3-dithiole effects the position of the charge transfer band obtained.

The effect of increasing the conjugated spacer unit should produce a more bathochromic (low energy) shift in the charge transfer band by lowering the energy gap between the HOMO and the LUMO producing a lower energy transition and materials with increasing values of λ_{max}.

2.4 Synthesis of Donor-Acceptor Systems With an Increased Conjugated Link.

The synthesis of systems with two or more π bond spacer units required the use of the known 1,3-dithiole Wittig reagents **79a-c**.

2.4.1 Synthesis of 1,3-Dithiole Derived Wittig Reagents

These were prepared from the corresponding methylthio salts **77a,b** (Scheme 2.7) according to the procedures outlined in Scheme 2.2. The methylthio salts **77a,b** were treated with sodium borohydride to yield thioethers **80a,b** which were protonated by tetrafluoroboric acid with the simultaneous loss of methane thiol yielding dithiolium cations **81a,b** which were treated with trialkyl phosphines (PR_3) to yield the Wittig reagents **79a,b** or trialkyl phosphite [$P(OMe)_3$] and sodium iodide to yield the phosphonates **82a,b** (Scheme 2.10).

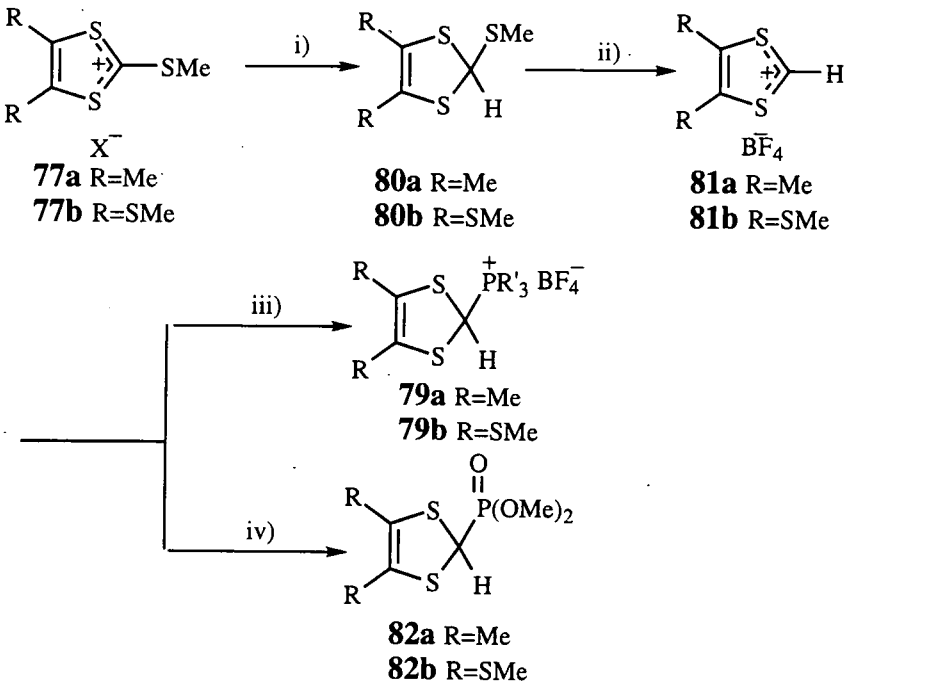

Scheme 2.11 Synthesis of Functionalised Wittig and Wittig-Horner Derivatives Reagents i) $NaBH_4$, propan-2-ol, ii) HBF_4, Et_2O, iii) PR'_3, MeCN, iv) $P(OMe)_3$, NaI, MeCN

The diester Wittig reagent **79c** was prepared *via* a one step procedure in which DMAD **73** and tetrafluoroboric acid were added to a cooled (-30°C) solution of adduct **83** formed from carbon disulfide and tributylphosphine (Scheme 2.11) in diethyl ether yielding compound **79c**[64] as a white solid in high yield.

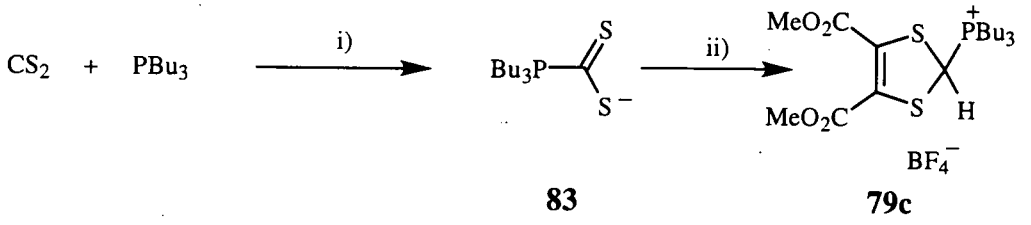

Scheme 2.11 Synthesis of Wittig Reagent 79c Reagents i) MeOH, 0°C, ii) DMAD **73**, HBF_4, -30°C

With quantities of these Wittig reagents in hand, the subsequent reactions with glyoxal **84** in THF and triethylamine were performed yielding compounds **85a-c**[65,66] (Scheme 2.12) in moderate to good yields.

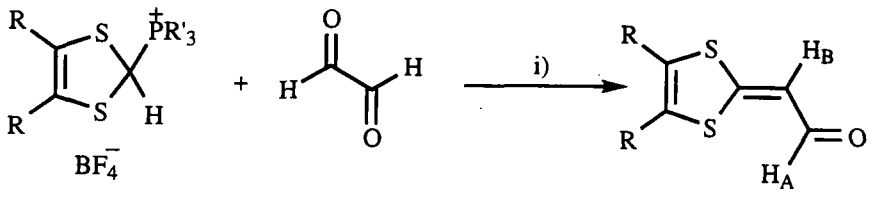

79a R=Me
79b R=SMe
79c R=CO_2Me

84

85a R=Me
85b R=SMe
85c R=CO_2Me

Scheme 2.12 The Wittig Reaction of 1,3-dithiole Wittig Reagents 79a-c with Glyoxal Reagents i) Et_3N, THF, 20°C

The coupling constants of the vinyl protons of **85a** and the remainder of the series were lower that might be expected for the trans system shown in Scheme 2.12. The J values of H_A and H_B of 3 Hz indicated a *cis* conformation **85a'** in which we assume there is a close contact between the dithiole sulfur and the aldehyde oxygen. This structural characteristic has been observed in similar dithiole systems in which S--S,[67] and S--N[68] stabilised structures lead to aromatic dithiolium species similar to compound **85a'**

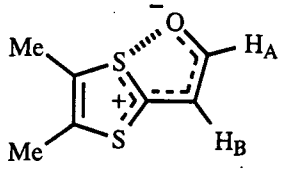

85a'

2.4.2 Synthesis of Dicyanomethylene and Cyanoimine Donor-π-Acceptor Systems

To investigate the effects of increasing the conjugated link between the donor and the acceptor groups on the position of the charge transfer band, we converted aldehydes **85a-c** into dicyanomethylene derivatives *via* the use of Lehnert reagents[69] [$TiCl_4$, $CH_2(CN)_2$ and pyridine] in refluxing dichloromethane to yield **86a-c** as red or orange solids (Scheme 2.13). To vary the acceptor strength we also utilised the cyanoimine acceptor units (Section 1.1.7.1) which were prepared following the procedure outlined by Aumüller and Hünig[70] ([$TiCl_4$ and *bis*-trimethylsilylcarbodiimide (BTC)] in dichloromethane at room temperature yielding **87a-c** as orange or red solids (Scheme 2.13).

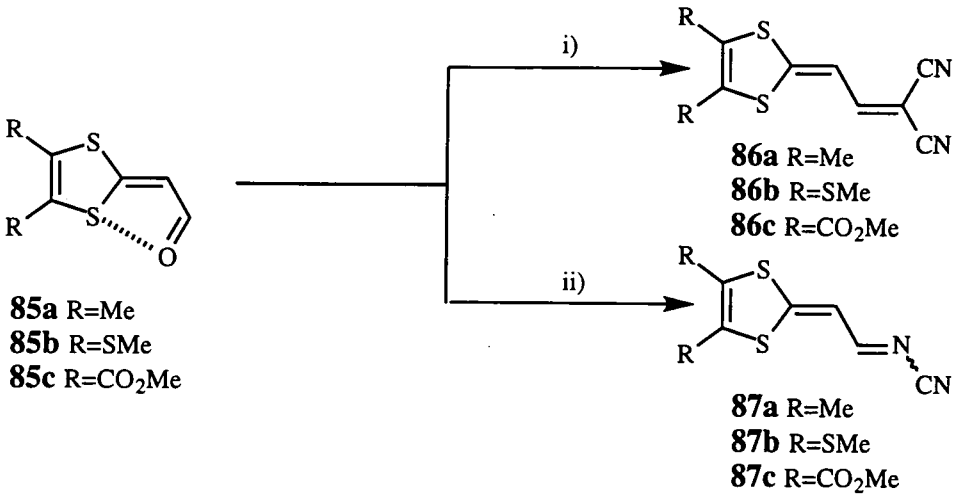

Scheme 2.13 **Synthesis of Dicyanomethylene and Cyanoimine Derivatives of 85a-c** Reagents i) $TiCl_4$, $CH_2(CN)_2$ pyridine, DCM, reflux, ii) $TiCl_4$, BTC, DCM, 20°C

2.4.3 UV-VIS Spectra of Compounds 86a-c and 87a-c

The orange or red colour of these compounds was indicative that the charge transfer absorption now falls within the visible region. This correlated with the increasing length of the conjugated spacer unit lowering the HOMO-LUMO gap thus causing a bathochromic shift into the visible region (400-800 nm). The cyanoimine systems comparably absorbed at higher energy than their dicyanomethylene analogues which was attributed to the increased stabilisation of the negative charge by the two nitrile groups in compound **86a-c** compared to **87a-c** (Table 2.2).

R	λ_{max}/nm	$\varepsilon/10^4 M^{-1}cm^{-1}$	λ_{max}/nm	$\varepsilon/10^4 M^{-1}cm^{-1}$
Me	489	4.2	450	5.0
SMe	475	5.3	448	1.3
CO_2Me	439	2.5	426	3.5

Table 2.2 **UV-VIS Data For Compounds 86 and 87**

Compounds **86a** and **87a**, which contain dimethyl functionality, produce a charge transfer absorption band that was markedly red shifted compared to the diester analogues **86c** and **87c** which was again attributed to the electron donating and accepting properties of these substituents. The methylthio functionalised again produced a disappointing result indicating their relatively weak electron donating properties.

2.4.4 NMR Spectra of Compounds 86 and 97

Comparison of the ^1H NMR spectra of compounds **86** and **87** revealed marked differences between these systems. For the former there was a noticeably large $^3H_{AB}$ coupling constants (J=12 Hz) which is indicative of the expected *s-trans* structure of compound **86** which is exemplified in Scheme 2.13; however the spectra of **87** was markedly different. The coupling constants for the vinylic protons in compounds **87a-c** was much smaller (J=5 Hz) which points to an *s-cis* conformation in which there is a significant intramolecular contact between the dithiole sulfur and the imine nitrogen analogous to compound **85a'**

2.4.5 X-Ray Structure of Compounds 86b and 87b

Slow evaporation of a dichloromethane solution of compound **86b** and **87b** produced crystals suitable for single crystal X-ray analyses. The X-ray crystal structures of compounds **86b** and **97b** were obtained to provide information on the extent of charge transfer in the ground state. The presence of charge transfer in the excited state had already been demonstrated *via* solution state UV spectroscopic studies (Section 2.3.3)

Molecule **87b** (Fig.2.2) is planar to within 0.03Å, except for the two methyl groups, C(4) and C(5) which deviate from this plane by 1.24 and 1.67Å respectively. The N(1) atom is in a *syn* orientation towards the 1,3-dithiole unit and forms a short intermolecular contact of 2.719(6)Å with S(1), which is substantially less than the sum of the van der Waals radii (3.35Å).[71] This, together with π-delocalisation along the C(1)C(6)C(7)N(1) chain, suggests some degree of N(1)-S(1) bonding interaction.

Molecule **86b** is, also planar (fig.2.3), but for small twists around the C(4)-C(5) and C(2)-S(3) bonds (3° and 7°, respectively) and a nearly orthogonal (86°) twist around the C(3)-S(4) bond. The 'butadiene' moiety has a *trans* configuration; the formally single C(4)-C(5) bond is only 0.016Å longer than the formally double bonds. Thus, the system is much closer to a cyanine (bond-equivalent) structure, than to genuine all-*trans* polyenes with the mean alteration (Δ) between single and double bond

lengths of 0.10-0.12Å.[72] In fact, such a degree of π-delocalisation (Δ≤0.02Å) is usual for polyene chains with a dicyanomethylene group on one end and electron-releasing (amino) substituents on the other (*e.g.* compounds **88** and **89**);[73] sulfur containing heterocycles have been shown to have a similar effect, as in **90** (Δ=0.02Å)[74] and **46**,[75] which has the same conjugated path and acceptor group as **86b**, with the same value of Δ (0.016Å).

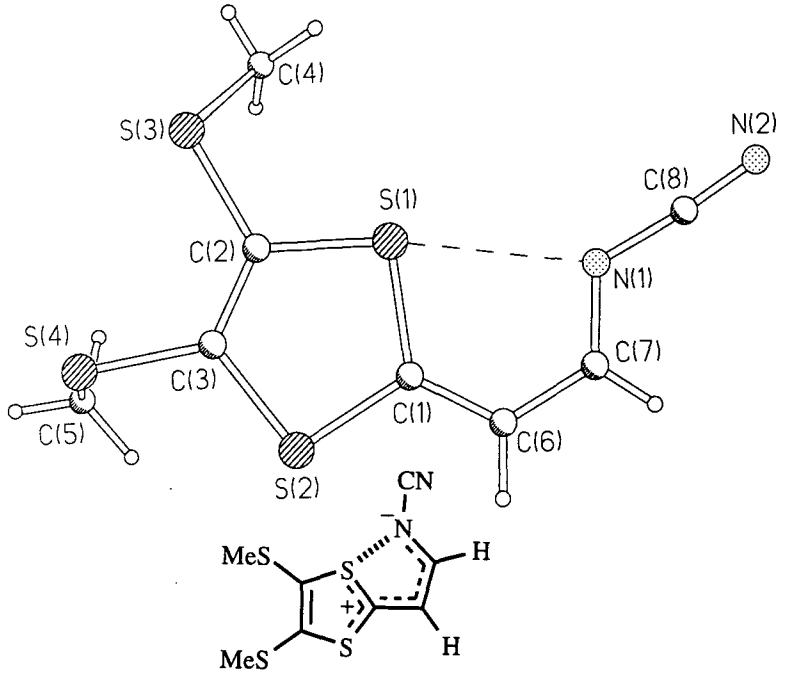

87b'

Fig.2.2 X-Ray Structure of Compound 87b

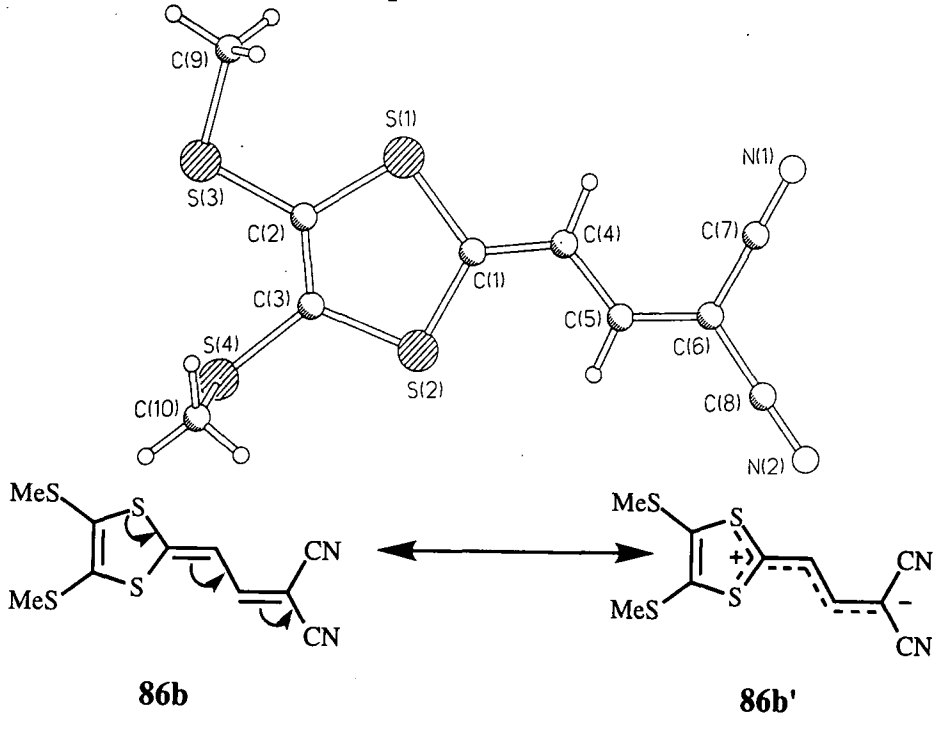

86b **86b'**

Fig. 2.3 X-Ray structure of 86b

Molecules in the crystal of **86b**, related *via* an *x* translation, form a stack with an interplanar separation of *ca.* 3.4Å and a lateral shift of 3.5Å, such that the oppositely charged dithiole and dicyanomethylene moieties (arising as a result of intramolecular electron transfer) of adjacent molecules are nearly overlapping.

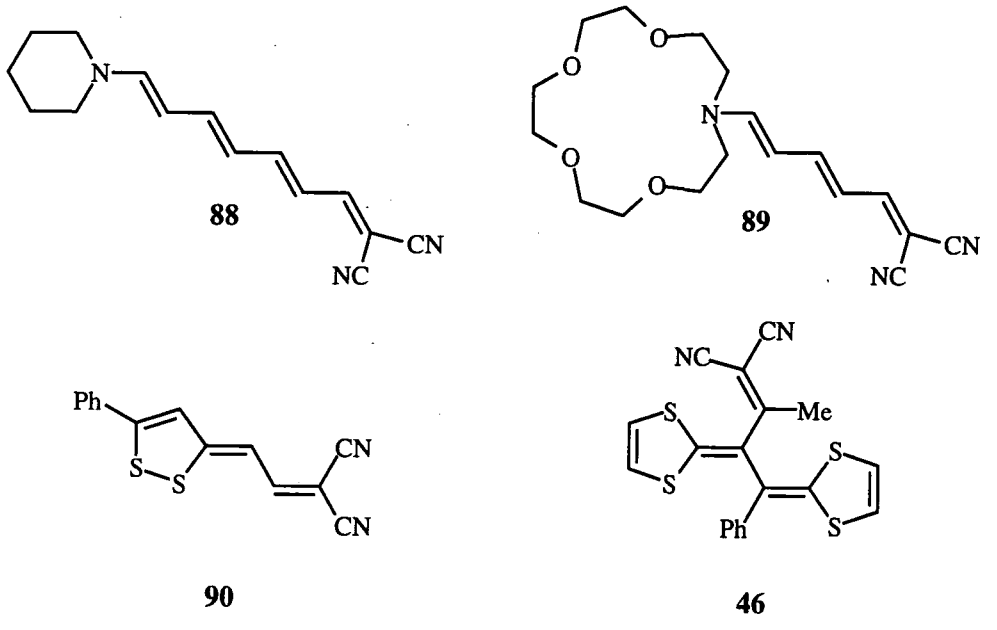

Fig 2.4 Molecules with Bond Alternate Structures Similar to Compound 86b

We have, therefore, shown that in the case of compound **86b** the zwitterionic state **86b'** makes a significant contribution to the ground state structure. Similarly, for compound **87b** there is both delocalisation from the donor to the acceptor and a close contact between dithiole sulfur and imine nitrogen which was earlier postulated from the ^{1}H NMR evidence (Section 2.4.4).

Similar S-S interactions have been utilised to produce stabilised thioaldehyde derivatives which are usually very unstable to dimerisation. Bryce *et al*[67] synthesised compound **91** and *via* X-ray crystal analysis a S-S interaction of 2.9 Å was observed which was considerably shorter than the sum of the Van der Waals radii (3.6 Å).

Moreover, we were attracted to the thioketone unit as a possible acceptor group as the resonance stabilised structure **91'** exhibits charge transfer properties similar to compound **86b** (Scheme 2.14). With that in mind we sought to synthesis dithiole derived donor-π-acceptor systems containing thioketone acceptor units.

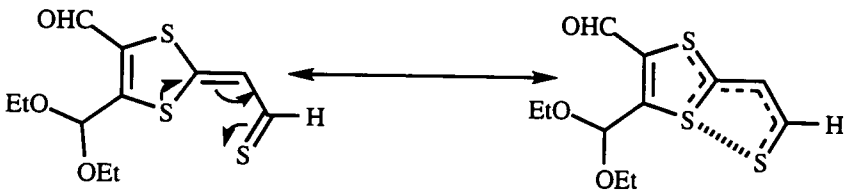

91 **91'**

Scheme 2.14 Charge Transfer in Compound 91

2.4.6 Synthesis of Donor-π-Acceptor Systems containing Thioketone Acceptor Units

To a solution of Wittig reagent **79a** in acetonitrile was added triethylamine and either phenylglyoxal **92** or methylglyoxal **93** to afford **94** and **95** as yellow solids in 72 and 48% yields respectively. Compound **95** was unstable even when maintained below 0°C, darkening over time to a red solid, and was thus used immediately following purification. Ketones **94** and **95** were subsequently thionated by the action of phosphorus pentasulfide in acetonitrile in the presence of sodium bicarbonate yielding thioketone derivatives **96** and **97** in 50 and 73% yields as red or brown solids (Scheme 2.15).

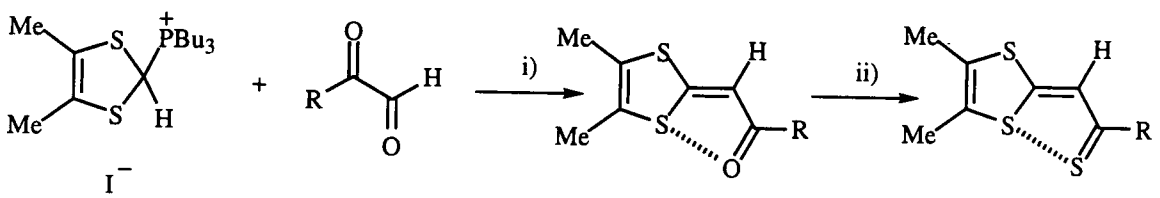

79a **92** R=Ph, **93** R=Me **94** R=Ph, **95** R=Me **96** R=Ph, **97** R=Me

Scheme 2.15 Synthesis of 1,3-Dithiole Derived Thioketone Derivatives
Reagents i) Et_3N, MeCN, ii) P_4S_{10}, $NaHCO_3$, MeCN

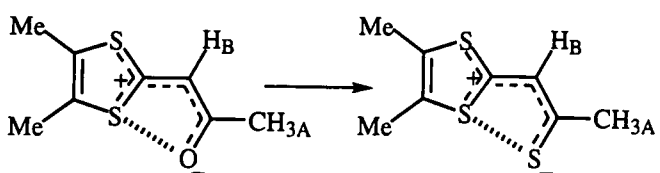

95' **97'**

Scheme 2.16 Proposed Charge Transfer in Compound 95

The ^1H NMR spectra of compound **97** exhibited noticeable peak shifts compared to compound **95**. Following thionation, protons H_A shifted from δ 2.2 ppm to 2.7 ppm and H_B from 6.6 Hz to 7.6 Hz upon thionation. If we assume that both the ketone and thioketones adopt the a similar structure, namely with S--S(O) close contacts, then the differences in the NMR spectra could be attributed to increased intramolecular electron transfer from donor to acceptor (Scheme 2.16).

2.4.7 UV-VIS Spectra of Compounds 96 and 97

Both materials displayed the expected low energy absorption in the UV-VIS spectra, the values of which are shown in Table 2.3 along with the corresponding data for compounds **86a** and **87a**.

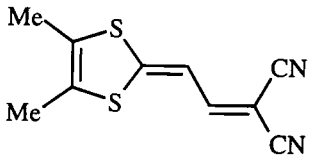

86a

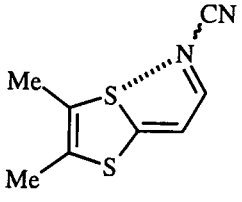

87a

Compound	λ_{max}/nm	$\varepsilon/10^4 M^{-1}cm^{-1}$
96	489	4.0
97	466	1.3
86a	489	4.2
87a	450	5.0

Table 2.3 A Comparison of the Thione Acceptor Ability Compared to the Dicyanomethylene and Cyanoimine Acceptor Units

Compound **96** and **86a** exhibited a charge transfer band at identical positions whereas compound **97** had a charge transfer absorption which was shifted slightly towards higher energy. This was due at least in part to the electron donating effects that the phenyl and methyl substituents have on the charge transfer bands. The phenyl group evidently exerts a greater effect as it possesses both an inductive and a conjugative (mesomeric) electron donating effect, where as the methyl group can only exert an inductive effect. Also, both compounds **96** and **97** produced a charge transfer band that was shifted bathochromically compared to compound **87a**. We, therefore,

propose that the thioketone unit is an excellent electron acceptor being comparable to the dicyanomethylene unit and superior to the cyanoimine group.

2.5 Synthesis of Extended Donor-Acceptor Systems Based around *E.E*-Mucondialdehyde.

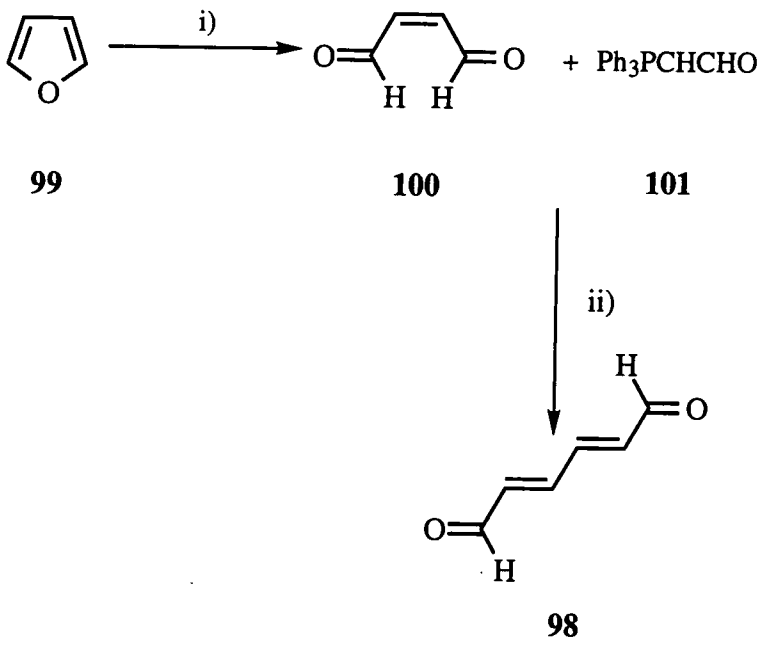

Scheme 2.17 Synthesis of *E,E*-Mucondialdehyde 98 from Furan 99 Reagents i) DMD, Acetone 0°C, ii) DCM

These encouraging results lead us to study the effect of increasing, still further, the conjugated spacer between the donor and the acceptor. We were, thus, attracted to *E,E*-mucondialdehyde **98**[76] which was prepared *via* the oxidative ring opening of furan **99** with dimethyldioxirane (DMD) in acetone to yield malealdehyde **100**.[77] Treatment of malealdehyde **100** with formylmethylene triphenylphosphorane **101**[78] afforded, after work up and thermal and iodine isomerisation *E,E* mucondialdehyde **98** (Scheme 2.17).

To a solution of Wittig salts **79a-c** and *E,E*-mucondialdehyde **98** in THF was added triethylamine which yielded compounds **102a-c** in 54-79% yields as the *trans* isomer in each case. It was interesting to note that when Wittig reagents **79a,b** were utilised the only products isolated were **102a,b** (even when an excess of Wittig reagent **79a,b** was utilised) whereas one equivalent of Wittig reagent **79c** produced compound **102c** as well as **103c** in 14% yield (Scheme 2.18).

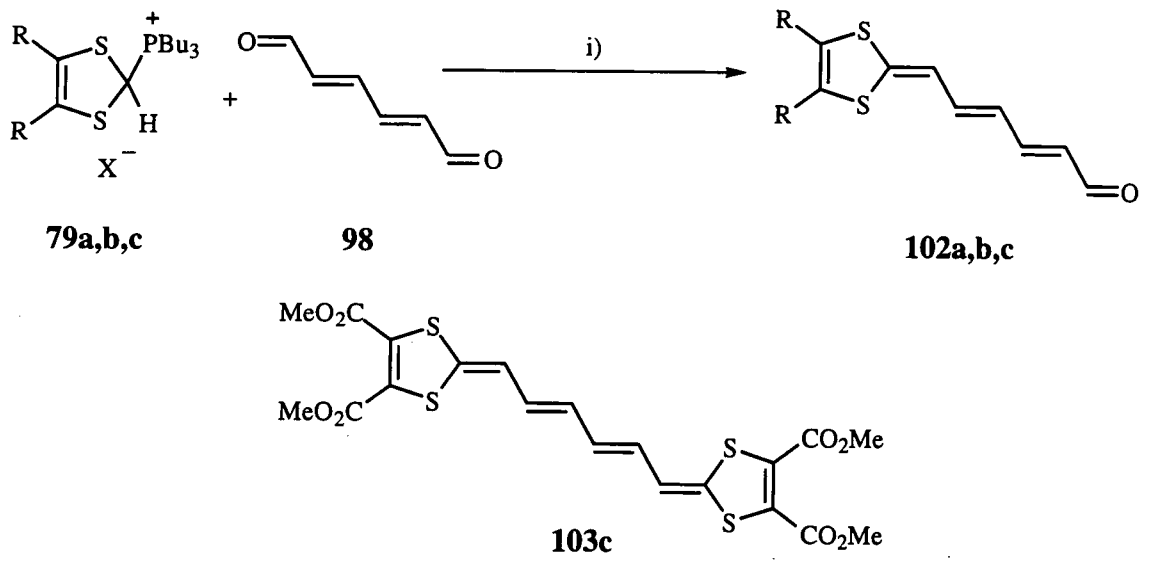

Scheme 2.18 Synthesis of Extended Aldehydes 102a-c Reagents THF, Et_3N

2.7.1 Synthesis of Dicyanomethylene and Cyanoimine Derivatives of 102a-c

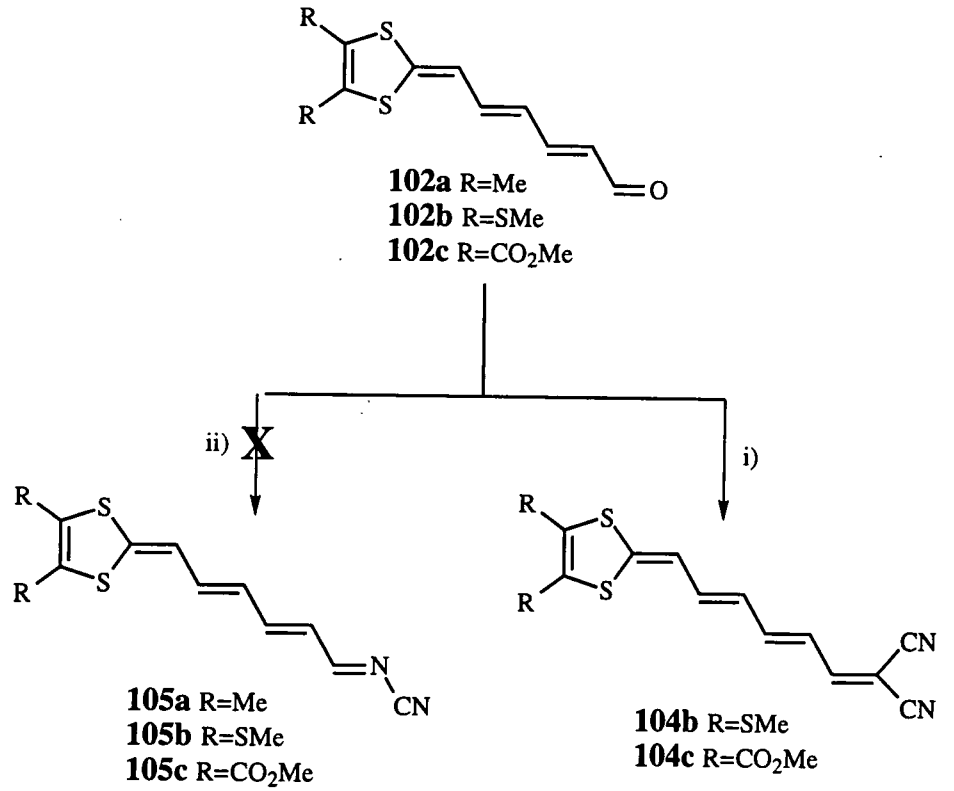

Scheme 2.19 Synthesis of Compounds 104b,c and Attempted Synthesis of Compounds 105a-c Reagents i) $TiCl_4$, $CH_2(CN)_2$, pyridine, DCM, reflux, ii) $TiCl_4$, BTC, DCM, 20°C and reflux.

With compounds **102a-c** in hand, reactions to form the dicyanomethylene derivatives **104a-c** were attempted using standard conditions (Section 2.4.3). These reactions lead to compounds **104b,c** as deep red solids in 43 and 87% respectively. Inexplicably a similar procedure to produce compound **104a** failed, with subsequent modifications (e.g. different solvents and reaction temperatures) producing none of the desired compound. Attempts to convert aldehydes **102a-c** into the corresponding cyanoimine derivatives **105a-c** also failed and only starting aldehydes **102a-c** were isolated (Scheme 2.19).

2.5.2 UV-VIS spectra of Compounds 104b,c

These materials produce low energy absorption bands that were further red shifted compared to the previously described systems **86a-c** which contained only two π bonds (Table 2.3).

R	λ_{max}/nm	$\varepsilon/10^4 M^{-1}cm^{-1}$
SMe	533	2.3
CO_2Me	492	7.5

Table 2.3 UV-VIS Data For Compounds 86b,c

A similar trend in donor ability was observed with the ester functionality acting as an electron acceptor and the methylthio derivative presumably acting as a weak donor, however this was difficult to determine without the data for compound **104a**.

2.6 Cyclic Voltammetic Data For Donor-π-Acceptor Systems

The solution redox properties of the donor-π-acceptor systems synthesised during the course of this work are summarised in Table 2.4. All materials produced a reversible one electron oxidation wave corresponding to the formation of the radical cation of the dithiole donor unit. Similarly, an irreversible one electron reduction wave was produced which was attributed to the formation of the radical anion, which was presumably located on the dicyanomethylene and cyanoimine groups.

A cathodic shift in both the oxidation and reduction peaks with increasing donor strength was observed. Similarly, on increasing the length of the conjugated spacer there was a cathodic shift in the oxidation wave and a anodic shift in the reduction wave which was attributed to increased π delocalisation within these systems.

Compound	E_{ox}[a]/V	E_{red} (V)
78a	1706	-1668
78b	1758	-1520
78c	2148	-1240
86a	1090	-1180
86b	1140	-1060
86c	1490	-1010
87a	1250	-1370
87b	1170	-1220
87c	1653	-1140
104b	730	-840
104c	970	-810

[a] 10^{-5}M compound in dry acetonitrile under argon *vs.* Ag/AgCl, Pt working and counter electrodes at 20°C.

Table 2.4 CV Data for Donor-π-Acceptor Systems

2.6 Solvatochromism and NLO Properties.

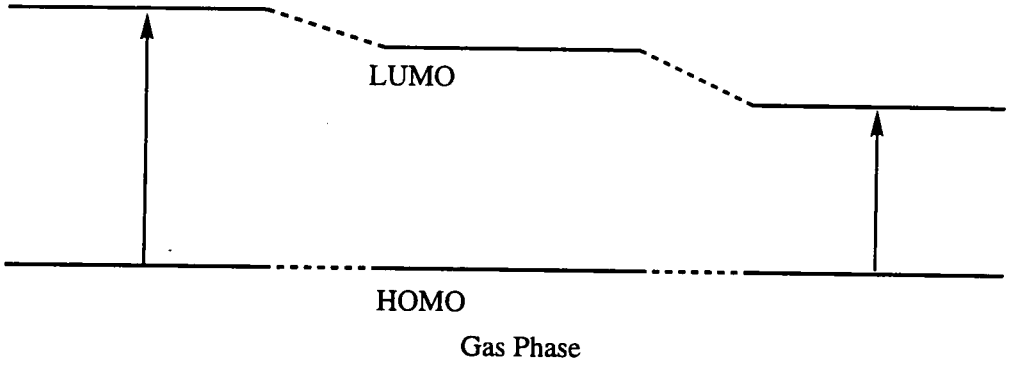

Fig.2.5 The Effects of Increasing Solvent Polarity Causing Positive and Negative Solvatochromism

The position of the low energy charge transfer band of compound **104b** was affected by solvent polarity. On passing from hexane to propan-2-ol a marked colour change

was observed. This was also demonstrated by a shift of the λ_{max} values to lower energy with increased solvent polarity. This phenomena is known as positive solvatochromism which is caused when the excited state is stabilised by more polar solvents. This leads to an increased stabilisation of the zwitterionic excited state more than the uncharged ground state leading to a lowering of the LUMO; this in tern was manifested in a decrease of the transition energy (HOMO-LUMO) and a longer wavelength absorption (fig.2.5). This indicated that the excited state in compound **104b** was zwitterionic, forming **104b'**, (Fig.2.6) similar to compound **86b'**.

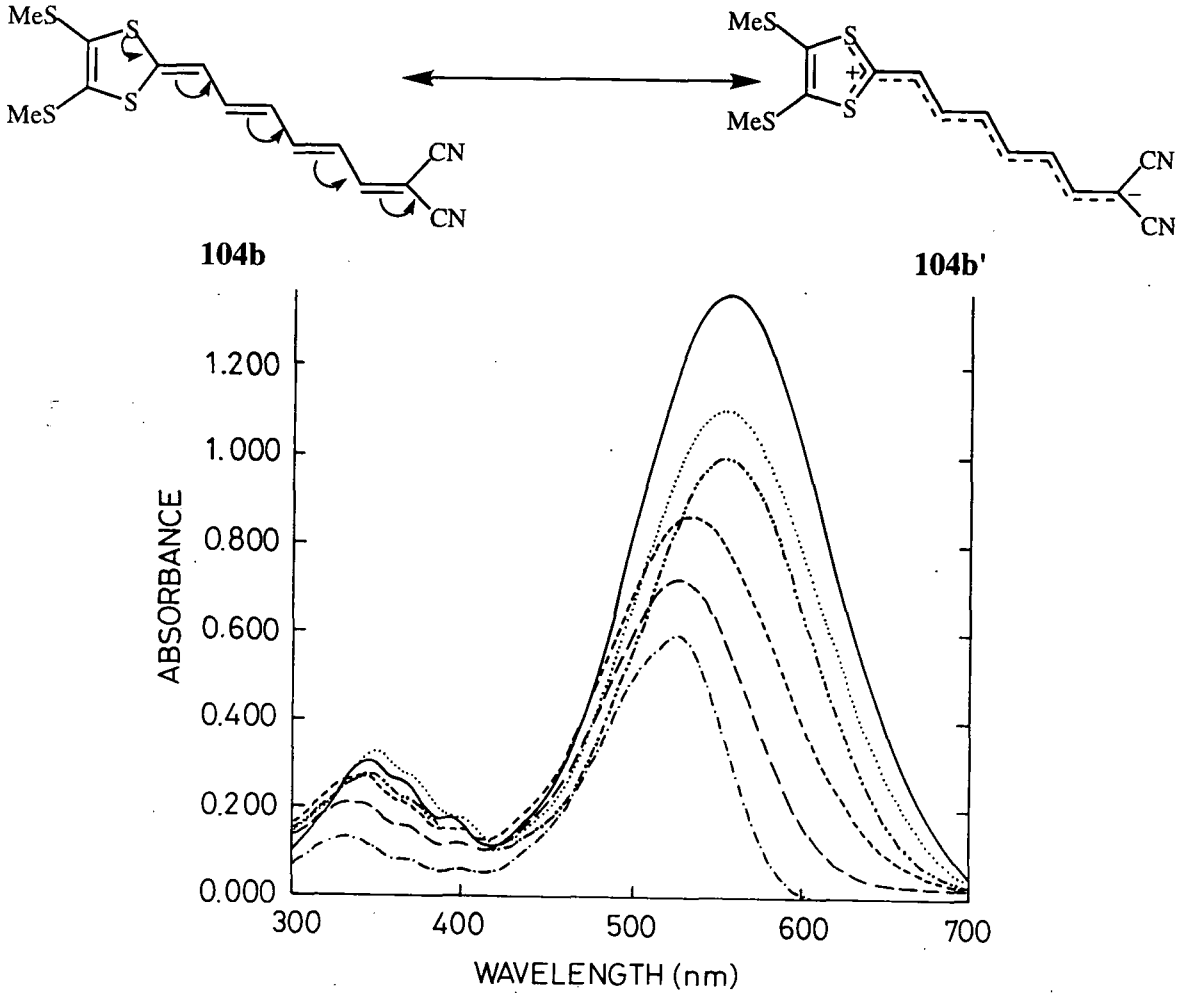

Fig 2.6 Solvatochromism in Compound 104b

Solvent	Hexane	Et_2O	MeCN	DMSO	CH_2Cl_2	CF_3CH_2OH
λ_{max}/nm	526	528	533	553	555	556

Table 2.5 The Variation of λ_{max} with Increased Solvent Polarity for Compound 104b

Materials that observe solvatochromism are also generally active molecules for non-linear optical materials.[79] With that in mind, NLO measurements were performed by Dr. I Ledoux on compounds **104b** and **86a-c** in order to determine whether these materials were NLO active and whether the modification of electron donor properties (*via* the functionality on the donor) has any effect on the value of β.

NLO data were recorded using an EFISH technique (electric field induced second harmonic generation) in chloroform solution measured at fundamental frequency of 1.34 μm (1340 nm) (Table 2.6).

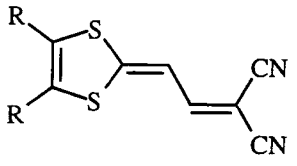

86a R=Me
86b R=SMe
96c R=CO_2Me

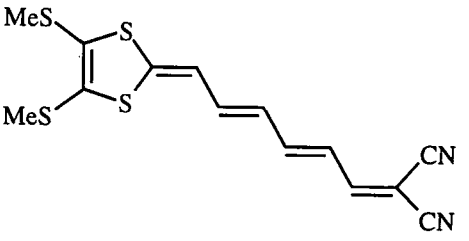

104b

Compound	μ/D[a]	β/10^{-30}esu	β_0/10^{-30}esu	μ.β_0/10^{-48}esu
86a	8.8	31	13	112
86b	6.9	37	15	105
86c	6.8	24	12	85
103b	*ca.* 9	μ.β=4554	*ca.* 130	1170

[a] 1D=10^{-18}esu

Table 2.6 NLO Data for Compounds 86a-c and 103b

Compounds **86a-c** exhibit only moderate NLO activity [the relevant parameter for application being μ.β_0] when compared to the materials discussed in chapter one. The dependence of $\mu\beta_0$ on the dithiole substituent is quite weak but does follow the expected trend *viz.* Me>SMe>CO_2Me which was consistent with UV-VIS data. Compound **104b** appears to be the most interesting material exhibiting a comparatively large values of $\mu\beta_0$.

2.7 Conclusions

We have synthesised a variety of novel functionalised dithiole derived donor-π-acceptor systems which display in their UV-VIS spectra a low energy absorption

which was attributed to intramolecular electron transfer from the donor to the acceptor. The position of this charge transfer absorption can be modulated by a number of factors. We have demonstrated that the donor strength decreases in the series Me>SMe>CO_2Me with the methylthio derivatives acting as a much poorer electron donor than was initially imagined. Increasing the length of the conjugated spacer unit (1, 2, and 4π bonds) produced a bathochromic shift in the UV-VIS spectra. The dicyanomethylene group acts as a stronger electron acceptor than the cynoimine group and the thioketone group has been shown to be excellent acceptor unit in these systems. X-ray crystallography of two of these donor-π-acceptor systems showed that there was considerable charge transfer in the solid state with zwitterionic structures produced. These materials were also NLO active.

Chapter 3

The Synthesis of Anthracene Derived Donor-π-Acceptor Systems

3.1 Intramolecular Donor-π-Acceptor Systems.

The linking of a 1,3-dithiole donor to acceptor units *via* an anthracene spacer unit could lead to a stabilised zwitterionic species: both the anthracene and the dithiole subunits could attain aromaticity upon charge transfer; the destabilising effect of the S-H peri interactions in the neutral form may be removed by rotation of both the dithiole and the dicyanomethylene units about the formally double bonds (Scheme 3.1).

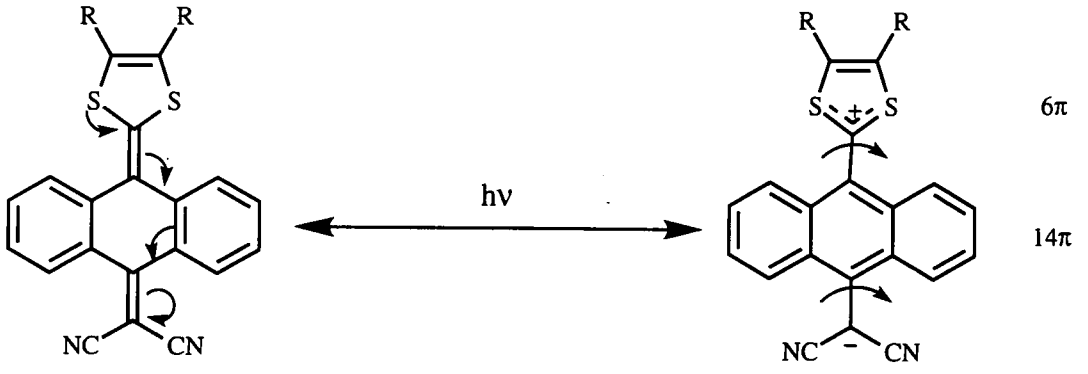

Scheme 3.1 The Effect of Intramolecular Electron Transfer

3.2 Synthesis

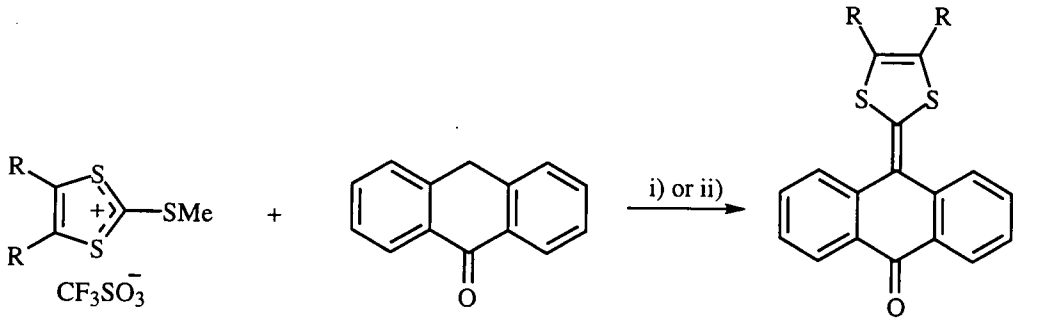

77a R=Me
77b R=SMe
77c R=H
77d R-R=SCH_2CH_2S

106

107a R=Me
107b R=SMe
107c R=H
107d R-R=SCH_2CH_2S

Scheme 3.2 The Synthesis of 107a-d Reagents i) Pyridine:Acetic acid 3:1 v/v, 50-60°C, ii) NaOEt, EtOH, 60-70°C

The synthesis of a 1,3-dithiole-2-ylidene unit linked to the 9-position of anthracene may be achieved from the corresponding methylthio salts **77a-d** (Section 2.3.1) and anthrone **106** in a mixture of pyridine and acetic acid following a literature procedure (Scheme 3.2).[80] We sought to synthesise derivatives with a variety of functionality on the donor in order to investigate further the effects of functionalisation upon the position and nature of the charge transfer bands obtained. Methylthio salts **77a-d** were added to a pre-prepared solution of anthrone **106** in a mixture of pyridine and acetic acid (3:1 v/v) yielding **107a,c,d** in good yields. The corresponding reaction of **77b** to form **107b** failed to yield any of the desired compound and a multitude of uncharacterised products was produced in the reaction mixture (TLC evidence). In order to overcome this problem, salt **77b** was added to a solution of anthrone **106** in sodium ethoxide and ethanol yielding compound **107b** in good yield.

3.3.1 The Synthesis of Dicyanomethylene Derived Donor-π-Acceptor Systems.

The ketone functionality in compounds **107a-d** may be directly converted to the dicyanomethylene derivatives **108a-d** *via* standard conditions (titanium tetrachloride, malononitrile and pyridine in refluxing chloroform) (Section 2.4.2). We found, however, that the use of a large excess of both malononitrile and pyridine (10 equivalents) lead to a reduction of the reaction time. Compounds **108a-d** were thus isolated as blue/purple crystalline solids in good to excellent yields (Scheme 3.3).

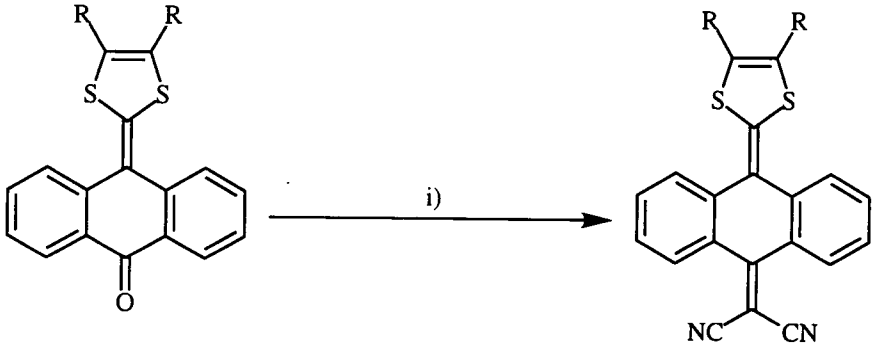

107a R=Me
107b R=SMe
107c R=H
107d R-R=SCH_2CH_2S

108a R=Me
108b R=SMe
108c R=H
108d R-R=SCH_2CH_2S

Scheme 3.3 The Synthesis of 108a-d Reagents i) $TiCl_4$, $CH_2(CN)_2$, pyridine, $CHCl_3$, reflux

3.2.2 Synthesis of Cyanoimine Derived Donor-π-Acceptor Systems

These materials were prepared in an analogous manner to those described previously in Section 2.4.2, following the procedure outlined by Aumüller and Hünig[21a] in which ketones **107a-d** were transformed into compounds **109a-d** *via* the use of titanium tetrachloride and *bis*-trimethylsilylcarbodiimide (BTC) in refluxing chloroform (Scheme 3.4). These reactions proceed much more slowly than the corresponding dicyanomethylation reactions and additional BTC was added periodically to the reaction until the starting material was exhausted (TLC evidence) yielding compounds **109a-d** as blue/black powders in moderate yields.

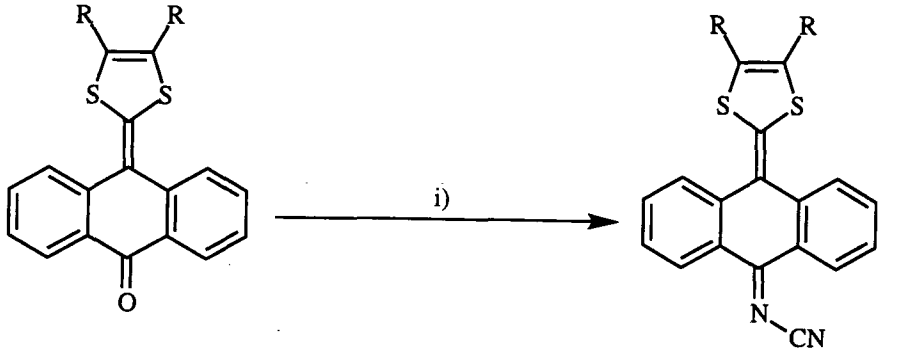

107a R=Me
107b R=SMe
107c R=H
107d R-R=SCH_2CH_2S

109a R=Me
109b R=SMe
109c R=H
109d R-R=SCH_2CH_2S

Scheme 3.4 The Synthesis of Compounds 109a-d Reagents i) $TiCl_4$, BTC, $CHCl_3$, reflux

3.2.2.1 ^{1}H NMR Study of Compound 109b

The ^{1}H NMR spectra of compounds **108a-d** were in most respects similar to the ketones **107a-d** from which they were derived. However, the spectra of compounds **109a-d** bears little or no similarity to either the starting ketones or compounds **108a-d**, as can be seen in fig 3.1. The NMR spectra of compound **109b** measured at 20°C were unusual in that they contained three broad, badly resolved peaks in the aromatic region (one doublet and two triplets) each corresponding to only two protons (fig.3.1). This broadness and the apparent loss of a two proton resonance was attributed to the motion of the nitrile group of compound **109b** on the NMR time scale, leading to the resonance of protons 4(4') being broadened to the extent that they were not observed.

The triplets were attributed to protons 2 (2') and 3 (3') which experience a $^3J_{HH}$ coupling to protons 1 (1'), 3 (3'), and 2 (2'), 4 (4') respectively. The low field doublet was similarly attributed to proton 1 (1') coupling to protons 2 (2') . The remaining, expected, peak should be attributed to protons 4 (4') which was not observed as they are time averaged into the baseline due to the proximity to the mobile nitrile group. These arguments were clarified by a variable temperature NMR study on compound **109b** which established that at -30°C the motion of the acceptor unit was slowed below that of the NMR time scale leading to resolution.

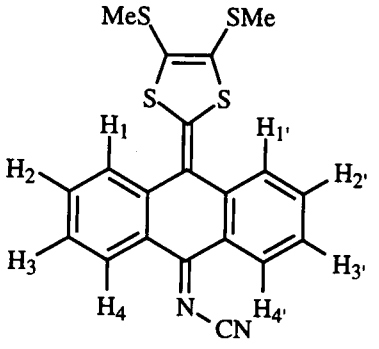

109b

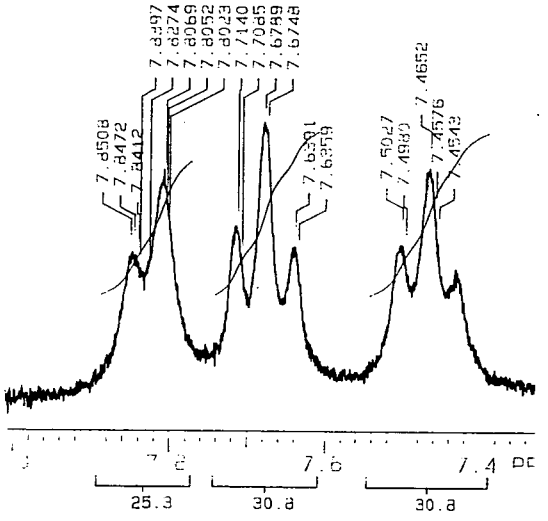

Fig.3.1 ^{1}H NMR Spectra of Compound 109b at 20°C

As can be seen from fig.3.2 as the sample was cooled from 20°C to -30°C there was improved resolution of the aromatic region with all eight aromatic protons observed to be inequivalent. The two low field doublets which developed on cooling were ascribed to protons 4 and 4', respectively, which become inequivalent as the motion

of the acceptor unit was suppressed. The remaining resonances being attributed to the non-symmetrical protons of **109b**.

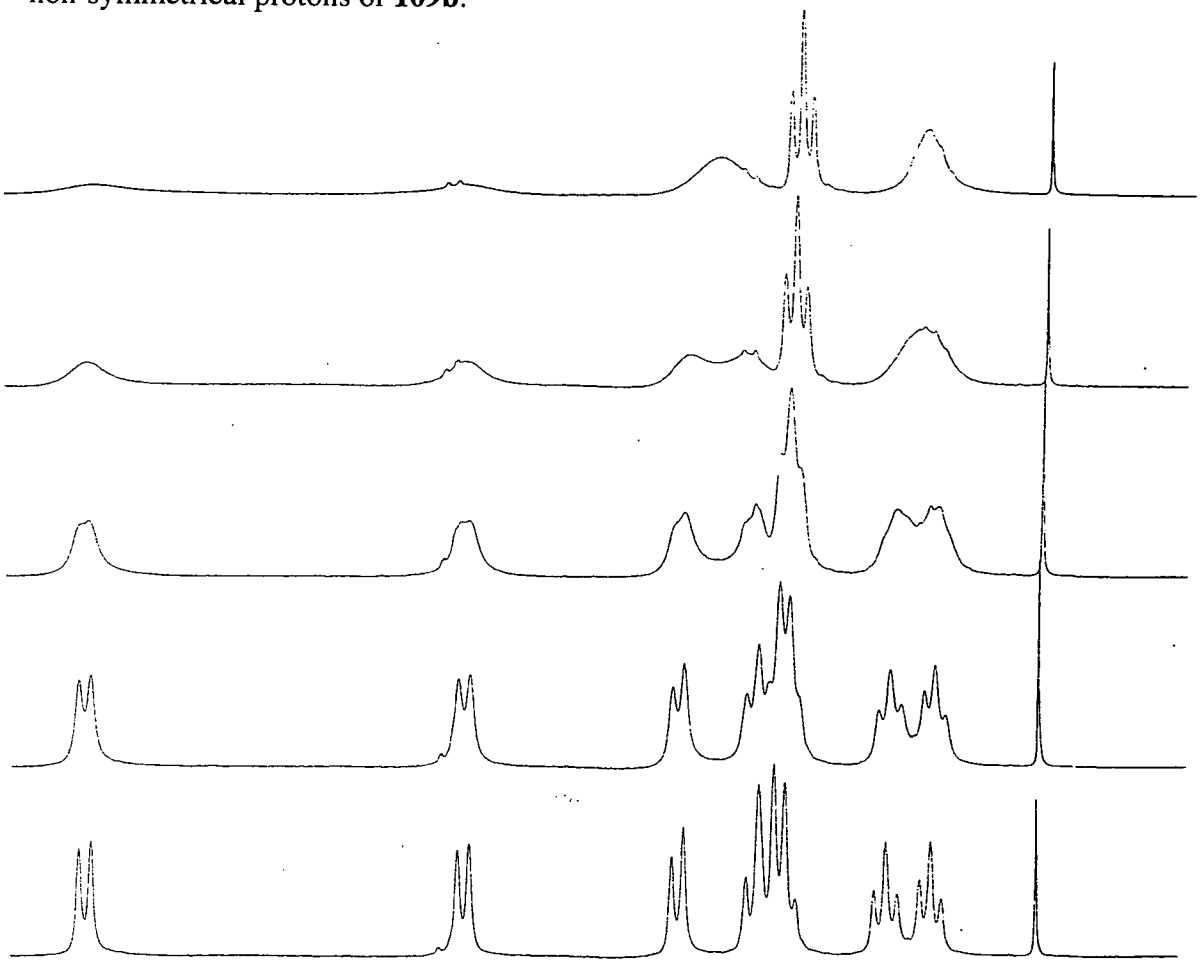

Fig.3.2 Variable Temperature ^{1}H NMR Studies of Compound 109b

3.3 UV-VIS Spectra of Compounds 108a-d and 109a-d

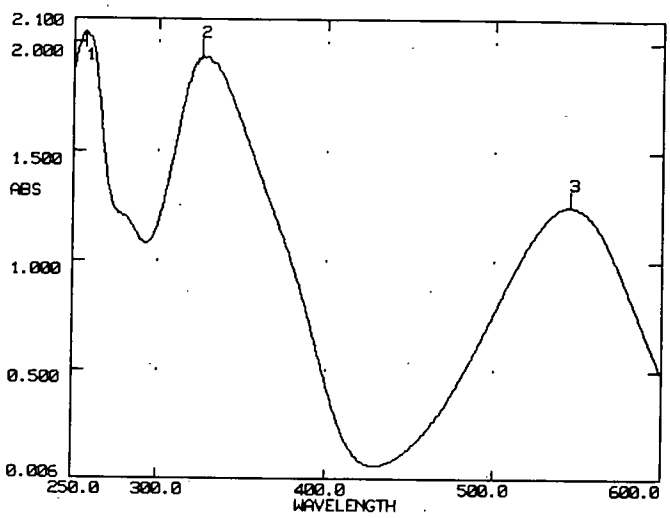

Fig. 3.3 UV-VIS Spectra of Compound 108a

The solution state UV-VIS spectra of donor-π-acceptor systems **108** and **109** possess the expected broad, low energy absorption arising from intramolecular electron transfer from the donor to the acceptor (fig.3.3). The charge transfer absorptions were shifted bathochromically (to low energy) compared to the species discussed previously in chapter two. This shift was presumably due to the aromatic stabilising effect of the anthracene unit upon charge transfer.

3.3.1 The Effect of Donor and Acceptor Strength on the Position of the Charge Transfer Absorption

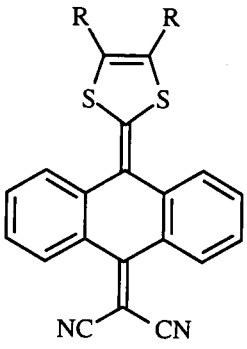

108a-d

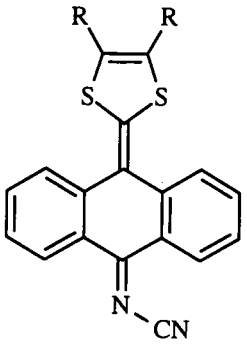

109a-d

R	λ_{max}/nm	$\varepsilon/10^4 M^{-1}cm^{-1}$	λ_{max}/nm	$\varepsilon/10^4 M^{-1}cm^{-1}$
Me	572	1.1	566	2.0
SMe	545	0.89	542	0.86
H	542	1.0	543	1.5
R-R=SCH_2CH_2S	550	0.73	558	0.93

Table 3.1 The Effect of Dithiole Substituents and Acceptor Units on the Position of the Charge Transfer Bands Observed

The position of the charge transfer absorption was again affected by the substituents placed on the 1,3-dithiole donor units in which, as before, the dimethyl derivatives **108a** and **109a** produced charge transfer bands that were noticeably red shifted compared to the other analogues (Table 3.1). Similarly, the dicyanomethylene acceptor unit produced charge transfer absorptions that were red shifted compared to the corresponding cyanoimines for compounds which were substituted with methyl and methylthio derivatives, which was in agreement with the results discussed in chapter two (Section 2.3.3). Slight anomalies were, however, noted for compounds **109c** and **109d**. In both of these systems, the cyanoimine materials produced charge transfer bands that were red shifted compared to the dicyanomethylene analogues.

These results are difficult to explain as, thus far, the dicyanomethylene acceptor units have always been considerably superior to the corresponding cyanoimine acceptors. The variation in apparent acceptor ability must, therefore, be attributed in some way to the donor functionality (i.e. R=H and R-R=SCH_2CH_2S) which has not previously received attention in this study.

It is, again, worth noting that the methylthio derivatives cause a blue shift in the position of the charge transfer band compared to dimethyl derivatives **108a** and **109a**. This indicates the excellent donor ability of dimethyl derived dithioles and the poor electron donating properties of the methylthio derivatives. This phenomenon was observed in chapter two and was attributed to the ability of sulfur to participate as both a $p\pi$ donor and a $d\pi$ acceptor with the interplay between these effects adjusting the position of the UV-VIS absorptions. If we consider compound **108c** (R=H), which is unsubstituted, as the parent system, then any red shifted charge transfer bands compared to **108c** contain substituents that act as true electron donors, with blue shifts arising from electron acceptors. We can see from Table 3.1 that the methylthio derivative **108b** produces a charge transfer absorption which was red shifted compared to compound **108c**, but by only 3 nm. Similarly for compounds **109c** and **109b** the position of the charge transfer band was extensively unchanged: although compounds **109c** and **109d** appear to be unusual as the cyanoimine derivatives were red shifted compared to the dicyanomethylenes. This indicates that there was little effect on substituting the 1,3-dithiole donor unit with methylthio groups, as the interplay between the $d\pi$ acceptor ability and the $p\pi$ donor ability causes little or no enhancement over the unsubstituted compounds **108c**. The effect of tethering the sulfur atoms in compounds **108d** and **109d** leads to a slight shift in the charge transfer band by 5 nm and 8 nm compared to **108c** and **109c** indicating that the ethylenedithio substituted dithiole donor units are moderate electron donors; however they are considerably weaker than the methyl substituents.

3.4 Solvatochromism

Whilst performing routine UV-VIS spectral studies on these donor-π-acceptor system it was noted that there was a noticeable colour variation between solvents at the extremes of polarity, namely hexane and propan-2-ol. Compound **108a** was pink in hexane solution but purple in propan-2-ol. This was also demonstrated by the position of the charge transfer absorption in the UV-VIS spectra, with a variation in the charge transfer band (Δ_{CT}) of 50 nm between the two solvents (fig.3.4).

A similar but slightly less marked effect was observed for compound **109b** for which Δ_{CT}= 44 nm. These initial experiments indicated that the charge transfer absorption in more polar solvents occurred at lower energy *i.e* these materials exhibited positive solvatochromism similar to compound **104b** discussed in chapter two (Section 2.6).

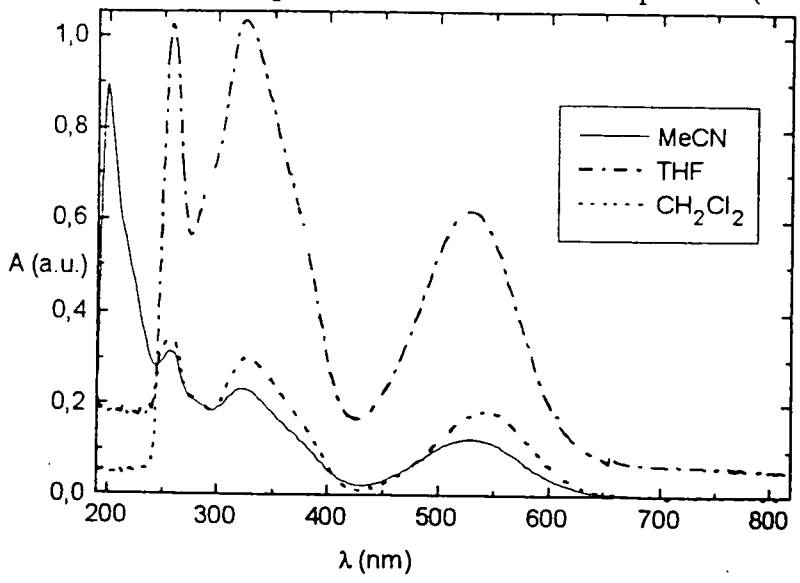

Fig.3.4 The Effect of Solvent Polarity on the Position of the Charge Transfer Absorptions for Compound 108a

These initial results lead us to perform a more detailed study of the solvatochromic behaviour of **108a** and **109b** in a variety of solvents. All spectra were recorded at room temperature on dilute solutions (1 x 10^{-5} M) with repeat scans giving absorption maxima within ± 2 nm. Solvents were selected to investigate a wide variety of possible effects on the nature and state of the charge transfer absorption namely:-

a) Dipolarity / polarisability
b) Hydrogen bond donor (HBD) effects
c) Hydrogen bond acceptor (HBA) effects

Solvent selection was aided by a hierarchical cluster analysis of the solvent descriptors which implies the use of solvents of such diverse polarity from fluorocarbons to water and formaldehyde. It was, however, noted that the solubility of the compounds in these solvents was too low for spectral analysis to be performed. The spectra of compounds **108a** and **109b** were recorded in 21 different solvents and some representative results are summarised in Table 3.2 along with the Kamlet-Taft (K-T) parameters[81] which are an indication of the solvent polarity (π^*), hydrogen bond donor (α), hydrogen bond acceptor (β) and a polarity correction parameter (δ) used occasionally for aromatic or halogenated solvents.

	λ_{max} /nm		Transition Energy /10^3 cm^{-1}		Kamlet-Taft Parameters			
Solvent	**109b**	**108a**	**109b**	**108a**	α	β	π*	δ
TFE[a]	554	586	18.051	17.065	1.51	0	0.73	0
DMSO	550	564	18.182	17.730	0	0.76	1	0
DMF	542	562	18.450	17.794	0	0.69	0.88	0
CH_2Cl_2	540	570	18.519	17.544	0.13	0.1	0.82	0.5
CH_3CN	533	551	18.762	18.149	0.19	0.4	0.75	0
Et_2O	519	546	19.286	18.315	0	0.47	0.27	0
Hexane	511	540	19.569	18.519	0	0	-0.04	0

[a] TFE is Trifluoroethanol (CF_3CH_2OH)

Table 3.2 Solvatochromism Analysis of Compounds 108a and 109b

From these results K-T based linear solvent energy relations (LSER) were derived of the form:-

$$E = c_0 + c_1\pi^* + c_2\alpha + c_3\beta + c_4\delta$$

The one basic assumption is that intermolecular solvent-solute interactions are treated as separate and additive. The coefficients c_1, c_2, c_3 and c_4 are regression coefficients which reflect the relative effect of each chosen solvent. Thus, these parameters will indicate how a solute interacts with a solvent upon photoexcitation and should give some indication of the electronic reorganisation occurring during photoexcitation with the coefficients determined by multilinear regression analysis (MLRA).

3.5.1 Correlation and Regression Analysis

The initial analysis was to plot the transition energy of compound **108a** against **109b** for the range of solvent polarities. This should indicate whether similar excitation was present in both solutes. As can be seen from fig.3.5 a good correlation exists between the eight solvents that are neither hydrogen bond donors nor hydrogen bond acceptors (α=0, β=0) with the remainder deviating from this ideal correlation line. This is indicative of different solvation behaviour for one class of solvents compared to another.

Non-polarisable hydrogen bond donor (HBD) ($\alpha>0,\beta=0$) solvents, with the exception of trifluoroethanol (TFE) all deviated to one side of the correlation line, whilst polarisable solvents and TFE, deviated to the other side. Furthermore, the slope of the line was far from unity indicating that the electron reorganisation on excitation of the two solutes differs. Thus the excited state of these two, seemingly similar molecules, appears to be different.

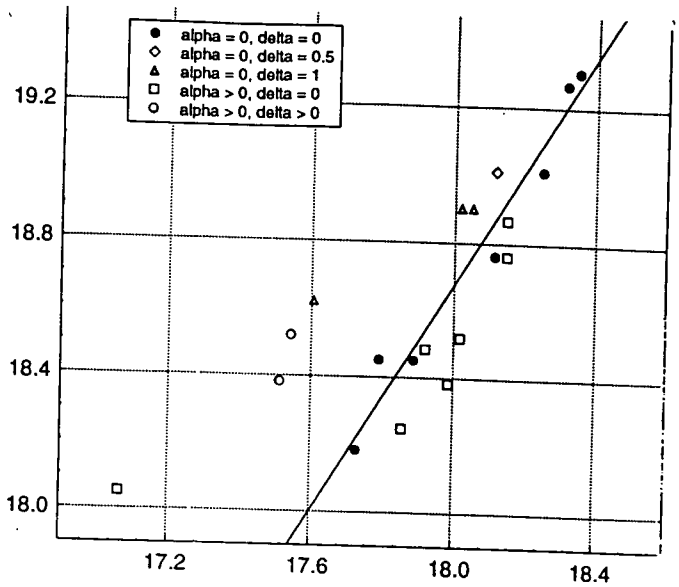

Fig.3.5 Plot of Transition Energies for Compounds 108a *vs.* 109b

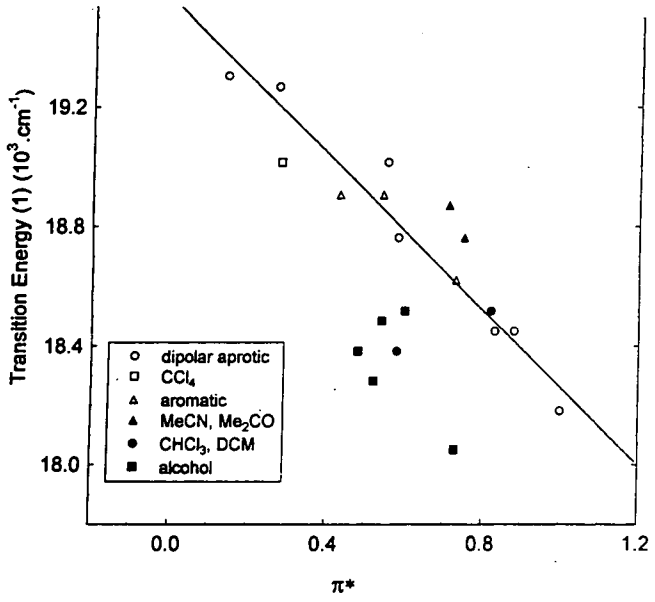

Fig.3.6 Plot of Transition Energy *vs.* π^* for Compound 109b

Initially considering compound **109b**, a plot of solvent dipolarity polarisability parameter π^* against transition energy (fig.3.6) exhibits a notable correlation for the

solvents which are neither hydrogen bond donors nor hydrogen bond acceptors. Thus for the eight solvents for which α=0, β=0 (non hydrogen bond donor or hydrogen bond acceptor) a good correlation with π^* was observed. Furthermore, data measured in polar solvents and carbon tetrachloride fell within the correlation line as well. The only major deviation from this correlation line occurs with the five alcohols and chloroform which are all hydrogen bond donor type solvents.

If the hydrogen bond donor effects and solvent polarity are considered within the MLRA then the plot of transition energy against predicted energy (derived *via* the MLRA) reveals that two parameter LSER, based on polarity and hydrogen bond donor effects, models the solvatochromism of compound **109b** acceptably well (fig.3.7). The standard deviation of the LSER was *ca.* 0.17 x 10^3 cm^{-1} which corresponds to 4 nm or only twice the accepted error in measurement.

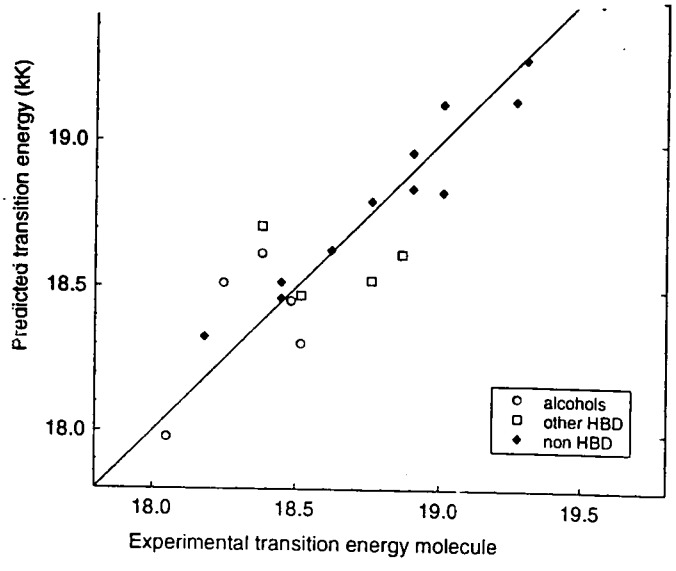

Fig.3.7 Plot of Predicted *vs.* Experimental Transition Energies for Compound 109b

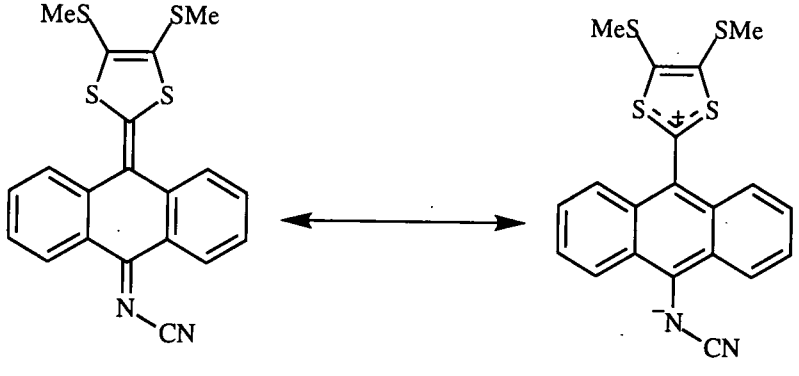

109b **109b'**

The negative values of the c_1 and c_2 coefficients of the important factors in the LSER indicated that an increase of both solvent dipolarity and hydrogen bond donor ability had the effect of lowering the energy of the charge transfer state, thus stabilising the excited state relative to the ground state, leading to charge separation being more prevalent in the excited state than in the ground state. The results acquired thus far could be readily explained by electron transfer from the dithiole donor unit to the imine nitrogen which will thus hydrogen bond with the hydrogen bond donor solvents, thereby lowering the energy of the observed excited state. This evidence is in complete agreement with the proposed intramolecular charge transfer in this system.

For compound **108a** a similar plot of transition energy of this solute against π^* reveals a good correlation for the eight non-polarisable (non-aromatic, non-halogenated) dipolar aprotic solvents. However, in contrast to derivative **109a**, inclusion of hydrogen bonding solvents into the LSER lead to a deterioration in the correlation, and even the addition of the polarising correction factor δ had little or no effect on the fit achieved in modelling the solvent effects. TFE appeared to be a rogue solvent, and if excluded from the calculations for compound **108a** the standard deviation for the remaining solvents was 0.16×10^3 cm^{-1} which was comparable with the previous data set. However, there still appears to be some additional interactions (exemplified for TFE and some aromatic molecules) which leads to a stabilising of the excited state (or destabilising of the ground state) of **108a** which was not easy to rationalise.

We conclude that the solvatochromism in compound **109b** may be explained by the polarity and hydrogen bond donor characteristics of the solvents. Similar calculations for compound **108a** lead to results which were difficult to rationalise; however, there appears to be an additional interaction between solvents and solutes which was not observed for compound **109b**.

3.5 X-Ray Structural Analysis of Compound 108a

Crystals of compound **108a** obtained by slow evaporation of a dichloromethane:hexane solution (1:1 v/v) were of suitable quality for X-ray analysis which was performed by Dr. A. Batsanov. The structure of compound **108a** is shown in fig.3.8 together with the atomic numbering scheme The asymmetric unit of compound **108a** contains two independent molecules with equivalent bond lengths. The structure revealed that the molecule was highly distorted, with the fused anthracene units folded along the C(9)....C(10) vector by 35

and 32°. Both molecules were folded into a U-shape, folding (in the same direction) at C(16), C(4a)....C(10) vector, C(8)....C(9a) vector, C(11) and S(1)...S(2) vector by 9.4, 22.2, 28.9, 4.1, and 10.0°, respectively, in one molecule and correspondingly by 10.0, 22.8, 29.5, 6.7, and 12.2° in the other. The crystal packing presents adjacent molecules embracing each other: there was, however, no stacking patterns or short S....S interactions, presumably due to the non-planar geometry of the molecule. There was, also, no charge transfer observable within this structure with all bond lengths identical to those expected for the neutral species.

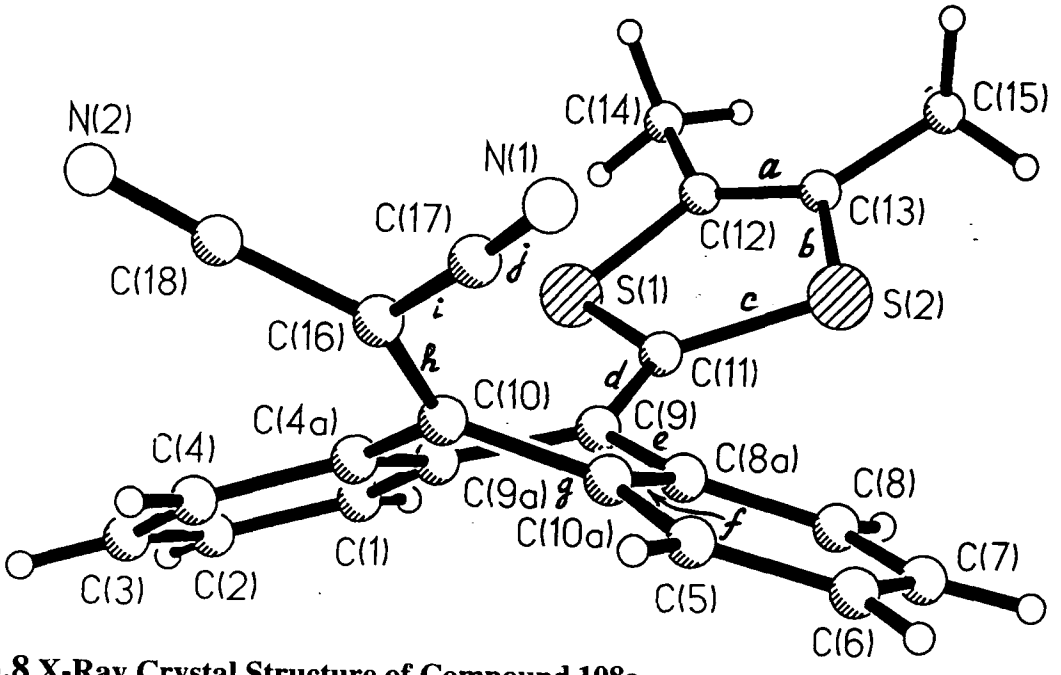

Fig.3.8 X-Ray Crystal Structure of Compound 108a

The lack of charge transfer in the solid state structure was unexpected as compound **86b** exhibited a significant degree of charge transfer as revealed by X-ray crystallography (Section 2.4.5). In compound **86b** the only stabilising effects following charge transfer was the formation of the 1,3-dithiolium cation and the stabilising effect of the dicyanomethylene unit on the negative charge. Whereas in compound **108a**, we expected the aromaticity of the anthracene spacer unit to produce materials with extensive charge transfer in the solid state. This result lead us to investigate further the nature of charge transfer within compound **108a** and with that in mind we studied the excitation kinetics utilising ultra-fast spectroscopy.

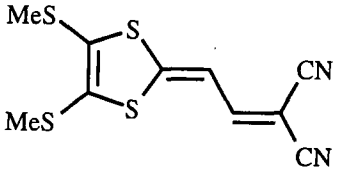

86b

3.6. Ultra-fast Spectroscopy of Compound 108a

Compound **108a** was studied by Dr. I. Lednev, Dr. J. N. Moore and Prof. R. Hester using ultra-fast spectroscopic techniques in order to acquire information about the nature of the charge transfer observed. It was again observed that compound **108a** exhibited a marked solvatochromic response and also weak luminescence in cyclohexane and chloroform solution, the lifetimes of luminescence being 170 and 500 ps, respectively (Table 3.3, fig 3.9).

Solvent	solvent polarity	λ_{max} /nm	$\lambda_{lumines}$ /nm	lumines. intensity	$\Delta\lambda_{stokes}$ /nm	lifetime /ps
C_6H_{12}	2.0	542	590	weak	48	ca. 500
$CHCl_3$	4.8	571	658	very weak	87	170
CH_3CN	37.5	553	-	-	-	-
H_2O	77	592	-	-	-	-

Table 3.2 Absorption and Luminescence Characteristics of Compound 108a

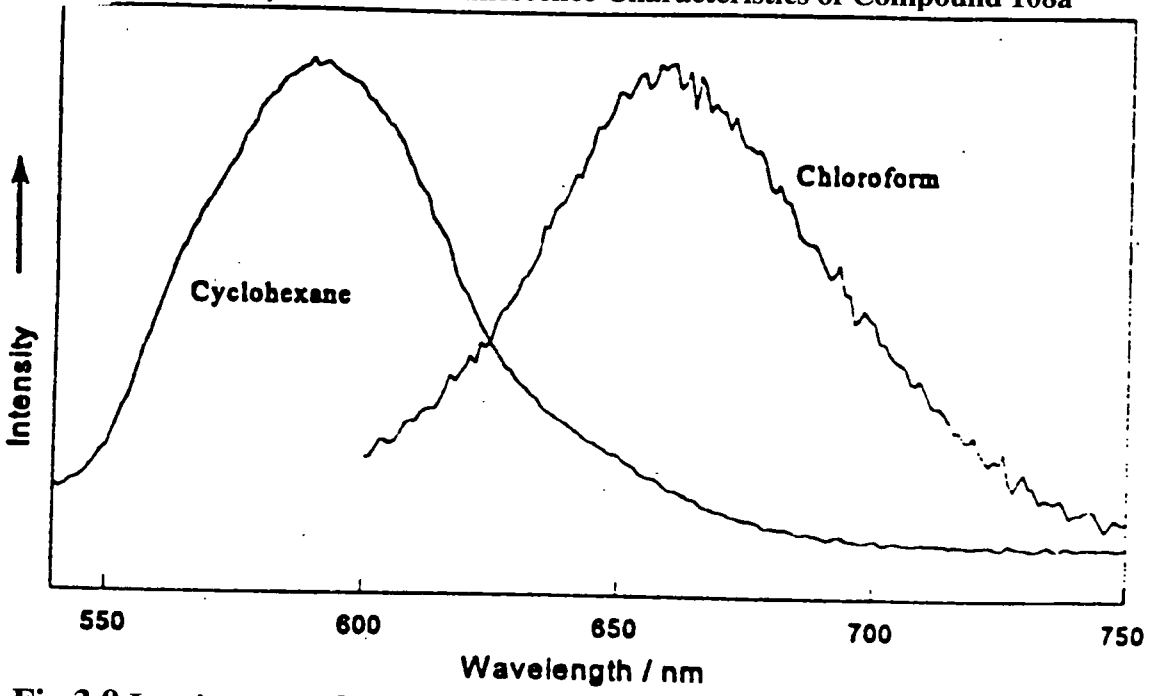

Fig 3.9 Luminescence Spectra of 108a in Cyclohexane and Chloroform

The red shift of λ_{max} with increasing solvent polarity agrees with the increase in Stokes shift for the luminescence bands with increasing solvent polarity (Table 3.2). Thus, both the charge transfer absorption and $\lambda_{lumines}$ strongly depend on the solvent polarity which is indicative that the nature of excitation in compound **108a** was zwitterionic. All transient spectra exhibit a gain at wavelengths longer than *ca.* 750

nm following UV or visible light excitation. There were neither ground state absorptions nor luminescence within this spectral region. The stimulated emission at $\lambda >$ *ca.* 750 nm cannot be attributed to the same excited state that is responsible for luminescence on steady state photolysis, which is indicative of at least two excited states. One possibility for this stimulated emission is a Twisted Intramolecular Charge Transfer state (TICT) and the formation of TICT states is more thermodynamically probable at higher solvent polarity as the luminescent transition states consist of zwitterionic species.

3.6.1 Photoexcitation of Compound 108a

When compound **108a** absorbs a photon the transition S_0 to S_1 occurs, which then either returns to S_0 emitting a quantity of energy hν producing a charge transfer band in the UV-VIS spectra (fig.3.10). This then exhibits luminescence at lower energy which is quenched due to the formation of the TICT state at even lower energy which is more prevalent in solvents with higher polarity. This explains why the luminescence lifetime in cyclohexane solution was greater than in chloroform.

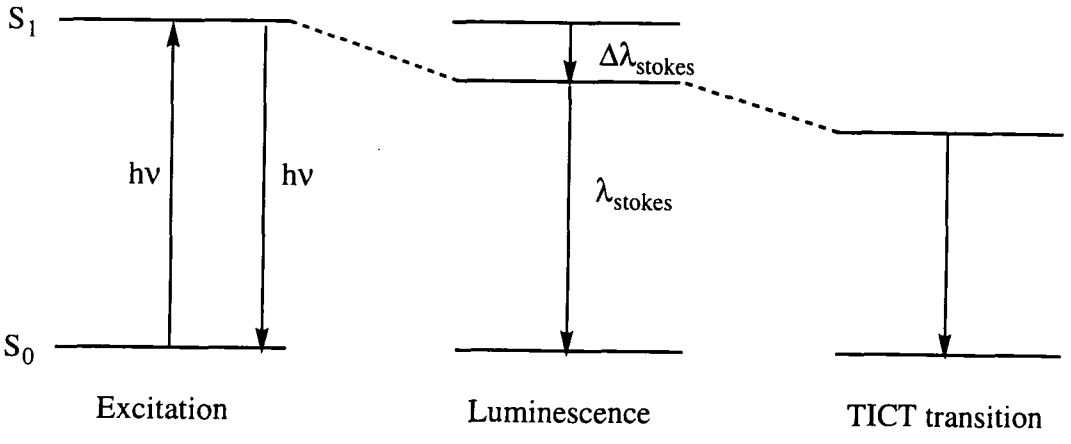

Fig.3.10 Photoexcitation in Compound 108a

3.6.2 The Nature of Excited States

On excitation electrons flow in an intramolecular fashion from the donor to the acceptor as expected leading to a zwitterionic intermediate, which was exemplified by compound **108a** exhibiting positive solvatochromism. This then interconverts to another singlet state at lower energy from which it luminesces. This state is still zwitterionic but more stabilised than S_1 by the Stokes energy and was assigned to the twisted structure initially postulated in Section 3.1. This twisted species was then able to deactivate *via* the TICT state back to S_0 (fig 3.11).

The current favoured method of TICT deactivation of photoexcited **108a** consists of a twisting about the C-C bond linking the dithiole donor unit to the anthracene spacer unit with a similar twist about the C-C bond to the dicyanomethylene unit. This could place the dithiolium cation close to a nitrogen on the dicyanomethylene anion possibly leading to the observed deactivation..

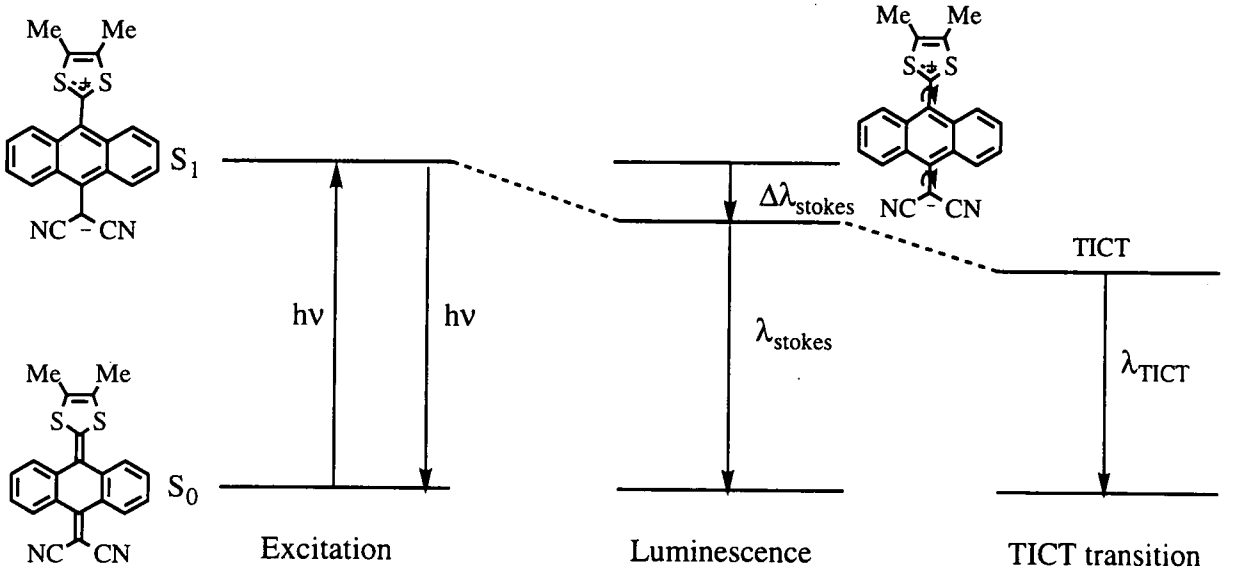

Fig. 3.11 Structural Modification Upon Photoexcitation

3.7 Cyclic Voltammetry Data

The solution CV data for compounds **108a-d** and **109a-d** were obtained under standard conditions (Section 7.1). Each exhibited a reversible oxidation corresponding to the formation of the radical cation of the 1,3-dithiole donor unit. Similarly, a reversible reduction wave corresponding to the formation of the radical anion of the acceptor was seen which is expected to be localised on the dicyanomethylene and cyanoimine groups, respectively.[82] Along with this reduction wave a second irreversible reduction wave was observed at lower potential which was attributed to a one electron reduction of the anthracene unit which is known to occur at comparable potentials under the same experimental conditions. The half wave potentials for compounds **108a-d** and **109a-d** as well as data for TTF, TCNQ, and anthracene are summarised in Table 3.3.

For both derivatives the lowest first oxidation potential was observed for the electron donating dimethyl derivatives **108a** and **109a**. There was a subsequent anodic shift with decreasing donor strength: *viz.* Me>SMe>H>SCH_2CH_2S for compounds **108a-d**.

Similarly the first reduction potential exhibit a similar trend, with the more negative (i.e. the worst acceptor) being compound **108a** with a similar cathodic shift with decreasing donor strength. Again data for compounds **109a-d** did not exhibit the same trends, with compound **109d** possessing the lowest reduction potential; however, these materials have been previously shown to produce anomalous charge transfer bands at lower energy than the corresponding dicyanomethylene systems.

Compound	$E^1_{1/2}$ ox/V[a]	$E^2_{1/2}$ ox/V	$E^1_{1/2}$ red/V	$E^2_{1/2}$ red/V
108a	0.892	-	-0.855	-1.286
108b	0.923	-	-0.869	-
108c	0.993	-	-0.901	-1.289
108d	0.944	-	-0.971	-1.491
109a	0.856	-	-0.999	-1.519
109b	0.974	-	-1.042	-1.511
109c	0.800	-	-1.004	-1.500
109d	0.972	-	-0.949	-1.365
TTF	0.36	0.70	-	-
TCNQ	-	-	0.22	-0.36
Anthracene	-	-	-	-1.40

[a] performed *vs* SCE; CH_2Cl_2; 0.1mol/dm^{-3} Bu_4NClO_4; scan rate 200 mV/s

Table 3.3 Cyclic Voltammetry Data for Compounds 108 and 109

3.8 Conclusions

We have synthesised a variety of functionalised 1,3-dithiole derived donor-π-acceptor systems linked to dicyanomethylene and cyanoimine acceptor units *via* an anthracene spacer. Both series of compounds exhibited low energy charge transfer absorption bands in the UV-VIS spectra attributed to intramolecular electron motion from the donor to the acceptor. Functionalisation of the donor fragment with electron releasing methyl units produced charge transfer bands with a lower energy absorption. The methylthio group has been shown to be a similar donor to the unfunctionalised systems with the ethylenedithio derivatives acting as moderate electron donors. Both series of compounds exhibit solvatochromism and a detailed study of cyanoimine derivative **109a** indicated that charge transfer from donor to acceptor does occur leading to a zwitterionic excited state. Compound **108a** has also been studied by ultra fast absorption spectroscopy and shown to luminesce *via* two independent pathways of which one has been attributed to a species in which the dithiolium cations are

twisted out of plane compared to the anthracene spacer unit. Cyclic voltammograms of these species show the presence of two active redox sites, namely the donor and the acceptor moieties. X-ray crystallography of compound **108a** indicates that there was no charge separation in the ground state; however, charge separation in solution has been demonstrated by other techniques.

Chapter 4

Tetrathiafulvalene and Related 1,3-Dithiole Derived Donor-π-Acceptor Systems

4.1 Introduction to Tetrathiafulvalene Chemistry

The propensity of tetrathiafulvalene (TTF) **2** (Section 1.1) to undergo a variety of reactions has led to the formation of a multitude of new TTF derivatives. TTF may be functionalised by two completely independent routes. The most direct route is *via* the lithiation of TTF followed by addition of an electrophile, whilst a more complex method involves the coupling two 1,3-dithiole-2-one (or 2-thione) units. This chapter will be concerned with a brief review of monofunctionalised TTF synthesis and the subsequent formation of monofunctionalised TTF and 1,3-dithiole-2-thione donor-π-acceptor systems.

4.1.1 Lithiation of TTF

The lithiation of TTF **2** was first reported by Green in 1977, in which he successfully converted TTF **2** into mono-lithio TTF (TTF-Li) **110** *via* the addition of an equimolar amount of ^{n}BuLi or LDA.[83] TTF-Li **110** is stable in solution under an inert atmosphere only at low temperatures (-70°C), higher temperatures leading to disproportionation into multi-lithiated species and TTF **2**. Green showed that TTF-Li **110** was very susceptible to electrophilic attack to afford a wide variety of substituted products (Scheme 4.1, Table 4.1).[84]

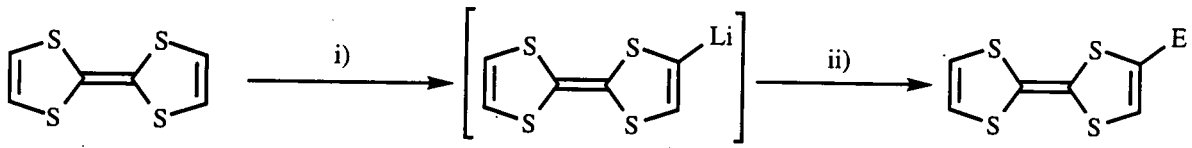

2 **110** **111-117**

Scheme 4.1 Lithiation of TTF 2 Reagents i) ^{n}BuLi/LDA -78°C, THF. ii) Electrophile (E^{+})

Electrophile	Product	Yield %
DMF	TTF-CHO **111**	44
$ClCO_2Et$	TTF-CO_2Et **112**	50
CO_2	TTF-CO_2H **113**	60
MeC(O)Cl	TTF-C(O)Me **114**	67
Me_2SO_4	TTF-Me **115**	80
HCOH	TTF-CH_2OH **116**	34
$Et_3O^{+}PF_6^{-}$	TTF-Et **117**	45

Table 4.1 Reactions of TTF-Li 110 With Electrophiles

Lithiation of substituted TTF derivatives is influenced by the type of substituent(s) present. Green showed that an electron donating substituent lowers the acidity of the proton on the same dithiole unit. Thus, mono-lithiation of methyl-TTF **115** followed addition of an electrophile, *e.g.* ethylchloroformate, produces compound **118** exclusively, whilst di-lithiation affords **119** (Scheme 4.2).

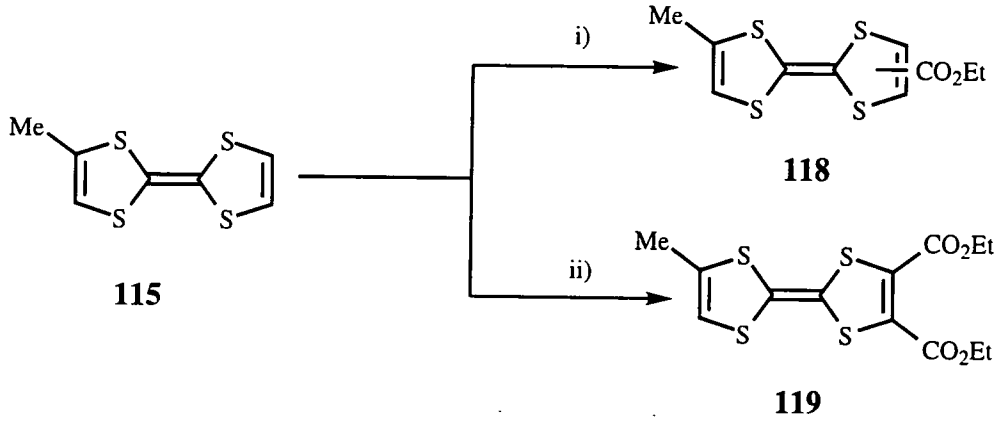

Scheme 4.2 Effect of Electron Donating Substituents Reagents i) LDA, $ClCO_2Et$ (1 equiv.), ii) LDA, $ClCO_2Et$ (2 equiv.)

Similarly, the presence of an electron withdrawing substituent on TTF renders the adjacent proton more acidic and therefore lithiation of **112** occurs adjacent to the substituent yielding **120** following addition of ethylchloroformate (Scheme 4.3).

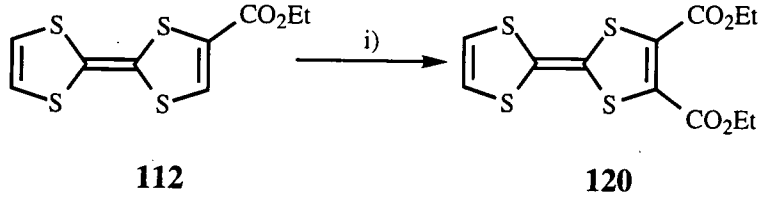

Scheme 4.2 Effect of Electron Withdrawing Substituents Reagents i) LDA, $ClCO_2Et$ (1 equiv.)

Generally, in all reactions to form mono-lithiated TTF, a small amount of multi-lithiated TTF is also formed. This fact is attributed to lithio-TTF **110** disproportionating into multi lithio species even at temperatures as low as -78°C. Thus for exclusive monolithiation of TTF in high yield a strict reaction protocol must be adhered to:-

1) The reaction temperature must be maintained below -70°C.
2) A precisely equimolar amount of LDA(or $^{n}BuLi$) must be added.

3) The reaction must be performed under dilute conditions to prevent TTF from precipitating from solution.

4.1.2 Coupling Methods to Functionalised TTF Derivatives.

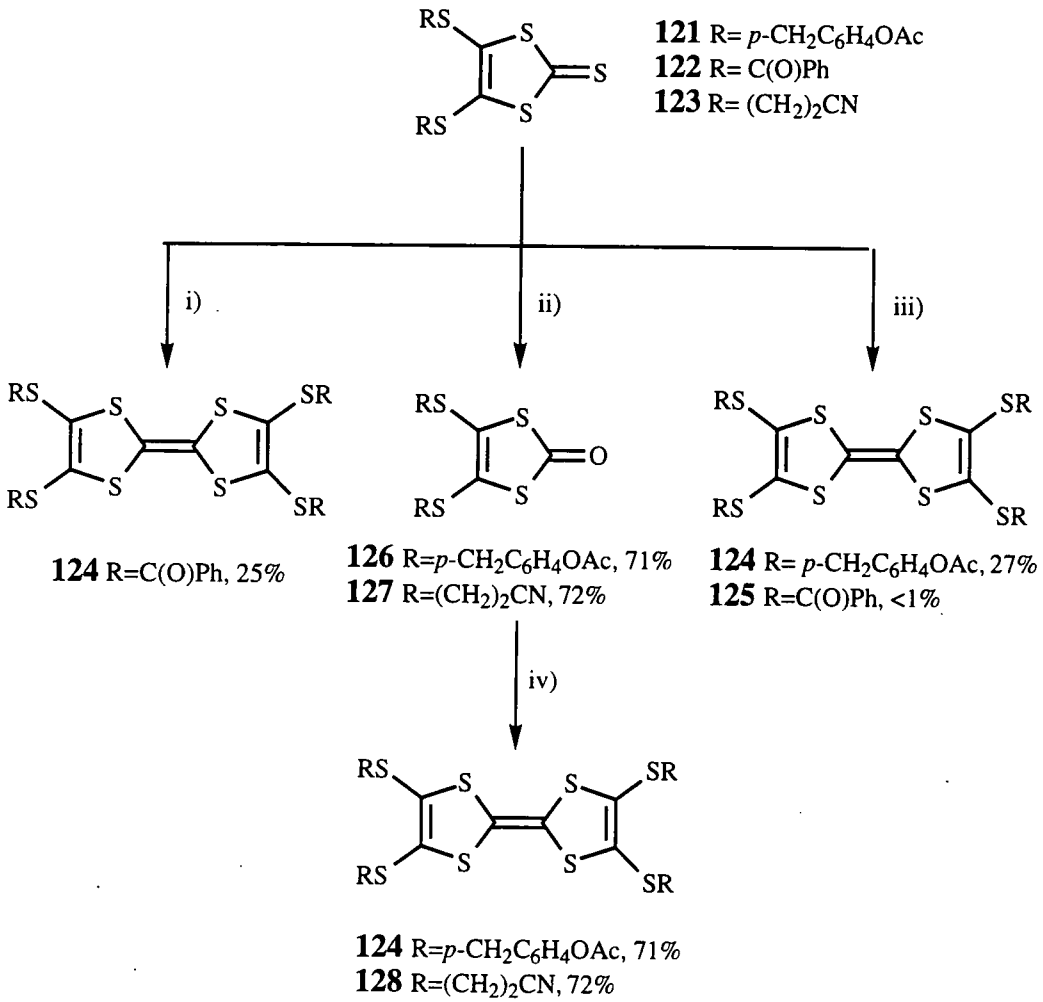

Scheme 4.4 Cross-coupling Methods to Functionalised TTF's Reagents i) $Co_2(CO)_8$, ii) $Hg(OAc)_2$, iii) and iv) $P(OEt)_3$

An alternative method to that described in Section 4.1.1 for the formation of functionalised TTF derivatives involves the coupling or cross-coupling of 1,3-dithiole-2-thione (or 2-one) units. Generally trialkyl phosphite mediated coupling proceeds efficiently affording the desired TTF derivative in good to excellent yields although for some substituents careful choice of coupling reagents is necessary. This is exemplified in Scheme 4.4 in which the self coupling of compound **122** to yield **125** occurs in less than 1% yield when triethyl phosphite is utilised.[85,86] In contrast, the identical reaction utilising dicobalt octacarbonyl to produce **124** occurs in 25% yield.[87] Coupling of compound **121** in triethylphosphite yields compound **124** in only

27% and any attempt to couple compound **123** in this manner failed to yield any of the desired TTF derivative **128**. The conversion of the thione unit of **121** and **123** into the more reactive ketones **126** and **127** may be achieved using mercuric acetate. The ketone unit may then be coupled to the desired TTF derivatives **124** and **128** in 71 and 72% yields respectively.[88,89] It is evident that in order to synthesise functionalised TTF derivatives by coupling methods a great deal of experimentation is required to achieve these transformations in good yields.

4.1.2.2 Coupling Methods to Monofunctionalised TTF Derivatives.

The corresponding reaction to form mono-functionalised TTF derivatives involving the cross coupling of a mono-functionalised thione or ketone **129** with vinylene trithiocarbonate **132** often occurs in extremely low yields. These reactions usually result in a complex mixture of products which requires extensive chromatography in order to isolate the desired product, and there are several functional groups which are incompatible to cross-coupling methodology. An improved yield is often achieved *via* cross coupling the desired mono functionalised dithiole-2-thione (or -2-one) **129** with 4,5-dicarbomethoxy-1,3-dithiole-2-thione (or -2-one) **130** X=O, **74** X=S. This yields the tris-functionalised TTF **131** which may be converted into the desired monofunctionalised TTF derivative **133** by the action of lithium bromide in HMPA.

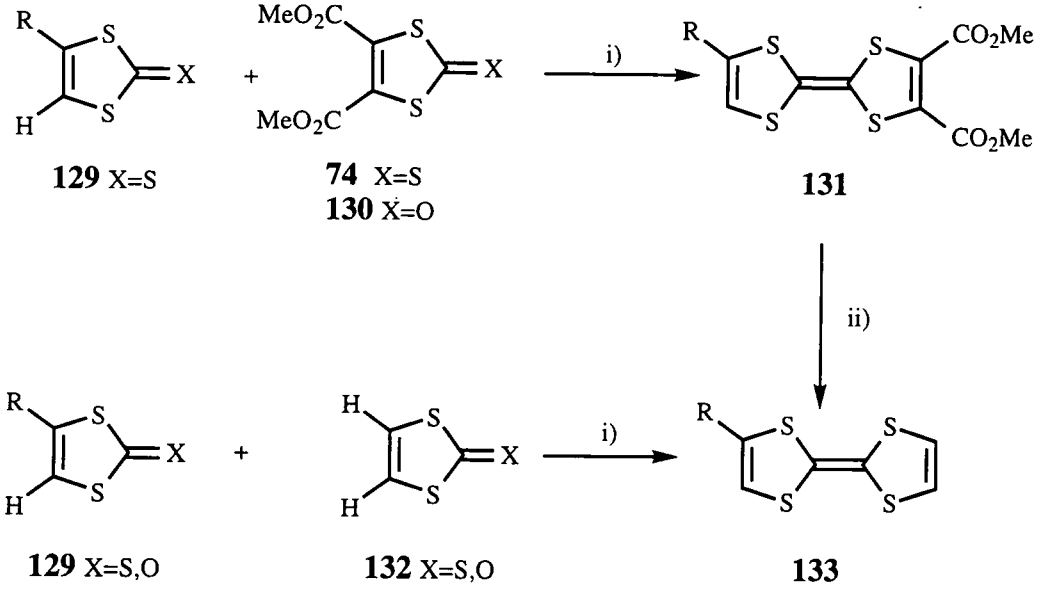

129 X=S **74** X=S **130** X=O **131**

129 X=S,O **132** X=S,O **133**

Scheme 4.5 Synthesis of Mono-functionalised TTF Derivatives Reagents i) $P(OMe)_3$, ii) LiBr, HMPA

4.2 Reactions of TTF-carboxaldehyde

Green reported that the reaction of lithio-TTF **110** with DMF yielded TTF-carboxaldehyde **111** in 44% yield.[90] However, previous work performed in Durham found this reaction to be highly capricious with isolated yields often as low as 5%, however using *N*-methyl-formanalide as a formylating reagent gave **111** in a much improved 85% yield.[90] Furthermore, it is well known that TTF-carboxaldehyde is highly reactive towards Wittig and Wittig-Horner Emmons derivatives and a variety of vinyl TTF derivatives **134-136** have been synthesised.[91,92,93]

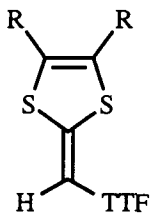

134

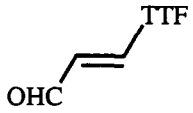

135

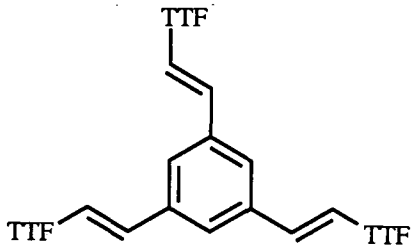

136

4.2.2 Intramolecular Donor-Acceptor Systems Based on TTF

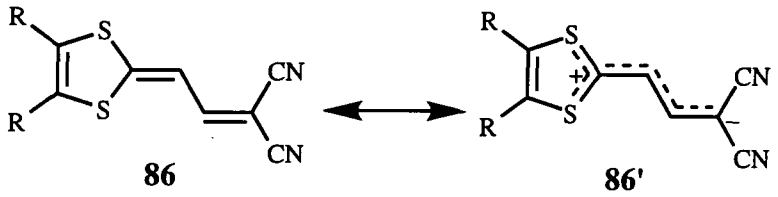

86 **86'**

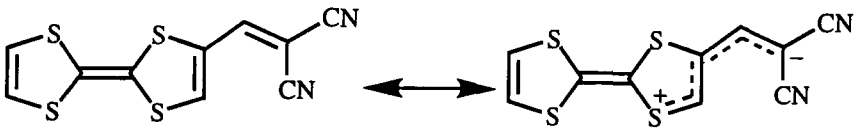

137 **137'**

Scheme 4.6 Differing Modes of Charge Transfer in 1,3-Dithiole and TTF Derived Donor-π-Acceptor Systems

The basic framework of TTF has been extensively modified to produce materials with a range of conductivity properties (Section 1.1.2). However, to date TTF has received only scant attention within the field of intramolecular donor-π-acceptor systems which is surprising as TTF is a powerful electron donor and would be expected to produce a variety of donor-acceptor systems analogous to the materials extensively

studied in chapters 2 and 3. The only conceivable difference between systems such as **86** (Section 2.4.2) and comparable TTF derived donor-acceptor system **137** is the nature of the charge transfer due to the different positions of the acceptor unit with respect to the donor (Scheme 4.6).

In the systems with a 1,3-dithiole donor linked to an acceptor *via* the C(2) position of the dithiole, intramolecular charge transfer was observed both in the UV-VIS spectra and by X-ray crystallography (Section 2.4.5). However, in the case of the prototype TTF system **137**, the acceptor is linked to C(4) and thus the nature of the electron transfer could be markedly different. The source of π-electron donation occurs from the dithiole sulfur atoms in both cases. However there is only one conjugated sulfur atom in the TTF system whereas for the dithiole there is two. Thus, the aim of this chapter is to investigate whether TTF can utilise its strong electron donor ability to produce donor-π-acceptor systems which exhibit improved intramolecular electron transfer properties compared to the compound **86**.

4.3 Synthesis of TTF Derived Donor-π-Acceptor Systems

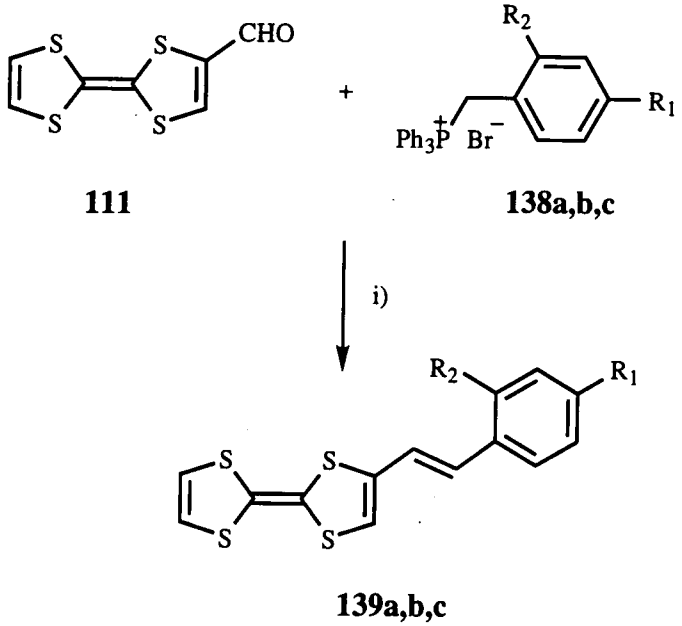

111 **138a,b,c**

139a,b,c

Scheme 4.7 Synthesis of Compounds 139a-c Reagents i) Et_3N, DCM 20°C or benzene, reflux

The reaction of TTF carboxaldehyde **111** with a variety of electron withdrawing aromatic Wittig reagents **138a-c** yielded TTF donor-acceptor systems **139a-c**. To a solution of Wittig reagent **138a-c** in dichloromethane was added triethylamine which produced an immediate colour change from yellow to deep red corresponding to the

formation of the phosphorus stabilised ylid, to which TTF-carboxaldehyde **111** was added. The ^1H NMR spectra of these materials indicated that both *cis* and *trans* isomers of **139a-c** were present, which proved to be inseparable by chromatography or recrystallisation. However, refluxing the isomer mixtures in benzene for 2-3 hours resulted in the isolation of the *trans* isomer as the sole product in each case, without the need for further chromatography (Scheme 4.7).

4.3.1 UV-VIS Spectra of TTF-π-Acceptor systems

Compounds **139a,b,c** were isolated as purple/black solids in 67-80% yield and their UV spectra reveal the presence of a charge transfer band at low energy (Table 4.2).

Compound	R_1	R_2	λ_{max}/nm	$E/10^3 M^{-1}cm^{-1}$
139a	NO_2	H	502	3.55
139b	H	NO_2	467	4.67
139c	CN	H	460	3.73

Table 4.2 UV-VIS Data for compounds 139a-c

The extinction coefficient of these charge transfer bands was low (*ca.* 3×10^3 $M^{-1}cm^{-1}$) compared to the corresponding dithiole derivative for which these values are an order of magnitude higher (Section 2.4.3). This is indicative that the charge separated species is not particularly prevalent even in the excited state and that the majority of the molecules remain in their ground state on UV excitation. This is presumably due to the nature of the charge transfer occurring within these systems, where the electron transfer occurs in the opposing direction to that observed in chapter 2. The discrepancy in the extinction coefficients between the two types of systems can be explained by the amount of available π-donation which is more limited in the case of the TTF derivatives. The acceptor strength being:-

$$p\text{-}NO_2 > o\text{-}NO_2 > p\text{-}CN$$

The fact that the *para* nitro derivative **139a** has a lower energy charge transfer band than the *ortho* nitro **139b** can be attributed to the increased length of the conjugated link between the donor and acceptor moieties in the former compound which will reduce the HOMO-LUMO energy gap.

Compound **41** previously reported by Katz *et al* [94] is the closest analogue to compound **139a** with the TTF donor exchanged for the 1,3-dithiole unit. It is, therefore, possible to compare directly the effects that the two donor units have on the position and nature of the intramolecular charge transfer properties.

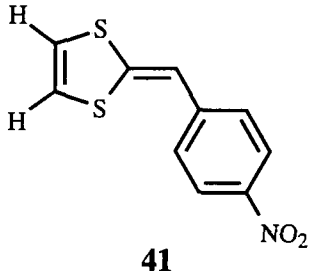

41

Compound	λ_{max}	$E/10^3 M^{-1}cm^{-1}$
139a	508	3.55
41	446	49.8

Table 4.3 UV-VIS Data for compounds 139a and 41

As can be seen from Table 4.3 even though the dithiole system **41** exhibits a larger extinction coefficient, the TTF derivative **139a** produces a markedly red shifted charge transfer band, confirming that the increased donor ability of TTF produces an excellent prototype donor-acceptor system.

4.3.2 Synthesis of Trimethyl TTF Derivatives

In order to increase, still further, the amount of intramolecular charge transfer, a superior donor unit to the parent TTF was required. We, therefore, turned our attention to trimethyl-TTF (Trim-TTF) which has the following advantages over TTF:

1) The presence of the three methyl groups prevents multi lithiation, which can be a major problem with TTF.
2) The methyl substituents lower the oxidation potential of Trim-TTF with respect to TTF, thus increasing the donor ability.
3)Trim-TTF is obtained in multigram quantities *via* a modified literature procedure developed by Moore and Bryce, and its reaction with *N*-methyl formanalide to yield Trim-TTF-carboxaldehyde **140** in 84% yield, which undergoes similar reactions to TTF carboxaldehyde **111**.[95]

Treatment of Trim-TTF-carboxaldehyde **140** with the pre-formed ylid of *para* -nitrobenzyltriphenylphosphonium bromide **138a** (derived from the Wittig reagent **138a** and triethylamine) in benzene afforded **141** as the *trans* isomer in 62% yield (Scheme 4.8). Attempts to purify this compound (or indeed any Trim-TTF derivative) using silica gel resulted in decomposition, which is attributed to the acidity of silica which could protonate the central double bond in Trim-TTF: all products were, therefore, chromatographed on neutral alumina with acid-free solvents.

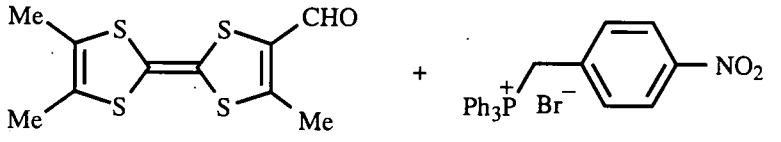

140 **138a**

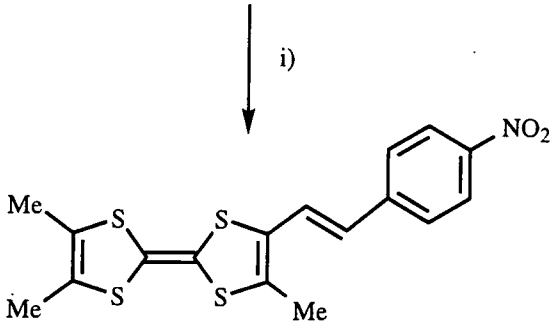

141

Scheme 4.8 Synthesis of Trim TTF Donor-π-Acceptor System 141 Reagents i) Et_3N, Benzene, reflux

4.3.2.1 UV-VIS Spectra of Compound 141 and Similar Derivatives

Compound **141** was isolated as a black solid and its UV spectra exhibited a charge transfer band which was further red shifted compared to the parent derivative **139a**. In order to compare further the effect that TTF has on the position of the charge transfer band compound **142** was similarly synthesised from Wittig reagent **79a** (Section 2.4.1) and *para*-nitrobenzaldehyde **143** in acetonitrile and triethylamine producing compound **142** as bright purple crystals (Scheme 4.9).

The UV spectra of compounds **141** and **142** exhibited the expected low energy charge transfer bands, the data for which are collected in Table 4.4 along with data for compound **139a** for comparison.

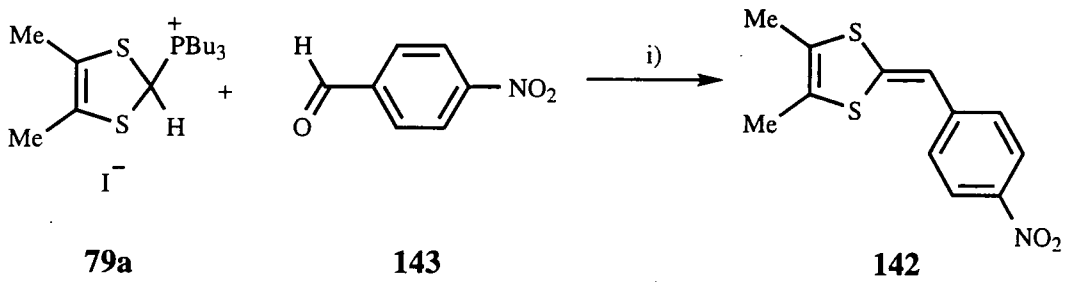

79a **143** **142**

Scheme 4.9 Synthesis of Compound 142 Reagents i) Et_3N, MeCN, 20°C

Compound	λ_{max}/nm	$E/10^3 M^{-1}cm^{-1}$
139a	502	3.55
141	517	7.12
142	467	21.4

Table 4.4 λ_{max} Values for Compounds 139a and 141-142

Converting the donor unit from TTF to Trim-TTF in compounds **139a** and **141** leads to a noticeable red shift in the position of λ_{max}. Both of these compounds possess a charge transfer band that was red shifted compared to compound **86** which contains a further conjugated sulfur than both compounds **139a** and **141**. Again it is noticeable that **142** possesses a charge transfer band that is blue shifted compared to the TTF derivatives.

4.3.3 Extending the Conjugated Spacer Between the Donor and the Acceptor

The linking of a donor and an acceptor unit by an increasing conjugated length generally causes the charge transfer band produced to be red shifted (Section 2.1.3). We therefore sought to explore this effect in our systems. Treatment of TTF carboxaldehyde **111** with formylmethylene triphenylphosphorane **101** in benzene produced compound **135**. It is interesting to note that a small amount of compound **144** was isolated, in which the desired compound reacts again with the Wittig reagent **101**, the yield of which increased with reaction time. Refluxing the reaction mixture for 24 hours led to the formation of a multitude of products, as indicated by TLC, which were inseparable by chromatography or recrystallisation. A previous report of this reaction made no mention of this competing side reaction.[90] Compound **135** undergoes similar reactions with Wittig reagents with the same ease as the parent TTF-carboxaldehyde **111** yielding compound **145** following treatment with Wittig

4.3.4 CV Data

The solution CV data for compounds **139a-c**, **141** and **145** were obtained under standard conditions (Section 7.1). As expected, two independent one-electron oxidation waves were observed, which were shifted anodically compared to the TTF and Trim-TTF due to the presence of the electron acceptor units. For compound **145** the oxidation potential was similarly anodically shifted compared to TTF due to the distance between the acceptor and the donor

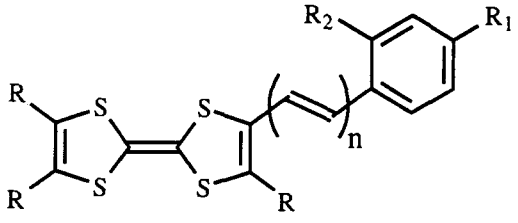

139a R=H R_1=H R_2=NO_2 n=0
139b R=H R_1=NO_2 R_2=H n=0
139c R=H R_1=H R_2=CN n=0
141 R=Me R_1=H R_2=NO_2 n=0
145 R=H R_1=H R_2=NO_2 n=1

Compound	$E^1_{ox}/V^{a,}$	E^2_{ox}/V^a
139a	0.45	0.77
139b	0.45	0.81
139c	0.45	0.81
141	0.37	0.74
145	0.42	0.78
TTF	0.43	0.77
Trim-TTF	0.29	0.69

[a] All values are the corresponding half wave potentials

Table 4.6 CV Data for TTF and Trim-TTF Donor-π-Acceptors

4.4 Dicyanomethylene Acceptor Systems

In order to modify further the position of any charge transfer band we recognised that TTF-derived donor-acceptor systems with more powerful acceptor units (*e.g.* dicyanomethylene **137** and cyanoimine **146** groups described previously in chapters 2 and 3) were attractive targets. The conditions previously utilised to convert aldehydes

into dicyanomethylene and cyanoimine units (Section 2.4.2) were attempted. In all cases, however, no products corresponding to either compounds **137** or **146** were isolated (Scheme 4.11). This was disappointing as these systems appear to be ideal candidates for TTF-derived donor-acceptor units possessing both strong donor and acceptor units.

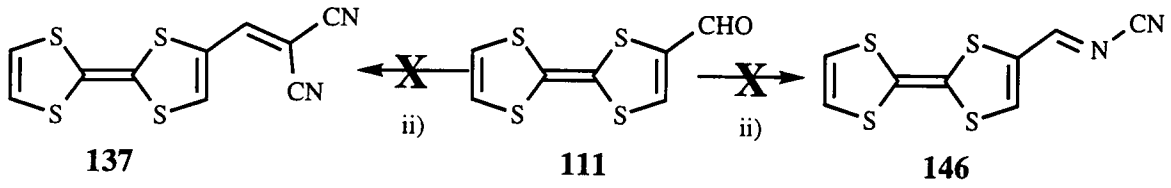

137 **111** **146**

Scheme 4.11 Attempted Synthesis of Compounds 137 and 146 Reagents i) $TiCl_4$, $CH_2(CN)_2$, pyridine, $CHCl_3$, ii) $TiCl_4$, BTC, $CHCl_3$

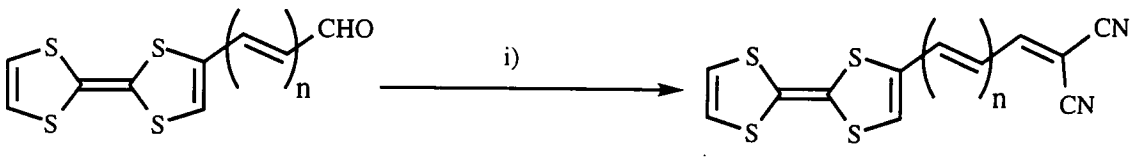

111 n=0
135 n=1

147 n=0
148 n=1

Scheme 4.12 Martín's Route to Compounds 147-148 Reagents i) $CH_2(CN)_2$, $AcONH_4$/AcOH, Benzene, reflux

Compound	λ_{max}/nm[a]	E^1_{ox}/V[b]	E^2_{ox}/V[b]	E^1_{red}/V[b]
111	475	0.60	1.03	-
135	500	0.59	1.00	-
147	624	0.69	0.97	-0.89
148	618	0.59	0.92	-0.88
TTF	-	0.43	0.77	

[a] CH_2Cl_2, [b] *vs.* SCE $Bu_4N^+ClO_4^-$, CH_2Cl_2, Scan rate 200 mV s^{-1}

Table 4.7 UV-VIS and CV Data

More recently compound **137** and analogues have been synthesised by Martín *et al* utilising a different methodology.[96] They report that TTF-carboxaldehyde **111** may be converted into the dicyanomethylene derivatives in excellent yields using ammonium acetate-acetic acid as a catalyst (Scheme 4.12). The UV spectra of these compounds exhibit the expected broad low energy absorption centred around 620 nm.

Interestingly, when a longer conjugated spacer was placed between the donor and the acceptor, the low energy absorption band was blue shifted in a manner analogous to that observed for the series **139a** to **144**. Similarly, on increasing the length of the conjugated spacer between the donor and the acceptor the oxidation potential of the TTF moiety decreased due to the separation of the acceptor unit from the site of oxidation. The UV spectra and cyclic voltammetric data are summarised in Table 4.7.

4.5 NLO Measurements of TTF Derived Donor-Acceptor Systems

NLO measurements of compounds **139a,c** were determined by Dr. I Ledoux using the EFISH technique previously mentioned in chapter 2. The values are summarised in Table 4.8, along with values for TTF-carboxaldehyde **111**.

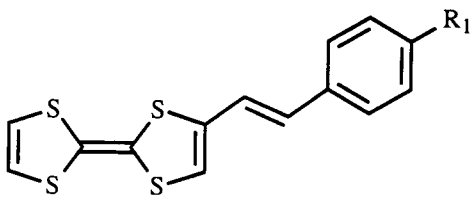

139a R=NO_2
139c R=CN

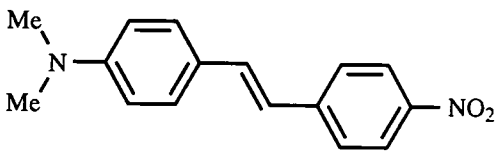

26

Compound	$\beta(0)/10^{-30}$esu[a,b]	$\beta/10^{-30}$esu[a,b]	μ/D	$\mu\beta(0)/10^{-48}$esu
111	-	18	4.8	85
139a	17	46	7.0	135
139c	17	36	6.7	115

[a] $1D=10^{-18}$esu

[b] Measured at 1340 nm

Table 4.8 EFISH Measurements

As can be seen, from Table 4.8, TTF-carboxaldehyde **111** exhibits NLO activity and the addition of an improved electron acceptor unit has a positive effect on the value of the dipole moment (μ) and the hyperpolarisability (β). However, a similar effect on $\beta(0)$ is not observed. These values demonstrate that although these systems are NLO active, their efficiency is quite poor. The value of $\mu\beta$ for a comparative aromatic donor unit **26** being 580 $x10^{-48}$ esu[97] compared to 322 x 10^{-48} esu for compound **139a**. Thus, although the TTF unit is an excellent donor which produces materials with large values of λ_{max}, the efficiency of these systems as NLO materials was disappointing.

4.6 1,3-Dithiole-2-thione Derived Donor-π-Acceptor Systems

As mentioned previously, the nature of π-electron donation in TTF donor-acceptor systems is different from the 1,3-dithiole donor-π-acceptor systems described previously. However, charge transfer was observed with the λ_{max} values for the TTF systems red shifted compared to similar 1,3-dithiole compounds. This begs the question: is it the powerful donor ability of TTF that enhances the intramolecular charge transfer, or would the simple 1,3-dithiole-2-thione derivatives **150** functionalised at the C(4) position perform as well?

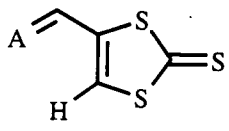

150 A=$CHC_6H_4NO_2$ or $C(CN)_2$

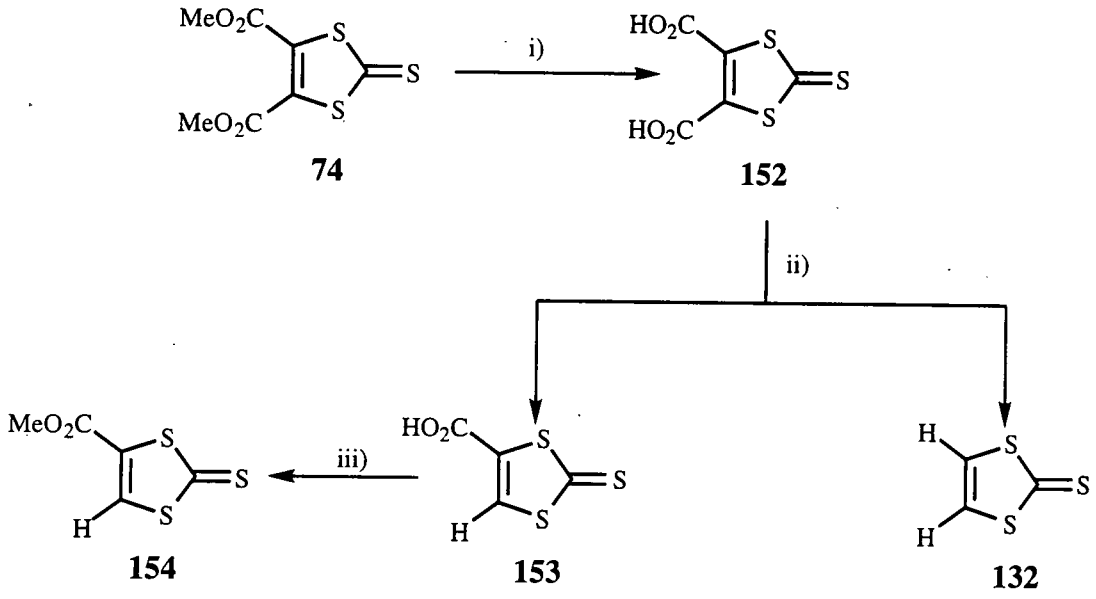

Scheme 4.13 Initial Synthetic Route to Compound 154 Reagents i) HCl, $MeCO_2H$, ii) Heat, iii) MeOH, c. H_2SO_4

Thus, our attention was drawn to a recent synthesis of 2-thioxo-1,3-dithiole-4-ylmethyl(triphenyl)phosphonium bromide **151** by Gorgues *et al*[98] which may be utilised in the synthesis of extended donor-acceptor systems comparable to those previously mentioned in chapter 2. The Wittig reagent was synthesised from the corresponding 4,5-dicarbomethoxy-1,3-dithiole-2-thione **74**[99] (Section 2.2.4). This rather cumbersome synthesis initially involves the hydrolysis[100] of the diester **74** to the diacid **152**[101] which can subsequently be monodecarboxylated to form mono acid

153 which is then re-esterified to the desired monoester **154** (Scheme 4.13).[102] The decarboxylation reaction, however, did not proceed in high yield (generally <20%) and often produced large quantities of the doubly decarboxylated product vinylenenetrithiocarbonate **132** leading to the abandonment of this route.

4.6.1 Thiadiazoles as 1,3-Dithiole Precursors

Whilst we were experiencing problems with Scheme 4.13, another route was reported involving the formation of a thiadiazole intermediate **155** which spontaneously ring opened when treated with base (potassium *tert*-butoxide or sodium hydride) to form the intermediate acetylenic thiolate **156** which was intercepted with carbon disulfide to form the desired 1,3-dithiole-2-thione derivatives **157** (Scheme 4.14).[103]

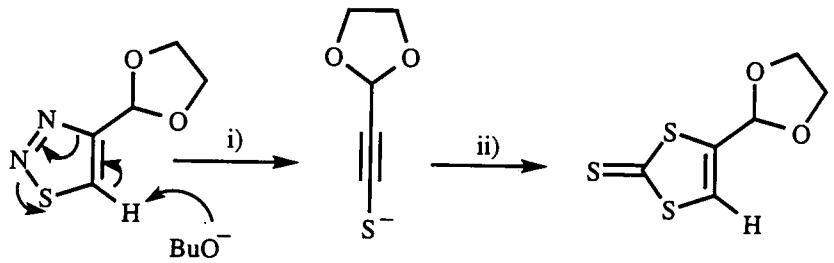

155 **156** **157**

Scheme 4.14 The Use of a Thiadiazole as a 1,3-Dithiole Intermediate Reagents i) KO^{t}Bu/^{t}BuOH, ii) CS_2

The thiadiazole of interest **158** can be prepared in three step (Scheme 4.15) from methylglyoxal **93** and ethyl carbazate **159** to afforded the *bis*imine **160** in 75% yield (Scheme 4.15) which was cyclised to yield the imine functionalised 1,2,3-thiadiazole **161** using thionyl chloride *via* a Hund-Mori reaction.[104] The imine **161** can be readily converted into the desired aldehyde **158** using formaldehyde and concentrated sulfuric acid. The reported yields of these steps are high, although the conversion of the aldehyde **158** into the 4-formyl-1,3-dithiole-2-thione **162** was not reported presumably because the electron withdrawing substituent interfered. To overcome this the aldehyde group was first converted to the acetal prior to formation of the dithiole which was subsequently removed to facilitate compound **162**.

153 which is then re-esterified to the desired monoester **154** (Scheme 4.13).[102] The decarboxylation reaction, however, did not proceed in high yield (generally <20%) and often produced large quantities of the doubly decarboxylated product vinylenenetrithiocarbonate **132** leading to the abandonment of this route.

4.6.1 Thiadiazoles as 1,3-Dithiole Precursors

Whilst we were experiencing problems with Scheme 4.13, another route was reported involving the formation of a thiadiazole intermediate **155** which spontaneously ring opened when treated with base (potassium *tert*-butoxide or sodium hydride) to form the intermediate acetylenic thiolate **156** which was intercepted with carbon disulfide to form the desired 1,3-dithiole-2-thione derivatives **157** (Scheme 4.14).[103]

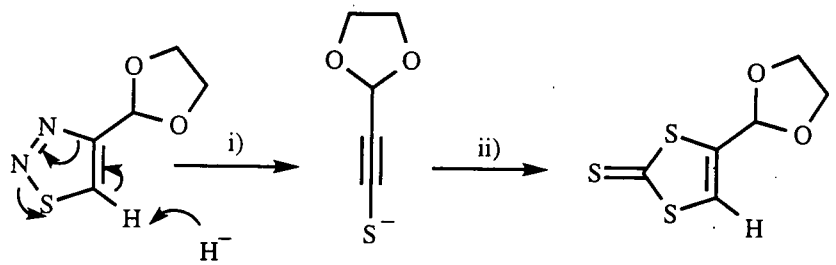

155 **156** **157**

Scheme 4.14 The Use of a Thiadiazole as a 1,3-Dithiole Intermediate Reagents i) $KO^tBu/^tBuOH$, ii) CS_2

The thiadiazole of interest **158** can be prepared in three step (Scheme 4.15) from methylglyoxal **93** and ethyl carbazate **159** to afforded the *bis*imine **160** in 75% yield (Scheme 4.15) which was cyclised to yield the imine functionalised 1,2,3-thiadiazole **161** using thionyl chloride *via* a Hund-Mori reaction.[104] The imine **161** can be readily converted into the desired aldehyde **158** using formaldehyde and concentrated sulfuric acid. The reported yields of these steps are high, although the conversion of the aldehyde **158** into the 4-formyl-1,3-dithiole-2-thione **162** was not reported presumably because the electron withdrawing substituent interfered. To overcome this the aldehyde group was first converted to the acetal prior to formation of the dithiole which was subsequently removed to facilitate compound **162**.

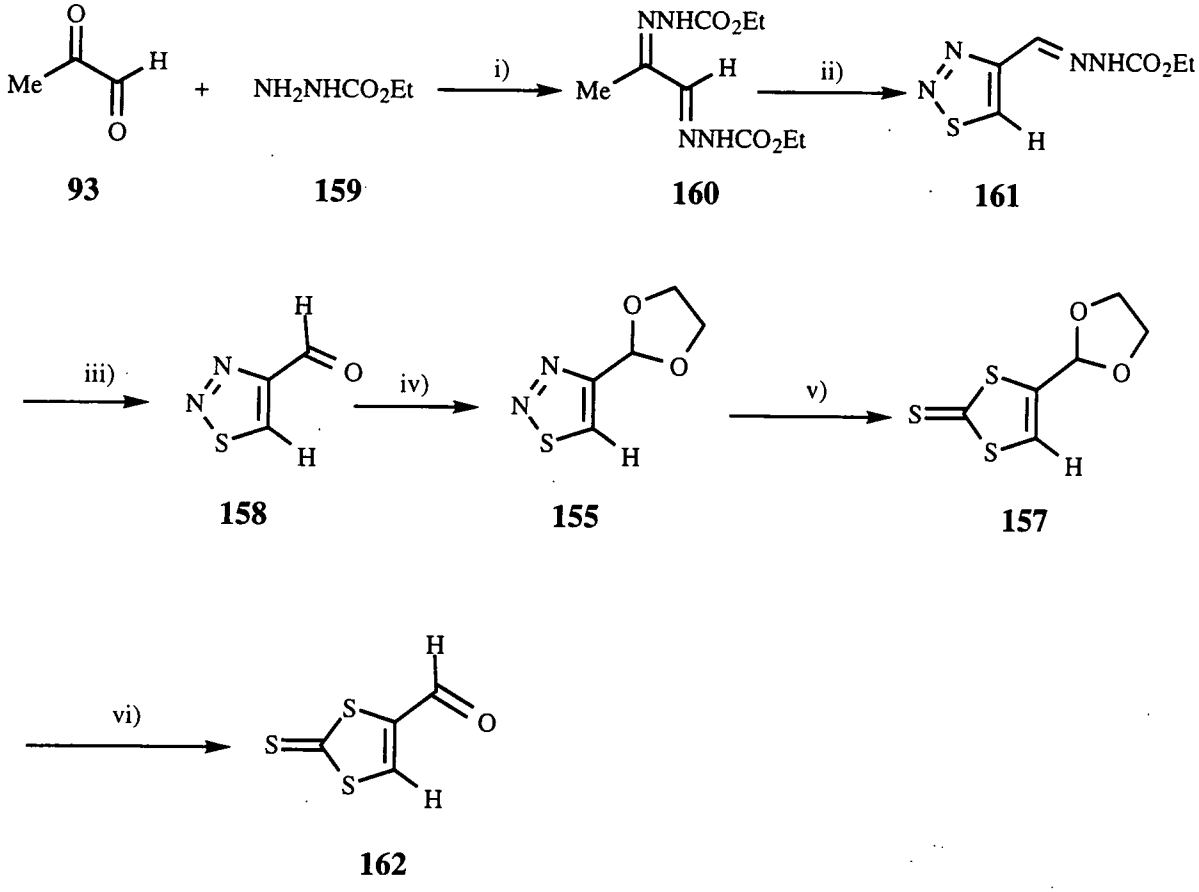

Scheme 4.15 Synthesis of 162 *Via* Thiadiazole Intermediate 157 Reagents i) EtOH, ii) $SOCl_2$, iii) HCHO, c. H_2SO_4, iv) $HOCH_2CH_2OH$, H^+, v) NaH, CS_2,, vi) H^+

4.6.2 A One-Pot Synthesis of 4-Carbomethoxy-1,3-dithiole-2-thione

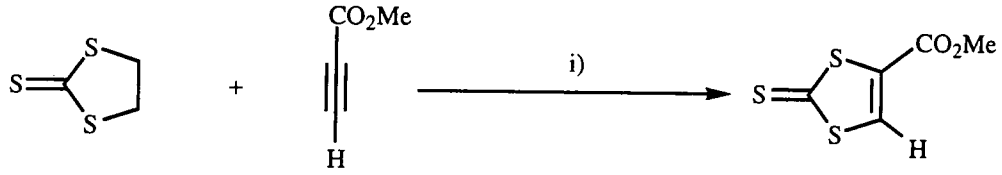

Scheme 4.16 A One-pot Route to Compound 154 Reagents i) xylene, reflux

A more suitable pathway for the synthesis of monoester **162** was devised which utilised methodology similar to that used in the synthesis of the diester **74** (Section 2.2.4) In the synthesis of **74**, ethylenetrithiocarbonate **72** reacts with DMAD **73** in a 3+2 cycloaddition reaction. If methylpropiolate **163** is employed instead of DMAD the monoester **154** is formed albeit in low yield <10%. The yield may, however, be

augmented by performing the reaction in refluxing xylene instead of the usual solvent toluene (Scheme 4.16).

4.6.3 Synthesis of Wittig Reagent 151

Monoester **154** was converted to the corresponding Wittig reagent **151** in a multi-stage synthesis. The first step being the selective reduction of the ester group to the alcohol using diisobutylaluminium hydride at low temperature. The choice of temperature in this reaction is critical as it is possible to produce either aldehyde **162** or alcohol **164** by modulating the reaction conditions. Alcohol **164** may similarly be prepared *via* the borohydride reduction of monoester **154** at room temperature in excellent yields[105] and this is currently the method of choice (Scheme 4.17).

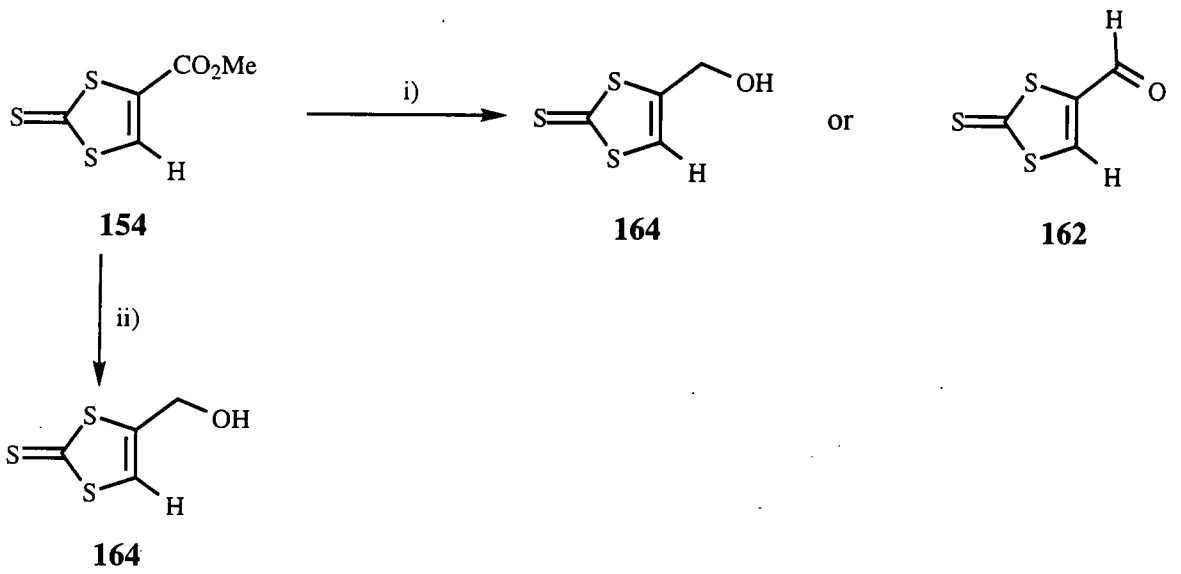

Scheme 4.17 Synthesis of Aldehyde 162 and Alcohol 164 Reagents i) DIBALH, -85 to -25°C, CH_2Cl_2 ii) $NaBH_4$, 20°C, MeOH

With alcohol **164** in hand, the synthesis of the Wittig reagent **151** is relatively straightforward producing the compound **151** in 35% overall yield from the alcohol **164**. Having successfully synthesised both the aldehyde **162** and the Wittig reagent **151** there was scope for a convergent synthetic pathway to C(4)-substituted 1,3-dithiole-2-thione donor-π-acceptor systems. An excellent comparative example of the usefulness of this was the synthesis of the *para*-nitrobenzyl donor-acceptor system **165** which could be directly compared to the previously discussed TTF derivative **139a**. Aldehyde **162** was, therefore, treated with *para*-nitrobenzyl triphenylphosphonium bromide **138a** in dichloromethane, utilising triethylamine as base, to yield **165** in good yield as the *trans* isomer. Under the similar conditions,

Wittig reagent **151** and *para*-nitrobenzaldehyde **143** yielded **165** which was identical to that prepared by the initial route (Scheme 4.18). In both cases, the ^1H NMR spectra indicated that the *trans* isomer is formed exclusively with no evidence for the *cis* isomer.

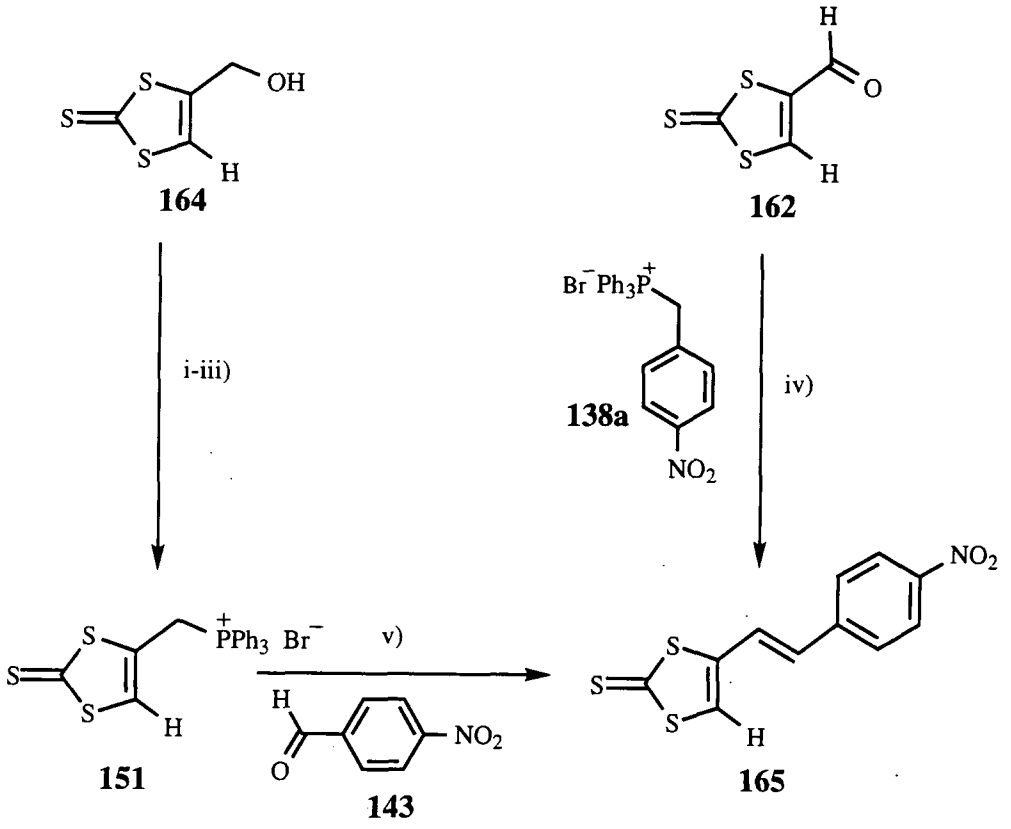

Scheme 4.18 Convergent Synthetic Pathway to Compound 165 Reagents i) Et_3N, MsCl, ii) Bu_4NBr, iii) PPh_3, iv and v) Et_3N

4.7 A Comparison of the UV-VIS Data.

Unlike the TTF donor-acceptor systems compound **165** was a yellow solid and a relatively high energy absorption band is observed at 415 nm in the UV-VIS spectra. This type of spectra is characteristic of 1,3-dithioles which generally absorb within the UV and near visible regions. This indicates that the nature of charge transfer in this dithiole system is different to that observed in the TTF systems and those previously described in chapter 2. Indeed what are the charge transfer characteristics in compound **165**?

As can be seen from Table 4.9, both of the TTF donor-acceptor systems and the C(2) substituted dithiole donor-acceptor systems exhibit charge transfer absorptions above 430 nm whereas compound **165** does not. The driving force for the C(2) substituted

dithiole donor-acceptor systems is the extra π donation that these systems implicitly exhibit, and the stabilising effect that the 1,3 dithiole unit has on the positive charge that is formed (Scheme 4.19). These two effects seem to indicate that the direction of any charge transfer for compound **165** is towards the thione sulfur which has previously been shown to be an excellent acceptor unit (Section 2.4.6).

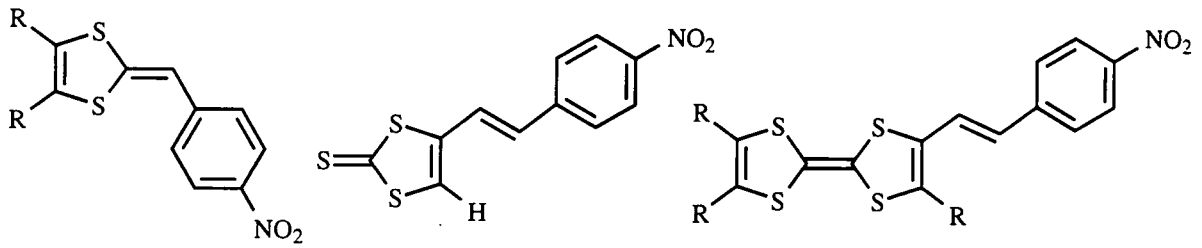

41 R=H
142 R=Me

165

139a R=H
141 R=Me

Compound	Colour	λ_{max}/nm
139a	Purple/Black	502
141	Black	517
165	Yellow	415
41	Purple	446
142	Purple	467

Table 4.9 UV-VIS Data for TTF and 1,3-Dithiole Donor-Acceptor Systems

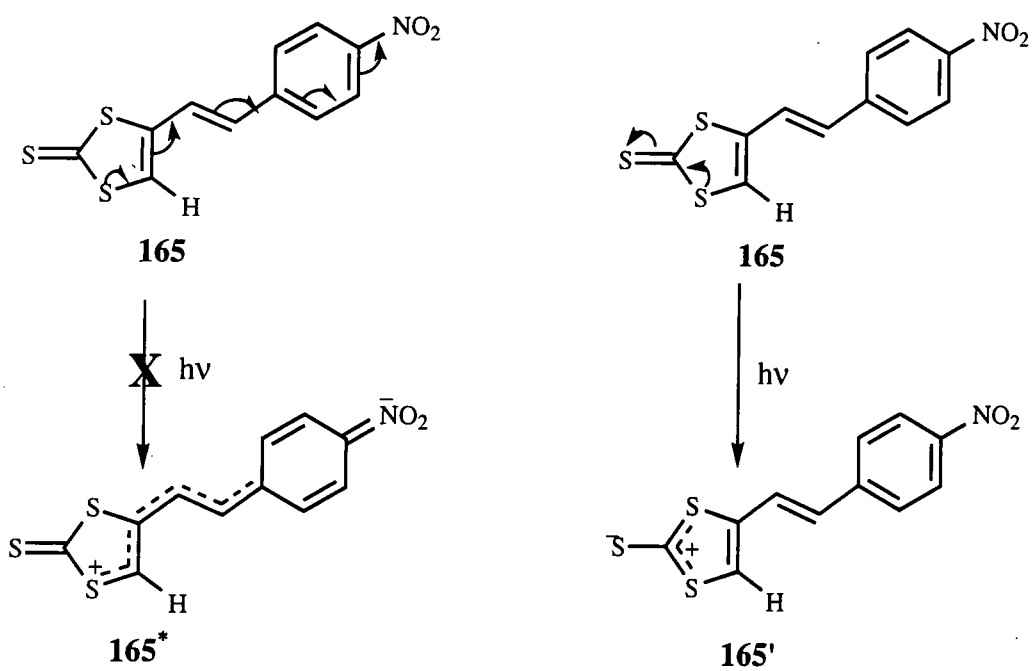

165 **165**

165* **165'**

Scheme 4.19 The Dual Mode of Charge Transfer in Compound 165

The thione unit must, therefore, be acting as an electron acceptor which appears to be superior to the corresponding dicyanomethylene systems **77a-c** (Section 2.4.6). It is worth noting that compounds **77** possess marked charge transfer properties but do not absorb in the visible region (even when functionalised with the electron donating methyl substituents) whereas the 1,3-dithiole-2-thione unit does (Table 4.10).

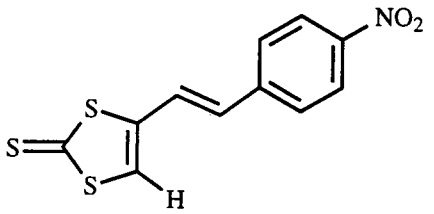

165

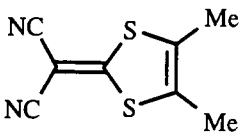

77a

Compound	λ_{max}/nm
165	415
77a	387

Table 4.10 UV-VIS Data For Compounds 77a and 165

The TTF and Trim-TTF derivatives **139a** and **141** also produce systems with red shifted charge transfer absorption frequencies compared to their corresponding dithiole-2-ylidene systems **41** and **142**: the addition of methyl substituents to both TTF and 1,3-dithiole units leads to the expected red shift compared to their parent systems (R=H). Thus, in conclusion, although the charge transfer within these TTF donor-acceptor systems is different in nature it is in fact superior to the 1,3-dithiole-2-ylidene donor-π-acceptor systems (chapter 2) which is attributed to the excellent donor properties of TTF.

4.8 Dicyanomethylene Derived Donor-π-Acceptor Systems

The presence of a strong electron acceptor unit within these C(4) derived dithiole donor-π-acceptor systems should provide a degree of intramolecular charge transfer within these systems. In order to determine whether this was the case, potential building blocks **166-168** containing suitable functionality were synthesised. These new aldehydes **166** and **168** and ketone **167** were prepared from Wittig reagent **151** and glyoxal **84**, methylglyoxal **93** and *E,E*-mucondialdehyde **98** (Section 2.5) respectively. To a solution of Wittig reagent **151** in dichloromethane was added, sequentially, triethylamine followed by the corresponding aldehyde **84**, **93** and **98**

(Scheme 4.20). All compounds were isolated in a pure state as yellow solids in high yield. The reaction with methyl glyoxal occurred solely at the aldehyde site and no reaction was observed with the ketone. Several reactions of Wittig reagent **151** with ketones were attempted but no products were detected even after long reaction times at elevated temperature. This was attributed to the steric interactions that are encountered on performing reactions between phenyl Wittig reagents and ketones similarly the electron releasing effects of the phenyl groups reduces the efficiency of these Wittig reactions.

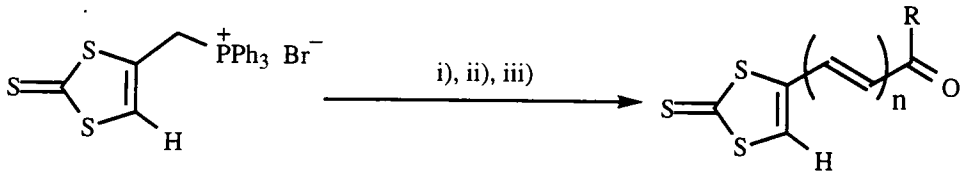

151

166 n=1 R=H
167 n=1 R=Me
168 n=3 R=H

Scheme 4.20 Synthesis of Compounds 166-168 Reagents i) CH_2Cl_2, Et_3N, glyoxal **84**, ii) CH_2Cl_2, Et_3N, methylglyoxal **93**, iii) CH_2Cl_2, Et_3N, *E,E*-mucondialdehyde **98**

The attempted conversion of aldehydes **166-168** into the corresponding dicyanomethylene derivatives using standard conditions (Section 2.4.2) proved unsuccessful and only starting aldehydes were recovered in 70-80% yield. The interaction of ketones and aldehydes with titanium reagents is the initial step of the titanium tetrachloride induced Knoevenagel reaction.[106] Thus the thione unit within **151** could interfere with this reaction (even with a large excess of titanium tetrachloride, no reaction was observed). A method was therefore required which involved either protecting the thione unit or using another heterocycle as a latent source of the desired dithiole. The latter case makes use of the previously mentioned 1,2,3-thiadiazole (Section 4.6.1).

To this end 4-formyl-1,2,3-thiadiazole **158** was converted to the corresponding dicyanomethylene derivative **169** using standard conditions (Section 2.4.2). However, the base-induced ring opening of **169** failed and only starting materials were recovered, presumably due to the strongly electron withdrawing dicyanomethylene group suppressing the ring opening reaction. Indeed the ring opening reaction of 4-formyl-1,2,3-thiadiazole **158** has never been reported, probably

for similar reasons. The weaker para-nitrobenzyl acceptor system was thus investigated forming **170** in good yield (Scheme 4.21) which was subsequently ring opened to form **165** indicating that this ring opening reaction can proceed when functionalised with electron withdrawing substituents. To date, our attempts to synthesise C(4) substituted dithiole donor-acceptor systems containing stronger electron acceptor units have proved unsuccessful with none of the target compounds being formed. The Wittig reagent **151** has, however, been utilised to yield several novel extended 1,3-dithiole-2-thione derivatives which may still find use within the wider field of organic materials.

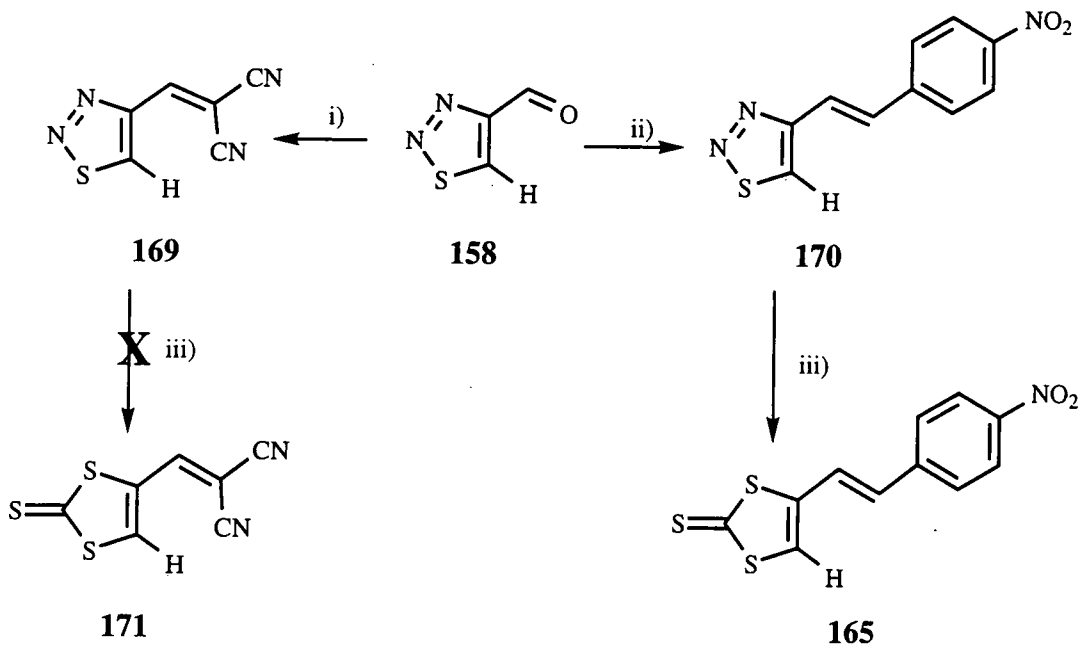

Scheme 4.21 Thiadiazole and Dithiole Derived Donor-π-Acceptor Systems
Reagents i) $TiCl_4$, $CH_2(CN)_2$, Pyridine, CH_2Cl_2, ii) **138a**, Et_3N, iii) NaH, CS_2

4.9 Conclusions

The conjugative linking of the strong π-electron donor TTF to simple aromatic acceptor units has been performed and these compounds exhibit intramolecular electron transfer properties. The corresponding 1,3-dithiole donor systems exhibit no charge transfer properties toward the aromatic acceptor. These systems are yellow in colour which has been attributed to the more favourable charge transfer between the two dithiole sulfurs and the thione acceptor. These results are consistent with the improved donor ability of TTF compared to monocyclic dithiole units. NLO measurements of the TTF donor-acceptor systems show them to be active materials

for second order NLO properties; the values of the second order hyperpolarisability coefficient β are, however, modest.

Chapter 5

The Use of 1,3-Diselenole-2-ylidene Donor Units

5.1 Introduction

The 1,3-diselenole-2-ylidene unit is the selenium analogue of the 1,3-dithiole-2-ylidene unit utilised as the π electron donor fragment in the majority of this work. 1,3-Diselenoles have received considerable interest within the field of organic conductors[107] since the discovery that the hexafluorophosphate salt of tetramethyltetraselenafulvalene **6** was superconducting under pressure[16a] (Section 1.1.5.2). This chapter will briefly discuss the general synthetic routes to functionalised 1,3-diselenole units and the synthesis of diselenole derived donor-π-acceptor systems analogous to those discussed in chapters 2 and 3.

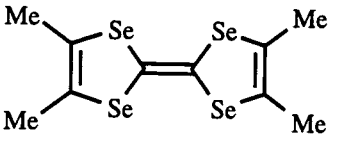

6

5.2 Synthesis of 1,3-Diselenole-2-ylidene Systems

The synthesis of 1,3-diselenole-2-ylidene derivatives employs similar procedures to those outlined in chapter 2, in which carbon diselenide is the source of selenium. This is exemplified by the preparation of 4,5-dicarbomethoxy-1,3-diselenole-2-tributylphosphonium tetrafluoroborate **172a** from tributyl phosphine, carbon diselenide, and DMAD **73** (Scheme 5.1). Carbon diselenide is, however, a highly toxic, fetid and commercially unavailable source of selenium and its preparation requires very specific reaction conditions.[108,109]

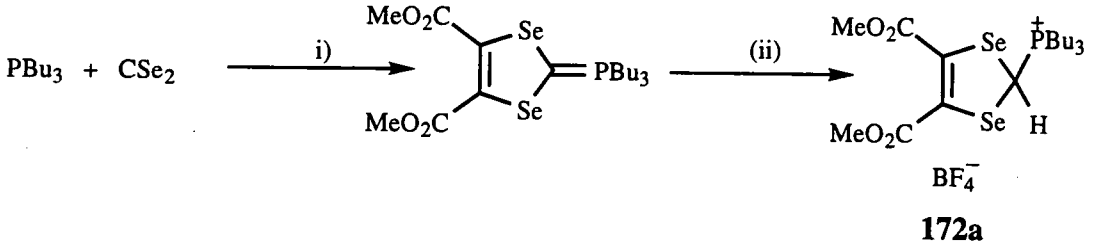

172a

Scheme 5.1 The Synthesis of 172a Using Carbon Diselenide Reagents i) DMAD **73**, MeOH, 0°C, ii) HBF_4, Et_2O, -30°C

5.2.1 Synthesis of 1,3-Diselenole Derivatives Utilising Hydrogen Selenide

It is possible to prepare 1,3-diselenole derivatives *via* the use of gaseous hydrogen selenide which is a commercially available source of selenium. To this end ethane triselenocarbonate **173**, which is an important synthetic building block, was synthesised from hydrogen selenide independently by Fabre[110] and Wudl.[111]

The treatment of gaseous hydrogen selenide with triethylamine in dry chloroform at 0°C produces triethylammonium hydrogen selenide **174**. This was subsequently treated with *N,N*-dimethyl-phosgene imminium chloride **175** to yield salt **176** *via* the substitution of both chlorine atoms for selenium. To this was added 1,2 dibromoethane **177** to afford the bromide salt **178** which was subsequently treated with hexafluorophosphoric acid to yield the hexafluorophosphate salt **179** as a white solid. Treatment of salt **179** with either hydrogen selenide or sodium hydrogen selenide produced the desired selone **173** which by analogy with **74** (Section 2.2.4) reacts with DMAD **73** to yield **180b** in 85% yield (Scheme 5.2).

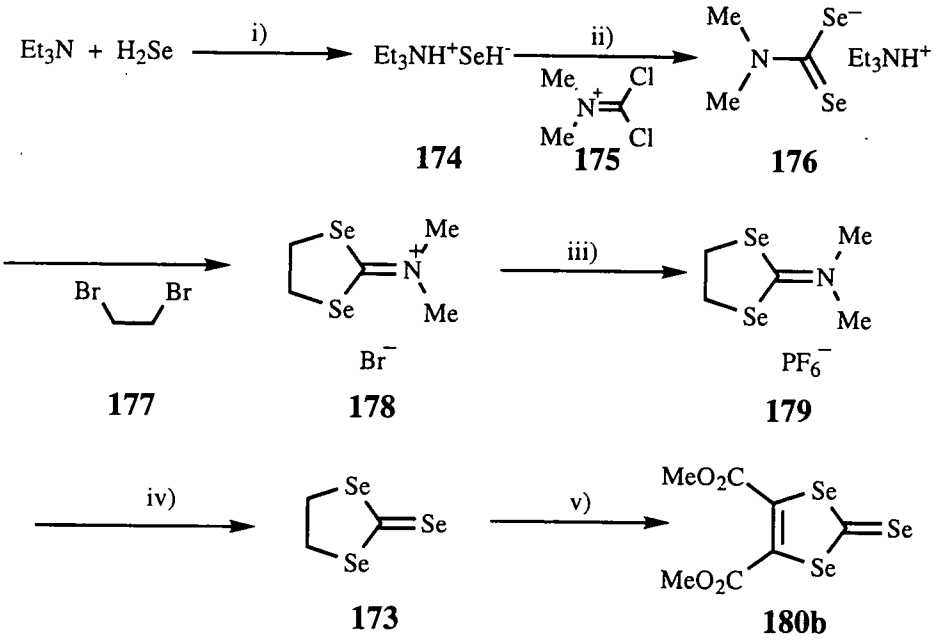

Scheme 5.2 The Synthesis of Compound 180b *via* the use of Hydrogen Selenide
Reagents i) $CHCl_3$, 0°C, ii) Et_3N, iii) HPF_6, iv) H_2Se or NaHSe v) DMAD **73**, toluene, reflux

5.2.2 Synthesis of 4,5-Dimethyl-1,3-diselenole-2-selone 180a

The synthesis of the 4,5-dimethyl-1,3-diselenole-2-selone **180a** was accomplished as shown in Scheme 5.3 following the literature procedure (Scheme 5.3).[111] This route was based upon analogous chemistry to 4,5-dimethyl-1,3-dithiole-2-thione **65** (Section 2.2.2) commencing with compound **176** (Section 5.2.1).

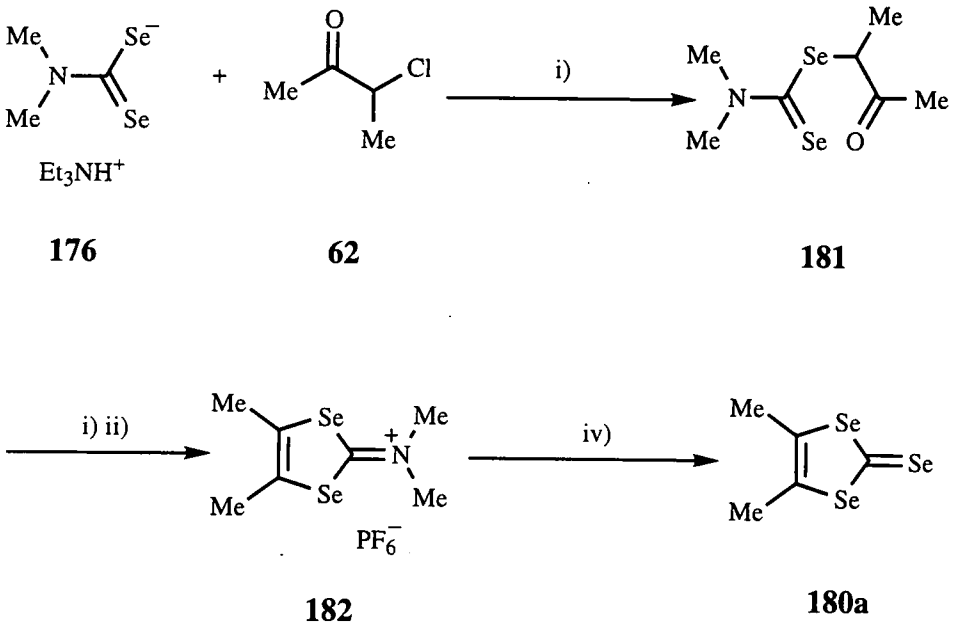

Scheme 5.3 Synthesis of Compound 180a Reagents i) $CHCl_3$, ii) c. H_2SO_4, iii) HPF_6, iv) H_2Se or NaHSe

5.3 Synthesis of Wittig Derivatives of 1,3-diselenole

As previously mentioned in Chapter 2, thiones may be converted into Wittig and Wittig-Horner derivatives by employing standard transformations (Section 2.4.1) and both the dimethyl and the diester 1,3-diselenoles derivatives **180a,b** have been transformed into the corresponding Wittig derivatives **172a,b.** Wittig reagent **172b** could be prepared in one step (Section 5.2); however, this requires the use of carbon diselenide.

The functionalised diselenole Wittig reagents **172a,b** were subsequently prepared by literature procedures from the corresponding selones **180a,b** and have been trapped with aldehydes to yield functionalised derivatives (Scheme 5.4).[112,113]

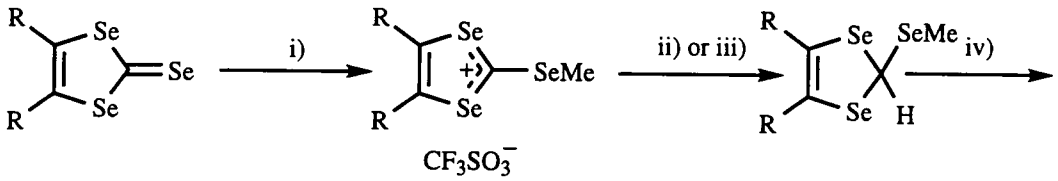

180a R=Me
180b R=CO_2Me

181a R=Me
181b R=CO_2Me

182a R=Me
182b R=CO_2Me

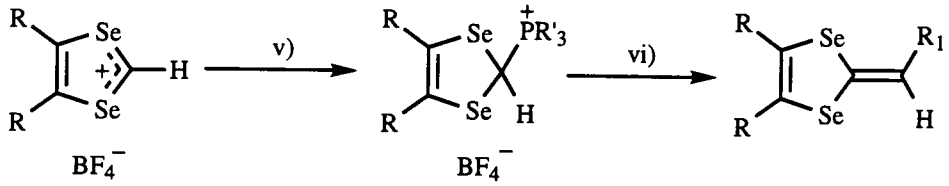

183a R=Me
183b R=CO_2Me

172a R=Me
172b R=CO_2Me

Scheme 5.4 Synthesis of Diselenole Wittig Reagents Reagents i) $MeSO_3CF_3$, CH_2Cl_2, ii) R=CO_2Me $NaCNBH_4$, propan-2-ol; R=Me $NaBH_4$, propan-2-ol, iv) HBF_4, v) PR'_3, MeCN, vi) Et_3N, R_1CHO

5.4 Diselenole Donor-π-Acceptor Systems

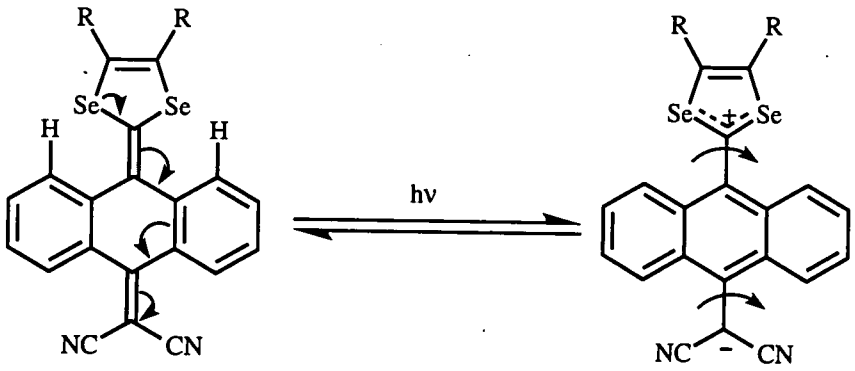

Scheme 5.5 Neutral and Zwitterionic States of Anthracene Donor-π-Acceptor Systems

Within the context of chalcogen containing donor-π-acceptor systems it was of interest to investigate the effect that the 1,3-diselenole donor unit has on intramolecular charge transfer. The linking of these donor fragments to the established acceptor units (Section 2.4.2) *via* conjugated spacer groups (chapter 2 and 3) should allow us to compare directly the donor ability of dithiole and diselenole fragments. Similarly, for the anthracene derived donor acceptor systems discussed in chapter 3, it was envisaged that the larger selenium atoms within the donor unit

should produce an even more congested (Se--H) peri interaction. This was expected to encourage the charge separated state to adopt the wholly aromatic structure first postulated in chapter 3 (Section 3.1.1) in which the diselenole donor fragment is expected to rotate out of plane (Scheme 5.5).

5.3.1 Donor-π-Acceptor Systems Containing an Ethylenic Spacer

The only previous report of a 1,3-diselenole donor unit being used in the context of donor-π-acceptor chemistry was in 1967 by Hendricksen.[114] This material was similar to the earlier work by Gompper *et al*[51] and Mayer *et al*[52] (Section 1.3) with the donor units linked to the dicyanomethylene acceptor units *via* a single π bond. The diselenole derivative **185** was synthesised by reaction of selenoether **184** with malononitrile in a mixture of triethylamine and pyridine (Scheme 5.6).

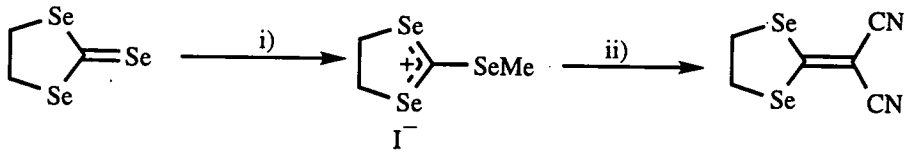

173 **184** **185**

Scheme 5.6 Hendricksen's Synthesis of Diselenole Donor-π-Acceptor System 185 Reagents i) MeI, ii) $CH_2(CN)_2$, Et_3N, Pyridine

During the course of Hendricksen's work ethane triselenocarbonate **173** and a variety of similar compounds **186a-e**, all containing the general triselenocarbonate unit, were reported to be highly coloured with λ_{max} values up to 565 nm. Although not interpreted in this work, this UV-VIS data can be attributed to intramolecular electron transfer from diselenole donor to the selone acceptor. The corresponding 1,3-dithiole-2-thione subunit contains a UV-VIS absorption at 415 nm which was attributed to electron transfer from dithiole donor to the thione acceptor unit (Section 4.3.4). This indicates that either the selone is an improved acceptor unit compared to the thione or the 1,3-diselenole is a superior donor. Unfortunately the UV-VIS spectrum of compound **185** was not reported, so a direct comparison of the dicyanomethylene and selone acceptor units could not be made.

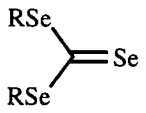

186a R-R=CH_2CH_2
186b R-R=$CH_2CH_2CH_2$
186c R=$CH_2C_6H_5$
186d R=CH_2CO_2H
186e R=Me

Compound	λ_{max}/nm[a]
186a	565
186b	554
186c	547
186d	545
186e	545

[a] Spectra measured in ethanol solution

Table 5.1

5.3.1.1 Synthesis of Functionalised 1,3-Diselenole-2-ylidene Donor-π-Acceptor Systems

With quantities of functionalised 1,3-diselenole-2-selone units in hand we initially focused our attention on preparing functionalised analogues of compound **185**, via the corresponding selenoether derivatives **181a,b** (Scheme 5.7), using Gompper's methodology.[51]

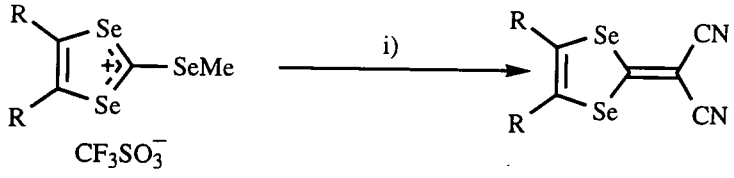

181a R=Me
181b R=CO_2Me

187a R=Me
187b R=CO_2Me

Scheme 5.7 Synthesis of Functionalised 1,3-Diselenole Donor-π-Acceptor Systems Reagents i) $CH_2(CN)_2$, pyridine, propan-2-ol, 20°C

To a propan-2-ol solution of the selenoether **181a,b** was added malononitrile and pyridine at room temperature. Following addition of pyridine a cream/white

precipitate developed which was collected by filtration yielding compounds **187a,b** in 53 and 65% yields respectively.

5.3.1.2 UV-VIS Spectra of compounds 187a,b

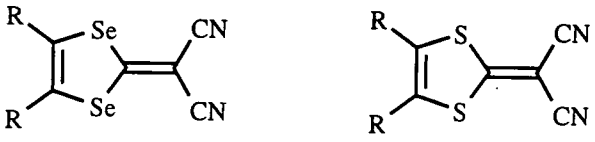

R	λ_{max}/nm[a]	λ_{max}/nm[a]
Me	388	387
CO_2Me	356	354

[a] all spectra recorded in dichloromethane solution

Table 5.2 The Effect of Diselenole and Dithiole Functionality on the Low Energy Charge Transfer Bands

As expected, both systems **187a,b** exhibited a low energy absorption similar to their dithiole counterparts (Section 2.4.3) with **187a** being red shifted compared to **187b** which was in complete agreement with the dithiole analogues (Section 2.4.3). However, There was a negligible difference between the dithiole and the diselenole donor units which is exemplified in Table 5.2.

5.3.2 Donor-π-Acceptor Systems Derived From Diselenole Wittig Reagents 172a,b

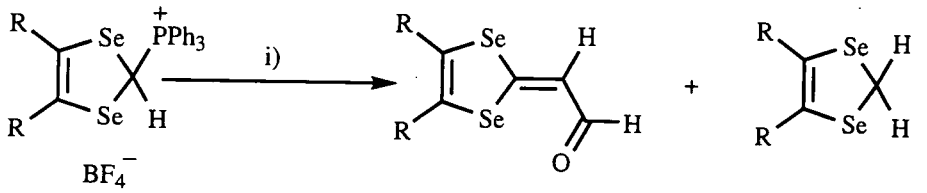

172a R=Me
172b R=CO_2Me

188a R=Me
188b R=CO_2Me

189a R=Me
189b R=CO_2Me

Scheme 5.9 Synthesis of Compounds 188a,b Reagents i) Et_3N, MeCN, Glyoxal **84**

The stimulus for this work was the previously reported reaction between compound **172b** and glyoxal in triethylamine which proceeded in 36% yield to form compound **188b**.[18] Comparable reactions performed in Durham lead to the formation of

compound **189b** which was attributed to the age of the tetrafluoroboric acid used.[115] Subsequent reactions to form **188a** lead to no formation of **189a** independent of the age of the acid used, with **188a** being isolated as a yellow solid albeit in only 20% yield (Scheme 5.9)

The ^{1}H NMR spectra of compounds **188a,b** showed coupling constants (J= 1.2Hz) similar to those observed for **85a,c** in chapter two, again suggesting a close contact between selenium and oxygen. The presence of such interactions has been established by X-ray analysis for the nitroso derivative **190** of the 1,3-diselenole-2-ylidene system.[115]

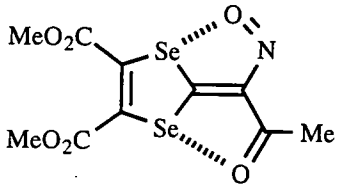

190

5.3.2.1 Dicyanomethylene Derived Donor-Acceptors

The dicyanomethylation of aldehydes **188a,b** under standard conditions (Section 2.4.2) yielded the corresponding diselenole derived donor-acceptor systems **191a,b** in 73 and 70% yields respectively as red or orange solids (Scheme 5.10).

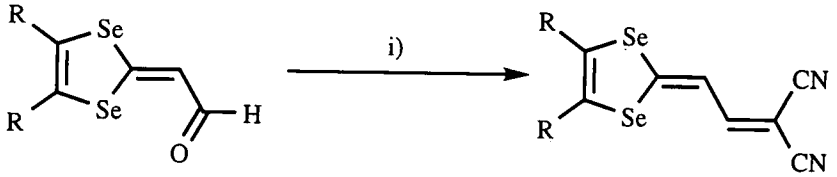

188a R=Me
188b R=CO_2Me

191a R=Me
191b R=CO_2Me

Scheme 5.10 Synthesis of Diselenole Donor-π-Acceptor Systems Reagents i) $TiCl_4$, $CH_2(CN)_2$, pyridine, CH_2Cl_2

The ^{1}H NMR spectra of these compounds **190a,b** indicated that the butadiene chain was in the *trans* conformation (J=12 Hz) which is in contrast to the *cis* conformation in the starting aldehydes **188a,b**.

5.3.2.2 A Comparison of UV-VIS Data for Compounds 191a,b

In order to gain a direct comparison of dithiole *vs.* diselenole donor units we compared compounds **191a,b** with the corresponding dithiole-dicyanomethylene systems prepared in chapter two (section 2.4.3): the data for which are collected in Table 5.3.

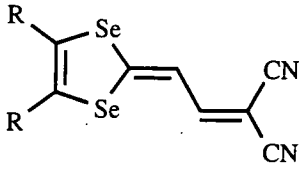

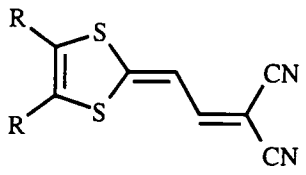

R	λ_{max}/nm[a]	λ_{max}/nm[a]
Me	482	489
CO_2Me	437	439

[a] Spectra measured in dichloromethane solution

Table 5.3 UV-VIS Data for Compounds 191a,b and 86a,c

It is evident that the 1,3-diselenole-2-ylidene is a poorer donor fragment than the corresponding dithiole donor unit with the charge transfer band being noticeably blue shifted. This was attributed to the diffuse nature of the p and dπ electrons leading to less π-donation from the 1,3-diselenole donor than from the 1,3-dithiole units. The extension of the conjugated spacer between donor and acceptor should shift the position of the charge transfer band bathochromically so the use of an aromatic spacer unit was employed utilising diselenole donor fragments.

5.4 The Use of Aromatic Spacer Units.

We, therefore, proposed to study the effect of the 1,3- diselenole donor unit with an aromatic spacer unit between the donor and the acceptor. The dithiole analogues are similarly unexplored and were synthesised to allow a direct comparison to be drawn.

Crude Wittig reagent **172b** reacted with triethylamine and two equivalents of teraphthalaldehyde **192** to yield **194** in 70% yield. The corresponding dithiole derivative **193** was similarly prepared in 52% yield from Wittig reagent **79c** (Scheme 5.11).

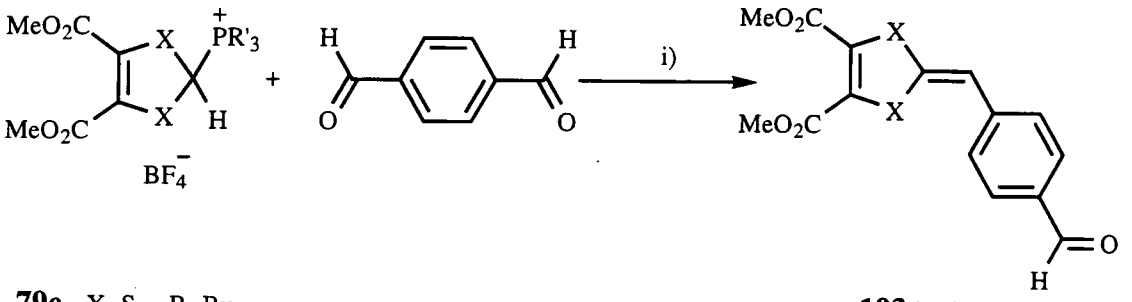

79c X=S R=Bu
172b X=Se R=Ph

192

193 X=S
194 X=Se

Scheme 5.11 Synthesis of Compounds 193 and 194 Reagents i) Et_3N, MeCN

Dithiole **193** and diselenole **194** were converted to the corresponding dicyanomethylene derivatives by utilising standard reaction conditions (Section 2.4.2). An immediate colour change on warming was observed yielding compounds **195** and **196** which were easily purified by chromatography (Scheme 5.12).

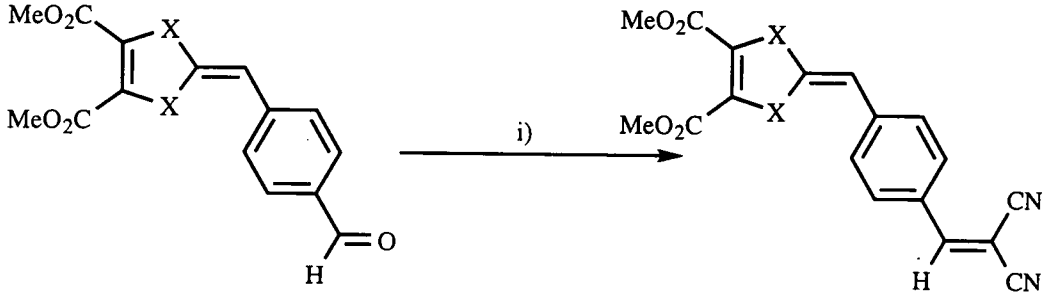

193 X=S
194 X=Se

195 X=S
196 X=Se

Scheme 5.12 Synthesis of Compounds 195 and 196 Reagents i) $TiCl_4$, $CH_2(CN)_2$, pyridine, CH_2Cl_2

5.4.1 UV-VIS Spectra of Compounds 195 and 196

Compounds **195** and **196** both contained the expected low energy absorptions in the UV-VIS spectra which were attributed to intramolecular electron transfer. The effects that the different heterocyclic donor units have on the wavelength of this charge transfer band are exemplified in Table 5.4, with additional data for compound **104c** (Section 2.5.2) added for comparison.

Again the position of the charge transfer absorptions for the diselenole derivative **196** was blue shifted compared to the corresponding dithiole **195**. The charge transfer band for compound **104c** was considerably red shifted compared to both compounds

195 and **196**. The length of the conjugated spacer between the donor and the acceptor in both compounds consists of four π bonds. However, the position of the charge transfer bands in compounds **195** and **196** was blue shifted due to the destabilising effects of the aromatic spacer unit which becomes quinoidal upon excitation.

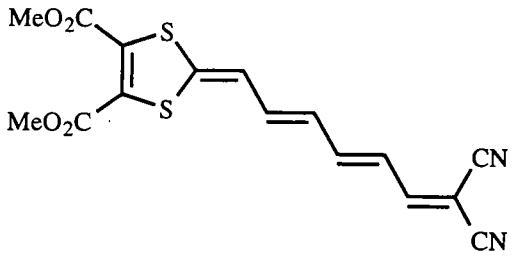

104c

Compound	λ_{max}/nm
195	462
196	458
104c	492

Table 5.4 UV-VIS Data for Compounds 195, 196 and 104c

5.5 Anthracene Spacer Units

When an anthracene diylidine spacer unit was placed between the dithiole donor and the dicyanomethylene acceptor fragments in compound **108a** the charge transfer absorption was shifted towards lower energy compared to the all other materials discussed herein (λ_{max} =572 nm). This was indicative that the anthracene diylidine is an excellent conjugated spacer unit which was attributed to the gain in aromaticity upon charge transfer. Furthermore we proposed that the destabilising (S--H) peri interactions would cause the dithiolium cation produced to twist out of plane to eleviate this interaction. This, however was not observed and a highly distorted "butterfly" structure was instead produced. As discussed previously (Section 5.4) the presence of the larger selenium atoms was expected to increase these peri interactions and, thus the zwitterionic structure was, again, postulated.

The diselenole was, however, expected to produce a higher energy charge transfer band than compound **108a** due to the poorer donor ability of the diselenole compared to the dithiole. Having studied the effect of substituents at the 4,5 position only the superior dimethyl derivatives will now be considered as a direct comparison to compound **108a**.

5.4.1 Synthesis

In an analogous reaction to that previously performed in chapter 2 (Section 2.2.2) 4,5-dimethyl-1,3-diselenole imminium salt **182a** was converted into the corresponding thione **197** by the action of sodium thiole in acetic acid which was cleanly methylated by methyl trifluoromethylsulfonate to yield the thioether salt **198** in 42% yield (Scheme 5.13).

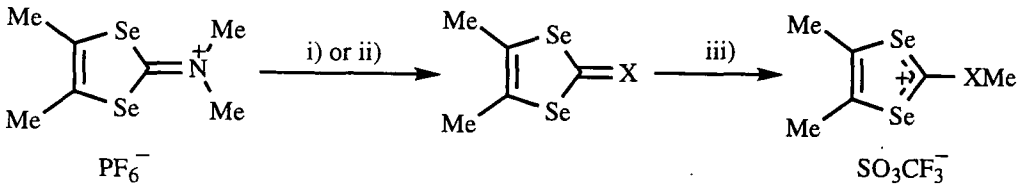

182a **197** R=S, **180a** R=Se **198** R=S, **181a** R=Se

Scheme 5.13 Synthesis of Selenoether and Thioether Salts Reagents i) X=S, NaSH, Acetic acid:DMF 1:1, reflux ii) X=Se, H_2Se, 20°C iii) CF_3SO_3Me, DCM, Et_2O, 20°C

Subsequent added of **198** to a solution of anthrone **106** in pyridine:acetic acid yielding compound **199** in 73% yield as a red solid. Correspondingly, if the selenoether **180a** (Scheme 5.14) was utilised in the same reaction the formation of **199** was almost instantaneous at room temperature occurring in 86% yield (Scheme 5.14).

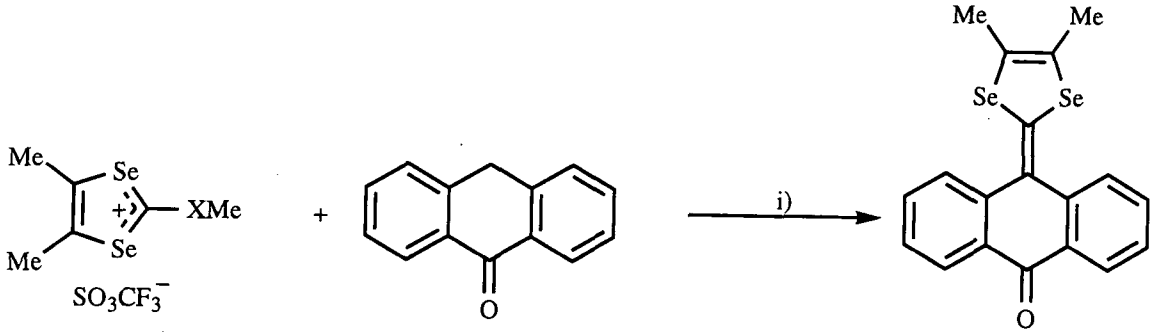

198 X=S, **181a** X=Se **106** **199**

Scheme 5.14 Synthesis of Compound 199 Reagents i) Pyridine:Acetic acid 3:1, 50-60°C

5.4.2 Synthesis of Donor-π-Acceptor Systems

The ketone functionality of **199** was converted using standard reaction conditions into the dicyanomethylene and cyanoimine donor-π-acceptor systems (Section 3.3.1 and 3.3.2) **200** (64%) and **201** (20%) respectively, as blue or black powders (Scheme 5.15).

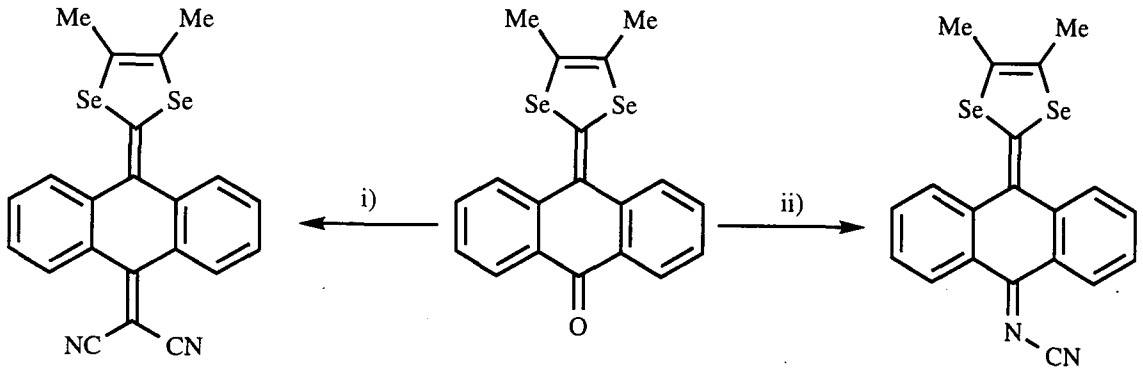

200 **199** **201**

Scheme 5.15 Synthesis of Compounds 200 and 201 Reagents i) $TiCl_4$, $CH_2(CN)_2$, pyridine, $CHCl_3$, ii) $TiCl_4$, BTC, $CHCl_3$

5.4.3 UV-VIS Spectra of Compounds 200 and 201

The values of the low energy charge transfer absorption for compound **200** and **201** are listed in Table 5.5 along with comparative values for the corresponding dithiole derivatives **108a** and **109a**. As expected, the diselenole donor unit acts as a poorer donor than the dithiole leading to charge transfer bands that are blue shifted by *ca.* 15 nm.

Compound	λ_{max}/nm[a]
200	556
201	552
108a	572
109a	561

[a] Spectra measured in dichloromethane solution

Table 5.5 UV-VIS Data for Compounds 108a, 109a and 200-201

5.4.4 X-Ray Structure of Compound 200

During the course of this work we were able to obtain crystals of compound **200** which were suitable for a full X-ray analysis (fig.5.1). This allows a direct comparison to be drawn between the structure of compounds **108a** (Section 3.5) and **200**.

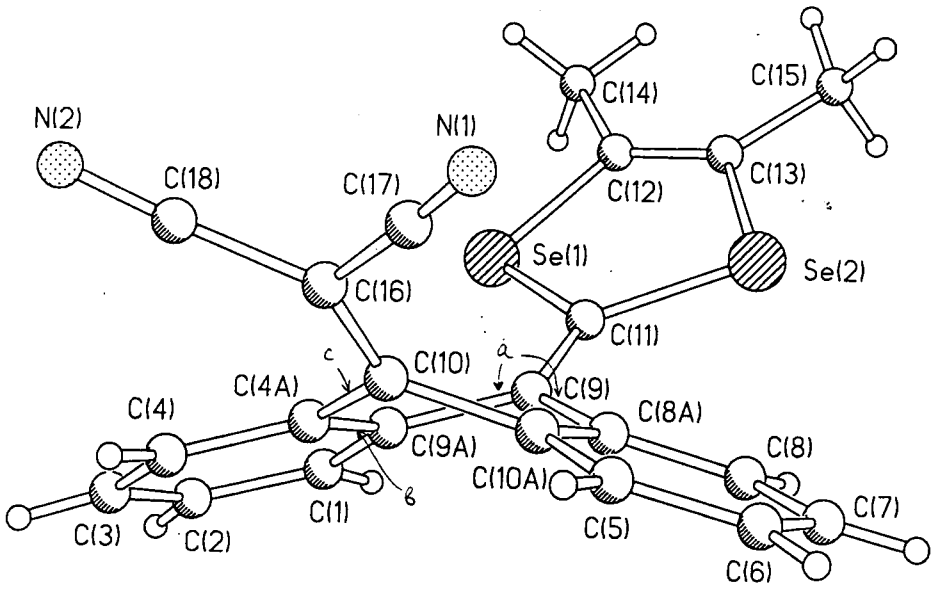

Fig.5.1 X-Ray Structure of Compound 200

Crystals of **200** were not isostructural with compound **108a** and their molecular conformation, although similar, is different. The central anthracene ring in compound **200** adopts a boat conformation folded along C(8a)---C9(a) by 32.7° compared with 29.2° for compound **108a**. The entire anthracene system is also folded greater for compound **200** compared with compound **108a** (36.0 to 33.8°). This increased folding can be attributed to the steric repulsion between the larger selenium atoms and the peri hydrogens. Indeed the difference between the corresponding Se---H and S---H distances (average 2.68 *vs.* 2.50Å, for the idealised C---H distances of 0.95Å) is almost the same as the Van der Waals radii of selenium (2.00Å) and sulfur (1/85Å).

Even though we have now converted the dithiole donor unit for the sterically more demanding diselenole there is still no evidence of charge transfer in the solid state for compound **200**.

5.5 Towards Extended Tetramethyltetraselenafulvalene Derivatives

In order to provide some structural evidence that the size of the selenium atoms within the 1,3-diselenole donor causes the 1,3-diselenole donor units to adopt a different conformation we were attracted to *bis*-(1,3-diselenole-2-ylidene) derivatives of compound **10**.

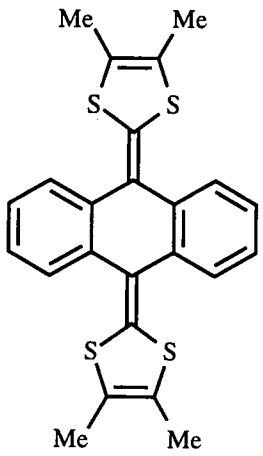

10

The interchanging of one or two sulfur atoms of **10** using 1,3-selenothiole reagents has been previously reported by Moore and Bryce (Scheme 5.16).[80] The reaction of **203** with anthraquinone **204** yielded both isomers of compound **205** which were inseparable. However, no crystallographic data or salt formation was reported and, thus, the synthesis of compounds in which one or both of the dithioles are converted into a diselenole would be of great interest.

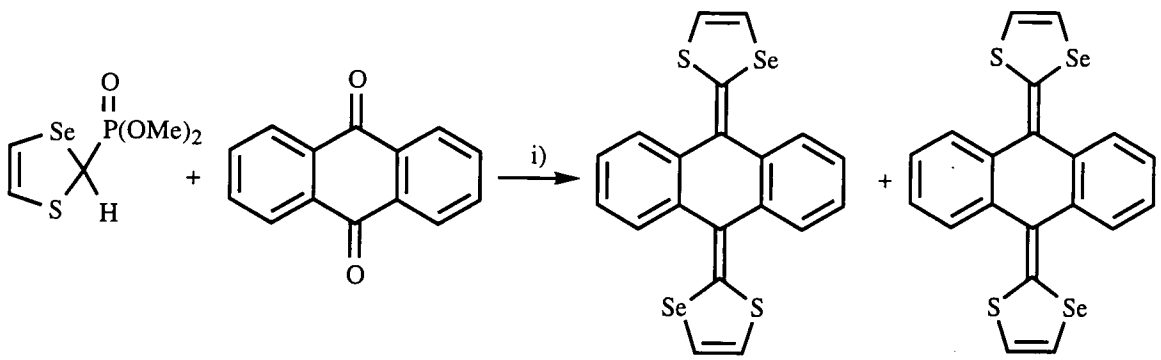

203 **204** **205** **205**

Scheme 5.16 Synthesis of Compound 205 Reagents i) n-BuLi, THF, -78°C

5.5.1 Synthesis

With compound **199** in house we were attracted to the possibility of performing Wittig reactions at the ketone functionality. We proposed to react 4,5-dimethyl-1,3-diselenole tributylphosphine Wittig reagent **172a** with ketone **199** to obtain compound **202.** To a solution of Wittig reagent **172a** in acetonitrile was added base (triethylamine or dry potassium *tert*-butoxide) which formed the ylid as a pale yellow solution in both instances. A solution of **199** was added; however, following work-up, only starting materials were recovered in 40% yield (Scheme 5.17).

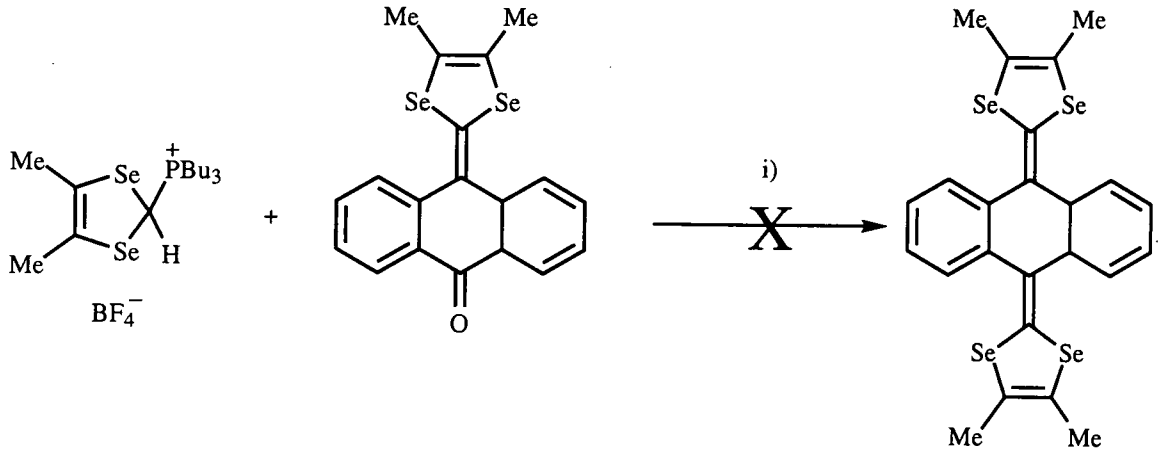

172a **199** **202**

Scheme 5.17 Attempted Synthesis of Compound 202 Reagents i) Et_3N or KO^tBu, MeCN, 20°C

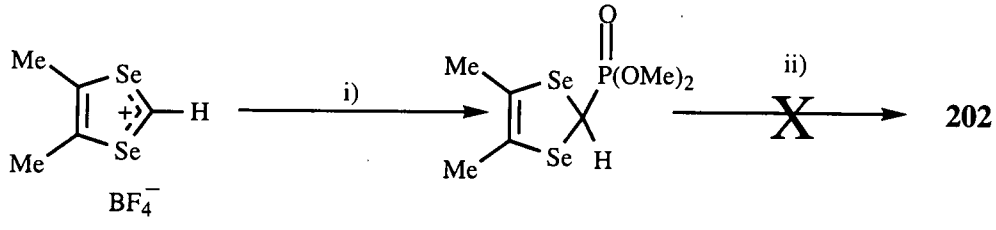

183a **206**

Scheme 5.18 Attempted Synthesis of Compound 202 Reagents i) $P(OMe)_3$, NaI, ii) n-BuLi, THF, -78°C, **199**.

The use of the more reactive phosphonate ester **206** to yield compound **202** was subsequently attempted. Compound **206** was prepared from the corresponding tetrafluoroborate salt **183a** (Scheme 5.5) by the action of trimethyl phosphite and sodium iodide which yielded essentially pure **206** (by ^1H NMR analysis) which was

subsequently used without purification, however, the desired compound **202** was not obtained (Scheme 5.18).

The phosphonate **206** appeared to be very unstable even when maintained in solution at -78°C and it presumably decomposes prior to reaction. Attempted reactions of phosphonate **206** with benzaldehyde and ferrocene aldehyde similarly failed indicating the general lack of reactivity or rapid decomposition of the phosphonate.

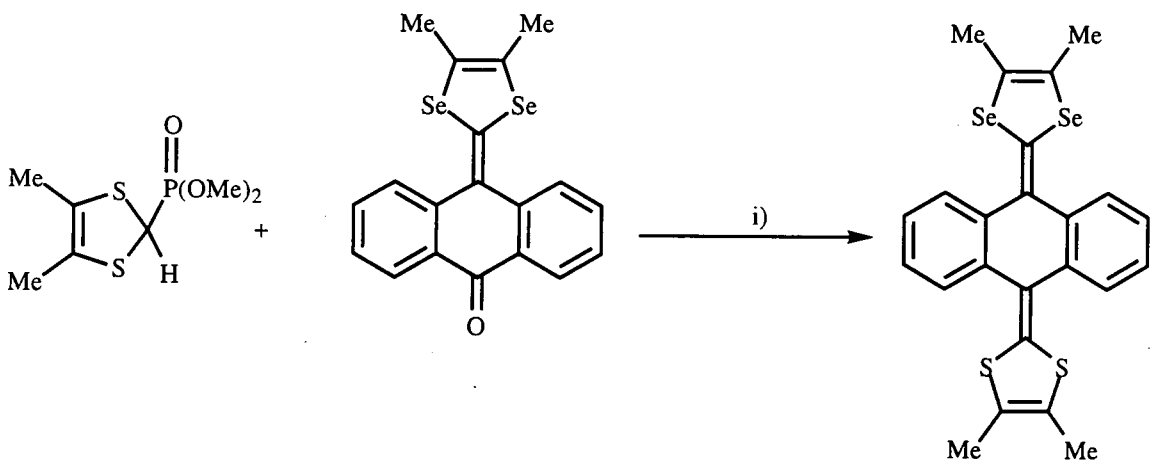

82a **199** **207**

Scheme 5.19 Synthesis of Compound 207 Reagents i) n-BuLi, THF, -78°C

In order to ascertain the viability of these reactions we performed the reaction between Wittig-Horner reagent **82a** (Section 2.4.1) with ketone **199**. To a solution of **82a** in THF at -78°C was added n-butyl lithium followed by ketone **199** which yielded compound **207** in 20% yield (Scheme 5.19) confirming that **199** is reactive towards Wittig-Horner reactions, and the failure to form **202** was most likely due to the decomposition of **206**. Unfortunately attempts to produce suitable crystals of compound **207** similarly failed.

5.6 Conclusions

We have investigated the effects of converting a dithiole into a diselenole within the context of intramolecular donor-π-acceptor charge transfer compounds. It has been shown that the presence of the more polarisable selenium atoms shifts the position of the charge transfer band towards higher energy. The effects of substituents on the heterocycle have again established that the electron donating methyl substituents induced a small but noticeable low energy shift in the value of λ_{max} compared to the electron withdrawing ester functionality. The destabilising effect of selenium on the

extent of peri interactions in anthracene-spaced donor and donor-acceptor systems was proposed and X-ray evidence indicated that the structure was highly buckled but not zwitterionic as proposed.

Chapter 6

Synthesis of Mixed Donor-π-Acceptor Systems

6.1. Dendralenes Derived From 1,3-Dithiole Donors

The synthesis of [3]- and [4]-dendralenes[116,117] bearing the 1,3-dithiole donor unit has been previously reported by Yoshida *et al*[118] and Bryce *et al.*[119] Interest in these systems lies in their potential to form cross-conjugated radicals. X-Ray structural analysis of [3]-dendralene **208** showed that two of the 1,3-dithiole units were co-planar with the third orthogonal to this plane(fig.6.1). CV Data for compound **208** indicated that the two 1,3-dithioles that were co-planar interacted in a similar way to compound **12** (Section 1.1.6), whereas the third 1,3-dithiole unit acted as an isolated unit (Table 6.1).

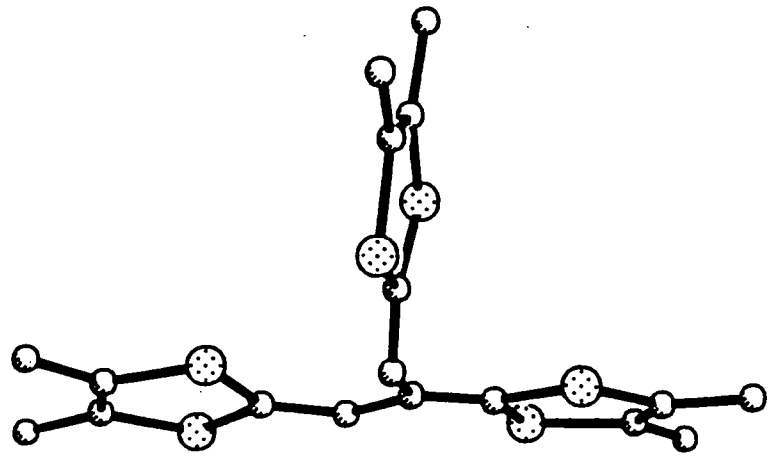

Fig.6.1 X-Ray Crystal Structure of Compound 208

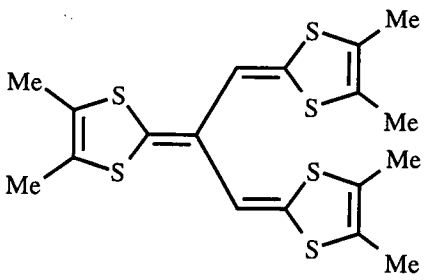

208

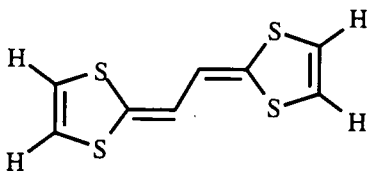

12

Compound	E_1/V	E_2/V	E_3/V
208	0.084	0.327	1.246
12	0.20	0.36	-

Table 1.1 CV Data For Compounds 208 and 12

We were attracted to systems with two acceptor and one donor unit, and two donor and one acceptor unit, as an extension of the work performed in chapter 2, as the nature of charge transfer in these type of systems is virtually unexplored. For

example, in prototype compound **209**, would a charge transfer band attributable to donor-dicyanomethylene, donor-*para*-nitrobenzene, or a combination of the two be observed?

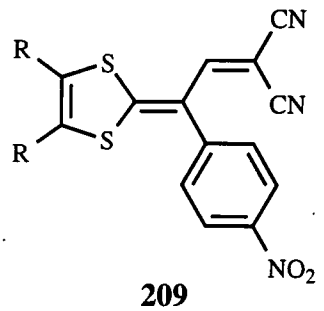

209

To investigate this effect we were attracted to compound **142** (Section 4.3.2) which may be functionalised at the α position *via* Vilsmeier methodology to provide a reactive handle for attachment of further acceptor units.

6.2 Dithiole Derived Donor-π-Acceptor-π-Acceptor Systems.

Compound **210** was prepared *via* addition of oxalyl chloride to a ice cooled mixture of **142** in DMF which furnished, following basic hydrolysis, compound **210** as an orange solid (Scheme 6.1).

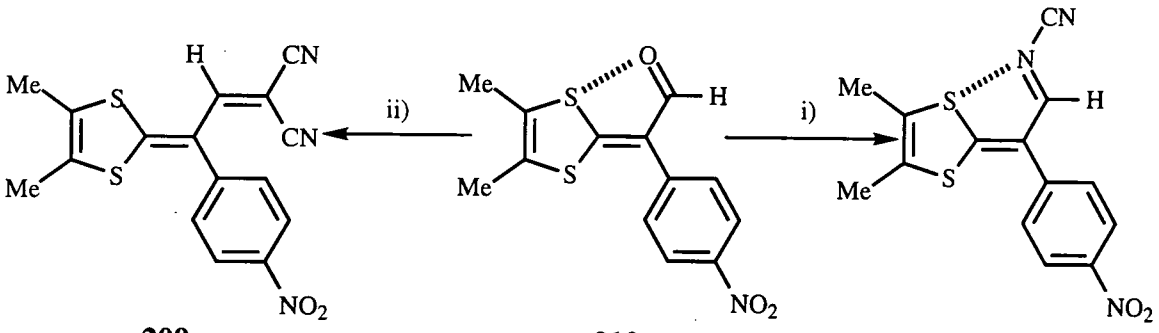

209 **210** **211**

Scheme 6.1 Synthesis of 1,3-Dithiole Derived Donor-π-Acceptor-π-Acceptor Systems Reagents i) $(ClCO)_2$, DMF, 0°C, ii) 1M NaOH, iii) $TiCl_4$, BTC, CH_2Cl_2, reflux, iv) $TiCl_4$, $CH_2(CN)_2$, pyridine, CH_2Cl_2, reflux

Compound **210** was converted into cyanoimine derivatives **211** under standard conditions (Section 2.4.2) as a orange solid. It was postulated that both compounds **210** and **211** would exhibit non-bonded interactions between the sulfur and the oxygen or nitrogen as was observed in chapter 2. The addition of a more powerful dicyanomethylene acceptor unit should similarly lead to both a bathochromic shift in

the value of λ_{max} and an acceptor unit which would not engage in such non bonded interactions. To that end compound **209** was synthesised from aldehyde **210** under standard conditions (Section 2.4.2) to yield compound **209** as a red solid.

6.2.1 UV-VIS Spectra of Donor-Acceptor-Acceptor Units

Compound **142** (λ_{max}= 476 nm) was purple which was attributed to intramolecular charge transfer from the donor to the acceptor (Section 4.3.2.1). However, following formylation to yield **210** a marked colour change to orange was observed corresponding to a hypsochromic shift in the value of λ_{max} to 431 nm. Allied with this shift, a shoulder developed at 379 nm which was not observed in compound **142** or any of the donor-π-acceptor systems previously discussed (fig.6.2). Furthermore, there was no charge transfer band which could be attributed to compound **142**. The low energy charge transfer band for compound **142** could arise from charge transfer from the dithiole donor to the weakly accepting aldehyde group.

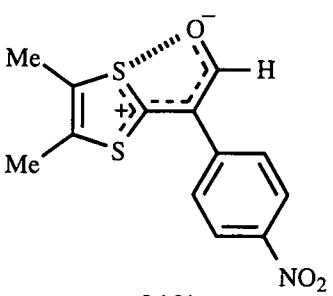

210'

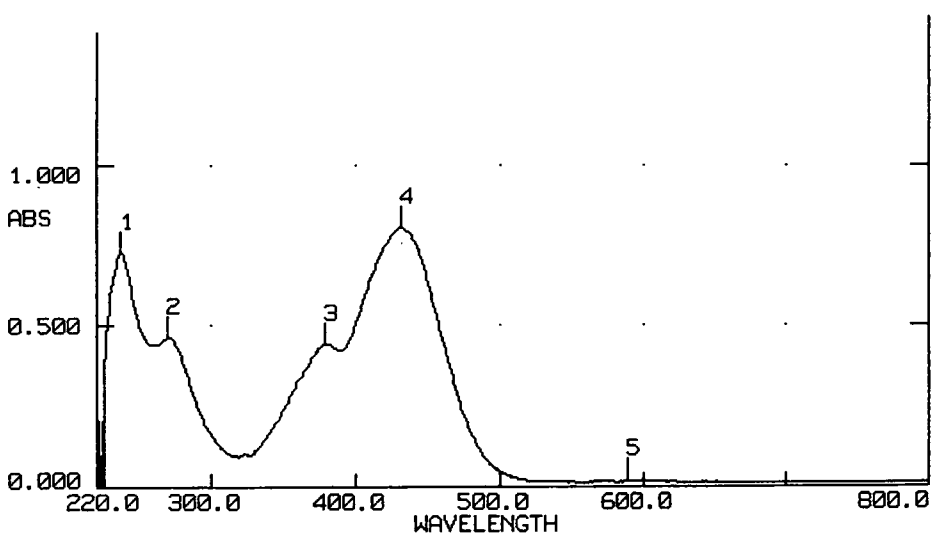

Fig.6.2 UV-VIS Spectrum of Compound 210

Zwitterion **210'**, which presumably contributes to the ground state structure of **210**, possesses a pseudo-aromatic bicyclic system which would explain the lack of charge transfer to the *para*-nitro acceptor unit in this compound. The high energy shoulder in the UV-VIS spectra may, therefore, be attributed to an increase in the overall π delocalisation within the system.

The UV-VIS spectra of compounds **211** and **209** exhibited a low energy absorption along with a high energy shoulder similar to that observed for compound **210**. The position of the low energy band for both compounds **211** and **209** was red shifted compared to compound **210** due to the improved acceptor ability. Compounds **211** and **209** exhibited charge transfer absorptions which were red shifted compared to the parent donor-π-acceptor systems **86a** and **87a**, respectively (Section 2.4.3) (Table 1.2).

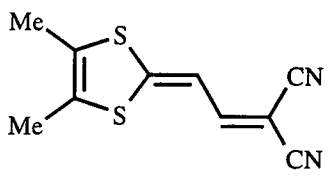

86a

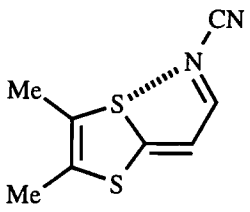

87a

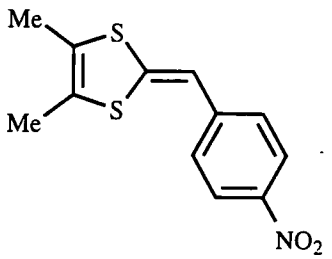

142

Compound	λ_{max}/nm[a]	$\lambda_{shoulder}$/nm[a]
142	467	none
210	431	379
211	463	400
87a	452	none
209	495	450
86a	492	none

[a] All spectra measured in dichloromethane solution

Table 6.2 UV-VIS Data

The observed red shifts, which were more marked for compound **211** than for **209**, were attributed primarily to intramolecular charge transfer from the donor to the cyanoimine and dicyanomethylene, respectively. The red shift for this band may arise from a lowering in energy of the LUMO due to increased π overlap. X-Ray data

could have shed light upon the nature of the conjugation in these molecules, but no suitable crystals were obtained.

6.2.2 Donor-π-Acceptor-π-Acceptor Systems Utilising the Same Acceptor Units

The lack of observable charge transfer from the dithiole donor to the *para*-nitrobenzyl acceptor fragment in compounds **209-211** could arise from steric interactions between the aromatic ring proton and the second acceptor unit leading to the dicyanomethylene and cyanoimine charge transfer absorptions predominating. We may, therefore, consider these systems to be analogous to the [3]-dendralene system **208** in which in this instance one acceptor moiety is forced out of plane due to steric constraints. The conversion of aldehyde **210** for a *para*-nitrobenzyl unit leading to compound **212** should limit any steric interactions by distancing the acceptor unit by a further π-bond. The attempted conversion of aldehyde **210** into **212** using Wittig reagent **138a** and triethylamine in dichloromethane failed to afford compound **212** at either 20°C or under reflux, and proceeded only sluggishly in refluxing benzene (Scheme 6.2). The tardiness of this reaction may be due to the S---O interaction in **210** (for the conversion to the dicyanomethylene and cyanoimine derivatives **209** and **211** titanium tetrachloride was employed which forms a co-ordination complex with the aldehyde oxygen, activating it for subsequent reactions).

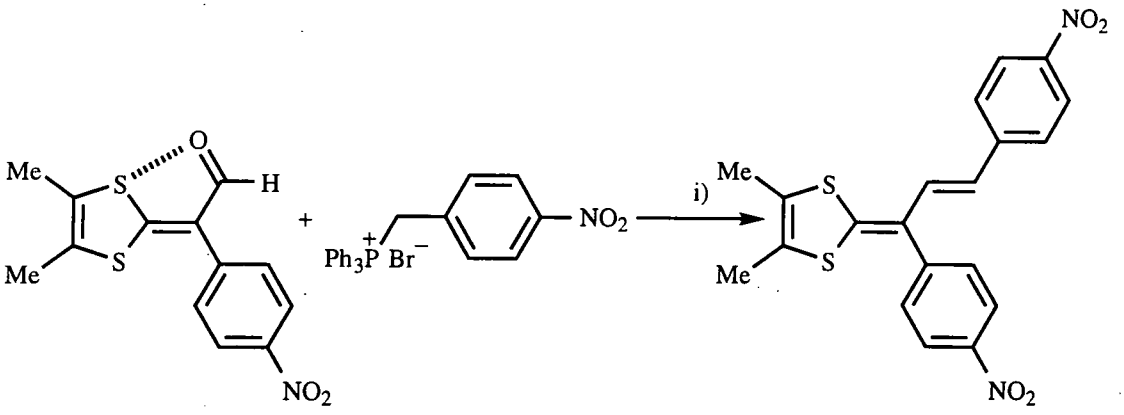

210 **138a** **212**

Scheme 6.2 Synthesis of Compound 212 Reagents i) Et_3N, Benzene, reflux

For comparison, compound **213** was synthesised to probe the effect of adding a nitrobenzyl acceptor unit which was separated from the donor by two π bonds. To a

solution of Wittig reagent **79a** (Section 2.4.1) in acetonitrile was added *para*-nitrocinamaldehyde **214** and triethylamine yielding compound **213** as a black solid (Scheme 6.3).

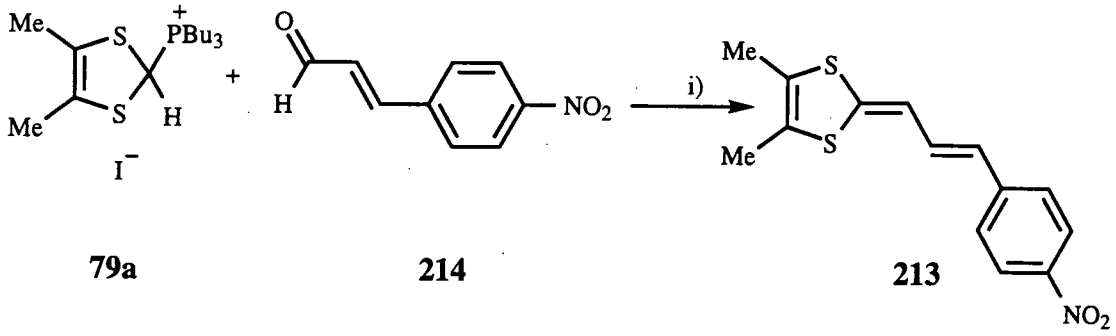

79a **214** **213**

Scheme 6.3 Synthesis of Compound 213 Reagents i) Et_3N, MeCN, 20°C

6.2.2.1 UV-VIS Comparison of Nitrobenzyl Acceptor Units

The positions of the low energy charge transfer bands for compounds **212-213** are summarised in Table 6.3 along with data for compound **215**, containing three π bond spacers between the donor and the acceptor, which was recently prepared by Gorgues *et al.*[120]

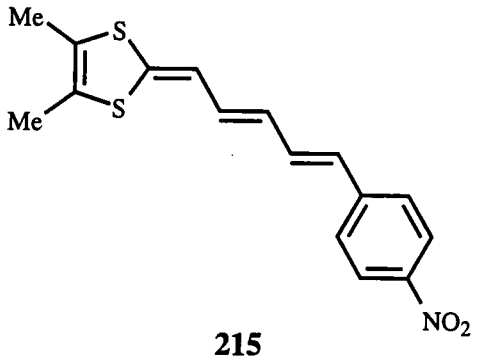

215

Compound	λ_{max}/nm[a]
142	467
213	488
215	499
212	487

[a] All spectra measured in dichloromethane solution

Table 6.3 UV-VIS Data for Aromatic Donor-π-Acceptor-π-Acceptor Systems

The charge transfer absorption of compound **213** was red shifted compared to compound **142** as has previously been observed in chapter two for systems containing an extra conjugated spacer (Section 2.4.3). Similarly compound **215**, which contained an extra conjugated spacer unit, has a charge transfer band which was red shifted still further, showing no sign of reaching saturation point. The charge transfer absorption of compound **212** was consistent with that of compound **213** which possessed a band at almost identical wavelength. However, for compound **212** no shoulder was observed in the UV-VIS spectra. We can, therefore, consider that charge transfer proceeds from the 1,3-dithiole donor unit to the acceptor *via* the longer conjugated spacer, with no evidence for charge transfer to the other acceptor.

6.2.3 Donor-π-Acceptor-π-Donor Systems

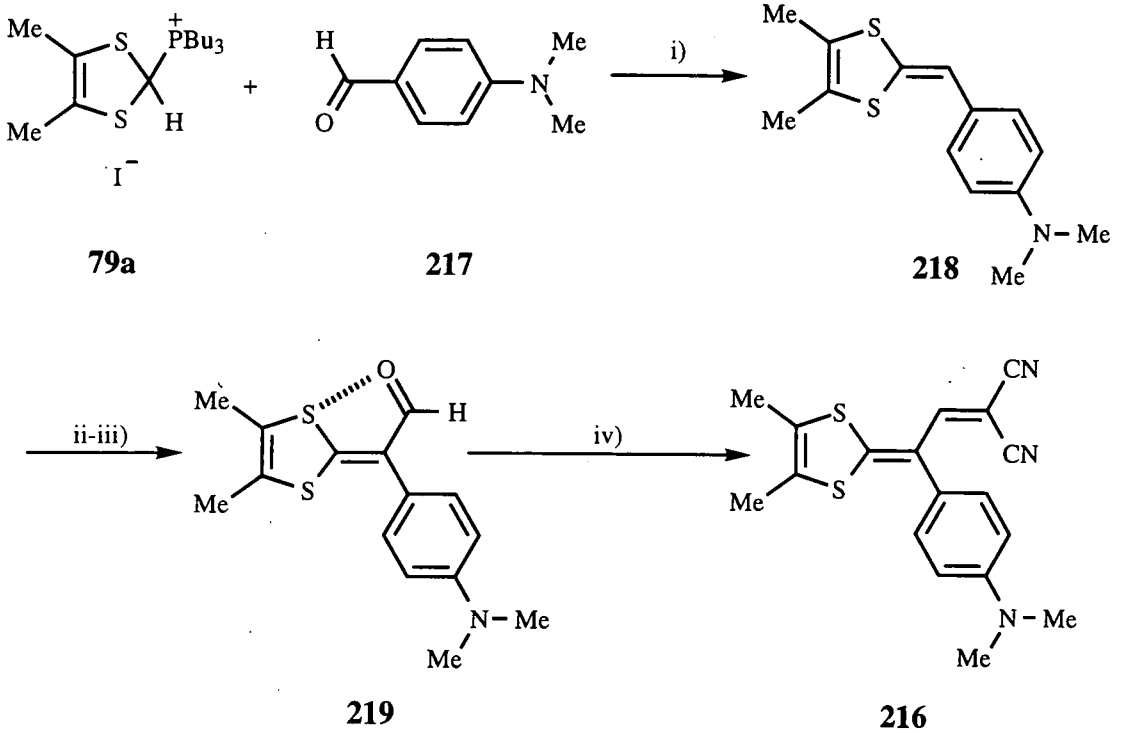

79a **217** **218** **219** **216**

Scheme 6.4 Synthesis of Dimethylamino Derived Donor-π-Acceptor-π-Donor Systems Reagents i) Et_3N, MeCN, 20°C, ii) $(ClCO)_2$, DMF, 0°C, iii) 1M NaOH, iv) $TiCl_4$, $CH_2(CN)_2$, pyridine, CH_2Cl_2, reflux

In a prototypical donor-π-acceptor-π-donor system such as **216** the 1,3-dithiole donor unit is conjugated to the dicyanomethylene acceptor unit with the aromatic donor unit formally cross conjugated to the acceptor, therefore, prevented from contributing to any intramolecular charge transfer processes.

The *N,N*-dimethylamino group is an attractive donor in this context. It may readily be linked to the dithiole unit by the reaction between Wittig reagent **79a** and *N,N*-dimethylaminobenzaldehyde **217** in acetonitrile and triethylamine, yielding compound **218** in 23% yield. Compound **218** was isolated as a cream/white solid which rapidly turned red (even under an inert atmosphere at 0°C) and, thus, was not obtained analytically pure. Instead compound **218** was immediately formylated (oxalyl chloride in DMF at 0°C) to yield **219** in 61% yield as an air stable yellow solid. Compound **219** can be considered as a donor-π-acceptor-π-donor with the aldehyde presumably locked in a non-bonded interaction.

Subsequent reaction of compound **219** with titanium tetrachloride, malononitrile and pyridine in refluxing dichloromethane afforded the target compound **216** as an air stable red solid in 42% yield (Scheme 6.4).

6.2.3.1 UV-VIS Spectra of Donor-π-Acceptorπ-Donor Systems

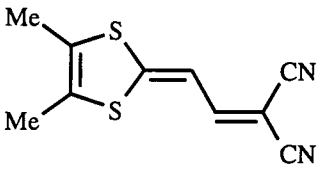

86a

Compound	λ_{max}/nm
218	none > 350
219	411
216	499
86a	492

Table 6.4 UV-VIS Data for Donor-π-Acceptor-π-Acceptor Systems

The position of the low energy charge transfer absorption for compounds **216** and **218-219** are collected in Table 6.4 along with data for compound **86a**. In all three cases a small shoulder was observed at high energy in the UV-VIS spectra indicating the presence of more than one charge transfer process.

Compound **218** possessed no absorption band above 350 nm as there was no intramolecular charge transfer inherent in this system. The conformationally locked

aldehyde **219** exhibited a charge transfer absorption maximum at 411 nm. Conversion of the aldehyde into the dicyanomethylene acceptor system **216** resulted in the expected red shift from 411 nm to 499 nm. In comparison compound **86a** exhibited a charge transfer band at 492 nm demonstrating that the addition of a formally cross conjugated donor unit induces a small red shift in the position of the charge transfer absorption. This was attributed to the positive inductive effect that the dimethylamino donor unit exerts. The presence of the high energy shoulder was, however, difficult to explain and a convincing rationale could not be put forward other than an effect arising from an increase in the overall π conjugation.

6.2.4 Conclusions

It is apparent that a second acceptor unit produces a red shift in the low energy charge transfer band compared to the parent donor-π-acceptor system. Allied to this red shift an unusual high energy shoulder was also observed which was similarly red shifted with increased acceptor strength. Both of these bands may be attributed to increased π delocalisation within these compounds. The presence of the shoulder was difficult to rationalise but is presumably due, at least in part, to the presence of the second acceptor unit as such shoulders were not observed for the parent donor-π-acceptor systems. The addition of the dimethylamino donor had a similar effect on the position of the charge transfer absorption possibly due to a positive inductive effect. However, the presence of a high energy shoulder in these systems was harder to explain as there appears to be only one mode of electron transfer as the dimethylamino donor unit was cross conjugated to the acceptor unit. The limitations of this simple interpretation cannot be overestimated and there remains considerable scope for structural or theoretical calculations to probe further this interesting class of compounds.

6.3 The Use of Ferrocene Donor Units.

Ferrocene is a π electron donor with a half wave potential $E_1^{1/2}$ = 0.36V *vs.* Ag/AgCl (corresponding to Fe^{2+} to Fe^{3+} oxidation) which is comparable to that of TTF $E_1^{1/2}$=0.34V, $E_2^{1/2}$=0.71V. With ferrocene derivatives readily available, a natural progression was to utilise ferrocene as a π-electron donor in donor-π-acceptor-π-donor systems with the aim of probing further the intramolecular charge transfer effects discussed above.

6.3.1 Ferrocene-Dithiole Donor-π-Acceptor-π-Donor Systems

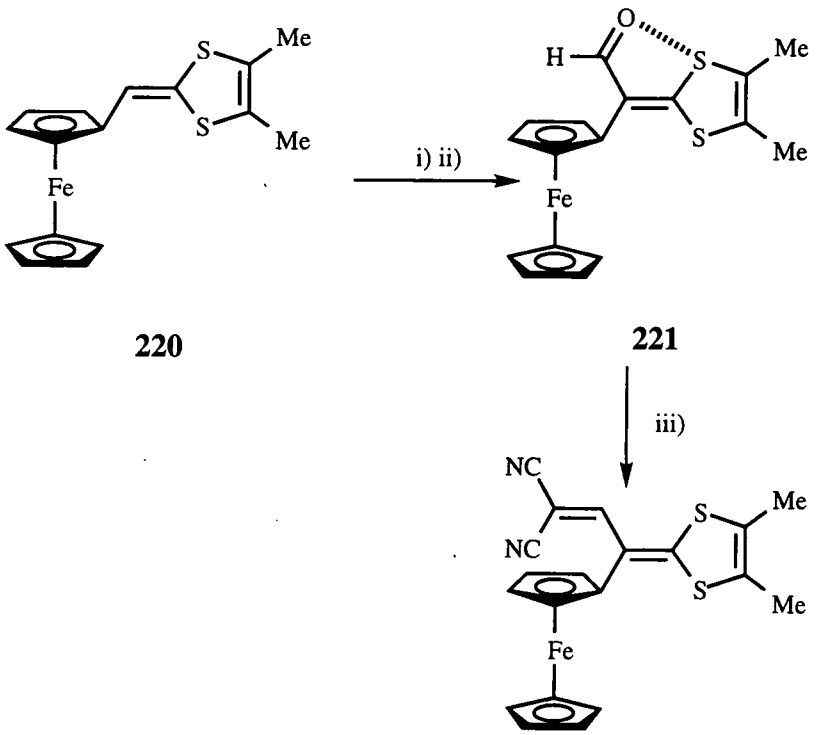

220 **221** **222**

Scheme 6.5 Synthesis of Ferrocene Derived Donor-π-Acceptor-π-Donor Systems Reagents i) $(ClCO)_2$, DMF, 0°C, ii) 1M NaOH, iii) $TiCl_4$, $CH_2(CN)_2$, pyridine, CH_2Cl_2, reflux

Our interest was in systems which contained a 1,3-dithiole unit conjugated to ferrocene and the known compound **220** was an attractive building block.[121] Formlyation of **220** proceeded in good yield yielding compound **221**.[122] The conversion of compound **221** into the corresponding dicyanomethylene derivative **222** was achieved using standard reaction conditions (Section 2.4.2) producing **222** in 35% yield as a black solid (Scheme 6.5). The corresponding dithiole-π-dicyanomethylene **86a** is a red solid and, thus, the effect of adding ferrocene (although formally cross conjugated) has a marked effect on the colour of this compound.

6.3.1.1 UV-VIS spectrum of Compound 222

The UV-VIS spectrum of compound **222** was different from the donor-π-acceptor-π-donor systems described previously in this chapter (fig.6.3). A sharp charge transfer band was observed at 491 nm with a very broad low energy shoulder also observed.

The former absorption could reasonably be attributed to charge transfer from dithiole to dicyanomethylene (compound **86a** λ_{max}= 492 nm), however, this absorption was not augmented by an inductive effect from the ferrocene unit. The low energy absorption was, again, difficult to explain, however, by slow evaporation of a dichloromethane:hexane solution of compound **222** black crystals were deposited which were suitable for X-ray structural analysis.

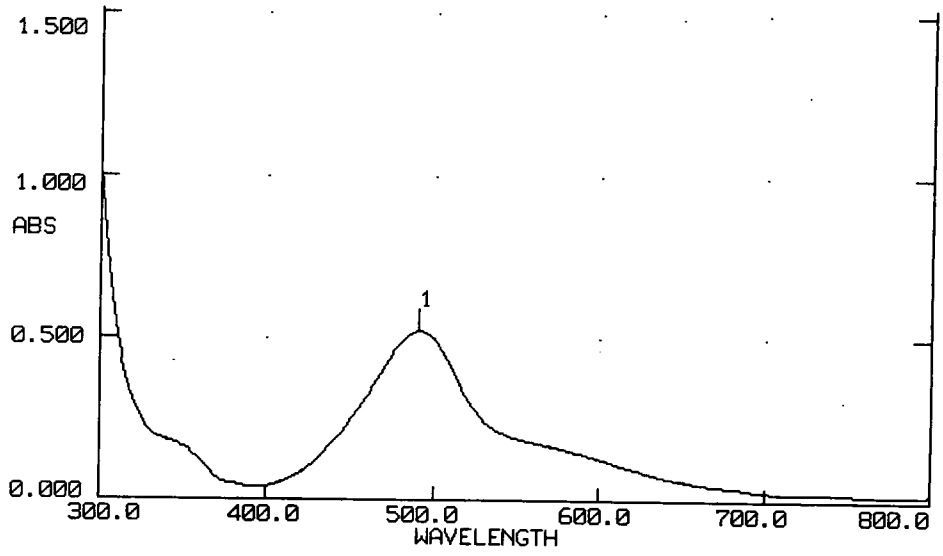

Fig.6.3 UV-VIS Spectrum of Compound 222

6.3.1.2 X-Ray Structure of Compound 222

Compound **222** (fig.6.4) was substantially non-planar, with the dithiole ring folded along the S(1)...S(2) vector by 7.9(1)°. The butadiene system adopts a twist of 21.3(3)° around the central C(6)-C(7) bond, sufficient to interfere with π-conjugation. The twists around the C(1)-C(6) and C(7)-C(8) bonds are also substantial, 6.7(3) and 7.4(3)° respectively. Correspondingly, the difference Δ=0.05 Å between the central ('single') and peripheral ('double') bonds in the butadiene moiety was notably larger than in chemically similar (but essentially planar) donor-π-acceptor systems **86a** (Section 2.4.5) and **46** (Δ=0.016 Å in both cases) and in the 1,2-dithiole analogue **90** (Δ=0.02 Å) (fig.6.5).

The twist of 36.1(2)° around the C(6)-C(11) bond leaves little possibility for conjugation between the cyclopentadienyl and butadiene π-systems. Due to steric overcrowding of the molecule, the S(1) atom is 'wedged' into the sandwich moiety (perfectly at its equatorial plane), making the cyclopentadienyl rings appreciably non-parallel (dihedral angle of 5.8(2)°), although the Fe...S(1) distance of 3.681(1) Å is too long for direct interactions.

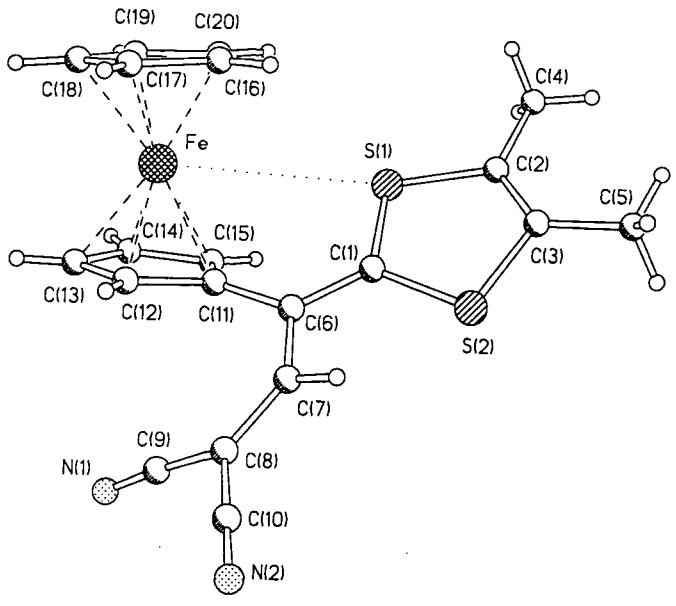

Fig.6.4 The X-Ray Structure of Compound 222

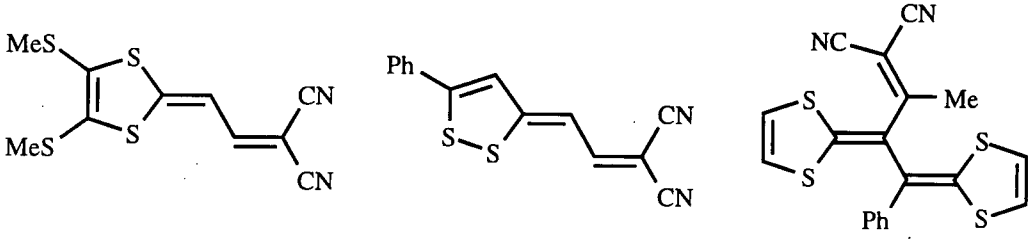

86b **90** **46**

Fig.6.5 Dithiole-π-C(CN)$_2$ Compounds Which Possess a Large Degree of Electron Delocalisation

The UV-VIS spectra of compound **222** contained a charge transfer absorption corresponding to electron motion from the dithiole donor to the dicyanomethylene acceptor. This was observed in the X-ray structure, however the nature of this charge transfer was not as extensive as in compound **86b** due to the steric effects of the ferrocene unit forcing the conjugated spacer unit to be substantially buckled. As mentioned previously this charge transfer band was not enhanced by the presence of the electron donating ferrocene unit which was unsurprising due to the twist of 36.1(2)° around the C(6)-C(11) precluding electron donation. This data, however does not explain the broad low energy absorption observed (fig 6.3). We initially postulated that this might be due to some type of iron-sulfur interaction, however, although the iron and sulfur are considerably closer than in other ferrocene-dithiole derivatives no contact was observed but the possibility of interaction during an excited state process, such as UV-VIS photolysis could lead to a considerable

interaction. This system is still interesting and further work is needed to rationalise fully this unusual compound.

6.3.1.3 CV Data

Cyclic voltammetric data for compounds **210-211**, **216** and **222** is collected in Table 6.5 along with data for compound **86a** for comparison (Section 2.6)

Compound	$E^1_{ox}/V^{a,b}$	E^2_{ox}/V^b	E_{red}/V^b
86a	1.090	-	-1.180
210	1.449	-	-
211	0.994	-	-1.324
216	0.772	-	-1.230
222	0.476[c]	1.081	-1.268

[a] 10^{-5}M compound in dry acetonitrile under argon *vs.* Ag/AgCl, Pt working and counter electrodes at 20°C.

[b] All potentials irreversible unless otherwise stated

[c] Reversible potential

Table 6.5 Cyclic Voltammetric Data

As can be see from Table 6.5 all systems (with the exception of compound **210**) possess an irreversible oxidation and reduction couple, with the oxidation potentials for compounds **210-216** being attributed to oxidation of the 1,3-dithiole. The two oxidation potentials for compound **222** correspond to the oxidation of the ferrocene unit (0.476 V) and the 1,3-dithiole respectively. The corresponding reduction potentials are all attributed to the reduction of the dicyanomethylene or cyanoimine units with no observable reduction of the aromatic nitro unit or oxidation of the dimethylamino donor unit. It can be seen that the oxidation and reduction potentials correlate well with the data acquired in chapter 2 (Section 2.6).

6.5 Conclusions.

The addition of two acceptor units conjugated to one dithiole donor unit has the effect of red shifting the position of the charge transfer compared to the parent donor-π-acceptor system. Allied to this red shift a high energy shoulder was also observed which may be attributed to either electron motion from the heteroaromatic donor unit to the acceptor of simply increased π delocalisation within the systems. The

conversion of the aromatic acceptor into an aromatic donor induces a similar red shift in the position of the low energy charge transfer band compared to the simple donor-π-acceptor systems which was the result of an inductive effect. A high energy shoulder was again observed which was difficult to rationalise as only one mode of conjugative charge transfer was available. If the donor was converted into ferrocene the major charge transfer absorption was attributed to the parent donor-π-acceptor system without the inductive increase observed due to the ferrocene unit being twisted thus, precluding conjugation. Noticeably a broad low energy shoulder in the UV-VIS spectra was observed which was very tentatively assigned to an iron sulfur interaction in the excited state. Cyclic voltammetric studies on these systems confirm the presence of a good degree of charge transfer.

Chapter 7

Experimental Details

7.1 General Methods

Melting points were recorded on a Reichert-Kofler hot stage microscope apparatus and are uncorrected.

Infra-red spectra were obtained on a Perkin-Elmer 1720 FT-IR spectrophotometer operating a Gramms 1600 program: with samples embedded in KBr discs.

Proton NMR spectra were recorded on Varian Gemini-200, XL-200 or Varian VXR-200 operating at 199.9 MHz. ^{13}C NMR spectra were recorded on a Varian-400 spectrometer operating at 100.582 MHz. Chemical shifts are quoted in parts per million (ppm) relative to tetramethylsilane an internal reference (0 ppm).

Mass spectra were recorded on a VG7070E instrument with ionising modes as indicated; ammonia was used as impingent gas in chemical ionisation mode.

Elemental analysis were obtained on a Carlo-Erba Strumentazione instrument.

UV-VIS spectra were recorded using a Perkin-Elmer II UV-VIS spectrophotometer with 1cm quartz cells.

Column chromatography was carried out using either Merck or Prolabo silica gel (70-230 mesh) or Merck alumina (activity I to III 70-230 mesh); the latter was neutralised by pre-soaking basic alumina in ethyl acetate for 24 h. Solvents were distilled prior to use for chromatography, with the exception of dichloromethane and cyclohexane which were used as supplied. All reactions were performed under an inert atmosphere (nitrogen or argon) which was pre-dried by passing over a column of phosphorus pentoxide.

Reaction solvents were dried over, and distilled from, the following reagents under an inert atmosphere. Diethyl ether, tetrahydrofuran and toluene (sodium metal / benzophenone), acetonitrile, dichloromethane and benzene (calcium hydride), acetone (potassium carbonate), methanol (magnesium methoxide) triethylamine (3 Å molecular sieves). All other reagents were reagent grade and used without further purification.

Cyclic voltammetry experiments were performed in a one-compartment cell with platinum working and counter electrodes. The reference electrode was silver/silver chloride. Electrochemical measurements were carried out using a BAS 50 electrochemical analyser and were compensated for internal resistance. The cell concentrations consisted of test compound (1×10^{-5}M) with dry tetrabutylammonium perchlorate as supporting electrolyte (1×10^{-1}M) in dry acetonitrile (*ca.* 15 ml). All solutions were purged with argon and sonicated for 15 min prior to measurements being taken.

7.2 Experimental for Chapter 2

7.2.1 General Procedure for Compounds 78a-c

To a stirred suspension of salt **77a-c** (15 mmol) in dry propan-2-ol (25 ml) (THF for compound **78b**) at room temperature was added sequentially malononitrile (1.06 ml, 16.8 mmol, 1.1 equiv.) and dry pyridine (3 ml, excess) dropwise. After stirring for 3h, water (1 l) was added and the mixture extracted into dichloromethane (3 x 75 ml) and the organic phase washed with water (2 x 200 ml). After drying ($MgSO_4$), and evaporation *in vacuo*, the residue was purified by silica gel column chromatography (eluent dichloromethane) and, if necessary, recrystallisation from chloroform, which yielded **78a-c**. There was thus obtained:

(4,5-Dimethyl-1,3-dithiole-2-ylidene)-dicyanomethane 78a, as tan needles, (2.04g, 67%). Mpt: 228-229°C (sublimes from *ca.* 150°C). Anal. calc. for $C_8H_6N_2S_2$: C, 49.5; H, 3.1; N,14.4, found: C, 50.2; H, 2.9; N, 14.2. ^1H NMR ($CDCl_3$; 200 MHz) δ: 2.21 (6H, s) ppm. m/z (EI) = 194 (M^+, 100%), (CI) = 195 (M^++1, 25%), 212 (M^++18, 100%). IR (KBr) (cm^{-1}): 2205. UV ($\varepsilon/M^{-1}cm^{-1}$) (DCM) 233 (1.3 x$10^4$) , 370 (1.5 x$10^4$), 387 (4.8 x$10^4$) nm.

(4,5-Dimethylthio-1,3-dithiole-2-ylidene)-dicyanomethane 78b, as a pale yellow solid (2.36g, 61%), Mpt: 100-101°C. (Analysis found: C, 37.4; H, 2.4; N, 11.0; $C_8H_6N_2S_4$ requires: C, 37.2; H, 2.3; N, 10.8%); m/z (EI) 258 (M^+, 100%); m/z (CI) 259 (M^++1, 50%), 276 (M^++ NH_4, 100%); δ_H ($CDCl_3$) 2.52 (6H, s); ν_{max} (KBr) 2207 cm^{-1}; λ_{max} (DCM) (ε) 214 (9.2 x 10^3), 353 (1.6 x 10^4), 364 (1.3 x 10^4) nm.

(4,5-Dicarbomethoxy-1,3-dithiole-2-ylidene)-dicyanomethane 78c, as a cream solid, (2.34 g, 65%). Mpt: 104-105°C. Anal. Calc. for $C_{10}H_6N_2O_4S_2$: C, 42.55; H, 2.14; N, 9.92%, found: C, 42.59; H, 2.10; N, 9.86. ^1H NMR ($CDCl_3$; 200 MHz) δ: 3.96 (6H, s) ppm. m/z (EI) = 251 (30%), 282 (M^+, 100%). IR (KBr) (cm^{-1}): 2207. UV ($\varepsilon/M^{-1}cm^{-1}$) (DCM) 235 (1.5 x 10^4), 354 (2.3 x 10^4) nm.

7.2.2 General Procedure for Compounds 86a-c

To a stirred solution of aldehyde **85a-c** (2.5 mmol) in dry dichloromethane (50 ml) at room temperature was added sequentially (i) titanium tetrachloride (1M in dichloromethane, 3.75 ml, 3.75 mmol), ii) malononitrile (0.24 ml, 3.75 mmol,), and

allowed to cool, diluted with dichloromethane (250 ml) and washed with water (3 x 100 ml). After drying ($MgSO_4$), the solvent was evaporated *in vacuo* and the residue was chromatographed on silica gel (eluent dichloromethane) to afford the products **86a-c**. There was thus obtained:

1-(4,5-Dimethyl-1,3-dithiole-2-ylidene)-3,3-dicyano-2-propene 86a, as a red solid, (358 mg, 65%). Mpt: 222-223°C (sublimes from *ca.* 185°C). Anal. calc. for $C_{10}H_8N_2S_2$: C, 54.5; H, 3.7; N, 12.7%, found: C, 54.2; H, 3.6; N, 12.9. ^1H NMR ($CDCl_3$; 200 MHz) δ: 7.35 and 6.54 (each 1H, AB J = 12.8Hz), 2.15 (3H, s), 2.13 (3H, s) ppm. m/z (EI) = 220 (M^+, 100%); (CI) m/z = 221 (M^++1, 25%), 238 (M^++ 18, 100%). IR (KBr) (cm^{-1}): 2208, 2200, 1540. UV ($\varepsilon/M^{-1}cm^{-1}$) (DCM) 249 ($7.4x10^3$), 489 ($4.2x10^4$) nm.

1-(4,5-Dimethylthio-1,3-dithiole-2-ylidene)-3,3-dicyano-2-propene 86b, as a red solid, (504 mg, 71%). Mpt: 149-150°C. Anal. calc. for $C_{10}H_8N_2S_4$: C, 42.2; H, 2.8; N, 9.9%, found: C, 42.2; H, 2.8; N, 9.8. ^1H NMR ($CDCl_3$; 200 MHz) δ: 7.30 and 6.56 (each 1H, AB J = 12.7Hz), 2.47 (s, 3H), 2.46 (s, 3H) ppm. ^{13}C NMR ($CDCl_3$) 164.2, 150.8, 130.8, 130.3, 115.1, 113.1, 108.0, 71.7, 19.2, 19.1 ppm. m/z (CI) = 285 (M^++1, 100%), 302 (M^++ 1 12%). IR (KBr) (cm^{-1}): 2210, 2198, 1554. UV ($\varepsilon/M^{-1}cm^{-1}$) (DCM) 244 ($1.0x10^4$), 318 ($1.0x10^4$), 475 ($5.3x10^4$) nm. A crystal suitable for X-ray analysis was grown by slow evaporation of a CH_2Cl_2 solution.

1-(4,5-Dicarbomethoxy-1,3-dithiole-2-ylidene)-3,3-dicyano-2-propene 86c, as an orange solid, (492 mg, 64%). Mpt: 202-203°C (sublimes from *ca.* 150°C). Anal. calc. for $C_{12}H_8N_2O_4S_2$: C, 46.8; H, 2.6; N, 9.1%, found: C, 46.9; H, 2.7; N, 9.0. ^1H NMR ($CDCl_3$; 200 MHz) δ: 7.32 and 6.60 (each 1H, AB J = 12.5Hz), 3.92 (6H, s) ppm. m/z (CI) = 309 (M^++1, 80%), 326 (M^++18, 100%). IR (KBr) (cm^{-1}): 2218, 2208, 1707. UV ($\varepsilon/M^{-1}cm^{-1}$) (DCM) 241 ($5.8x10^3$), 439 ($2.5x10^4$) nm.

7.2.3 General Procedure for Compounds 87a-c

To a stirred solution of aldehyde **85a-c** (3 mmol) in dichloromethane (25 ml) at 20°C was added sequentially (i) titanium tetrachloride (1M in dichloromethane, 3.3 ml, 3.3 mmol) and (ii) *bis*-trimethylsilylcarbodiimide (BTC) (0.75 ml, 3.3 mmol) and the reaction stirred for 48h. After which time the reaction was diluted with dichloromethane (250 ml) and washed with water (3 x 100 ml). After drying ($MgSO_4$), the solvent was evaporated *in vacuo* and the residue was chromatographed on silica gel (eluent ethyl acetate) to afford the compounds **87a-c**. There was thus obtained:

1-*N*-Cyanoimine-2-(4,5-dimethyl-1,3-dithiole-2-ylidene)-ethane 87a, as an orange solid, (459 mg, 78%). Mpt: 181-182°C (sublimes from *ca.* 130°C). Anal. calc. for $C_8H_8N_2S_2$: C, 49.0; H, 4.1; N, 14.3%, found: C, 48.8; H, 3.8; N, 14.3. ^{1}H NMR ($CDCl_3$; 200 MHz) δ: 8.25 and 6.41 (each 1H, AB J = 4.9Hz), 2.24 (6H, s) ppm. m/z (CI) =197 (M^++1, 100%). IR (KBr) (cm^{-1}): 2155, 1542, 1457. UV ($\varepsilon/M^{-1}cm^{-1}$) (DCM) 236 ($9.7x10^3$), 432 ($3.7x10^4$), 450 ($5.0x10^4$) nm.

1-*N*-Cyanoimino-2-(4,5-dimethylthio-1,3-dithiole-2-ylidene)-ethane 87b, as an orange solid, (660 mg, 85%). Mpt: 127-128°C. Anal. calc. for $C_8H_8N_2S_4$: C, 36.9; H, 3.1; N, 10.7%, found: C, 37.0; H, 2.9; N, 10.9. ^{1}H NMR ($CDCl_3$; 200 MHz) δ: 8.32 and 6.48 (each 1H, AB, J = 4.8Hz), 2.56 (3H, s), 2.51 (3H, s) ppm. ^{13}C NMR ($CDCl_3$) 167.3, 166.1, 134.9, 129.5, 117.9, 105.4, 19.2, 19.0 ppm. m/z (CI) = 261 (M^++1, 100%). IR (KBr) (cm^{-1}): 2161, 1540, 1455. UV ($\varepsilon/M^{-1}cm^{-1}$) (DCM) 201 ($8.1x10^3$), 307 ($2.5x10^3$), 448 ($1.3x10^4$) nm. A crystal suitable for X-ray analysis was grown by slow evaporation of a dichloromethane solution

1-*N*-Cyanoimino-2-(4,5-dicarbomethoxy-1,3-dithiole-2-ylidene)-ethane 87c, as a bright yellow solid, (681 mg, 80%). Mpt: 156-157°C. Anal. calc. for $C_{10}H_8N_2O_4S_2$: C,42.2; H, 2.8; N, 9.9%, found: C, 42.0; H, 2.7; N, 10.2. ^{1}H NMR ($CDCl_3$; 200 MHz) δ: 8.45 and 6.59 (each 1H, AB J = 4.9Hz), 3.95 (3H, s), 3.93 (3H, s) ppm. m/z (CI) = 261 (M^++1, 100%). IR (KBr) (cm^{-1}): 2189, 2169, 1733, 1710, 1575, 1559, 1471. UV ($\varepsilon/M^{-1}cm^{-1}$) (DCM) 227 ($1.3x10^4$), 414 ($3.6x10^4$), 426 ($3.5x10^4$) nm.

7.2.3 Experimental Detail to Section 2.4.6

1-(4,5-Dimethyl-1,3-dithiole-2-ylidene)-2-phenyl-ethanone 94. To a solution of Wittig reagent **79a** (3.0 g, 6.52 mmol) in acetonitrile (25 ml) was added sequentially triethylamine (1.0 ml, 6.52 mmol) and phenylglyoxal **92** (1.0 g, 6.52 mmol) and the resultant yellow solution was stirred at 20°C for 13h. After which time a yellow solid developed which was collected by filtration to yield **94** a bright yellow solid (1.18 g, 72%). Mpt: 171°C. Anal. calc. for $C_{13}H_{12}S_2O$: C, 62.87; H, 4.87, found: C, 63.04; H, 4.66. ^{1}H NMR ($CDCl_3$; 200 MHz) δ: 7.98-7.93 (2H, m), 7.46-7.43 (3H, m), 7.33 (1H, s), 2.16 (6H, s) ppm. m/z (DCI) 249 (M^++1, 100). IR (KBr) (cm^{-1}): 1567, 1495, 1470, 1229, 755, 630. UV ($\varepsilon/M^{-1}cm^{-1}$) (DCM) 236 (2.2 x 10^3), 432 (4.1 x 10^4) nm.

1-(4,5-Dimethyl-1,3-dithiole-2-ylidene)-propan-2-one 95. To a solution of Wittig reagent **79a** (2.11 g, 4.58 mmol) in acetonitrile (10 ml) was added triethylamine (0.67

ml, 4.58 mmol) and the resultant solution was stirred for 15 mins. To this was added methylglyoxal **93** (1.05 ml, 6.88 mmol) and the solution was stirred at 20°C for 1.5 h. The solvent was removed *in vacuo* and the residue chromatographed on silica gel (eluent dichloromethane) to yield **95** as a yellow solid (0.41 g, 48%) which slowly darkened to a red solid and was not obtained analytically pure. Mpt: 130-131°C. ^{1}H NMR ($CDCl_3$; 200 MHz) δ: 6.65 (1H, s), 2.17 (3H, s), 2.01 (6H, s) ppm. m/z (DCI) 186 (M^++1, 100). UV ($\varepsilon/M^{-1}cm^{-1}$) (DCM) 235 (3.4 x 10^3), 420 (5.0 x 10^4) nm.

1-(4,5-Dimethyl-1,3-dithiole-2-ylidene)-2-phenyl-ethanthione 96. To a solution of compound **94** (0.3 g, 1.21 mmol) in acetonitrile (40 ml), was added phosphorus pentasulfide (0.81 g, 1.81 mmol) followed by sodium bicarbonate (0.15 g, 1.81 mmol) and the solution was warmed to 50°C for 6h. The solution was allowed to cool and the solvent removed *in vacuo*. Purification was achieved by silica gel chromatography (eluent dichloromethane:hexane 4:1 v/v) to yield compound **96** as a brown crystalline solid (0.16 g, 50%). Mpt: 200-201°C. Anal. calc. for $C_{13}H_{12}S_3$: C, 59.05; H, 4.57, found: C, 58.51; H, 4.74. ^{1}H NMR ($CDCl_3$; 200 MHz) δ: 8.16 (1H, s), 7.88-7.83 (2H, m), 7.40-7.37 (3H, m), 2.28 (3H, s), 2.25 (3H, s) ppm. m/z (DCI) 189 (30%), 233 (35%), 249 (55%), 265 (M^++1, 100). IR (KBr) (cm^{-1}): 1457, 1294, 1260, 767. UV ($\varepsilon/M^{-1}cm^{-1}$) (DCM) 220 (3.0 x 10^4), 489 (4.0 x 10^4) nm.

1-(4,5-Dimethyl-1,3-dithiole-2-ylidene)-propan-2-thione 97. To a solution of compound **95** (0.38 g, 2.04 mmol) in acetonitrile (30 ml) was added phosphorus pentasulfide (1.36 g, 3.06 mmol, 1.5 equiv.), followed by sodium bicarbonate (0.27 g, 3.06 mmol, 1.5 equiv.) and the solution was warmed to 50°C for 6 h. The solution was allowed to cool and the solvent was removed *in vacuo* to yield a dark residue which was extracted into dichloromethane (100 ml) and washed with water (3 x 200 ml). The organic phase was dried ($MgSO_4$) and the solvent removed *in vacuo*. Purification of the dark residue was achieved by silica gel chromatography (eluent dichloromethane) to yield compound **97** as a red crystalline solid (0.30 g, 73%). Mpt: 121-123°C. Anal. calc. for $C_8H_{10}Se_3$: C, 47.48; H, 4.98, found: C, 47.04; H, 4.92. ^{1}H NMR ($CDCl_3$; 200 MHz) δ: 7.63 (1H, s), 2.74 (3H, s), 2.25 (3H, s), 2.21 (3H, s) ppm. m/z (DCI) 127 (30%), 187 (45%), 203 (M^++1, 100). IR (KBr) (cm^{-1}): 1460, 1245, 1205, 1095, 765. UV ($\varepsilon/M^{-1}cm^{-1}$) (DCM) 235 (2.2 x 10^4), 466 (1.3 x 10^4) nm.

7.2.4 General Procedure for Compounds 102a-c

To a stirred solution of Wittig reagent **79a-c** (1.5 mmol) and *E,E*-mucondialdehyde **98** (1.5 mmol) in dry tetrahydrofuran (50 ml) at room temperature was added triethylamine (1 ml, excess) and the solution was stirred for 16h at 20°C. After evaporation of the solvent *in vacuo*, the residue was extracted with dichloromethane (250 ml) and washed with water (3 x 100 ml). The organic layer was dried ($MgSO_4$) and the solvent evaporated *in vacuo*. Purification of the products was achieved by silica gel column chromatography. There was thus obtained:

6-(4,5-Dimethyl-1,3-dithiole-2-ylidene)-*trans,trans*-2,4-hexadieneal 102a, by eluting with dichloromethane, as a red solid, (150 mg, 45%). Anal. calc. for $C_{11}H_{12}OS_2$: C, 58.81; H, 5.35%, found: C, 59.01; H, 5.40. Mpt: 108-110°C. ^1H NMR ($CDCl_3$; 200 MHz) δ: 9.50 (1H, d, J_{EF} = 8.1Hz), 7.14 (1H, dd, J_{DC} = 11.5Hz, J_{DE} = 15.0Hz), 6.57 (1H, dd, J_{BA} = 12.0Hz, J_{BC} = 11.2Hz), 6.21-6.02 (3H, m, H_A,H_C,H_E) ppm. m/z (DCI) = 225 (M^++1, 100%). IR (KBr) (cm^{-1}): 1667, 1603, 1567, 1501. UV ($\varepsilon/M^{-1}cm^{-1}$) (DCM) 229 ($6.4x10^4$), 280 ($9.9x10^3$), 451 ($1.5x10^4$) nm.

6-(4,5-Dimethylthio-1,3-dithiole-2-ylidene)-*trans,trans*-2,4-hexadieneal 102b, by eluting with dichloromethane, as a deep red solid, (341 mg, 79%). Mpt: 95-96°C. Anal. calc. for $C_{11}H_{12}OS_4$: C, 45.8; H, 4.2%, found: C, 45.8; H, 4.4. ^1H NMR ($CDCl_3$; 200 MHz) δ: 9.52 (1H, d, J_{EF} = 8.1Hz), 7.12 (1H, dd, J_{DC} = 11.1Hz, J_{DE} = 15.0Hz), 6.52 (1H, dd, J_{BA} = 11.6Hz, J_{BC} = 14.1Hz), 6.20 (1H, dd, J_{CB} = 14.1Hz, J_{CD} = 11.1Hz), 6.13 (1H, d, J_{AB} = 11.6Hz), 6.09. (1H, dd, J_{ED} = 15.0Hz, J_{EF} = 8.1Hz,), 2.41 (3H, s), 2.40 (3H, s) ppm. ^{13}C NMR ($CDCl_3$) 193.2, 152.2, 143.3, 137.5, 129.6, 127.8, 126.7, 125.4, 113.2, 19.0, 18.9 ppm. m/z (CI) = 289 (M^++1, 100%). IR (KBr) (cm^{-1}): 1670, 1595, 1573. UV ($\varepsilon/M^{-1}cm^{-1}$) (DCM) 229 ($4.4x10^3$), 293 ($7.6x10^3$), 438 ($2.1x10^4$) nm.

6-(4,5-Dicarbomethoxy-1,3-dithiole-2-ylidene)-*trans,trans*-2,4-hexadieneal 102c. Initial elution with dichloromethane afforded compound **103c** as a dark-orange solid, (108 mg, 14%). Mpt: 186-188°C. Anal. calc. for $C_{20}H_{18}O_8S_4$ requires: C, 46.7; H, 3.5, found: C, 46.5; H, 3.6;). ^1H NMR ($CDCl_3$; 200MHz) δ: 6.05-5.97 (6H, m), 3.83 (12H, s). m/z (CI) 515 (M^++1, 100%). IR (KBr) (cm^{-1}) 1749, 1730, 1702, 1598 1563 UV ($\varepsilon/M^{-1}cm^{-1}$) (DCM) 433 ($9.6 \times 10^4$), 410 ($8.5 \times 10^4$), 388 ($5.0 \times 10^4$), 239 ($1.5 \times 10^4$) nm. continued elution with dichloromethane/ acetone (10:1 v/v) afforded compound **102c** as an orange solid, (252 mg, 54%). Mpt: 147-148°C. Anal. calc. for

$C_{13}H_{12}O_5S_2$:C,50.0; H, 3.9%, found: C, 50.3; H, 3.7. ^1H NMR ($CDCl_3$; 200 MHz) δ: 9.55 (1H, d, J_{EF} = 8.0Hz), 7.11 (1H, dd, J_{DE} = 15.1Hz, J_{DC} = 11.1Hz), 6.47 (1H, dd, J_{BA} = 11.2Hz, J_{BC} = 14.3Hz), 6.25 (1H, dd, J_{CB} = 14.3Hz, J_{CD} = 11.1Hz), 6.16 (1H, d, J_{AB} = 11.2Hz), 6.10 (1H, dd, J_{ED} = 15.1Hz, J_{EF} = 8.0Hz), 3.86 (6H, s) ppm. m/z (CI) = 313 (M^++1, 100%). IR (KBr) (cm^{-1}): 1730, 1702, 1664, 1603, 1581. UV (ε/$M^{-1}cm^{-1}$) (DCM) 229 ($7.8x10^3$), 264 ($8.2x10^3$), 410 ($2.9x10^4$) nm.

7.2.5 General Procedure for Compounds 104b,c

Compounds **104b,c** were prepared according to the procedure outlined in Section 7.2.2 from aldehydes **102b,c** (0.7 mmol, 1.0 equiv.), dichloromethane (50 ml), titanium tetrachloride (1.0 ml, 0.75 mmol, 1.1 equiv.), malononitrile (0.06 ml, 1 mmol, 1.4 equiv.), and pyridine (1 ml, excess). The mixture was then heated under reflux for 24h and allowed to cool. The solvent was removed *in vacuo* and the residues purified by silica gel chromatography. There was thus obtained:

1-(4,5-Dimethylthio-1,3-dithiole-2-ylidene)-7,7-dicyano-*trans,trans,trans*-2,4,6-heptatriene 104b, by eluting with dichloromethane/ hexane (2:1 v/v), as a deep red solid, (101 mg, 43%). Mpt: 160-162°C. Anal. Calc. for $C_{14}H_{12}N_2S_4$: C, 50.0; H, 3.6; N, 8.3%, found: C, 50.1; H, 3.7; N, 8.2. ^1H NMR ($CDCl_3$; 200 MHz) δ: 7.42 (1H, d, J_{EF} = 11.9Hz), 6.95 (1H, dd, J_{DC} = 11.5Hz, J_{DE} = 14.1Hz), 6.65 (1H, dd, J_{ED} = 14.1Hz, J_{EF} = 11.9Hz), 6.55 (1H, dd, J_{BA} = 11.6Hz, J_{BC} = 13.9Hz), 6.24 (1H, d, J_{AB} = 11.6Hz), 6.18. (1H, dd, J_{CB} = 13.9Hz, J_{CD} = 11.5Hz), 2.45 (3H, s), 2.43 (3H, s) ppm. m/z (CI) = 337 (M^++1, 100%). IR (KBr) (cm^{-1}): 2215 , 1581. UV (ε/$M^{-1}cm^{-1}$) (DCM) 264 ($6.2x10^3$), 326 ($6.8x10^3$), 533 ($2.3x10^4$) nm.

1-(4,5-Dicarbomethoxy-1,3-dithiole-2-ylidene)-7,7-dicyano-*trans,trans,trans*-2,4,6-heptatriene 104c, by eluting with dichloromethane, as an deep red solid, (219 mg, 87%). Mpt: 213-214°C. Anal. Calc. for $C_{16}H_{12}N_2O_4S_2$: 53.3; H, 3.3; N, 7.7%, found: C, 53.4; H, 3.5; N, 7.6 ^1H NMR ($CDCl_3$; 200 MHz) δ: 7.39 (1H, d, J_{EF} = 12.0Hz), 6.92 (1H, dd, J_{DC} = 11.6Hz, J_{DE} = 14.1Hz), 6.67 (1H, dd, J_{DE} = 14.1Hz, J_{EF} = 12.0Hz), 6.50 (1H, dd, J_{BA} = 11.5Hz, J_{BC} = 13.9Hz), 6.22 (1H, d, J_{AB} = 11.5Hz), 6.21. (1H, dd, J_{CB} = 13.9Hz, J_{CD} = 11.6Hz), 3.87 (6H, s) ppm . ^{13}C NMR ($CDCl_3$) 159.1, 159.0, 158.8, 147.9, 142.8, 138.8, 133.0, 131.1, 127.3, 125.1, 114.0, 112.1, 109.7, 79.8, 53.8, 53.7 ppm. m/z (CI) = 361 (M^++1, 100%). IR (KBr) (cm^{-1}): 2217, 1717, 1700, 1566. UV (ε/$M^{-1}cm^{-1}$) (DCM) 252 ($1.0x10^4$), 302 ($1.0x10^4$), 492 ($7.5x10^4$) nm.

7.3 Experimental for Chapter 3

10-(4,5-Dimethyl-1,3-dithiole-2-ylidene)-anthracene-9-(10H)-one 107a.[80] This compound was prepared *via* a modified literature procedure in which anthrone **106** (3.83 g, 19.7 mmol) was added to a stirred solution of pyridine:acetic acid (3:1v/v) (100 ml) and the resulting yellow solution was stirred at 20°C for 0.25h. After this time, 4,5-dimethyl-1-methylthio-1,3-dithiolium iodide **77a** (6.0 g, 19.7 mmol) was added and the solution warmed to 50-60°C for 16h. The solvent was partially removed *in vacuo* to leave a volume of *ca.* 50 ml whence a red solid precipitated. This solid was filtered, washed with hexane (200 ml), taken up into dichloromethane (150 ml) and the resulting white precipitate removed by filtration. The filtrate was concentrated *in vacuo* to yield compound **107a** as a red crystalline solid (3.7 g, 60%) Mpt: 222-224°C (dichloromethane:cyclohexane), (lit[80] 217-218°C). Spectroscopic and analytical data was entirely consistent with those reported previously for compound **107a**.

10-(4,5-Dimethylthio-1,3-dithiole-2-ylidene)-anthracene-9(10H)-one 107b. To a solution of sodium ethoxide [prepared from finely grated sodium (0.21 g, 8.9 mmol) in dry ethanol (50 ml)] was added anthrone **106** (1.71 g, 8.8 mmol) and the resulting yellow solution was stirred for 15 mins. After this time 2,4,5 trimethylthio-1,3-dithiolium tetrafluoroborate **77b** (3.0 g, 8.8 mmol) was added and the solution warmed to 60°C for 16h. The solution was allowed to cool and the solid that precipitated was filtered and purified by silica gel chromatography (eluent dichloromethane:cyclohexane 1:1 v/v) to afford compound **107b** as an orange solid (1.71 g, 50%). Mpt: 185°C (from cyclohexane/dichloromethane). Anal. calc. for $C_{19}H_{14}OS_4$: C, 59.06; H, 3.62, found: C, 59.31; H, 3.50. ^{1}H NMR ($CDCl_3$; 200 MHz) δ: 8.27, 7.79, (both 2H, d, J=8Hz), 7.65, 7.44 (both 2H, t, J=8Hz) 2.42 (6H s) ppm. ^{13}C NMR ($CDCl_3$) 184.0, 140.6, 139.1, 132.3, 131.2, 127.8, 127.4, 127.3, 126.7, 119.9, 19.8 ppm. m/z (DCI) 387 (M^++ 1, 100%). IR (KBr) (cm^{-1}): 1607. UV ($\varepsilon/M^{-1}cm^{-1}$) (DCM) 225 (1.6 x 10^3), 455 (9.8 x 10^3) nm.

10-(4,5-Dihydro-1,3-dithiole-2-ylidene) anthracene-9-(10H)-one 107c.[80]
This compound was prepared according to a literature procedure in 86% yield.

10-(4,5-Ethylenedithio)-1,3-dithiole-2-ylidene) anthracene-9-(10H)-one 107d. This was prepared in an analogous manner to compound **107a** using 4,5-ethylenedithio-2-methylthio-1,3-dithiolium tetrafluoroborate **77d** yielding compound **107d** as a red solid in 69% yield. Mpt: 201-203°C. Anal. calc. for $C_{19}H_{12}S_4O$: C,

59.37; H, 3.13:, found: C, 59.20; H, 3.04. ^{1}H NMR ($CDCl_3$; 300 MHz) δ: 8.27, 7.74, (both 2H, d, J=8Hz) 7.66, 7.45 (both 2H, t , J=8Hz) 3.33 (4H s) ppm. ^{13}C NMR ($CDCl_3$, 75 MHz) 153.7, 138.7, 138.1, 136.4, 135.4, 131.7, 130.5, 127.1, 126.8, 126.2 ppm.. m/z (EI) 384 (M^+, 100%). IR (KBr) (cm^{-1}): 1756, 1547, 1540, 1520, 1499. UV ($\varepsilon/M^{-1}cm^{-1}$) (DCM) 222 (3.2 x 10^3), 460 (4.5 x 10^4) nm.

7.3.2 General Procedure for Compounds 108a-d

To a stirred solution of ketone **107a-d**, (1 equiv.) in dry chloroform, was added sequentially (i) malononitrile (10 equiv.), titanium tetrachloride (2.5 equiv.) and finally dry pyridine (10 equiv.), the resulting dark solution was heated under reflux for 20h. The solution was then allowed to cool and the solvent removed *in vacuo* to leave a dark residue which was purified by silica gel chromatography (eluent dichloromethane) to afford compounds **108a-d**. There was thus obtained:

10-(4,5-Dimethyl-1,3-dithiole-2-ylidene)-9-(2,2-dicyanomethane) anthracene 108a. From ketone **107a** (0.16 g, 0.5 mmol), chloroform (20 ml), malononitrile (0.33 g, 5.0 mmol), titanium tetrachloride (0.42 ml, 5.0 mmol) and dry pyridine (0.42 ml, 5.0 mmol) and isolated as a purple solid, (0.122g 66%). Mpt: >250°C. ^{1}H NMR ($CDCl_3$; 200 MHz) δ: 8.14, 7.94, (both 2H, d, J=8Hz) 7.80, 7.39 (both 2H, t, J=8Hz) 2.04 (6H s) ppm. ^{13}C NMR ($CDCl_3$) 162.2, 143.6, 135.5, 131.2, 128.4, 126.3, 126.2, 125.6, 122.5, 116.8, 115.1,13.1 ppm. m/z (DCI) 371 (M^+, 100%). HRMS:- found 371.0529 $C_{22}H_{14}S_2N_2$ requires 371.0526. IR (KBr) (cm^{-1}): 2210. UV ($\varepsilon/M^{-1}cm^{-1}$) (DCM) 231 (3.2 x 10^3), 572 (1.1 x 10^4) nm. Slow evaporation of a dichloromethane:hexane solution (1:1 v/v) of compound **108a** afforded X-ray quality crystals.

10-(4,5-Dimethylthio-1,3-dithiole-2-ylidene)-9-(2,2-dicyanomethane) anthracene 108b. From ketone **107b** (0.104 g, 0.27 mmol), chloroform (50 ml), malononitrile (0.178 g, 2.7 mmol), titanium tetrachloride (0.08 ml, 0.68 mmol), and dry pyridine (0.23 ml, 2.7 mmol) as a purple solid (0.08 g, 65%). Mpt: 250°C (dec.). ^{1}H NMR ($CDCl_3$; 200 MHz) δ: 8.14, 7,80 (both 2H, d, J=8Hz) 7.59, 7.44 (both 2H, t, J=8Hz), 2.42 (6H s) ppm. ^{13}C NMR ($CDCl_3$) 162.4, 140.1, 135.0, 131.4, 128.6, 127.0, 126.8, 126.5, 125.7, 119.8, 19.8 ppm. m/z (EI) 434 (M^+, 100). HRMS :- found 434.0034 $C_{22}H_{14}S_4N_2$ requires 434.0039. IR (KBr) (cm^{-1}): 2220 UV ($\varepsilon/M^{-1}cm^{-1}$) (DCM) 243 (5.6 x 10^4) nm.

10-(4,5-Dihydro-1,3-dithiole-2-ylidene)-9-(2,2-dicyanomethane) anthracene 108c. From ketone **107c** (0.1 g, 0.34 mmol), chloroform (50 ml), malononitrile (0.22 ml, 3.4

mmol), titanium tetrachloride (0.85 ml, 0.85 mmol) and dry pyridine (0.23 ml, 3.4 mmol), yielding compound **108c** as a black solid (0.09 g, 84%) following silica gel column chromatography (eluent dichloromethane). Mpt: 199-201°C. Anal. calc. for $C_{20}H_{10}N_2S_2$: C, 69.09; H, 3.03; N, 8.13 found: C, 68.88; H, 3.21: N, 7.98 ^{1}H NMR ($CDCl_3$; 200 MHz) δ: 8.14, 7.98, (both 2H, d, J=8Hz) 7.60, 7.41 (both 2H, t, J=8Hz) 6.52 (2H s)ppm. ^{13}C NMR ($CDCl_3$) 162.5, 139.3, 131.8, 130.5, 127.0, 126.4, 126.0, 118.0, 117.5 ppm. m/z (DCI) 344 (M^++1, 100%). IR (KBr) (cm^{-1}): 2240. UV ($\varepsilon/M^{-1}cm^{-1}$) (DCM) 245 (2.9 x 10^3), 542 (1.0 x 10^4) nm.

10-(4,5-Ethylenedithio-1,3-dithiole-2-ylidene)-9-(2,2-dicyanomethane) anthracene 108d. From ketone **107d** (0.1 g, 0.26 mmol), chloroform (50 ml), malononitrile (0.17 g, 2.6 mmol), titanium tetrachloride (0.65 ml, 0.65 mmol) and dry pyridine (0.15 ml, 2.6 mmol), yielding compound **108d** as a purple solid (0.06 g, 54%). Mpt: >250°C. Anal. calc. for $C_{22}H_{12}N_2S_4$: C, 61.11; H, 2.77; N, 6.45, found: C, 61.24; H, 3.01; N, 6.50. ^{1}H NMR ($CDCl_3$; 200 MHz) δ: 8.13, 7.78 (both 2H, d, J=8Hz), 7.78, 7.59 (Both 2H, t, J=8Hz), 3.35 (4H, s) ppm. ^{13}C NMR ($CDCl_3$) 153.8, 135.0, 131.3, 128.6, 126.8, 126.5, 125.7, 114.7, 111.8, 29.3 ppm. m/z (EI) 434 (M^+, 100). IR (KBr) (cm^{-1}): 2220, 1600, 1570, 1540, 1500, 1450. UV ($\varepsilon/M^{-1}cm^{-1}$) (DCM) 254 (0.9 x 10^4), 550 (0.73 x 10^4) nm.

7.3.3 General Procedure for Compounds 109a-d

To a stirred solution of ketone **107a-d** (1 equiv.) in dry chloroform was added titanium tetrachloride (3.5 equiv.) followed by *bis*-trimethylsilycarbodiimide (BTC) (3 equiv.) The resulting dark solutions were heated under reflux for 48-72h with periodic addition of more BTC until no starting material was observable (TLC analysis). The solution was allowed to cool, the solvent removed *in vacuo* and the residue purified by silica gel chromatography, to afford compounds **109a-d**. There was thus obtained:

10-(4,5-Dimethyl-1,3-dithiole-2-ylidene)-9-*N*-cyanoimine anthracene 109a. From ketone **107a** (0.1 g, 0.31 mmol), chloroform (30 ml), titanium tetrachloride (1.1 ml, 1.1 mmol) and BTC (0.20 ml, 0.93 mmol) yielding compound **109a** as a black solid (0.09 g, 85%) following column chromatography, eluent dichloromethane. Mpt: 234-236°C. Anal. calc. for $C_{20}H_{14}N_2S_2$: C, 69.36; H, 4.04, N, 8.09 found: C, 69.44; H, 4.20; N, 7.82. ^{1}H NMR ($CDCl_3$; 200 MHz) δ: 8.00-7.92 (2H, m), 7.89-7.85 (2H, m), 7.66 (2H, t, J=8Hz), 7.42 (2H, t, J=8Hz), 2.04 (6H, s) ppm. m/z (EI) 346 (M^+, 100%). IR (KBr) (cm^{-1}): 2150, 1600, 1570, 1530, 1485, 1430. UV ($\varepsilon/M^{-1}cm^{-1}$) (DCM) 243 (5.4 x 10^3), 566 (2.0 x 10^4) nm.

10-(4,5-Dimethylthio-1,3-dithiole-2-ylidene)-9-*N*-cyanoimine anthracene 109b. From ketone **107b** (0.14 g, 0.36 mmol), chloroform (20 ml), titanium tetrachloride (1.27 ml, 1.27 mmol) and BTC (0.24 ml, 1.08 mmol) to yield compound **109b** as a blue/black solid (eluent dichloromethane) (0.05 g, 47%). Mpt: 175-178°C. ^{1}H NMR ($CDCl_3$; 400 MHz, -30°C) δ: 8.83 (1H, d, J=8Hz), 8.21 (1H, d, J=8Hz), 7.85 (1H, d, J=8Hz), 7.74-7.67 (3H, m), 7.52 (1H, t, J=8Hz), 7.45 (1H, t, J=7.6Hz) ppm. ^{13}C NMR ($CDCl_3$) 173.3, 142.4, 136.9, 132.4, 127.4, 127.0, 126.8, 126.0 (b), 119.2, 115.6, 19.3 ppm. m/z (DCI) 411 (M^++ 1, 100%). HRMS :- found 410.0040 $C_{20}H_{14}S_4N_2$ requires 410.0040. IR (KBr) (cm^{-1}): 2253. UV ($\varepsilon/M^{-1}cm^{-1}$) (DCM) 232 (2.6 x 10^3), 542 (0.86 x 10^4) nm..

10-(4,5-Dihydro-1,3-dithiole-2-ylidene)-9-*N*-cyanoimine anthracene 109c. From ketone **107d** (0.1 g, 0.34 mmol), chloroform (50 ml), titanium tetrachloride (1M, 1.19 ml, 1.19 mmol) and BTC (0.23 ml, 1.02 mmol), (eluent dichloromethane:hexane 3:5 v/v) yielded unchanged ketone **107d** (0.01 g, 10%) continued elution yielded compound **109d** as a purple solid, (0.025 mg, 23%). Mpt: 185-186°C. Anal. calc. for $C_{18}H_{10}N_2S_2$: C, 67.92; H, 3.14; N,8.80, found: C, 68.01; H, 3.00; N, 8.95. ^{1}H NMR ($CDCl_3$; ; 400 MHz -30°C) δ: 8.85, 8.23, 8.01, 7.93 (all 1H d J=8Hz), 7.71 (2H m), 7.48, 7.43 (both 1H t J=8Hz) ppm. ^{13}C NMR ($CDCl_3$; 50MHz) 173.3, 137.6, 134.3, 132.4, 127.3, 126.7, 125.8 (b), 118.5, 118.4, 117.5) ppm. m/z (DCI) 218 (100%), 319 (M^++ 1, 40%). IR (KBr) (cm^{-1}): 2155. UV ($\varepsilon/M^{-1}cm^{-1}$) (DCM) 229 (1.7 x 10^3), 543 (1.5 x 10^4) nm.

10-(4,5-Ethylenedithio-1,3-dithiole-2-ylidene)-9-*N*-cyanoimine anthracene 109d. From ketone **107d** (0.1 g, 0.26 mmol), titanium tetrachloride (1M, 0.86 ml, 0.86 mmol) and BTC (0.12 ml, 0.78 mmol) to yield compound **109c** as a black solid (0.08 g, 77%) (eluent dichloromethane). Mpt: 178-179°C. ^{1}H NMR ($CDCl_3$; 200 MHz) δ: 7.81-7.73 (4H, m), 7.68 (2H, t, J=8Hz), 7.47 (2H, t, J=8Hz) 3.35 (4H, s) ppm. Anal. Calc. for $C_{20}H_{12}N_2S_4$: C, 58.82; H, 2.94; N, 6.93, found: C, 58.80; H, 3.06; N, 7.19. IR (KBr) (cm^{-1}): 2135. m/z (DCI) 409 (M^++1, 100%). UV ($\varepsilon/M^{-1}cm^{-1}$) (DCM) 254 (0.5 x 10^4), 558 (0.93 x 10^4) nm.

7.4 Experimental for Chapter 4

7.4.1 General Procedure for Compounds 139a-c

To a stirred suspension of the corresponding Wittig reagent **138a-c** (3.0 equiv.) in dry benzene was added triethylamine (3.0 equiv.) followed by 4-formyl-tetrathiafulvalene[90]**111** (1.0 equiv.) in one portion against a positive flow of argon. The resulting dark solution was heated under reflux for 4h. The solution was allowed to cool and the solvent removed *in vacuo* to yield a black residue which was purified by silica gel chromatography yielding compounds **139a-c**: There was thus obtained.

1-(4'-Tetrathiafulvalenyl)-2-(4-nitrobenzyl)-ethene 139a. From Wittig reagent **138a** (3.71 g, 7.76 mmol), benzene (50 ml), triethylamine (1.08 ml, 7.76 mmol) and 4-formyltetrathiafulvalene **111** (0.6 g, 2.59 mmol) eluent dichloromenthane:hexane (5:3 v/v) yielded compound **139a** as a purple solid, (0.73 g, 80%). Mpt: >250°C. Anal. calc. for $C_{14}H_9NO_2S_4$: C, 47.86; H, 2.56; N, 3.96, found: C, 47.85; H, 2.33; N, 3.72. ^{1}H NMR ($CDCl_3$; 200 MHz) δ: 8.18 (2H, d, J=9Hz), 7.56 (2H, d, J=9Hz), 7.07 (1H, d, J=15Hz), 6.72 (1H, d, J=15Hz), 6.61 (1H, s), 6.38 (2H, s) ppm. ^{13}C NMR ($CDCl_3$) 146.2, 143.1, 134.6, 131.7, 131.5, 128.5, 127.2, 124.9, 124.5, 123.9, 120.0, 123.0 ppm.. m/z (EI) 351 (M^+, 100%) (CI) 352 (M^++ 1, 100%). IR (KBr) (cm^{-1}): 1567, 1522, 1290, 1106, 975, 545 UV (ε/$M^{-1}cm^{-1}$) (DCM) 235 (1.4 x 10^4), 267 (2.2 x 10^4), 502 (3.5 x 10^3) nm.

1-(4'-Tetrathiafulvalenyl)-2-(2-nitrobenzyl)-ethene 139b. From Wittig reagent **138b** (2.06 g, 4.31 mmol), benzene (50 ml), triethylamine (0.60 ml, 4.31 mmol) and 4-formyl-tetrathiafulvalene **111** (0.1 g, 0.43 mmol) eluent dichloromenthane:hexane 1:1 v/v yielded compound **139b** as a black solid, (0.1 g, 67%). Mpt: 159-160°C. Anal. calc. for $C_{14}H_9NO_2S_4$: C, 47.86; H, 2.56; N, 3.98, found: C, 47.42; H, 2.58; N, 3.76. ^{1}H NMR ($(CD_3)_2CO$; 200 MHz) δ: 8.01 (1H, d, J=8Hz), 7.92 (1H, d, J=8Hz), 7.72 (1H, t, J=8 Hz), 7.56 (1H, t, J=8Hz), 7.28 (1H, d, J=16Hz), 6.98 (1H, s), 6.85 (1H, d, J=16Hz), 6.67 (2H, s) ppm. m/z (EI) 351 (M^+, 100%), (CI) 352 (M^++ 1, 100%). IR (KBr) (cm^{-1}): 1513, 1471, 1346, 1331, 1273, 1253. UV (ε/$M^{-1}cm^{-1}$) (DCM) 229 (2.3 x 10^4), 281 (3.2 x 10^4), 467 (4.6 x 10^3) nm.

1-(4'-Tetrathiafulvalenyl)-2-(4-cyanobenzyl)-ethene 139c. From Wittig reagent **138c** (1.78 g, 4.31 mmol), benzene (50 ml), triethylamine (0.6 ml, 4.31 mmol) and 4-formyltetrathiafulvalene **111** (0.1 g, 0.43 mmol) eluent dichloromethane yielded compound **139c** as a deep purple solid (0.1 g, 70%). Mpt: 121-122°C. Anal. calc. for

$C_{15}H_9NS_4$: C, 54.35; H, 2.74; N, 4.23, found: C, 54.56; H, 2.77; N, 4.00. ^1H NMR ($CDCl_3$; 200 MHz) δ: 7.76 (4H, s), 7.41 (1H, d, J=13Hz), 6.97 (1H, s), 6.79 (2H, s), 6.52 (1H, d, J=13Hz) ppm. m/z (DCI) 332 (M^++1, 100). IR (KBr) (cm^{-1}): 1654, 1548, 1468, 1245, 1095, 995. UV ($\varepsilon/M^{-1}cm^{-1}$) (DCM) 221 (4.1 x 10^4), 277 (2.4 x 10^4), 460 (3.7 x 10^3) nm.

7.4.2 Experimental for Section 4.3

1-([4-]4',5,5'Trimethyltetrathiafulvalenyl)-2-(4-nitrobenzyl)-ethene 141. This compound was prepared according to the general procedure outlined in Section 7.4.1. From Wittig reagent **138b** (0.55 g, 1.14 mmol), benzene (50 ml), triethylamine (1 ml, excess), and 4-formyl-4',5,5'-trimethyltetrathiafulvalene **140** (0.1 g, 0.38 mmol) yielded compound **141** as a black solid (0.85 g, 75%). Mpt:>250°C. Anal. calc. for $C_{17}H_{15}NO_2S_4$: C, 69.86; H, 3.81; N, 3.56, found: C, 69.88; H, 4.01; N, 3.45. ^1H NMR ($CDCl_3$; 200 MHz) δ: 8.12 (2H, d, J=8Hz), 7.86 (2H, d, J=8Hz), 6.99 (1H, d, J=15Hz), 6.75 (1H, d, J=15Hz), 2.30 (3H, s), 2.18 (6H, s) ppm. m/z (DCI) 394 (M^++1, 100). IR (KBr) (cm^{-1}): 1543, 1520, 1277, 1100, 938, 510. UV ($\varepsilon/M^{-1}cm^{-1}$) (DCM) 213 (1.6 x 10^4), 244 (3.2 x 10^4), 512 (5.2 x 10^3) nm.

1-(4,5-Dimethyl-1,3-dithiole-2-ylidene)-4-nitrobenzene 142. To a solution of Wittig reagent **79a** (3.4 g, 7.39 mmol) in dry acetonitrile (15 ml) was added triethylamine (1 ml, excess) and the resulting yellow solution was stirred for 15 mins at 20°C. 4-Nitrobenzaldehyde **143** (1.7 g, 11.09 mmol, 1.5 equiv.) was then added and the reaction mixture stirred for 1h at 20°C, after which time a purple solid developed, which was removed by filtration and washed with cold acetonitrile (2 x 20 ml) to yield **142** as a purple crystalline solid (1.90g, 98%). Mpt: 143-145°C. Anal. calc. for $C_{12}H_{11}NO_2S_2$: C, 54.34; H, 4.15; N,5.28. Found: C, 54.10; H, 4.00; N, 5.40. ^1H NMR ($CDCl_3$; 200 MHz) δ: 8.18 (2H, d, J=9Hz), 7.28 (2H, d, J=9Hz), 6.50 (1H, s), 2.05 (3H, s), 2,02 (3H, s) ppm. MS (DCI) *m/z* 236 (99%), 266 (M^++1, 100). IR (KBr) (cm^{-1}): 1586, 1543, 1497, 1481, 1322, 1307. UV ($E/M^{-1}cm^{-1}$) (DCM) 240 (8.2 x 10^3), 280, (1.1 x 10^4), 467 (2.4 x 10^4) nm.

1-(4'Tetrathiafulvalenyl)-prop-2-eneal 144.[90] This was prepared *via* a literature procedure from 4-formyltetrathiafulvalene **111** in 65% yield Mpt: 212-213°C (Lit: 214-215°C).

1-(4'-Tetrathiafulvalenyl)-4-(4-nitrobenzyl)-*trans*-*trans*-hexa-2-4-diene 145. To a solution of Wittig reagent **138a** (1.70 g, 3.55 mmol) in dichloromethane (50 ml) was added triethylamine (3 ml, excess) followed by compound **144** (0.1 g, 1.18 mmol)

dropwise as a solution in dichloromethane (50 ml). The solution was stirred at 20°C for 48h after which time the solvent was removed *in vacuo* and the residue purified by silica gel chromatography (eluent dichloromethane:hexane 1:1 v/v) followed by recrystallisation from dichloromethane:hexane (1:10 v/v) to yield compound **145** (0.1 g, 87%), Mpt: >250°C. Anal. calc. for $C_{16}H_{11}NO_2S_4$: C, 52.71; H, 2.91; N, 3.71, found: C, 52.68; H, 3.11; N, 3.79. ^{1}H NMR ($CDCl_3$; 200 MHz) δ: 8.23 (2H, d, J=8Hz), 8.01 (2H, d, J=8Hz), 7.65 (1H, d, J=15Hz), 7.34-7.32 (2H, m), 6.99 (1H, s), 6.96 (1H, d, J=15Hz) 6.40 (2H, s) ppm. m/z (DCI) 378 (M^++1, 100). IR (KBr) (cm^{-1}): 1657, 1644, 1590, 1499, 1488, 1205. UV ($\varepsilon/M^{-1}cm^{-1}$) (DCM) 231 (4.2 x 10^4), 277 (1.2 x 10^4), 487 (4.68 x 10^3) nm.

1,2-(Bis-carboethoxyimine) propane 160.[104] To a stirred solution of methyl glyoxal **93** (21.8 g, 0.117 mol) in dry ethanol (100 ml) was added ethyl carbazate **159** (25.2g, 0.24 mol) portion-wise over 15 mins. The solution was stirred for 3 h at room temperature after which time a white precipitate developed which was removed by filtration to yield compound **160** as a white solid (23.4 g, 80%). Mpt: 220-222°C (Lit:221-222)

4-(Carboethoxyimino)-1,2,3-thiadiazole 161. Compound **160** (15 g, 0.06 mol) was carefully added to a stirred solution of thionyl chloride (20 ml) and the resulting suspension stirred for 24 h at room temperature. After which time toluene (100 ml) was added and the precipitate that developed was filtered to yield compound **161** (10.7 g, 87%). Mpt: 166-168°C. ^{1}H NMR ($CDCl_3$; 200 MHz) δ: 9.33 (1H, s), 8.74 (1H, s), 8.65 (1H, s), 4.24 (2H, q, J=3Hz), 1.23 (3H, t, J=3Hz).ppm. Anal. Calc. for $C_6H_8N_4O_2S$: C, 36.00; H, 2.00; N, 7.00, found C, 35.98; H, 1.79; N,6.82. IR (KBr) (cm^{-1}): 3398, 3103, 3095, 1720, 1650, 1540. m/z (EI) 200 (M^+, 100).

4-Formyl-1,2,3-thiadiazole 158. To a suspension of compound **161** (10 g, 10 mmol) in sulfuric acid (100 ml) was added formaldehyde (20 ml) and the resultant suspension was heated under reflux for 5 h. At which point the solution was allowed to cool and the mixture extracted with dichloromethane (5x 50 ml). The organic layer was washed with water (2 x 50 ml) and dried ($MgSO_4$). The residue was chromatographed on silica gel (eluent dichloromethane) to yield **158** as a white solid which rapidly darkened to a pink solid over time (3.4 g, 50%). Mpt: 92-94°C. ^{1}H NMR ($CDCl_3$; 200 MHz) δ: 10.52 (1H, s), 9.33 (1H, s) ppm m/z (EI) 114 (M^+, 100).

4-(Ethan-1,2-acetal)-1,2,3-thiadiazole 155. To a solution of compound **158** (3.4 g, 29 mmol) in toluene (200 ml) was added ethan-1,2-diol (1.85 g, 30 mmol) and *p*-toluene sulfonic acid (5 mg). The solution was heated under reflux in a Dean-Stark

trap for 4 h. After which time the solvent was removed *in vacuo* and the crude residue thus obtained was chromatographed on silica gel (eluent dichloromethane) to yield **155** as a yellow oil (2.87 g 59%). ^{1}H NMR ($CDCl_3$; 200 MHz) δ: 8.63 (1H, s), 6.46 (1H, s), 4.11-4.22 (4H, m) ppm. m/z (EI) 158 (M^+, 100). IR (KBr) (cm^{-1}): 3004, 1689.

4-(Ethan-1,2-acetal)-1,3-dithiole-2-thione 157. To a suspension of carbon disulfide (0.5 g, 7 mmol) and sodium hydride (50 mg, 75 mmol) in acetonitrile (20 ml) was added compound **155** (1 g, 6.3 mmol) in one portion. After stirring for 1.5 h the solution was poured into water (100 ml), extracted with diethyl ether (2 x 50 ml) and filtered through a small pad of silica gel (eluent dichloromethane) to yield compound **157** (0.9g, 85%) as a yellow oil. ^{1}H NMR ($CDCl_3$; 200 MHz) δ: 8.63 (1H, s) 6.46 (1H, s) 4.20-4.10 (4H, m) ppm. m/z (EI) 194 (M^+, 100). IR (KBr) (cm^{-1}): 1645, 1234, 1224, 1200.

4-Formyl-1,3-dithiole-2-thione 162.[98] To a solution of **157** (0.45 g, 2.34 mmol) in acetone (20 ml) was added sulfuric acid (10 ml) and the solution stirred for 2 h. After which time diethyl ether (2 x 30 ml) was added and the organic fraction extracted, washed with water (2 x 50 ml) and dried ($MgSO_4$) and purified by silica gel chromatography (eluent dichloromethane) to yield compound **162** (0.34 g, 77%) as a yellow solid. Mpt: 84°C. Lit:- 83-84°C

Alternatively compound **162** may be prepared *via* a literature procedure[98] from compound **154** and diisobutylaluminium hydride in dichloromethane at -85°C, to yield **162** (0.48g, 65%). Mpt: 84°C. Lit: 83-84°C.

4-Carbomethoxy-1,3-dithiole-2-thione 154.[101] To a solution of ethylene trithiocarbonate **72** (10 g, 73 mmol) in xylene (100 ml) was added methyl propiolate **163** (17.9 g, 22.1 mmol, 3 equiv.) and the resulting yellow solution was heated under reflux for 3 days. The solution was allowed to cool, the solvent removed *in vacuo* and the residue purified by silica gel chromatography (eluent hexane:acetone 9:1 v/v) to yield **154** as a yellow crystalline solid (9.0 g, 63%). Mpt: 91-93°C (Lit: 92-94°C).

4-Hydroxymethyl-1,3-dithiole-2-thione 164.[98] This was prepared *via* a literature procedure[98] from compound **154** and diisobutylaluminium hydride in dichloromethane at -85°C to -25°C to yield **164** (0.91 g, 79%). Mpt 62-64°C. Lit :66-68°C

Alternative Procedure for Compound 164. To a suspension of compound **154** (0.71 g 3.7 mmol) in dry methanol (50 ml) was added sodium borohydride (0.56 g, 14.8 mmol, 4 equiv.) in small portions over 30 min and the solution stirred for 16 h. The resulting yellow solution was poured into water (100 ml) and extracted with dichloromethane (200 ml). The organic layer was washed with brine (200 ml) and dried ($MgSO_4$). The solvent was removed in *vacuo* and the residue purified by silica gel chromatography (eluent dichloromethane) to afford **164** a yellow solid (0.45 g 80%). This alcohol was unstable and darkened over a few hours at 20°C and thus was used immediately or maintained at -20°C.

1,3-Dithiole-2-thione-4-ylmethyl(triphenyl)phosphonium bromide 151[98].
This was prepared by a literature procedure[98] from compound **164** yielding compound **154** as a yellow powder 35%. Mpt: 250°C(decomp.), Lit: 250°C (decomp.)

7.4.3 Convergent Methodology to Compound 165.

3-[(4)-1,3-Dithiole-2-thione]-1-nitrobenzyl-ethene 165. To a solution of aldehyde **162** (0.5 g, 3.1 mmol) in dichloromethane was added triethylamine (0.48 ml, 3.2 mmol) and Wittig reagent **138a** (1.48 g, 3.1 mmol). The solution was stirred for 24 h after which time a yellow precipitate developed which was removed by filtration to yield compound **165** as a yellow solid (0.42 g, 55%), Mpt: 131-133°C. Anal. calc. for $C_{11}H_7NO_2S_3$: C, 47.00; H, 2.49; N, 5.00, found: C, 46.70; H, 2.23; N, 4.81. ^1H NMR ($CDCl_3$; 200 MHz) δ: 8.26 (2H, d, J=8.7 Hz), 7.85 (2H, d, J=8.7 Hz), 7.66 (1H, s), 7.54 (1H, d, J=16.2 Hz), 6.94 (1H, d, J=16.2Hz) ppm. m/z (DCI) 282 (M^++1, 100). IR (KBr) (cm^{-1}): 1540, 1521, 1149, 1278, 1108, 893. UV ($\varepsilon/M^{-1}cm^{-1}$) (DCM) 215 ($2.3 \times 10^4$), 415 ($4.2 \times 10^3$) nm.

Alternative method to Compound 165. To a solution of compound **151** (0.24 g, 0.5 mmol) in dry chloroform (20 ml) was added triethylamine (0.07 ml, 0.5 mmol) followed by *para*-nitrobenzaldehyde **143** (0.37 g, 2.5 mmol, 5 equiv.) and the solution was stirred at 20°C for 20h. After which time the solvent was removed *in vacuo* and the resultant residue purified by silica gel chromatography (eluent dichloromethane:hexane 3:2 v/v) yielding compound **165** which was identical to that described above.

7.5 Experimental Details for Chapter 5

1-(4,5-Dimethyl-1,3-diselenole-2-ylidene)-2,2-dicyanomethane 187a.
To a suspension of **181a**[112] (85 mg, 0.19 mmol) in propan-2-ol (20 ml), was added sequentially malononitrile (0.122 ml, 1.95 mmol), and pyridine (3 ml, excess) dropwise over a period of 0.25 h. Following the addition of pyridine a yellow/white precipitate developed which was removed by filtration, washed with ice cold propan-2-ol (10 ml), and dried *in vacuo* to yield compound **187a** as a pale yellow solid, (30 mg, 53%). Mpt: >250°C. Anal. calc. for $C_8H_6N_2Se_2$: C, 33.10; H, 2.07; N,9.65, found: C, 33.18; H, 2.01; N, 9.46. ^{1}H NMR ($CDCl_3$; 200 MHz) δ: 2.30 (6H, s) ppm. *m/z* (^{80}Se, DCI) 276 (100%), 290 (M^++1, 37%), 308 (M^++18, 100%). IR (KBr) (cm^{-1}): 2209, 2201, 1457, 1439, 1389, 417. UV ($\varepsilon/M^{-1}cm^{-1}$) (DCM) 250 (7.9 x 10^3), 357 (1.65 x 10^4) nm.

1-(4,5-Dicarbomethoxy-1,3-diselenole-2-ylidene)-2,2-dicyanomethane 187b. This compound was prepared according in an identical manner to that for compound **187a** from **181b**[115] (100 mg, 0.18 mmol), propan-2-ol (20 ml), malononitrile (0.12 ml, 0.2 mmol) and pyridine (3 ml, excess). Yielding compound **187b** as a white solid (50 mg, 65 %) Mpt: >250°C, ^{1}H NMR ($CDCl_3$; 200 MHz) δ: 3.99 (6H, s) ppm. Anal. calc. for $C_{10}H_6N_2O_4Se_2$: C, 31.74; H, 1.58; N,7.41, found: C,31.82; H, 1.60; N, 7.60. MS (^{80}Se, DCI) *m/z* 379 (M^++1, 100). IR (KBr) (cm^{-1}): 1720, 1670, 1570, 1520, 1289, 1200. UV (DCM) ($\varepsilon/M^{-1}cm^{-1}$) 248 (8.95 x 10^3), 338 (1.83 x 10^4) nm.

1-(4,5-Dimethyl-1,3-diselenole-2-ylidene)-3,3-dicyano-propene 191a. This compound was prepared in an analogous manner to compound **86** (Section 7.2.2) from **188a**[18] (44 mg, 0.15 mmol), dichloromethane (75 ml), titanium tetrachloride (1M, 0.37 ml, 0.37 mmol), malononitrile (0.09 ml, 1.65 mmol) and pyridine (0.12 ml, 1.56 mmol) and the resultant solution heated under reflux for 3 days. After this time the solution was allowed to cool and the solvent removed *in vacuo* to yield a residue which was purified by silica gel chromatography (eluent dichloromethane) to yield compound **191a** as a red solid (36 mg, 73%). Mpt: 235-236°C. Anal. calc. for $C_{10}H_8N_2Se_2$: C, 38.24; H, 2.54; N,8.92, Found: C, 38.09; H, 2.57; N, 8.40. ^{1}H NMR ($CDCl_3$; 200 MHz) δ: 7.16 (1H, d, J=12Hz), 7.04 (1H, d, J=12Hz) 2.16 (3H, s) 2.14 (3H, s) ppm. *m/z* (^{80}Se, DCI) 317 (M^++1, 100%), 334 (M^++18). IR (KBr) (cm^{-1}): 2210, 1654, 1578, 1442, 1035 UV ($\varepsilon/M^{-1}cm^{-1}$) (DCM) 274 (6.3 x 10^3), 295 (5.3 x 10^3), 492 (3.4 x 10^4) nm.

1-(4,5-Dicarbomethoxy-1,3-diselenole-2-ylidene)-2,2-dicyano-ethene 191b. This compound was prepared in an analogous manner to compound **191a** utilising **188b**[117] (125 mg, 0.35 mmol), dichloromethane (50 ml), titanium tetrachloride (1M, 0.9 ml, 0.9 mmol), malononitrile (0.22 ml, 3.5 mmol), pyridine (0.28 ml, 3.5 mmol) and the resultant orange solution was heated under reflux for 24h. After this time a yellow solid developed which was filtered and purified by flash silica column chromatography (eluent dichloromethane) and recrystallisation from dichloromethane:hexane (1:15 v/v) yielded compound **191b** as an orange solid (100 mg, 70%). Mpt: 220°C. ^{1}H NMR ($CDCl_3$; 200 MHz) δ: 7.12 (1H, d J=12Hz), 7.05 (1H, d, J=12Hz), 3.90 (6H, s) ppm. *m/z* (^{80}Se, DCI, rel int) 404 (M^++1, 70%), 422 (M^++18, 100%). HRMS :- 403.8788 $C_{12}H_8Se_2O_4N_2$ requires 403.8814. IR (KBr) (cm^{-1}): 2218, 1693 1573, 1533, 1285, 1215. UV (DCM) ($\varepsilon/M^{-1}cm^{-1}$) 275 (8.6 x 10^3), 447 (3.2 x 10^4) nm.

7.5.1 General Procedure for Compounds 193 and 194

To a solution of Wittig reagent **79c**[66] or the crude Wittig reagent **172b**[112] (1.0 equiv.) in acetonitrile (50 ml) was added triethylamine (1.1 equiv.) followed by teraphthalaldehyde **192** (2.0 equiv.) in one portion against a positive flow of argon and the resulting solution stirred for 16h at 20°C. The solvent was removed *in vacuo* and the residue chromatographed on silica gel: There was thus obtained.

1-(4,5-Dicarbomethoxy-1,3-dithiole-2-ylidine)-4-formyl benzene 193. From Wittig reagent **79c** (3.0 g, 5.47 mmol), triethylamine (0.85 ml, 6.02 mmol) and teraphthalaldehyde **192** (1.47 g, 10.94 mmol) which yielded compound **193** (eluent (dichloromethane:hexane 1:1 v/v) as a yellow solid, (0.96 g, 52%). Mpt: 120°C. Anal. calc. for $C_{15}H_{12}O_5S_2$: C, 53.56; H, 3.60, found: C, 53.30; H, 3.51. ^{1}H NMR ($CDCl_3$; 200 MHz) δ: 9.96 (1H, s), 7.87 (2H, d, J=8Hz), 7.35 (2H, d, J=8 Hz), 6.52 (1H, s), 3.88 (3H, s), 3.87 (3H, s) ppm. *m/z* (DCI) 279 (90%), 337 (M^++1, 100). IR (KBr) (cm^{-1}): 1737, 1689, 1543, 1258, 1165, 1034. UV ($\varepsilon/M^{-1}cm^{-1}$) (DCM) 230 (6.1 x 10^3), 410 (6.5 x 10^4) nm.

1-(4,5-Dicarbomethoxy-1,3-diselenole-2-ylidine)-4-formyl benzene 194. From the crude Wittig reagent **172b** (400 mg, 0.20 mmol), triethylamine (0.03 ml, 0.22 mmol) and teraphthalaldehyde **192** (53 mg, 0.40 mmol) which yielded compound **194** (eluent dichloromethane) as a yellow solid, (60 mg, 70%). Mpt: 128-130°C. Anal. calc. for $C_{15}H_{12}O_5Se_2$: C, 41.70; H, 2.27, found: C, 42.01; H, 2.98. ^{1}H NMR ($CDCl_3$; 200 MHz) δ: 9.98 (1H, s), 7.89 (2H, d, J=8Hz), 7.28 (2H, d, J=8Hz), 7.02 (1H, s), 3.86 (3H, s), 3.64 (3H, s) ppm. *m/z* (^{80}Se, DCI) 433 (M^++1, 100). IR (KBr) (cm^{-1}): 1736,

1718, 1581, 1566, 1238, 1162. UV ($\varepsilon/M^{-1}cm^{-1}$) (DCM) 221 (4.0 x 10^3), 401 (4.4 x 10^4) nm.

1-(4,5-Dicarbomethoxy-1,3-dithiole-2-ylidine)-4-(2,2-dicyanomethylene)-benzene 195 which was prepared in an analogous manner to compound **86** (Section 7.2.2) utilising aldehyde **193** (0.4 g, 1.19 mmol), titanium tetrachloride (2.97 ml, 2.97 mmol), malononitrile (0.75 ml, 11.9 mmol) and pyridine (0.96 ml, 11.9 mmol) and the solution was heated under reflux for 24h and allowed to cool. The solvent was removed *in vacuo* to leave a residue which was purified by silica gel chromatography (eluent dichloromethane:hexane 1:3 v/v) to yield compound **195** as a deep red solid, (430 mg, 95%). Mpt: 131°C. Anal. calc. for $C_{18}H_{12}N_2O_4S_2$: C, 56.25; H, 3.13; N,7.29, found: C, 56.45; H, 3.13; N, 7.39 ^{1}H NMR ($CDCl_3$; 200 MHz) δ: 7.99 (2H, d, J=12Hz) 7.65 (2H, d, J=12Hz), 7.29 (1H, s), 6.82 (1H, s), 3.98 (3H, s), 3.97 (3H, s) ppm. m/z (DCI) 385 (M^++1, 100). IR (KBr) (cm^{-1}): 2220, 1653, 1553, 1512, 1495, 1209. UV ($\varepsilon/M^{-1}cm^{-1}$) (DCM) 230 (6.9 x 10^3), 462 (2.6 x 10^4) nm.

1-(4,5-Dicarbomethoxy-1,3-diselenole-2-ylidine)-4-(2,2-dicyano methylene)-benzene 196 which was prepared in an analogous manner to compound **195** using aldehyde **193** (51 mg, 0.12 mmol), dichloromethane (50 ml), titanium tetrachloride (0.3 ml, 0.3 mmol), malononitrile (0.07 ml, 1.18 mmol) and pyridine (0.07 ml, 1.18 mmol) and the solution was heated under reflux for 48h. After which time the solution was allowed to cool and the solvent removed *in vacuo* . The residue thus obtained was purified by silica gel chromatography (eluent dichloromethane) followed by recrystallisation from dichloromethane:hexane (1:20 v/v) to yield compound **196** as a red solid (46 mg, 81%). Mpt: 165-166°C. Anal. calc. for $C_{18}H_{12}N_2O_4Se_2$: C, 45.00; H, 2.91; N,5.83, found: C, 44.88; H, 3.08; N, 5.69. ^{1}H NMR ($CDCl_3$; 200 MHz) δ: 7.65 (2H, d, J=12Hz), 7.24 (2H, d, J=12Hz), 5.12 (1H, s), 6.87 (1H, s), 3.90 (3H, s), 3.88 (3H, s) ppm. m/z (^{80}Se, DCI) 481 (M^++1, 100). IR (KBr) (cm^{-1}): 2251, 1643, 1633, 1599, 1554, 1421. UV ($\varepsilon/M^{-1}cm^{-1}$) (DCM) 229 (4.8 x 10^3), 458 (3.2 x 10^4) nm.

7.5.3 Experimental Detail to Section 5.4.1

10-(4,5-Dimethyl-1,3-diselenole-2-ylidene)-anthracene-9-(10H)-one 199. This compound was prepared by a similar methodology utilised for compound **107a** (Section 7.3.1) from anthrone **106** (0.14 mg, 0.72 mmol) in pyridine:acetic acid (40 ml, 3:1v/v) to which was added selenoether salt **181a** (350 mg, 0.74 mmol) in one portion against a positive flow of argon. Following addition of **181a**, the solution

which became a deep red colour was heated at 60-70°C for 16h. After this time the solvent is removed *in vacuo*. The residue extracted into dichloromethane (3 x 100 ml) washed with water (2 x 100 ml), sodium bicarbonate solution (1 M, 2 x 50 ml) and dried ($MgSO_4$). The solvent was removed *in vacuo* and the residue purified by silica gel chromatography (eluent dichloromethane:hexane 1:1 v/v) followed by recrystallisation from dichloromethane:hexane (1:1v/v) to yield compound **199** as thin red needles (264 mg, 86%). Mpt: >220°C. Anal. calc. for $C_{19}H_{14}OSe_2$: C, 54.83; H, 3.39. Found: C, 54.49; H, 3.28. ^1H NMR ($CDCl_3$; 200 MHz) δ:8.24 (2H, d, J=8Hz), 7.76 (2H, d, J=8Hz), 7.64 (2H, t, J=8Hz), 7.44 (2H, t, J=8Hz), 2.02 (6H, s) ppm. ^{13}C NMR ($CDCl_3$) 183.7, 140.7, 135.8, 131.9, 130.5, 127.0, 126.7, 125.7, 125.4, 125.1, 14.8 ppm. *m/z* (^{80}Se, DCI) 419 (M^++1, 100). IR (KBr) (cm^{-1}): 1655, 1593, 1495, 1301, 771, 687. UV ($\varepsilon/M^{-1}cm^{-1}$) (DCM) 249 (1.2 x 10^4) 275 (9.7 x 10^3) 380 (2.1 x 10^3) 475 (7.6 x 10^3) nm.

10-(4,5-Dimethyl-1,3-diselenole-2-ylidene)-9-(2,2-dicyanomethane) anthracene 200. This was prepared according to the general procedure outlined in Section 7.3.3 utilising ketone **199** (24 mg, 0.06 mmol), chloroform (25 ml), titanium tetrachloride (1M, 0.5 ml, 0.5 mmol), malononitrile (0.03 ml, 0.5 mmol) and pyridine (0.05 ml, 0.5 mmol). The resultant brown solution was heated under reflux for 24 h with periodic addition of additional malononitrile and pyridine until no starting material was evident (TLC analysis). The solution was allowed to cool, water (100 ml) was added, and the organic fraction separated. The aqueous layer was further extracted with dichloromethane (3 x 50 ml) and the combined organic fractions were washed with water (100 ml), and dried ($MgSO_4$). The solvent was removed *in vacuo* and the residue subjected to silica gel chromatography (eluent hexane:diethyl ether 5:1 v/v) to yield compound **200** as a black solid (17 mg, 60%). Mpt:>250°C. ^1H NMR ($CDCl_3$; 200 MHz) δ: 8.12, 7.81 (both 2H, d, J=7Hz), 7.57, 7.42 (both 2H, t, J=7Hz), 2.04 (6H, s) ppm.. *m/z* (^{80}Se, DCI) 276 (100), 391 (35), 467 (M^++1, 90). HRMS :- 465.9481 $C_{22}H_{14}N_2OSe_2$ requires 465.9487. IR (KBr) (cm^{-1}): 3054, 2305, 1421, 1665, 747, 705 UV ($\varepsilon/M^{-1}cm^{-1}$) (DCM) 253 (1.1 x 10^4), 322 (9.2 x 10^3), 556 (5.2 x 10^3) nm.

9-(4,5-Dimethyl-1,3-diselenole-2-ylidene)-10-*N*-cyanoimine anthracene 201. To a solution of **199** (50 mg, 0.12 mmol) in chloroform (50 ml) was added sequentially titanium tetrachloride (1M, 0.3 ml, 0.3 mmol), *bis*-trimethylsilylcarbodiimide (BTC) (0.27 ml, 1.2 mmol), and the resulting black solution was heated under reflux for 4 days with periodic addition of BTC. After this time the solution was allowed to cool and the solvent was removed *in vacuo* to yield a black oil. This oil was subjected to silica gel chromatography (eluent dichloromethane :cyclohexane 3:2 v/v) to yield unchanged **199** (20 mg), Continued elution with dichloromethane yielded compound

201 as a black solid (10 mg, 35 %). Mpt: >250°C. ^{1}H NMR ($CDCl_3$; 200 MHz -30°C) δ: 8.84 (1H, d, J=8Hz), 8.20 (1H, d, J=8Hz), 7.88 (1H, d, J=8Hz), 7.70-7.65 (3H, m), 7.51 (1H, t, J=8Hz), 7.43 (1H, t, J=8Hz) ppm. *m/z* (^{80}Se, DCI) 403 (20), 443 (M^++1, 100). HRMS :- 441.9491 $C_{20}H_{14}N_2Se_2$ requires 441.9487. IR (KBr) (cm^{-1}): 2180, 1644, 1552, 1095, 975, 721. UV ($\varepsilon/M^{-1}cm^{-1}$) (DCM) 256 (1.0 x 10^4), 315 (7.7 x 10^3), 552 (4.7 x 10^3) nm.

9-(4,5-Dimethyl-1,3-diselenole-2-ylidene)-10-(4,5-dimethyl-1,3-dithiole-2-ylidene)-anthracene 207. To a solution of **82a** (1.17 g, 4.87 mmol) in tetrahydrofuran (40 ml) at -78°C was added n-BuLi (1.6M in hexanes, 3.04 ml, 4.87 mmol). The solution was maintained at this temperature for 0.5 h, whence, compound **199** (50 mg, 0.12 mmol) was added dropwise as a solution in tetrahydrofuran (10 ml) and the reaction allowed to attain room temperature over 16 h. The solvent was removed *in vacuo*, water (100 ml) was added and the mixture was extracted with dichloromethane (3 x 50 ml). The organic fractions were combined and washed with water (100 ml), separated, and dried ($MgSO_4$). The solvent was removed *in vacuo* and the residue subjected to silica gel chromatography (eluent dichloromethane) followed by recrystallisation from dichloromethane to yield compound **207** as yellow crystals (13 mg, 20 %). Mpt: >250°C. Anal. calc. for $C_{24}H_{20}S_2Se_2$: C, 53.13; H, 3.76; N, 12.03. Found: C, 53.18; H, 3.56; N, 12.33. ^{1}H NMR ($CDCl_3$; 200 MHz) δ: 7.66-7.62 (2H, m), 7.55-7.49 (2H, m), 7.31-7.24 (4H, m), 1.96 (6H, s), 1.93 (6H, s) ppm *m/z* (^{80}Se, DCI) 321 (40%), 533 (M^++1, 100%). IR (KBr) (cm^{-1}): 1518, 1454, 1444, 771, 737, 638. UV ($\varepsilon/M^{-1}cm^{-1}$) (DCM) 239 (7.4 x 10^3), 371 (5.6 x 10^3), 436 (6.3 x 10^3) nm.

7.2.6 Experimental Details for Chapter 6

1-(4,5-Dimethyl-1,3-dithiole-2-ylidene)-1-(4-nitrobenzene)-ethanal 210. To a ice cooled 0°C solution of DMF (2 ml) was added oxalyl chloride (1.42 ml, 15.1 mmol) slowly over 10 mins. After this time compound **142** (1.0 g, 3.77 mmol) was added dropwise as a solution in DMF (5 ml). The orange solution was allowed to attain room temperature over 16 h and was then poured into a solution of sodium hydroxide (300 ml, 1M) and the resulting solid that developed was removed by filtration. The solid was then dissolved in dichloromethane (50 ml) and washed with water (3 x 50 ml). The organic phase was separated, dried ($MgSO_4$) and the solvent removed *in vacuo* to afford **210** as a yellow solid (0.92g 83%) which was sufficiently pure for further reactions. However, an analytically pure sample was obtained by silica gel chromatography (eluent dichloromethane). Mpt: 184-186°C. Anal. calc. for $C_{13}H_{11}NO_3S_2$: C, 53.24; H, 3.75; N,4.78. Found: C, 53.42; H, 3.83; N, 4.54. ^{1}H

NMR ($CDCl_3$; 200 MHz) δ: 9.36 (1H, s), 8.30 (2H, d, J=9Hz), 7.61 (2H, d, J=9Hz) 2.21 (3H, s), 2.17 (3H, s) ppm. MS (DCI) *m/z* 264 (100), 294 (M^++1, 80). IR (KBr) (cm^{-1}): 1632, 1624, 1588, 1509, 1427, 1341. UV ($\varepsilon/M^{-1}cm^{-1}$) (DCM) 327 (7.4 x 10^3), 270 (4.7 x 10^3) 379 (4.5 x 10^3), 431 (8.2 x 10^3) nm.

1-(4,5-Dimethyl-1,3-dithiole-2-ylidene)-1-(4-nitrobenzene)-2-*N*-cyanoimine-ethane 211. This compound was prepared according to the general procedure outlined in Section 7.2.3 using compound **210** (300 mg, 1.02 mmol), dichloromethane (50 ml) and BTC (2.26 ml, 2.56 mmol). The solution was heated under reflux for 48 h after which time the solution was allowed to cool, water (100 ml) was added and the organic fraction was separated and washed with water (3 x 200 ml), dried ($MgSO_4$) and the solvent removed *in vacuo*. The residue was purified by silica gel chromatography (eluent dichloromethane) to yield an orange solid (100 mg, 34%). Mpt: >250°C (sublimes >200°C). Anal. calc. for $C_{14}H_{11}N_3O_2S_2$: C, 55.43; H, 3.65; N, 9.23. Found: C, 55.12; H, 3.55; N, 9.06. ^1H NMR ($CDCl_3$; 200 MHz) δ: 8.31 (2H, d, J=9Hz), 8.35 (1H, s) 7.56 (2H, d, J=7Hz), 2.31 (3H, s) 2.23 (3H, s) ppm. *m/z* (DCI) 288 (85), 318 (M^++1, 100). IR (KBr) (cm^{-1}): 2188, 1559, 1401, 1377, 1369, 1341. UV ($\varepsilon/M^{-1}cm^{-1}$) (DCM) 252 (1.5 x 10^4), 380 (sh), 463 (2.3 x 10^4) nm.

1-(4,5-Dimethyl-1,3-dithiole-2-ylidene)-1-(4-nitrobenzene)-3,3-dicyano-ethene 209. This compound was prepared according to the general procedure outlined in Section 2.2.2 using compound **210** (100 mg 0.34 mmol), dichloromethane (75 ml), titanium tetrachloride (1M, 0.85 ml, 0.85 mmol), malononitrile (0.21 ml, 3.4 mmol) and pyridine (0.27 ml, 3.4 mmol). On adding all the reagents the solution turned immediately red and was heated under reflux for 14 h and subsequently cooled. The solvent was removed *in vacuo* and the residue purified by silica gel chromatography (eluent dichloromethane:hexane 2:1 v/v) yielding unchanged **210** (20 mg, 20%) followed by compound **209** as a deep red solid (40 mg, 41%). Mpt: >250°C (from dichloromethane:hexane). Anal. calc. for $C_{16}H_{11}N_2S_2$: C, 52.48; H, 3.21; N, 16.32. Found: C, 52.56; H, 3.00. N, 16.10. ^1H NMR ($CDCl_3$; 200 MHz) δ: 8.34 (2H, d, J=9Hz), 7.46 (2H, d, J=9Hz), 7.45 (1H, s), 2.18 (3H, s), 2.06 (3H, s) ppm. *m/z* (DCI) No peak corresponding to compound **209** was observed. IR (KBr) (cm^{-1}): 2210, 1654, 1595, 1535, 1509, 1331. UV ($\varepsilon/M^{-1}cm^{-1}$) (DCM) 252 (7.8 x 10^3) 430 (sh), 495 (1.6 x 10^4) nm.

1-(4,5-Dimethyl-1,3-dithiole-2-ylidene)-1-(4-nitrobenzene)-3-(4-nitrobenzene)-prop-2-ene 212. To a suspension of Wittig reagent **138a** (0.97 g, 3.0 mmol) in benzene (50 ml), was added triethylamine (1 ml, excess) and the solution stirred for 15 min. After this time compound **210** (200 mg, 1.0 mmol) was added in one portion

against an positive flow of argon. The resulting red/orange solution was heated under reflux for 6 days. After this time the solution was cooled and the solvent removed *in vacuo*. The residue was purified by silica gel chromatography (eluent dichloromethane) to yield compound **212** as a red solid (0.45 g, 35%) which could not be obtainable analytically pure. Mpt: 171-174°C sublimes >150°C. ^{1}H NMR ($CDCl_3$; 200 MHz) δ: 8.12 (4H, d, J=9Hz), 7.32 (4H, d, J=9Hz), 7.25 (1H, d, J=9Hz), 6.98 (1H, s, J=9Hz), 2.46 (6H, s) ppm. UV (ε/$M^{-1}cm^{-1}$) (DCM) 273 (1.3 x 10^3), 320 (1.1 x 10^4), 487 (1.5 x 10^4) nm.

1-(4,5-Dimethyl-1,3-dithiole-2-ylidene)-3-(4-nitrobenzene)-prop-2-ene 215. To a solution of Wittig reagent **79a** (0.85 g, 1.85 mmol) in dry acetonitrile (20 ml) was added triethylamine (0.30 ml, 2.22 mmol). To this solution was added para-nitrocinamaldehyde (0.30 g, 1.69 mmol). The resulting red solution was stirred for 3 h at 20°C. The solvent was removed *in vacuo* and the residue chromatographed on silica gel (eluent dichloromethane:hexane 1:1 v/v) yielding compound **215** as a brown solid (0.25g, 51%). Mpt: 163-163°C. Anal. calc. for $C_{14}H_{13}NO_2S_2$: C, 57.73; H, 4.46; N,4.81. Found: C, 57.98; H, 4.65; N, 4.99. ^{1}H NMR ($CDCl_3$; 200 MHz) δ: 8.11 (2H, d, J=9Hz), 7.42 (2H, d, J=9Hz), 6.98 (1H, d, J=10Hz), 6.67 (1H, d, J=10Hz), 6.43 (1H, d, J=10Hz), 2.23 (3H, s), 2.19 (3H, s) ppm. *m/z* (DCI) 262 (75), 292 (M^++1, 100). IR (KBr) (cm^{-1}): 1577, 1534, 1502, 1334, 1788, 1109. UV (ε/$M^{-1}cm^{-1}$) (DCM) 235 (7.7 x 10^3), 313 (7.1 x 10^3), 488 (1.8 x 10^4) nm.

1-(4,5-Dimethyl-1,3-dithiole-2-ylidene)-4-*N,N*-dimethylaminobenzene 218. To a solution of Wittig reagent **79a** (3.8 g, 8.26 mmol) in acetonitrile (20 ml) was added triethylamine (1 ml, excess) followed by 4-*N,N*-dimethylaminobenzaldehyde **217** (1.23 g, 8.26 mmol). The resultant yellow solution was stirred at 20°C for 24 h. Following this time the solvent was removed *in vacuo* and the residue chromatographed on silica gel (eluent dichloromethane:hexane 1:1 v/v) to yield compound **218** as a pale white solid (0.5g 23%) which decomposed rapidly even under an inert atmosphere at 0°C, and thus was used immediately without further purification. Mpt: 69-70°C. ^{1}H NMR ($CDCl_3$; 200 MHz) δ: 7.24 (2H, d, J=9Hz), 7.17 (2H, d, J=9Hz), 6.35 (1H, s), 2.96 (6H, s), 1.93 (6H, s) ppm.

1-(4,5-Dimethyl-1,3-dithiole-2-ylidene)-1-(4-*N,N*-dimethylamino benzene)-ethanal 219. This compound was prepared according to the general procedure outlined in Section 7.6.1 from **218** (0.40 g, 1.52 mmol), oxalyl chloride (0.53 ml, 6.08 mmol 4 equiv.) and DMF (5 ml) yielding compound **219** as a yellow solid (0.28 g, 61%). Mpt: 147-148°C. ^{1}H NMR ($CDCl_3$; 200 MHz) δ: 9.31 (1H, s), 7.25 (2H, d, J=7Hz), 6.77 (2H, d, J=7Hz), 3.00 (6H, s) 2,15 (3H, s), 2.09 (3H, s) ppm . Anal.

Calc. for $C_{15}H_{17}NOS_2$: C, 61.58; H, 5.84; N,4.81. Found: C, 62.10; H, 5.92; N, 5.06; IR (KBr) (cm^{-1}): 1610, 1524, 1435, 1419, 1364, 1276. *m/z* (DCI) 292 (M^++1, 100) ; UV ($\varepsilon/M^{-1}cm^{-1}$) (DCM) 235 (1.3 x 10^3), 273 (1.6 x 10^4), 411 (1.4 x 10^4) nm.

1-(4,5-Dimethyl-1,3-dithiole-2-ylidene)-1-(4-N,N-dimethylamino benzene)-2,2-dicyano-ethene 216. This compound was prepared according to the general procedure outlined in Section 2.2.2 utilising compound **219** (100 mg 0.34 mmol), dichloromethane (75 ml) titanium tetrachloride (0.90 ml, 0.90 mmol), malononitrile (0.22 ml, 3.6 mmol) and pyridine (0.29 ml, 3.6 mmol). The solution was heated under reflux for 12 hours yielding compound **216** as a red solid following silica gel chromatography eluent (dichloromethane:hexane 1:3 v/v) and recrystallisation from dichloromethane:hexane 1:10 v/v (50 mg, 42%). Mpt: 167-169°C. Anal. calc. for $C_{18}H_{17}N_3S_2$: C, 63.71; H, 5.01; N, 12.38, found: C, 64.00; H, 4.75; N, 12.61. ^1H NMR ($CDCl_3$; 200 MHz) δ: 7.07 (2H, d, J=7Hz), 6.76 (1H, s), 6.74 (2H, d, J=7Hz), 2.99 (6H, s) 2.12 (3H, s), 2.10 (3H, s) ppm. *m/z* (DCI) No peak corresponding to compound **216** was observed. IR (KBr) (cm^{-1}): 2207, 1607, 1525, 1444, 1319. UV ($\varepsilon/M^{-1}cm^{-1}$) (DCM) 254 (9.8 x 10^3), 281 (1.1 x 10^4), 499 (1.8 x 10^4) nm.

1-(4,5-Dimethyl-1,3-dithiole-2-ylidene)-1-ferrocenyl-ethanal 221. This compound was kindly supplied by Dr. A J. Moore[122]

1-(4.5-Dimethyl-1,3-dithiole-2-ylidene)-1-ferrocenyl-3,3-dicyano-propene 222. This compound was prepared according to the general procedure outlined in Section 2.2.2 using compound **221** (100 mg 0.29 mmol), dichloromethane (30 ml), titanium tetrachloride (0.34 ml, 0.34 mmol), malononitrile (0.02 ml, 0.34 mmol) and pyridine (0.03 ml, 0.34 mmol). The solution was heated under reflux for 12 h yielding compound **222** (40 mg, 35%) following silica gel chromatography (eluent dichloromethane) as a black solid. Mpt: 198-200°C (decomp.). Anal. calc. for $C_{20}H_{16}FeN_2S_2$: C, 59.41; H, 3.99; N, 6.93. Found: C, 59.55; H, 4.20; N, 2.50 ^1H NMR ($CDCl_3$; 200 MHz) δ: 7.49 (1H, s), 4.45-4.42 (4H, m), 4.23 (5H, s), 2.23 (6H, s)ppm. *m/z* (DCI) 405 (M^++1, 100). IR (KBr) (cm^{-1}): 2216, 1535, 1478, 1425, 1345, 1297. UV ($\varepsilon/M^{-1}cm^{-1}$) (DCM) 253 (7.6 x 10^3), 350 (1.2 x 10^4) 491 (1.8 x 10^4) nm. Slow evaporation of a dichloromethane:hexane (1:1 v/v) solution of compound **222** afforded X-ray quality crystals.

References

1 H. N. McCoy, W. C. Moore, *J. Am. Chem. Soc.*, 1911, **33**, 273.

2 H. J. Kraus, *J. Am. Chem. Soc.*, 1913, **34**, 1732.

3 H. Akamatsu, H. Inokuchi, Y. Matsunaga, *Nature*, 1954, **173**, 168.

4 L. R. Melby, R. J. Harder, W. R. Hertler, W. Mahler, R. E. Benson, W. E. Mochel, *J. Am. Chem. Soc.*, 1962, **84**, 3374.

5 J. Ferraris, D. O. Cowan, V. V. Walatka, J. H. Perlstein, *J. Am. Chem. Soc.*, 1973, **84**, 948.

6 H. Fröhlich, *Proc. R. Soc. London., Ser. A*, 1954, **223**, 296.

7 R. E. Peierls, 'Quantum Theory of Solids', Oxford University Press, London, 1955.

8 TTF was synthesised independently by two groups a) F. Wudl, G. M. Smith, E. J. Hufnagel, *J. Chem. Soc., Chem. Commun.*, 1970, 1453; b) S. Hünig, G. Kiesslich, D. Scheutzow, R. Zahradnik, P. Carsky, *Int. J. Sulfur Chem.*, Part C, 1971, 109.

9 F. Wudl, D. Wobschall, E. J. Hufnagel, *J. Am. Chem. Soc.*, 1972, **94**, 671.

10 a) T. E. Phillips, T. J. Kistenmacher, J. P. Ferraris, D. O. Cowan, *J. Chem. Soc., Chem. Commun.*, 1973, 471; b) T. J. Kistenmacher, T. E. Phillips, D. O. Cowan, *Acta Crystallogr.*, 1973, **B30**, 763.

11 J. S. Chappell, A. N. Bloch, W. A. Bryden, M. Maxfield, T. O. Pöehler, D. O. Cowan, *J. Am. Chem. Soc.*, 1981, **103**, 2442.

12 Y. A. Jackson, C. L. White, M. V. Lakshmikantham, M. P. Cava, *Tetrahedron Lett.*, 1987, **28**, 5635.

13 M. D. Mays, R. D. McCullough, D. O. Cowan, T. O. Poehler, W. A. Bryden, T. J. Kistenmacher, *Solid State Commun.*, 1988, **65**, 1089.

14 J. P. Ferraris, T. O. Poehler, A. N. Bloch, D. O. Cowan, *Tetrahedron Lett.*, 1973, 2553.

15 K. Bechgaard, D. O. Cowan, A. N. Bloch, *J. Chem. Soc. Chem. Commun.*, 1974, 937.

16 a) K. Bechgaard, C. S. Jacobsen, K. Mortensen, M. J. Pedersen, N. Thorup, *Solid State Commun.*, 1980, **33**, 1119; b) K. Bechgaard, K. Carneiro, F. G. Rasmussen, K. Olsen, G. Rindorf, C. S. Jacobsen, H. J. Pedersen, J. E. Scott, *J. Am. Chem. Soc.*, 1981, **103**, 2440.

17 M. Mizuno, A. F. Garito, M. P. Cava, *J. Chem. Soc., Chem. Commun.*, 1978, 18.

18 Z. Yoshida, T. Kawase, H. Awaji, S. Yoneda, *Tetrahedron Lett.*, 1983, **24**, 3473.

19 T. Kawase, H. Awaji, S. Yoneda, Z. Yoshida, *Heterocycles*, 1982, **18**, 123.

20 M. R. Bryce, A. J. Moore, *Synth. Met.*, 1988, **27**, B557.

21 M. R. Bryce, A. J. Moore, M. Hasan, G. J. Ashwell, A. T. Fraser, W. Clegg, M. B. Hursthouse, A. I. Karaulov, *Angew. Chem. Int. Ed. Engl.*, 1990, **29**, 1450.

22 a) A. Aumüller, S. Hünig, *Angew Chem. Int. Ed. Engl.*, 1984, **96**, 437; b) A. Aumüller, S. Hünig, *Liebigs Ann. Chem.*, 1986, 142; c) A. Aumüller, S. Hünig, *Liebigs Ann. Chem.*, 1986, 165.

23 A. Aumüller, P. Erk, S. Hünig, H. Meixner, J. U. von Schütz, H-P. Werner, *Liebigs Ann. Chem.*, 1987, 997.

24 S. Hünig, *J. Mater. Chem.*, 1995, **5**, 1469.

25 J. Y. Becker, J. Bernstein, S. Bittner, N. Levi, S. S. Shaik, *J. Am. Chem. Soc.*, 1983, **105**, 4468.

26 J. Y. Becker, J. Bernstein, S. Bittner, N. Levi, S. S. Shaik, N. Zer-Zion, *J. Org. Chem.*, 1988, **53**, 1689.

27 N. Martín, J. L. Segura, C. Seoane, A. Albert, F. H. Cano, *J. Chem. Soc., Perkin Trans. 1*, 1993, 2363.

28 a) N. Martín, M. J. Hanack, *J. Chem. Soc., Chem. Commun.*, 1988, 1522; b) N. Martín, R. Behnisch, M. J. Hanack, *J. Org. Chem.*, 1989, **54**, 2563.

29 P. Bando, K. Davidkov, N. Martín, J. L. Segura, C. Seoane, A. González, J. M. Pingarrón, *Synth. Met.*, 1993, **56**, 1721.

30 a) P. de la Cruz, N. Martín, F. Miguel, C. Seoane, A. Albert. F. H. Cano, A. Leverenz, *Synth. Met.*, 1992, **48**, 59; b) U. Schubert, S. Hünig, A. Aumüller, *Liebigs Ann. Chem.*, 1985, 1216.

31 A. Aviram, M. A. Ratner, *Chem. Phys. Lett.*, 1974, **29**, 277.

32 a) R. M. Metzger, C. A. Panetta, *J. Molec. Elect.*, 1989, **5**, 1; b) C. A. Panetta, N. E. Heimer, C. L. Hussey, R. M. Metzger, *Synlett.*, 1991, 301; c) P. Bando, N. Martín, J. L. Segura, E. Orti, P. M. Viruela, R. Viruela, A. Albert, F. H. Cano, *J. Org. Chem.*, 1994, **59**, 4618.

33 P. de Miguel, M. R. Bryce, unpublished results.

34 C. A. Panetta, J. Baghdadchi, R. M. Metzger, *Mol. Cryst. Liq. Cryst.*, 1984, **107**, 103.

35 L. R. Melby, R. J. Harder, W. R. Hertler, W. Mahler, R. E. Benson, W. E. Mochel, *J. Am. Chem. Soc.*, 1962, **84**, 3095.

36 a) G. J. Ashwell, E. J. C. Dawnay, A. P. Kuczynski, M. Szablewski, I. M. Sandy, M. R. Bryce, A. M. Grainger, M. Hasan, *J. Chem. Soc., Faraday Trans.*, 1990, **86**, 1117; b) G. J. Ashwell, G. Jefferies, E. J. C. Dawnay, A. P. Kuczynski, D. E. Lynch, G. Yu, D. C. Bucknell, *J. Mater. Chem.*, 1995, **5**, 975.

37 a) G. J. Ashwell, J. R. Sambles, A. S. Martin, W. G. Parker, M. Szablewski, *J. Chem. Soc., Chem. Commun.*, 1990, 1374; b) A. S. Martin, J. R. Sambles, G. J. Ashwell, *Phys. Rev. Lett.*, 1993, **70**, 218.

38 J. L. Oudar, D. S. Chemla, *J. Chem. Phys.*, 1977, **66**, 2664.

39 J. L. Oudar, D. S. Chemla, *Opt. Commun.*, 1975, **13**, 164.

40 B. F. Levine, C. G. Bethea, R. T. Thurmond, J. L. Bernstein, *J. Appl. Phys.*, 1979, **50**, 2523.

41 J. L. Oudar, *J. Chem. Phys.*, 1977, **67**, 446.

42 A. Dulic, C. Flytzanis, C. L. Tang, D. Pepin, M. Fitzon, Y. Hoppiliard, *J. Chem. Phys.*, 1981, **74**, 1559.

43 A. K. Jen, V. P. Rao, K. Y. Wong, K. J. Drost, *J. Chem. Soc., Chem. Commun.*, 1993, 90.

44 a) G . Bourhill, J. L. Bredas, L-T. Chen, S. R. Marder, F. Meyers, J. W. Perry, B. G. Tiemann, *J. Am. Chem. Soc.*, 1994, **116**, 2619; b) S. M. Risser, D. N. Beratan, S. R. Marder, *J. Am. Chem. Soc.*, 1993, **115**, 7719; c) J. C. Calabrese, L-T. Chen, J. C. Green, S. R. Marder, W. Tam, *J. Am. Chem. Soc.*, 1991, **113**, 7227.

45 A. Ullman, C. S. Willand, W. Köhler, D. R. Robello, D. J. Williams, L. Handley, *J. Am. Chem. Soc.*, 1990, **112**, 7083.

46 K. Ogura, S. Takahashi, Y. Kawamoto, M. Suzuki, M. Fujita, *Tetrahedron Lett.*, 1993, **34**, 2649.

47 A. Bahl, W. Grahn, S. Sadler, F. Freiner, G. Bourhill, C. Bräuchle, A. Reisner, P. G. Jones, *Angew. Chem. Int. Ed. Engl.*, 1995, **34**, 1485.

48 H. Ikeda, Y. Kawabe, T. Sakai, K. Kawasaki, *Chem. Lett.*, 1989, 1803.

49 V. P. Rao, A. K-Y. Jen, J. B. Cladwell, *Tetrahedron Lett.*, 1994, **35**, 3849.

50 H. E. Katz, K. D. Singer, J. E. Sohn, C. W. Dirk, L. A. King, H. M. Gordon, *J. Am. Chem. Soc.*, 1987, **109**, 6561.

51 R. Gompper, E. Kutter, *Chem. Ber.*, 1965, **98**, 2825.

52 R. Mayer, B. Gebhardt, *Chem. Ber.*, 1964, **97**,1298.

53 V. P. Rao, Y. M. Cai, A. K-Y. Jen, *J. Chem. Soc., Chem. Commun.*, 1994, 1689.

54 H. Hopf, M. Kreutzer, P. G. Jones, *Angew. Chem. Int. Ed. Engl.*, 1991, **30**, 1127.

55 M. Blanchard-Desce, I. Ledoux, J-M. Lehn, J. Malthête, J. Zyss, *J. Chem. Soc., Chem. Commun.*, 1988, 737.

56 a) M. Barzoucas, M. Blanchard-Desce, D. Josse, J-M. Lehn, J. Zyss, *J. Chem. Phys.*, 1989, **113**, 323; b) F. Meyers, J. L. Brédas, J. Zyss, *J. Am. Chem. Soc.*, 1992, **114**, 2914.

57 S. L. Gilat, S. H. Kawai, J-M. Lehn, *Chem. Eur. J.*, 1995, **1**, 275.

58 A. Mas, J. M. Fabre, E. Torreilles, L. Giral, G. Brun, *Tetrahedron Lett.*, 1977, 2579. Subsequently modified by A. J. Moore, M. R. Bryce, A. S. Batsanov, J. C. Cole, J. A. K. Howard, *Synthesis*, 1995, 675.

59 S. Wawzonec, S. M. Heilmann, *J. Org.Chem.*, 1974, **39**, 511.

60 B. T. Fetkenhauer, H. Fetkenhauer, *Ber.*, 1927, **60B**, 2528.

61 H. Kolbe, *Justus Leibig. Ann. Chem.*, 1868, 140.

62 J. Y. Becker, N. Svenstrup, *Synthesis*, 1995, 215.

63 G. Steimecke, R. Kirmse, E. Hoyer, *Z. Chem.*, 1975, **15**, 28.

64 a) M. Sato, N. C. Gonnella, M. P. Cava, *J. Org. Chem.*, 1979, **44**, 930, b) T. K. Hansen, PhD Thesis, University of Odense, Denmark, 1992.

65 T. Sugimoto, H. Awaji, Y. Misaki, T. Kawase, S. Yoneda, Z. Yoshida, T. Kobayashi, H. Anzai, *Chem. Mater.*, 1989, **1**, 535.

66 A. J. Moore, M. R. Bryce, *Tetrahedron Lett.*, 1992, **33**, 1373

67 P. Frère, A. Belysamine, Y. Gouriou, M. Jubalt, A. Gorgues, G. Duguay, S. Woods, C. D. Reynolds, M. R. Bryce, *Bull. Chim. Soc. Fr.*, 1995, **132**, 975.

68 M. R. Bryce, A. J. Moore, M. A. Chalton, A. S. Batsanov, J. A. K. Howard, *J. Chem. Soc., Perkin Trans.* 2, 1996, 2367.

69 a) W. Lehnert, *Tetrahedron Lett.*, 1970, 4723; b) W. Lehnert, *Synthesis*, 1974, 667

70 A. Aumüller, S. Hünig, *Angew. Chem. Int. Ed. Engl.*, 1984, **23**, 447.

71 a) A. Gavezzotti, *J. Am. Chem. Soc.*, 1983, **105**, 5220; b) G. Filippini, A. Gavezzotti, *Acta Crystallogr. Sect. B,* 1993, **49**, 868.

72 a) R. H. Baughman, B. E. Kohler, I .J. Levy and C. Spangler, *Synth. Met.* 1985, **11**, 37; b) A. Kiehl, A. Eberhardt, M. Adam, V. Enkelmann, K. Mullen, *Angew. Chem., Int. Ed. Engl.,* 1992, **31**, 1588; c) T. Hamanaka, T. Mitsui, T. Ashida, M. Kakudo, *Acta Crystallogr. Sect. B*, 1972, **28**, 214.

73 S. R. Marder, J. W. Perry, B. G. Tieman, C. B. Gorman, S. Gilmour, S. L. Biddle, G. Bourhill, *J. Am. Chem. Soc.*, 1993, **115**, 2524.

74 N.-H. Dung, J. Etienne, *Acta Crystallogr. Sect. B,* 1978, **34**, 683.

75 H. Hopf, M. Kreutzer, P .G. Jones, *Angew. Chem., Int. Ed. Engl.,* 1991, **30**, 1127.

76 B. Golding, G. Kennedy, W. P. Watson, *Tetrahedron Lett.*, 1988, **29**, 1220.

77 B. M. Adger, C. Barrett, J. Brennan, M. A. McKervey, R. W. Murray, *J. Chem. Soc., Chem. Commun.*, 1991, 1553.

78 B. J. Adger, C. Barrett, J. Brennan, P. McGuigan, M. A. McKervey, B. Tarbit, *J. Chem. Soc., Chem. Commun.*, 1993, 1220.

79 N. J. Long, *Angew Chem. Int. Ed. Engl.,* 1996, **13**, 1536.

80 A. J. Moore, M. R. Bryce, *J. Chem. Soc., Perkin Trans. 1*, 1991, 157.

81 M. J. Kamlet, J-L. M. Abboud, R. W. Taft, *J. Phys. Org. Chem.*, 1981, **13**, 486 and references cited therein.

82 F. Gerson, R. Heckerdorn, D. O. Cowan, A. M. Kini, M. Maxfield, *J. Am. Chem. Soc.*, 1983, **105**, 7071.

83 a) D. C. Green, *J. Chem. Soc., Chem. Commun.*, 1977, 161; b) D. C. Green, R. W. Allen, *J. Chem. Soc., Chem. Commun.*, 1978, 832.

84 D. C. Green, *J. Org. Chem.*, 1979, **44**, 1476.

85 V. Y. Khodorkovskii, Y. T. Katsen, O. Y. Neiland, *Zh. Org. Chem.*, 1985, **21**, 1582.

86 H. Poleschner, W. John, F. Hoppe, E. Fanghanel, *J. Prakt. Chem.*, 1983, **323**, 957.

87 T. K. Hansen, I. Hawkins, K. S. Varma, S. Edge, S. Larsen, J. Becher, A. E. Underhill, *J. Chem. Soc., Perkin Trans. 2*, 1991, 1963.

88 C. Gemmell, J. D. Kilburn, H. Ueck, A. E. Underhill, *Tetrahedron Lett.*, 1992, **33**, 3923.

89 N. Svenstrup, K. M. Rasmussen, T. K. Hansen, J. Becher, *Synthesis*, 1994, 809.

90 J. Garin, J. Orduna, S. Uriel, A. J. Moore, M. R. Bryce, S. Wegener, D. S. Yufit, J. A. K. Howard, *Synthesis*, 1994, 489.

91 M. Sallé, A. J. Moore, M. R. Bryce, M. Jubault, *Tetrahedron Lett.*, 1993, **34**, 7475.

92 M. Mizatuni, K. Tanaka, K. Ikeda, K. Kawabata, *Synth Met.*. 1992, **42**, 201.

93 M. Formigué, I. Johannsen, K. Boubekeur, C. Nelson, P. Batail, *J. Am. Chem. Soc.*, 1993, **115**, 3752.

94 H. E. Katz, K. D. Singer, J. E. Sohn, C. W. Dirk, L. A. King, H. M. Gordon, *J. Am. Chem. Soc.*, 1987, **109**, 6561.

95 A. J. Moore, M. R. Bryce, J. Cole, A. S. Batsanov, J. A. K. Howard, *Synthesis*, 1996, 675.

96 R. Andreu, A. I. de Lucas, J. Garín, N. Martín, J. Orduna, L. Sánchez, C. Seoane, *Synth. Met.* 1997, **86**, 1817.

97 V. P. Rao, in Nonlinear Optical Propeties of Organic Materials V, D. J. Williams, Ed,; *Proc. SPIE*, 1995, 32.

98 T. Nozdryn, J. Cousseau, A. Gorgues, M. Jubault, J. Orduna, S. Uriel, J. Garín, *J. Chem. Soc., Perkin Trans .I*, 1993, 1711.

99 D. B. Easton, D. Leaver, *J. Chem. Soc., Chem. Comun.*, 1965, 583.

100 E. Klinsberg, *J. Am. Chem. Soc.*, 1964, **86**, 5290.

101 L. R. Melby, H. D. Hartzler, W. A. Sheppard, *J. Org. Chem.*, 1974, **39**, 2456.

102 R. O. Clinton, S. C. Laskowski, *J. Am. Chem. Soc.*, 1948, **70**, 3135.

103 a) J Becher, Personal Communication; b) R. Andreu, J. Garin, J. Orduna, M. Savirón, J. Cousseau, A. Gorgues, V. Morrison, T. Nozdryn, J. Becher, R. P. Clausen, M. R. Bryce, P. J. Skabara, W. Dehaen, *Tetrahedron Lett.*, 1994, **35**, 9243.

104 C. D. Hund, R. I. Mori, *J. Am. Chem. Soc.*, 1955, **77**, 5359.

105 A. Gorgues, Personal communication.

106 a) W. Lehnert, *Tetrahedron Lett.*, 1970, 4723; b) W. Lehnert, *Synthesis*, 1974, 667.

107 N. Narita, C. U. Pittman, *Synthesis*, 1976, 489.

108 T Sugimoto, H. Awaji, I. Sugimoto, T. Kawase, S. Yoneda, Z. Yoshida, T. Kobayashi, H. Anzai, *Chem. Mater.*, 1989, **1**, 535.

109 a) L. S. Hendriksen, E. S. S. Kristiansen, *Int. J. Sulfur Chem.*, 1972, **2**, 133; b) W-H. Pan, J. P. Faccklet, H-W. Chen, *Inorg. Chem.* 1981, **20**, 856; c) L. Hendricksen, *Acta Chem. Scand.*, 1967, **21**, 1981.

110 S. Chakroune, PhD Thesis, Université Montpellier II, 1993.

111 F. Wudl, E. Aharon-Shalom, S. H. Bertz, *J. Org. Chem.*, 1981, **46**, 4612.

112 M. R. Bryce, A. Chesney, S. Yoshida, A. J. Moore, A. S. Basanov, J. A. K. Howard, *J. Mater. Chem.*, 1997, **7**, 381.

113 M. A. Chalton, PhD Thesis, University of Durham, 1996.

114 L. Hendricksen, *Acta Chem. Scand.*, 1967, **7**, 1981.

115 A. Chesney, M. R. Bryce, M. A. Chalton, A. S. Batsanov, J. A. K. Howard, J. M. Fabre, L. Binet, S. Chakroune, *J. Org. Chem.*, 1996, **61**, 2877.

116 H. Hopf, *Angew. Chem. Int. Ed. Engl.*, 1984, **23**, 948.

117 a) C. Reichardt, J. Knecht, W. Mrosek, D. Plass, R. Allmann, D. Kucharczyk, *Chem. Ber.*, 1983, **116**, 1982; b) A. Hosomi, T. Masunari, Y. Tomonaga, T. Yanagi, M. Hojo, *Tetrahedron Lett.*, 1990, **31**, 6201; c) J. I. G. Cadogan, S. Cradock, S. Gillam, I. Gosney, *J. Chem. Soc., Chem. Commun.*, 1991, 14.

118 Y. Masaki, Y. Matsumara, T. Sugimoto, Z. Yoshida, *Tetrahedron Lett.*, 1989, **30**, 5289.

119 M. A. Coffin, M. R. Bryce, A. S. Batsanov, J. A. K. Howard, *J. Chem. Soc., Chem. Commun.*, 1993, 552.

120 a) A. Gorgues Personal Communication; T. T. Nguyen, PhD Thesis, Université d' Angers, 1996.

121 P. J. Skabara, PhD Thesis, University of Durham, 1994.

122 A. J. Moore, M. R. Bryce, Unpublished Results.

Appendix 1

X-Ray Crystal Data

A1.1 Crystallographic Data for 1-*N*-Cyanoimino-2-(4,5-dimethylthio-1,3-dithiole-2-ylidene)-ethane 87b

Bond lengths [A] and angles [deg]

S(1)-C(1)	1.739(7)	S(1)-C(2)	1.751(7)
S(1)-N(1)	2.719(6)	S(2)-C(1)	1.741(7)
S(2)-C(3)	1.743(8)	S(3)-C(2)	1.759(8)
S(3)-C(4)	1.792(11)	S(4)-C(3)	1.758(7)
S(4)-C(5)	1.797(8)	N(1)-C(7)	1.313(9)
N(1)-C(8)	1.340(9)	N(2)-C(8)	1.148(9)
C(1)-C(6)	1.376(10)	C(2)-C(3)	1.352(9)
C(6)-C(7)	1.398(10)		
C(1)-S(1)-C(2)	95.9(4)	C(1)-S(1)-N(1)	75.5(3)
C(2)-S(1)-N(1)	171.4(3)	C(1)-S(2)-C(3)	96.9(3)
C(2)-S(3)-C(4)	101.5(5)	C(3)-S(4)-C(5)	100.0(4)
C(7)-N(1)-C(8)	119.8(6)	C(7)-N(1)-S(1)	95.4(5)
C(8)-N(1)-S(1)	144.7(5)	C(6)-C(1)-S(1)	124.3(5)
C(6)-C(1)-S(2)	121.7(5)	S(1)-C(1)-S(2)	113.9(4)
C(3)-C(2)-S(1)	117.4(6)	C(3)-C(2)-S(3)	124.2(6)
S(1)-C(2)-S(3)	118.4(4)	C(2)-C(3)-S(2)	115.8(5)
C(2)-C(3)-S(4)	125.9(6)	S(2)-C(3)-S(4)	118.2(4)
C(1)-C(6)-C(7)	122.9(7)	N(1)-C(7)-C(6)	121.8(7)
N(2)-C(8)-N(1)	174.7(8)		

Atomic coordinates (x 10^4) and equivalent isotropic displacement parameters (A^2 x 10^3) U(eq) is defined as one third of the trace of the orthogonalized Uij tensor.

	x	y	z	U(eq)
S(1)	6951(1)	6685(2)	5348(2)	32(1)
S(2)	8779(1)	7130(2)	5110(2)	37(1)
S(3)	7098(1)	3735(3)	7382(2)	44(1)
S(4)	9210(1)	4259(3)	7094(2)	44(1)
N(1)	6176(4)	9104(7)	3748(7)	32(2)
N(2)	4756(4)	10153(9)	3016(8)	46(2)
C(1)	7779(4)	7815(9)	4576(8)	31(2)
C(2)	7592(5)	5274(9)	6305(9)	33(2)
C(3)	8440(5)	5479(9)	6205(8)	33(2)
C(4)	6285(9)	3051(18)	6123(15)	70(4)
C(5)	9569(5)	3065(11)	5516(10)	42(2)
C(6)	7674(5)	9145(9)	3639(9)	34(2)
C(7)	6879(5)	9760(10)	3239(9)	36(2)
C(8)	5426(5)	9711(9)	3310(8)	34(2)

Anisotropic displacement parameters (A^2 x 10^3)
The anisotropic displacement factor exponent takes the form:
-2 pi^2 [h^2 a*^2 U11 + ... + 2 h k a* b* U12]

	U11	U22	U33	U23	U13	U12
S(1)	29(1)	33(1)	35(1)	3(1)	0(1)	1(1)
S(2)	26(1)	41(1)	42(1)	2(1)	-4(1)	4(1)
S(3)	47(1)	45(1)	42(1)	12(1)	0(1)	0(1)
S(4)	41(1)	59(1)	33(1)	3(1)	-5(1)	18(1)
N(1)	23(3)	28(3)	43(4)	3(3)	-2(3)	4(3)
N(2)	35(4)	42(4)	60(5)	10(4)	0(4)	7(4)
C(1)	24(4)	38(4)	30(4)	-11(4)	-5(3)	0(3)
C(2)	34(4)	37(4)	28(3)	-5(4)	-1(4)	9(4)
C(3)	33(4)	37(5)	30(4)	-1(4)	-4(3)	12(4)
C(4)	72(9)	82(10)	58(7)	5(7)	-8(7)	-26(8)
C(5)	37(5)	44(5)	45(5)	11(5)	13(4)	21(4)
C(6)	32(5)	28(4)	42(5)	4(4)	-5(4)	-4(4)
C(7)	31(5)	30(4)	48(5)	5(4)	-4(4)	3(4)
C(8)	37(5)	22(4)	45(5)	8(4)	3(4)	-4(4)

Hydrogen coordinates (x 10^4) and isotropic displacement parameters (A^2 x 10^3)

	x	y	z	U(eq)
H(4A)	6065(68)	2311(134)	6650(139)	95(45)
H(4B)	6599(71)	2658(163)	5310(155)	139(56)
H(4C)	5798(58)	3818(119)	6300(115)	75(36)
H(5A)	9980(48)	2284(108)	5905(95)	63(27)
H(5B)	9774(57)	3894(119)	4660(106)	96(35)
H(5C)	9081(48)	2321(100)	5224(106)	66(27)
H(6)	8181(47)	9742(90)	3431(82)	41(22)
H(7)	6868(33)	10647(69)	2546(59)	8(15)

A1.2 Crystallographic Data for 1-(4,5-Dimethylthio-1,3-dithiole-2-ylidene)-3,3-dicyano-2-propene 86b

Bond lengths [A] and angles [deg]

S(1)-C(1)	1.743(3)
S(1)-C(2)	1.757(3)
S(2)-C(1)	1.727(3)
S(2)-C(3)	1.753(3)
S(3)-C(2)	1.751(3)
S(3)-C(9)	1.811(3)
S(4)-C(3)	1.757(3)
S(4)-C(10)	1.815(4)
N(1)-C(7)	1.149(4)
N(2)-C(8)	1.148(4)
C(1)-C(4)	1.387(4)
C(2)-C(3)	1.343(4)
C(4)-C(5)	1.402(4)
C(4)-H(4)	0.99(3)
C(5)-C(6)	1.384(4)
C(5)-H(5)	0.97(3)
C(6)-C(8)	1.427(4)
C(6)-C(7)	1.432(4)
C(9)-H(9A)	0.98(4)
C(9)-H(9B)	0.97(4)
C(9)-H(9C)	0.96(4)
C(10)-H(10A)	0.93(3)
C(10)-H(10B)	0.96(4)
C(10)-H(10C)	0.92(4)
C(1)-S(1)-C(2)	96.10(13)
C(1)-S(2)-C(3)	96.37(13)
C(2)-S(3)-C(9)	102.5(2)
C(3)-S(4)-C(10)	99.1(2)
C(4)-C(1)-S(2)	125.0(2)
C(4)-C(1)-S(1)	120.7(2)
S(2)-C(1)-S(1)	114.3(2)
C(3)-C(2)-S(3)	122.3(2)
C(3)-C(2)-S(1)	116.4(2)
S(3)-C(2)-S(1)	121.3(2)
C(2)-C(3)-S(2)	116.8(2)
C(2)-C(3)-S(4)	124.5(2)
S(2)-C(3)-S(4)	118.6(2)
C(1)-C(4)-C(5)	121.4(3)
C(1)-C(4)-H(4)	119(2)
C(5)-C(4)-H(4)	120(2)
C(6)-C(5)-C(4)	125.2(3)
C(6)-C(5)-H(5)	118(2)
C(4)-C(5)-H(5)	117(2)
C(5)-C(6)-C(8)	121.8(3)
C(5)-C(6)-C(7)	121.5(3)
C(8)-C(6)-C(7)	116.7(3)
N(1)-C(7)-C(6)	179.9(4)
N(2)-C(8)-C(6)	178.8(3)
S(3)-C(9)-H(9A)	108(2)
S(3)-C(9)-H(9B)	111(2)
H(9A)-C(9)-H(9B)	110(3)
S(3)-C(9)-H(9C)	110(2)
H(9A)-C(9)-H(9C)	109(3)
H(9B)-C(9)-H(9C)	108(3)

S(4)-C(10)-H(10A)	108(2)
S(4)-C(10)-H(10B)	107(2)
H(10A)-C(10)-H(10B)	115(3)
S(4)-C(10)-H(10C)	108(3)
H(10A)-C(10)-H(10C)	103(3)
H(10B)-C(10)-H(10C)	117(3)

Atomic coordinates (x 10^4) and equivalent isotropic displacement parameters (A^2 x 10^3) U(eq) is defined as one third of the trace of the orthogonalized Uij tensor.

	x	y	z	U(eq)
S(1)	3221(1)	1782(1)	1854(1)	18(1)
S(2)	4472(1)	404(1)	3691(1)	20(1)
S(3)	-1281(1)	3685(1)	2804(1)	22(1)
S(4)	343(1)	2204(1)	4858(1)	23(1)
N(1)	12338(7)	-1775(4)	157(2)	43(1)
N(2)	14096(5)	-3745(3)	2955(2)	32(1)
C(1)	5257(5)	547(3)	2459(2)	17(1)
C(2)	1274(5)	2354(3)	2886(2)	16(1)
C(3)	1862(5)	1720(3)	3731(2)	18(1)
C(4)	7285(5)	-242(3)	1957(2)	18(1)
C(5)	8949(5)	-1233(3)	2434(2)	18(1)
C(6)	11085(5)	-2017(3)	1995(2)	19(1)
C(7)	11782(6)	-1882(3)	976(2)	26(1)
C(8)	12738(6)	-2972(3)	2536(2)	22(1)
C(9)	-862(7)	4288(4)	1540(2)	29(1)
C(10)	2592(7)	3613(4)	5074(2)	30(1)

Hydrogen coordinates (x 10^4) and isotropic displacement parameters (A^2 x 10^3)

	x	y	z	U(eq)
H(4)	7570(62)	-75(34)	1246(23)	21(8)
H(5)	8568(59)	-1379(33)	3124(22)	15(7)
H(9A)	-2163(74)	5091(41)	1435(26)	35(10)
H(9B)	-1136(70)	3494(41)	1148(26)	31(10)
H(9C)	894(74)	4642(38)	1354(25)	31(10)
H(10A)	1961(65)	3995(36)	5657(25)	22(8)
H(10B)	2667(73)	4305(41)	4526(27)	35(10)
H(10C)	4181(86)	3160(46)	5204(29)	49(12)

Anisotropic displacement parameters (A^2 x 10^3)
The anisotropic displacement factor exponent takes the form:
-2 pi^2 [h^2 a*^2 U11 + ... + 2 h k a* b* U12]

	U11	U22	U33	U23	U13	U12
S(1)	18(1)	20(1)	17(1)	-2(1)	-2(1)	3(1)
S(2)	20(1)	22(1)	18(1)	0(1)	0(1)	5(1)
S(3)	19(1)	21(1)	26(1)	-5(1)	-4(1)	5(1)
S(4)	20(1)	27(1)	19(1)	-4(1)	3(1)	1(1)
N(1)	56(2)	46(2)	24(1)	-2(1)	3(1)	14(2)
N(2)	31(1)	28(2)	39(2)	1(1)	-8(1)	6(1)
C(1)	16(1)	16(1)	20(1)	0(1)	-5(1)	-1(1)
C(2)	14(1)	16(1)	20(1)	-4(1)	-1(1)	-1(1)
C(3)	16(1)	19(1)	20(1)	-3(1)	-1(1)	2(1)
C(4)	18(1)	20(1)	17(1)	-1(1)	-2(1)	-1(1)
C(5)	19(1)	20(1)	16(1)	-2(1)	-1(1)	0(1)
C(6)	18(1)	18(1)	22(1)	-2(1)	-3(1)	2(1)
C(7)	28(2)	22(2)	28(2)	-3(1)	-2(1)	7(1)
C(8)	21(1)	20(1)	25(1)	-4(1)	0(1)	0(1)
C(9)	37(2)	26(2)	24(2)	1(1)	-7(1)	8(2)
C(10)	32(2)	32(2)	26(2)	-11(1)	-5(1)	1(1)

A1.3 Crystallographic Data for 10-(4,5-Dimethyl-1,3-dithiole-2-ylidene)-9-(2,2-dicyanomethane) anthracene 108a

Bond lengths [A] and angles [deg]

S(1)-C(12)	1.750(3)	S(1)-C(11)	1.753(2)
S(2)-C(13)	1.752(3)	S(2)-C(11)	1.755(3)
C(1)-C(2)	1.382(4)	C(1)-C(9A)	1.402(3)
C(2)-C(3)	1.383(4)	C(3)-C(4)	1.376(4)
C(4)-C(4A)	1.403(3)	C(4A)-C(9A)	1.410(3)
C(4A)-C(10)	1.465(3)	C(5)-C(6)	1.382(4)
C(5)-C(10A)	1.398(3)	C(6)-C(7)	1.379(4)
C(7)-C(8)	1.384(3)	C(8)-C(8A)	1.400(3)
C(8A)-C(10A)	1.410(3)	C(8A)-C(9)	1.472(3)
C(9)-C(11)	1.375(3)	C(9)-C(9A)	1.476(3)
C(10)-C(16)	1.373(3)	C(10)-C(10A)	1.462(3)
C(12)-C(13)	1.332(4)	C(12)-C(14)	1.502(4)
C(13)-C(15)	1.502(4)	C(16)-C(17)	1.438(4)
C(16)-C(18)	1.439(4)	C(17)-N(1)	1.147(3)
C(18)-N(2)	1.151(3)	S(3)-C(32)	1.748(3)
S(3)-C(31)	1.751(2)	S(4)-C(33)	1.751(3)
S(4)-C(31)	1.756(2)	C(21)-C(22)	1.382(3)
C(21)-C(29A)	1.400(3)	C(22)-C(23)	1.379(4)
C(23)-C(24)	1.380(4)	C(24)-C(24A)	1.403(3)
C(24A)-C(29A)	1.416(3)	C(24A)-C(30)	1.467(3)
C(25)-C(26)	1.384(4)	C(25)-C(30A)	1.401(3)
C(26)-C(27)	1.386(4)	C(27)-C(28)	1.381(3)
C(28)-C(28A)	1.403(3)	C(28A)-C(30A)	1.409(3)
C(28A)-C(29)	1.464(3)	C(29)-C(31)	1.373(3)
C(29)-C(29A)	1.467(3)	C(30)-C(36)	1.370(3)
C(30)-C(30A)	1.466(3)	C(32)-C(33)	1.330(4)
C(32)-C(34)	1.501(4)	C(33)-C(35)	1.498(4)
C(36)-C(37)	1.436(3)	C(36)-C(38)	1.441(3)
C(37)-N(3)	1.146(3)	C(38)-N(4)	1.147(3)
C(12)-S(1)-C(11)	97.43(12)	C(13)-S(2)-C(11)	97.75(12)
C(2)-C(1)-C(9A)	121.0(2)	C(1)-C(2)-C(3)	120.8(2)
C(4)-C(3)-C(2)	119.8(2)	C(3)-C(4)-C(4A)	120.3(2)
C(4)-C(4A)-C(9A)	120.4(2)	C(4)-C(4A)-C(10)	121.6(2)
C(9A)-C(4A)-C(10)	118.0(2)	C(6)-C(5)-C(10A)	120.2(2)
C(7)-C(6)-C(5)	119.5(2)	C(6)-C(7)-C(8)	121.0(2)
C(7)-C(8)-C(8A)	120.9(2)	C(8)-C(8A)-C(10A)	117.7(2)
C(8)-C(8A)-C(9)	123.2(2)	C(10A)-C(8A)-C(9)	119.1(2)
C(11)-C(9)-C(8A)	122.7(2)	C(11)-C(9)-C(9A)	122.8(2)
C(8A)-C(9)-C(9A)	114.2(2)	C(1)-C(9A)-C(4A)	117.7(2)
C(1)-C(9A)-C(9)	123.4(2)	C(4A)-C(9A)-C(9)	118.9(2)
C(16)-C(10)-C(10A)	122.2(2)	C(16)-C(10)-C(4A)	122.7(2)
C(10A)-C(10)-C(4A)	114.9(2)	C(5)-C(10A)-C(8A)	120.6(2)
C(5)-C(10A)-C(10)	121.5(2)	C(8A)-C(10A)-C(10)	117.9(2)
C(9)-C(11)-S(1)	124.8(2)	C(9)-C(11)-S(2)	123.8(2)
S(1)-C(11)-S(2)	111.24(14)	C(13)-C(12)-C(14)	126.8(2)
C(13)-C(12)-S(1)	117.0(2)	C(14)-C(12)-S(1)	116.2(2)
C(12)-C(13)-C(15)	127.8(2)	C(12)-C(13)-S(2)	116.0(2)
C(15)-C(13)-S(2)	116.2(2)	C(10)-C(16)-C(17)	123.6(2)
C(10)-C(16)-C(18)	122.8(2)	C(17)-C(16)-C(18)	113.0(2)
N(1)-C(17)-C(16)	176.4(3)	N(2)-C(18)-C(16)	177.1(3)
C(32)-S(3)-C(31)	97.45(12)	C(33)-S(4)-C(31)	97.31(12)
C(22)-C(21)-C(29A)	121.5(2)	C(23)-C(22)-C(21)	120.1(2)

Atomic coordinates (x 10^4) and equivalent isotropic displacement parameters (A^2 x 10^3) U(eq) is defined as one third of the trace of the orthogonalized Uij tensor.

	x	y	z	U(eq)
S(1)	4991(1)	5268(1)	3228(1)	33(1)
S(2)	4539(1)	5174(1)	1505(1)	35(1)
C(1)	3376(2)	5984(2)	3858(1)	32(1)
C(2)	3012(2)	6037(2)	4537(2)	37(1)
C(3)	2186(2)	5650(2)	4549(2)	38(1)
C(4)	1722(2)	5195(2)	3882(2)	32(1)
C(4A)	2085(2)	5123(2)	3190(1)	26(1)
C(5)	1021(2)	5194(2)	1058(1)	30(1)
C(6)	1166(2)	5595(2)	354(2)	33(1)
C(7)	1997(2)	5941(2)	310(2)	33(1)
C(8)	2680(2)	5924(2)	969(1)	29(1)
C(8A)	2558(2)	5518(2)	1690(1)	25(1)
C(9)	3256(2)	5493(2)	2412(1)	26(1)
C(9A)	2920(2)	5531(2)	3166(1)	26(1)
C(10)	1594(1)	4674(2)	2461(1)	25(1)
C(10A)	1716(2)	5130(2)	1719(1)	24(1)
C(11)	4138(2)	5364(2)	2388(2)	28(1)
C(12)	5823(2)	4869(2)	2735(2)	33(1)
C(13)	5618(2)	4820(2)	1942(2)	35(1)
C(14)	6700(2)	4624(2)	3254(2)	43(1)
C(15)	6202(2)	4504(2)	1379(2)	48(1)
C(16)	1104(2)	3848(2)	2470(1)	27(1)
C(17)	674(2)	3355(2)	1761(2)	31(1)
C(18)	1082(2)	3314(2)	3188(2)	32(1)
N(1)	315(2)	2926(2)	1220(2)	42(1)
N(2)	1064(2)	2851(2)	3743(2)	43(1)
S(3)	4860(1)	2144(1)	2304(1)	32(1)
S(4)	5461(1)	2320(1)	4011(1)	33(1)
C(21)	6365(2)	1491(2)	1551(1)	28(1)
C(22)	6625(2)	1510(2)	820(2)	33(1)
C(23)	7436(2)	1895(2)	755(2)	35(1)
C(24)	7988(2)	2272(2)	1417(1)	31(1)
C(24A)	7723(2)	2286(2)	2159(1)	25(1)
C(25)	8927(2)	2173(2)	4267(1)	32(1)
C(26)	8821(2)	1765(2)	4982(2)	37(1)
C(27)	8000(2)	1408(2)	5061(2)	35(1)
C(28)	7288(2)	1444(2)	4429(1)	30(1)
C(28A)	7368(2)	1870(2)	3702(1)	26(1)
C(29)	6633(2)	1916(2)	3016(1)	24(1)
C(29A)	6895(2)	1886(2)	2234(1)	24(1)
C(30)	8272(1)	2707(2)	2875(1)	24(1)
C(30A)	8202(2)	2243(2)	3631(1)	26(1)
C(31)	5771(2)	2071(2)	3095(1)	27(1)
C(32)	4101(2)	2618(2)	2844(2)	33(1)
C(33)	4381(2)	2717(2)	3626(2)	34(1)
C(34)	3201(2)	2856(2)	2365(2)	43(1)
C(35)	3891(2)	3147(2)	4221(2)	45(1)
C(36)	8755(1)	3534(2)	2862(1)	25(1)
C(37)	9194(2)	4013(2)	3575(2)	28(1)
C(38)	8773(2)	4098(2)	2158(2)	26(1)
N(3)	9539(2)	4438(2)	4122(1)	39(1)
N(4)	8814(1)	4596(2)	1630(1)	36(1)

Anisotropic displacement parameters (A^2 x 10^3)
The anisotropic displacement factor exponent takes the form:
-2 pi^2 [h^2 a*^2 U11 + ... + 2 h k a* b* U12]

	U11	U22	U33	U23	U13	U12
S(1)	24(1)	36(1)	37(1)	-1(1)	-1(1)	-1(1)
S(2)	27(1)	42(1)	37(1)	-2(1)	7(1)	0(1)
C(1)	29(1)	29(1)	35(2)	0(1)	0(1)	-4(1)
C(2)	40(2)	39(2)	31(1)	-7(1)	2(1)	-7(1)
C(3)	41(2)	45(2)	29(1)	-5(1)	8(1)	-2(1)
C(4)	28(1)	33(2)	36(2)	1(1)	7(1)	-2(1)
C(4A)	24(1)	23(1)	28(1)	1(1)	1(1)	3(1)
C(5)	24(1)	26(1)	36(2)	-2(1)	-1(1)	-2(1)
C(6)	35(2)	31(1)	31(1)	0(1)	-3(1)	1(1)
C(7)	41(2)	27(1)	28(1)	3(1)	3(1)	0(1)
C(8)	29(1)	25(1)	34(1)	-1(1)	5(1)	-2(1)
C(8A)	26(1)	18(1)	31(1)	-2(1)	3(1)	2(1)
C(9)	25(1)	22(1)	30(1)	0(1)	1(1)	-4(1)
C(9A)	25(1)	21(1)	31(1)	3(1)	2(1)	1(1)
C(10)	14(1)	25(1)	34(1)	-1(1)	3(1)	5(1)
C(10A)	25(1)	20(1)	27(1)	-3(1)	4(1)	1(1)
C(11)	27(1)	21(1)	35(1)	0(1)	2(1)	-5(1)
C(12)	25(1)	24(1)	49(2)	1(1)	5(1)	-1(1)
C(13)	25(1)	27(1)	53(2)	0(1)	10(1)	-2(1)
C(14)	29(2)	38(2)	60(2)	4(1)	2(1)	1(1)
C(15)	35(2)	50(2)	63(2)	-2(2)	19(2)	4(1)
C(16)	20(1)	28(1)	34(1)	-1(1)	5(1)	3(1)
C(17)	22(1)	25(1)	47(2)	-1(1)	6(1)	2(1)
C(18)	20(1)	27(1)	47(2)	-2(1)	7(1)	3(1)
N(1)	36(1)	32(1)	55(2)	-8(1)	2(1)	-2(1)
N(2)	41(1)	37(1)	52(2)	9(1)	14(1)	7(1)
S(3)	25(1)	36(1)	35(1)	-5(1)	4(1)	0(1)
S(4)	29(1)	39(1)	34(1)	-5(1)	12(1)	-5(1)
C(21)	28(1)	26(1)	31(1)	-4(1)	5(1)	-2(1)
C(22)	40(2)	31(1)	28(1)	-6(1)	3(1)	-3(1)
C(23)	45(2)	33(2)	29(1)	-4(1)	15(1)	-6(1)
C(24)	32(1)	27(1)	36(2)	2(1)	15(1)	-1(1)
C(24A)	28(1)	21(1)	28(1)	1(1)	8(1)	0(1)
C(25)	28(1)	29(1)	36(2)	2(1)	2(1)	-1(1)
C(26)	39(2)	36(2)	32(2)	6(1)	-5(1)	-1(1)
C(27)	45(2)	32(2)	27(1)	6(1)	4(1)	-2(1)
C(28)	32(1)	27(1)	33(1)	2(1)	10(1)	-4(1)
C(28A)	29(1)	23(1)	28(1)	-2(1)	6(1)	0(1)
C(29)	25(1)	20(1)	29(1)	0(1)	7(1)	-5(1)
C(29A)	24(1)	19(1)	31(1)	1(1)	8(1)	2(1)
C(30)	19(1)	25(1)	30(1)	0(1)	7(1)	4(1)
C(30A)	27(1)	23(1)	28(1)	1(1)	7(1)	0(1)
C(31)	28(1)	23(1)	30(1)	-3(1)	8(1)	-5(1)
C(32)	28(1)	24(1)	50(2)	1(1)	13(1)	-3(1)
C(33)	32(1)	25(1)	50(2)	0(1)	18(1)	-2(1)
C(34)	29(2)	38(2)	62(2)	4(1)	10(1)	6(1)
C(35)	47(2)	38(2)	60(2)	3(1)	32(2)	4(1)
C(36)	19(1)	26(1)	29(1)	0(1)	6(1)	1(1)
C(37)	23(1)	27(1)	34(2)	5(1)	9(1)	2(1)
C(38)	23(1)	24(1)	32(1)	-4(1)	7(1)	-1(1)
N(3)	39(1)	34(1)	42(1)	-3(1)	3(1)	-1(1)
N(4)	42(1)	32(1)	35(1)	4(1)	9(1)	-2(1)

C(28A)-C(29)-C(29A)	115.1(2)	C(21)-C(29A)-C(24A)	117.8(2)
C(21)-C(29A)-C(29)	123.6(2)	C(24A)-C(29A)-C(29)	118.6(2)
C(36)-C(30)-C(30A)	121.0(2)	C(36)-C(30)-C(24A)	123.2(2)
C(30A)-C(30)-C(24A)	115.6(2)	C(25)-C(30A)-C(28A)	120.6(2)
C(25)-C(30A)-C(30)	122.2(2)	C(28A)-C(30A)-C(30)	117.3(2)
C(29)-C(31)-S(3)	125.1(2)	C(29)-C(31)-S(4)	123.4(2)
S(3)-C(31)-S(4)	111.26(13)	C(33)-C(32)-C(34)	127.6(2)
C(33)-C(32)-S(3)	116.7(2)	C(34)-C(32)-S(3)	115.6(2)
C(32)-C(33)-C(35)	128.0(3)	C(32)-C(33)-S(4)	116.4(2)
C(35)-C(33)-S(4)	115.7(2)	C(30)-C(36)-C(37)	122.8(2)
C(30)-C(36)-C(38)	124.6(2)	C(37)-C(36)-C(38)	112.0(2)
N(3)-C(37)-C(36)	176.5(3)	N(4)-C(38)-C(36)	175.5(3)

Hydrogen coordinates (x 10^4) and isotropic displacement parameters (A^2 x 10^3)

	x	y	z	U(eq)
H(1)	3943(2)	6259(2)	3860(1)	38
H(2)	3336(2)	6342(2)	5000(2)	45
H(3)	1937(2)	5700(2)	5016(2)	46
H(4)	1154(2)	4927(2)	3889(2)	38
H(5)	450(2)	4957(2)	1094(1)	36
H(6)	696(2)	5635(2)	-96(2)	40
H(7)	2103(2)	6192(2)	-180(2)	39
H(8)	3239(2)	6195(2)	931(1)	35
H(14A)	6701(5)	3944(4)	3406(11)	82(7)
H(14B)	6791(7)	5025(11)	3735(6)	82(7)
H(14C)	7178(2)	4742(15)	2960(5)	82(7)
H(15A)	6062(11)	4878(12)	884(6)	100(8)
H(15B)	6104(12)	3818(5)	1257(11)	100(8)
H(15C)	6825(2)	4608(16)	1629(6)	100(8)
H(21)	5815(2)	1201(2)	1591(1)	34
H(22)	6243(2)	1260(2)	361(2)	40
H(23)	7615(2)	1900(2)	253(2)	42
H(24)	8551(2)	2523(2)	1372(1)	37
H(25)	9491(2)	2413(2)	4208(1)	38
H(26)	9312(2)	1720(2)	5414(2)	45
H(27)	7923(2)	1142(2)	5556(2)	42
H(28)	6736(2)	1172(2)	4489(1)	36
H(34A)	3037(6)	2378(9)	1940(8)	80(6)
H(34B)	3218(4)	3496(7)	2128(10)	80(6)
H(34C)	2762(3)	2850(15)	2713(3)	80(6)
H(35A)	4053(10)	3827(4)	4297(9)	73(6)
H(35B)	4053(10)	2806(9)	4730(4)	73(6)
H(35C)	3250(2)	3092(13)	4024(6)	73(6)

A1.4 Crystallographic Data for 10-(4,5-Dimethyl-1,3-diselenole-2-ylidene)-9-(2,2-dicyanomethane) anthracene 200

Bond lengths [A] and angles [deg]

Se(1)-C(12)	1.902(2)	Se(1)-C(11)	1.906(2)
Se(2)-C(13)	1.905(2)	Se(2)-C(11)	1.905(2)
N(1)-C(17)	1.132(3)	N(2)-C(18)	1.116(3)
C(1)-C(2)	1.389(3)	C(1)-C(9A)	1.402(3)
C(1)-H(1)	0.96(3)	C(2)-C(3)	1.394(3)
C(2)-H(2)	0.97(3)	C(3)-C(4)	1.387(3)
C(3)-H(3)	0.92(3)	C(4)-C(4A)	1.403(3)
C(4)-H(4)	0.92(3)	C(4A)-C(9A)	1.418(3)
C(4A)-C(10)	1.475(3)	C(5)-C(6)	1.390(3)
C(5)-C(10A)	1.408(3)	C(5)-H(5)	0.91(3)
C(6)-C(7)	1.392(3)	C(6)-H(6)	0.96(3)
C(7)-C(8)	1.389(3)	C(7)-H(7)	0.92(3)
C(8)-C(8A)	1.405(3)	C(8)-H(8)	1.01(3)
C(8A)-C(10A)	1.417(3)	C(8A)-C(9)	1.479(3)
C(9)-C(11)	1.364(3)	C(9)-C(9A)	1.483(3)
C(10)-C(16)	1.369(3)	C(10)-C(10A)	1.475(3)
C(12)-C(13)	1.334(3)	C(12)-C(14)	1.504(3)
C(13)-C(15)	1.509(3)	C(14)-H(141)	0.94(4)
C(14)-H(142)	0.96(4)	C(14)-H(143)	1.02(4)
C(15)-H(151)	0.95(3)	C(15)-H(152)	0.93(3)
C(15)-H(153)	0.97(4)	C(16)-C(17)	1.451(3)
C(16)-C(18)	1.459(3)		
C(12)-Se(1)-C(11)	95.3(1)	C(13)-Se(2)-C(11)	95.3(1)
C(2)-C(1)-C(9A)	120.8(2)	C(2)-C(1)-H(1)	118(2)
C(9A)-C(1)-H(1)	121(2)	C(1)-C(2)-C(3)	120.3(2)
C(1)-C(2)-H(2)	120(2)	C(3)-C(2)-H(2)	120(2)
C(4)-C(3)-C(2)	120.0(2)	C(4)-C(3)-H(3)	119(2)
C(2)-C(3)-H(3)	121(2)	C(3)-C(4)-C(4A)	120.3(2)
C(3)-C(4)-H(4)	121(2)	C(4A)-C(4)-H(4)	119(2)
C(4)-C(4A)-C(9A)	119.9(2)	C(4)-C(4A)-C(10)	122.9(2)
C(9A)-C(4A)-C(10)	117.2(2)	C(6)-C(5)-C(10A)	120.6(2)
C(6)-C(5)-H(5)	118(2)	C(10A)-C(5)-H(5)	121(2)
C(5)-C(6)-C(7)	119.6(2)	C(5)-C(6)-H(6)	119(2)
C(7)-C(6)-H(6)	121(2)	C(8)-C(7)-C(6)	120.6(2)
C(8)-C(7)-H(7)	118(2)	C(6)-C(7)-H(7)	121(2)
C(7)-C(8)-C(8A)	121.0(2)	C(7)-C(8)-H(8)	119.5(14)
C(8A)-C(8)-H(8)	119.4(14)	C(8)-C(8A)-C(10A)	118.4(2)
C(8)-C(8A)-C(9)	123.5(2)	C(10A)-C(8A)-C(9)	118.1(2)
C(11)-C(9)-C(8A)	123.3(2)	C(11)-C(9)-C(9A)	122.3(2)
C(8A)-C(9)-C(9A)	114.0(2)	C(1)-C(9A)-C(4A)	118.6(2)
C(1)-C(9A)-C(9)	122.8(2)	C(4A)-C(9A)-C(9)	118.6(2)
C(16)-C(10)-C(4A)	122.7(2)	C(16)-C(10)-C(10A)	122.1(2)
C(4A)-C(10)-C(10A)	115.1(2)	C(5)-C(10A)-C(8A)	119.9(2)
C(5)-C(10A)-C(10)	122.3(2)	C(8A)-C(10A)-C(10)	117.8(2)
C(9)-C(11)-Se(2)	124.4(2)	C(9)-C(11)-Se(1)	123.8(2)
Se(2)-C(11)-Se(1)	111.6(1)	C(13)-C(12)-C(14)	127.4(2)
C(13)-C(12)-Se(1)	118.5(2)	C(14)-C(12)-Se(1)	114.1(2)
C(12)-C(13)-C(15)	127.0(2)	C(12)-C(13)-Se(2)	118.5(2)
C(15)-C(13)-Se(2)	114.5(2)	C(12)-C(14)-H(141)	110(2)
C(12)-C(14)-H(142)	107(2)	H(141)-C(14)-H(142)	111(3)
C(12)-C(14)-H(143)	108(2)	H(141)-C(14)-H(143)	111(3)
H(142)-C(14)-H(143)	110(3)	C(13)-C(15)-H(151)	106(2)
C(13)-C(15)-H(152)	113(2)	H(151)-C(15)-H(152)	111(3)
C(13)-C(15)-H(153)	112(2)	H(151)-C(15)-H(153)	112(3)
H(152)-C(15)-H(153)	104(3)	C(10)-C(16)-C(17)	123.4(2)
C(10)-C(16)-C(18)	124.3(2)	C(17)-C(16)-C(18)	112.1(2)
N(1)-C(17)-C(16)	176.5(2)	N(2)-C(18)-C(16)	

Atomic coordinates (x 10^4) and equivalent isotropic displacement parameters (A^2 x 10^3) U(eq) is defined as one third of the trace of the orthogonalized Uij tensor.

	x	y	z	U(eq)
Se(1)	603.5(2)	4327.6(3)	3295.4(2)	27.3(1)
Se(2)	1701.0(1)	3660.4(3)	1909.2(2)	23.4(1)
N(1)	4427(2)	10459(2)	3480(2)	34(1)
N(2)	2897(2)	11327(3)	5250(2)	44(1)
C(1)	2082(2)	4920(3)	5423(2)	21(1)
C(2)	2089(2)	5588(3)	6304(2)	25(1)
C(3)	2570(2)	6949(3)	6662(2)	25(1)
C(4)	3054(2)	7634(3)	6145(2)	22(1)
C(4A)	3043(1)	6986(2)	5246(2)	17(1)
C(5)	4785(1)	6721(3)	4085(2)	20(1)
C(6)	5108(2)	5646(3)	3583(2)	23(1)
C(7)	4589(2)	4338(3)	3176(2)	23(1)
C(8)	3759(1)	4091(3)	3277(2)	20(1)
C(8A)	3414(1)	5165(2)	3774(2)	17(1)
C(9)	2541(1)	4962(2)	3914(2)	17(1)
C(9A)	2542(1)	5614(2)	4869(2)	17(1)
C(10)	3554(1)	7646(2)	4670(2)	18(1)
C(10A)	3934(1)	6510(2)	4171(2)	17(1)
C(11)	1771(1)	4370(2)	3191(2)	18(1)
C(12)	-66(2)	3854(3)	1916(2)	27(1)
C(13)	399(2)	3533(3)	1336(2)	25(1)
C(14)	-1087(2)	3824(4)	1622(2)	41(1)
C(15)	8(2)	3011(4)	253(2)	35(1)
C(16)	3626(1)	9199(3)	4554(2)	21(1)
C(17)	4076(2)	9867(3)	3938(2)	23(1)
C(18)	3208(2)	10368(3)	4972(2)	27(1)

Table 5. Hydrogen coordinates (x 10^4) and isotropic displacement parameters (A^2 x 10^3)

	x	y	z	U(eq)
H(1)	1792(17)	3937(30)	5229(19)	20(6)
H(2)	1781(18)	5080(33)	6686(20)	28(7)
H(3)	2610(18)	7367(33)	7265(21)	30(7)
H(4)	3408(19)	8492(35)	6397(22)	34(8)
H(5)	5145(17)	7558(30)	4361(18)	19(6)
H(6)	5697(18)	5797(31)	3545(20)	26(7)
H(7)	4788(19)	3614(33)	2840(21)	31(7)
H(8)	3420(16)	3099(30)	3029(18)	18(6)
H(141)	-1296(25)	4785(49)	1745(29)	68(12)
H(142)	-1215(24)	3031(44)	2017(28)	58(11)
H(143)	-1383(25)	3547(43)	879(29)	63(11)
H(151)	91(21)	1925(41)	270(24)	44(9)
H(152)	289(21)	3484(37)	-139(24)	43(9)
H(153)	-631(25)	3292(41)	-82(26)	55(10)

A1.5 Crystallographic Data for 1-(4.5-dimethyl-1,3-dithiole-2-ylidene)-1-ferrocenyl-3,3-dicyano-propene 220

Atomic coordinates (x 10^4) and equivalent isotropic displacement parameters (A^2 x 10^3) U(eq) is defined as one third of the trace of the orthogonalized Uij tensor.

	x	y	z	U(eq)
Fe	4173.1(2)	2360.6(4)	2113.3(2)	22.1(1)
S(1)	3606.1(4)	2836.9(9)	4221.8(4)	27.7(2)
S(2)	5201.2(4)	2371.3(8)	5439.3(3)	24.6(2)
N(1)	7316(2)	5568(3)	2644(2)	36(1)
N(2)	8901(2)	2227(4)	4366(2)	50(1)
C(1)	4830(2)	2733(3)	4415(1)	22(1)
C(2)	3343(2)	2237(3)	5202(2)	26(1)
C(3)	4079(2)	1996(3)	5763(1)	24(1)
C(4)	2304(2)	2073(5)	5308(2)	36(1)
C(5)	4070(2)	1505(4)	6640(2)	29(1)
C(6)	5462(2)	2967(3)	3835(1)	21(1)
C(7)	6441(2)	2677(3)	4097(1)	23(1)
C(8)	7234(2)	3260(3)	3774(1)	24(1)
C(9)	7250(2)	4524(3)	3132(2)	27(1)
C(10)	8157(2)	2667(4)	4102(2)	33(1)
C(11)	5150(2)	3492(3)	2986(1)	22(1)
C(12)	5581(2)	2939(3)	2280(2)	25(1)
C(13)	5143(2)	3850(4)	1594(2)	28(1)
C(14)	4423(2)	4931(3)	1854(2)	28(1)
C(15)	4417(2)	4714(3)	2712(2)	24(1)
C(16)	3570(2)	135(4)	2534(2)	31(1)
C(17)	4059(2)	-266(4)	1846(2)	34(1)
C(18)	3650(2)	759(4)	1181(2)	34(1)
C(19)	2909(2)	1788(4)	1458(2)	36(1)
C(20)	2866(2)	1403(4)	2294(2)	34(1)

Hydrogen coordinates (x 10^4) and isotropic displacement parameters (A^2 x 10^3)

	x	y	z	U(eq)
H(41)	2210(23)	1776(44)	5861(22)	53(9)
H(42)	1988(27)	3127(55)	5143(23)	74(12)
H(43)	2020(25)	1177(50)	4977(22)	62(11)
H(53)	4437(20)	494(40)	6769(16)	32(7)
H(52)	4334(21)	2446(39)	6999(18)	39(8)
H(51)	3426(24)	1195(45)	6754(19)	55(10)
H(7)	6566(18)	1895(37)	4573(16)	27(7)
H(12)	6056(19)	2150(35)	2283(15)	25(7)
H(13)	5290(18)	3749(36)	1076(17)	29(7)
H(14)	3975(19)	5672(37)	1486(16)	33(7)
H(15)	4005(19)	5310(37)	3031(16)	31(7)
H(16)	3700(19)	-308(38)	3059(17)	34(8)
H(17)	4580(20)	-1053(39)	1828(16)	35(8)
H(18)	3853(19)	788(38)	651(17)	37(8)
H(19)	2523(21)	2655(39)	1140(18)	39(8)

Anisotropic displacement parameters (A^2 x 10^3)
The anisotropic displacement factor exponent takes the form:
-2 pi^2 [h^2 a*^2 U11 + ... + 2 h k a* b* U12]

	U11	U22	U33	U23	U13	U12
Fe	20.7(2)	22.4(2)	22.8(2)	1.5(1)	0.2(1)	-2.1(1)
S(1)	19.8(3)	38.4(4)	25.1(3)	4.8(3)	3.3(2)	-0.4(3)
S(2)	21.7(3)	30.9(4)	21.4(3)	0.9(3)	3.8(2)	-0.3(3)
N(1)	31(1)	32(1)	47(1)	1(1)	13(1)	-5(1)
N(2)	30(1)	72(2)	48(2)	-18(1)	-5(1)	13(1)
C(1)	24(1)	20(1)	22(1)	1(1)	2(1)	-1(1)
C(2)	26(1)	26(1)	27(1)	2(1)	9(1)	-1(1)
C(3)	25(1)	24(1)	26(1)	1(1)	9(1)	0(1)
C(4)	26(2)	48(2)	35(2)	5(2)	7(1)	-1(1)
C(5)	34(2)	29(2)	24(1)	2(1)	8(1)	1(1)
C(6)	22(1)	20(1)	22(1)	0(1)	3(1)	-1(1)
C(7)	27(1)	24(1)	20(1)	-2(1)	2(1)	3(1)
C(8)	20(1)	28(1)	24(1)	-6(1)	2(1)	1(1)
C(9)	19(1)	28(1)	34(1)	-7(1)	7(1)	-4(1)
C(10)	26(1)	40(2)	32(1)	-10(1)	4(1)	1(1)
C(11)	19(1)	23(1)	24(1)	1(1)	5(1)	-4(1)
C(12)	22(1)	28(1)	26(1)	1(1)	4(1)	0(1)
C(13)	30(1)	31(2)	24(1)	3(1)	5(1)	-6(1)
C(14)	31(1)	24(1)	29(1)	5(1)	-1(1)	-4(1)
C(15)	25(1)	19(1)	30(1)	0(1)	2(1)	-1(1)
C(16)	34(2)	27(1)	33(2)	2(1)	1(1)	-10(1)
C(17)	38(2)	25(1)	38(2)	-5(1)	1(1)	-4(1)
C(18)	39(2)	35(2)	28(1)	-4(1)	-3(1)	-9(1)
C(19)	29(2)	38(2)	38(2)	2(1)	-9(1)	-7(1)
C(20)	23(1)	37(2)	41(2)	0(1)	2(1)	-8(1)

Torsion angles (degrees)

S(1)-C(1)-C(6)-C(7)	-174.5(2)
C(1)-C(6)-C(7)-C(8)	-158.6(3)
C(6)-C(7)-C(8)-C(9)	8.5(4)
C(11)-C(6)-C(7)-C(8)	21.3(4)
S(2)-C(1)-C(6)-C(7)	7.7(3)

Fe-C(12)	2.040(3)	Fe-C(13)	2.044(3)
Fe-C(20)	2.047(3)	Fe-C(19)	2.048(3)
Fe-C(18)	2.048(3)	Fe-C(14)	2.049(3)
Fe-C(16)	2.058(3)	Fe-C(17)	2.058(3)
Fe-C(15)	2.065(3)	Fe-C(11)	2.085(2)
Fe...S(1)	3.681(1)	S(1)-C(1)	1.738(2)
S(1)-C(2)	1.764(2)	S(2)-C(1)	1.745(2)
S(2)-C(3)	1.758(2)	N(1)-C(9)	1.146(3)
N(2)-C(10)	1.152(4)	C(1)-C(6)	1.392(3)
C(2)-C(3)	1.337(4)	C(2)-C(4)	1.509(4)
C(3)-C(5)	1.500(3)	C(6)-C(7)	1.432(3)
C(6)-C(11)	1.484(3)	C(7)-C(8)	1.370(3)
C(8)-C(9)	1.438(4)	C(8)-C(10)	1.439(4)
C(11)-C(15)	1.437(3)	C(11)-C(12)	1.438(3)
C(12)-C(13)	1.420(4)	C(13)-C(14)	1.415(4)
C(14)-C(15)	1.431(3)	C(16)-C(20)	1.419(4)
C(16)-C(17)	1.429(4)	C(17)-C(18)	1.425(4)
C(18)-C(19)	1.427(4)	C(19)-C(20)	1.424(4)
C(1)-S(1)-C(2)	97.0(1)	C(1)-S(1)...Fe	81.8(1)
C(2)-S(1)...Fe	159.3(1)	C(1)-S(2)-C(3)	97.5(1)
C(6)-C(1)-S(1)	124.8(2)	C(6)-C(1)-S(2)	122.7(2)
S(1)-C(1)-S(2)	112.5(1)	C(3)-C(2)-C(4)	127.7(2)
C(3)-C(2)-S(1)	116.7(2)	C(4)-C(2)-S(1)	115.6(2)
C(2)-C(3)-C(5)	128.5(2)	C(2)-C(3)-S(2)	115.8(2)
C(5)-C(3)-S(2)	115.7(2)	C(1)-C(6)-C(7)	116.5(2)
C(1)-C(6)-C(11)	122.6(2)	C(7)-C(6)-C(11)	120.9(2)
C(8)-C(7)-C(6)	130.1(2)	C(7)-C(8)-C(9)	125.7(2)
C(7)-C(8)-C(10)	120.3(2)	C(9)-C(8)-C(10)	114.0(2)
N(1)-C(9)-C(8)	175.7(3)	N(2)-C(10)-C(8)	178.6(3)
C(15)-C(11)-C(12)	106.8(2)	C(15)-C(11)-C(6)	127.6(2)
C(12)-C(11)-C(6)	125.5(2)	C(13)-C(12)-C(11)	108.5(2)
C(14)-C(13)-C(12)	108.3(2)	C(13)-C(14)-C(15)	108.3(2)
C(14)-C(15)-C(11)	108.1(2)	C(20)-C(16)-C(17)	108.1(3)
C(18)-C(17)-C(16)	107.7(3)	C(17)-C(18)-C(19)	108.1(3)
C(20)-C(19)-C(18)	107.8(3)	C(16)-C(20)-C(19)	108.3(3)

Appendix 2

List of Research Colloquia, Lectures and Seminars

A2.1 List of Research Colloquia, Lectures and Seminars

The following is a list of research colloquia, lectures and seminars that have been addressed by external speakers and arranged by the Department of Chemistry during the period of the authors residence as a postgraduate student at Durham.

* Denotes attendance by the author.
† Denotes invited specially for the graduate training programme.

August 1 1993-July 31 1994

1993

September 13 Prof. Dr. A.D. Schlüter, Freie Universität Berlin, Germany
Synthesis and Characterisation of Molecular Rods and Ribbons

September 13 Dr. K.J. Wynne, Office of Naval Research, Washington, USA
Polymer Surface Design for Minimal Adhesion

September 14 Prof. J.M. DeSimone, University of North Carolina, Chapel Hill, USA
Homogeneous and Heterogeneous Polymerisations in Environmentally Responsible Carbon Dioxide

September 28 Prof. H. Ila, North Eastern Hill University, India
Synthetic Strategies for Cyclopentanoids via Oxoketene Dithioacetals

October 4 Prof. F.J. Feher†, University of California, Irvine, USA
Bridging the Gap between Surfaces and Solution with Sessilquioxanes

October 14 Dr. P. Hubberstey, University of Nottingham
Alkali Metals: Alchemist's Nightmare, Biochemist's Puzzle and Technologist's Dream*

October 20 Dr. P. Quayle†, University of Manchester
Aspects of Aqueous ROMP Chemistry

October 21 Prof. R. Adams†, University of South Carolina, USA
Chemistry of Metal Carbonyl Cluster Complexes : Development of Cluster Based Alkyne Hydrogenation Catalysts

October 27 Dr. R.A.L. Jones†, Cavendish Laboratory, Cambridge
Perambulating Polymers

November 10 Prof. M.N.R. Ashfold†, University of Bristol
High Resolution Photofragment Translational Spectroscopy : A New Way to Watch Photodissociation

November 17 Dr. A. Parker†, Rutherford Appleton Laboratory, Didcot
Applications of Time Resolved Resonance Raman Spectroscopy to Chemical and Biochemical Problems

November 24 Dr. P.G. Bruce†, University of St. Andrews
Structure and Properties of Inorganic Solids and Polymers

November 25 Dr. R.P. Wayne, University of Oxford
The Origin and Evolution of the Atmosphere

December 1 — Prof. M.A. McKervey†, Queen's University, Belfast
Synthesis and Applications of Chemically Modified Calixarenes*

December 8 — Prof. O. Meth-Cohn†, University of Sunderland
Friedel's Folly Revisited - A Super Way to Fused Pyridines*

December 16 — Prof. R.F. Hudson, University of Kent
Close Encounters of the Second Kind

1994

January 26 — Prof. J. Evans†, University of Southampton
Shining Light on Catalysts

February 2 — Dr. A. Masters†, University of Manchester
Modelling Water Without Using Pair Potentials

February 9 — Prof. D. Young†, University of Sussex
Chemical and Biological Studies on the Coenzyme Tetrahydrofolic Acid*

February 16 — Prof. K.H. Theopold, University of Delaware, USA
Paramagnetic Chromium Alkyls : Synthesis and Reactivity

February 23 — Prof. P.M. Maitlis†, University of Sheffield
Across the Border : From Homogeneous to Heterogeneous Catalysis

March 2 — Dr. C. Hunter†, University of Sheffield
Noncovalent Interactions between Aromatic Molecules*

March 9 — Prof. F. Wilkinson, Loughborough University of Technology
Nanosecond and Picosecond Laser Flash Photolysis*

March 10 — Prof. S.V. Ley, University of Cambridge
New Methods for Organic Synthesis*

March 25 — Dr. J. Dilworth, University of Essex
Technetium and Rhenium Compounds with Applications as Imaging Agents

April 28 — Prof. R. J. Gillespie, McMaster University, Canada
The Molecular Structure of some Metal Fluorides and Oxofluorides: Apparent Exceptions to the VSEPR Model.

May 12 — Prof. D. A. Humphreys, McMaster University, Canada
Bringing Knowledge to Life

August 1 1994-July 31 1995

1994

October 5 — Prof. N. L. Owen, Brigham Young University, Utah, USA
Determining Molecular Structure - the INADEQUATE NMR way

October 19 Prof. N. Bartlett, University of California
Some Aspects of Ag(II) and Ag(III) Chemistry

November 2 Dr P. G. Edwards, University of Wales, Cardiff
The Manipulation of Electronic and Structural Diversity in Metal Complexes - New Ligands

November 3 Prof. B. F. G. Johnson, Edinburgh University
Arene-metal Clusters

November 9 Dr G. Hogarth, University College, London
New Vistas in Metal-imido Chemistry

November 10 Dr M. Block, Zeneca Pharmaceuticals, Macclesfield
Large-scale Manufacture of ZD 1542, a Thromboxane Antagonist Synthase Inhibitor*

November 16 Prof. M. Page, University of Huddersfield
Four-membered Rings and β-Lactamase*

November 23 Dr J. M. J. Williams, University of Loughborough
New Approaches to Asymmetric Catalysis

December 7 Prof. D. Briggs, ICI and University of Durham
Surface Mass Spectrometry

1995

January 11 Prof. P. Parsons, University of Reading
Applications of Tandem Reactions in Organic Synthesis*

January 18 Dr G. Rumbles, Imperial College, London
Real or Imaginary Third Order Non-linear Optical Materials*

January 25 Dr D. A. Roberts, Zeneca Pharmaceuticals
The Design and Synthesis of Inhibitors of the Renin-angiotensin System*

February 1 Dr T. Cosgrove, Bristol University
Polymers do it at Interfaces

February 8 Dr D. O'Hare, Oxford University
Synthesis and Solid-state Properties of Poly-, Oligo- and Multidecker Metallocenes*

February 22 Prof. E. Schaumann, University of Clausthal
Silicon- and Sulphur-mediated Ring-opening Reactions of Epoxide

March 1 Dr M. Rosseinsky, Oxford University
Fullerene Intercalation Chemistry*

March 22 Dr M. Taylor, University of Auckland, New Zealand
Structural Methods in Main-group Chemistry

April 26 Dr M. Schroder, University of Edinburgh

Redox-active Macrocyclic Complexes : Rings, Stacks and Liquid Crystals

May 4 Prof. A. J. Kresge, University of Toronto
The Ingold Lecture Reactive Intermediates : Carboxylic-acid Enols and Other Unstable Species

August 1 1995-July 1996

1995

October 11 Prof. P. Lugar, Frei Univ Berlin, FRG
Low Temperature Crystallography

October 13 Prof. R. Schmultzer, Univ Braunschwieg, FRG.
Calixarene-Phosphorus Chemistry: A New Dimension in Phosphorus Chemistry

October 18 Prof. A. Alexakis, Univ. Pierre et Marie Curie, Paris,
Synthetic and Analytical Uses of Chiral Diamines

October 25 Dr.D.Martin Davies, University of Northumbria
Chemical reactions in organised systems.

November 1 Prof. W. Motherwell, UCL London
New Reactions for Organic Synthesis*

November 3 Dr B. Langlois, University Claude Bernard-Lyon
Radical Anionic and Psuedo Cationic Trifluoromethylation

November 8 Dr. D. Craig, Imperial College, London
New Stategies for the Assembly of Heterocyclic Systems*

November 15 Dr Andrea Sella, UCL, London
Chemistry of Lanthanides with Polypyrazoylborate Ligands

November 17 Prof. David Bergbreiter, Texas A&M, USA
Design of Smart Catalysts, Substrates and Surfaces from Simple Polymers

November 22 Prof. I Soutar, Lancaster University
A Water of Glass? Luminescence Studies of Water-Soluble Polymers.

November 29 Prof. Dennis Tuck, University of Windsor, Ontario, Canada
New Indium Coordination Chemistry

December 8 Professor M.T. Reetz, Max Planck Institut, Mulheim
Perkin Regional Meeting*

1996

January 10 Dr Bill Henderson, Waikato University, NZ
Electrospray Mass Spectrometry - a new sporting technique

January 17 Prof. J. W. Emsley , Southampton University
Liquid Crystals: More than Meets the Eye

January 24	Dr Alan Armstrong, Nottingham Univesity Alkene Oxidation and Natural Product Synthesis*
January 31	Dr J. Penfold, Rutherford Appleton Laboratory, Soft Soap and Surfaces
February 7	Dr R.B. Moody, Exeter University Nitrosations, Nitrations and Oxidations with Nitrous Acid
February 12	Dr Paul Pringle, University of Bristol Catalytic Self-Replication of Phosphines on Platinum(O)
February 14	Dr J. Rohr, Univ Gottingen, FRG Goals and Aspects of Biosynthetic Studies on Low Molecular Weight Natural Products
February 21	Dr C R Pulham , Univ. Edinburgh Heavy Metal Hydrides - an exploration of the chemistry of stannanes and plumbanes
February 28	Prof. E. W. Randall, Queen Mary & Westfield College New Perspectives in NMR Imaging
March 6	Dr Richard Whitby, Univ of Southampton New approaches to chiral catalysts: Induction of planar and metal centred asymmetry
March 7	Dr D.S. Wright, University of Cambridge Synthetic Applications of Me_2N-p-Block Metal Reagents
March 12	RSC Endowed Lecture - Prof. V. Balzani, Univ of Bologna Supramolecular Photochemistry*
March 13	Prof. Dave Garner, Manchester University Mushrooming in Chemistry
April 30	Dr L.D.Pettit, Chairman, IUPAC Commission of Equilibrium Data pH-metric studies using very small quantities of uncertain purity

Appendix 3

Publications and Conferences Attended

A3.1 Publications

Part of the work contained within this thesis has been reported in the following publications:-

1) Andrei S. Batsanov, Adrian J. Moore, Neil Robinson, Andrew Green, Martin R. Bryce, Judith A. K. Howard, Allan E. Underhill. *J. Mater. Chem.*, 1997, **7**, 387.

2)Martin R. Bryce, Enrique Chinarro, Andrew Green, Nazario Martín, Adrian J. Moore, Louis Sánchez, Carlos Seoane. *Synth. Met.*, 1997, **86**, 1857.

3) Andrew Green, Martin R. Bryce, Enrique Chinarro, Nazario Martín, Louis Sánchez, Carlos Seoane, Andrei S. Batsanov, Adrian J. Moore, Judith A. K. Howard. Manuscript in preparation.

4) Adrian J. Moore, Martin R. Bryce,, Andrei S. Batsanov, Andrew Green, Judith A. K. Howard, M. Anthony McKervey, Peter McGuigan, Isabelle Ledoux, Enrique Ortí, Brian Tarbit. Manuscript in preparation.

5) Antony Chesney, Martin R Bryce, Andrew Green, Alexander K. Lay, Shimon Yoshida, Andrei S. Batsanov, Judith A. K. Howard, Jean-Marc Fabre. Manuscript in preparation.

A3.2 Conferences Attended

Dec. 1995	ICI Poster Competition, University of Durham*
March 1996	SCI Symposia on Novel Organic Chemistry, University of York$
April 1996	North East Graduate Symposia, University of Sunderland$

May 1996 Graduate Symposia, University of Durham$

July 1996 13th Conference on the Science and Technology of Synthetic Metals, Snowbird, Utah, USA*

* Indicates poster presented by the author

$ Indicates oral presentation by the author